
Dissertation zur Erlangung des Doktorgrades
der Fakultät für Chemie und Pharmazie
der Ludwig-Maximilians-Universität München



Optimization of shielding and targeting domains within
sequence-defined, cationic carriers for pDNA delivery

Stephan Wolfgang Morys
aus Forchheim, Deutschland

2017

Erklärung

Diese Dissertation wurde im Sinne von § 7 der Promotionsordnung vom 28. November 2011 von Herrn Prof. Dr. Ernst Wagner betreut.

Eidesstattliche Versicherung

Diese Dissertation wurde eigenständig und ohne unerlaubte Hilfe erarbeitet.

München, 09.11.2017

.....
Stephan Morys

Dissertation eingereicht am: 09.11.2017

1. Gutachter: Prof. Dr. Ernst Wagner
2. Gutachter: Prof. Dr. Wolfgang Frieß

Mündliche Prüfung am: 11.01.2018

Meiner Familie

„Science, my lad, is made up of mistakes, but they are mistakes which it is useful to make, because they lead little by little to the truth.“

Jules Verne

Table of contents

| | | |
|-----------|--|-----------|
| 1 | Introduction | 11 |
| 1.1 | Non-viral gene therapy | 11 |
| 1.1.1 | The delivery pathway of non-viral nucleic acid carriers | 13 |
| 1.1.2 | Cationic carriers: From polydisperse polymers towards sequence-defined oligomers..... | 18 |
| 1.1.2.1 | SPS as a method to develop sequence-defined cationic vectors for structure activity relationships..... | 19 |
| 1.1.2.2 | Tailoring topologies and functionalizing oligomers to improve nucleic acid delivery | 21 |
| 1.1.2.2.1 | Polyplex shielding | 25 |
| 1.1.2.2.2 | Approaches of pre-PEGylation, post-PEGylation..... | 26 |
| 1.1.2.3 | Receptor targeting..... | 27 |
| 1.1.2.3.1 | HGFR targeting..... | 28 |
| 1.1.2.3.2 | EGFR targeting..... | 28 |
| 1.2 | Aim of the thesis | 30 |
| 2 | Materials and Methods | 32 |
| 2.1 | Materials | 32 |
| 2.1.1 | Equipment for solid-phase synthesis..... | 34 |
| 2.1.2 | Plasmid DNA..... | 34 |
| 2.1.3 | Cell culture | 35 |
| 2.2 | Methods..... | 36 |
| 2.2.1 | Synthesis of oligomers and PEGylation reagents via solid phase synthesis (SPS)..... | 36 |

| | | |
|-----------|--|----|
| 2.2.1.1 | General procedure for solid phase synthesis (SPS) | 36 |
| 2.2.1.1.1 | Loading of a 2-chlorotrityl chloride resin with an Fmoc protected amino acid | 36 |
| 2.2.1.1.2 | Procedure of a manually conducted solid phase synthesis | 36 |
| 2.2.1.1.3 | Kaiser test | 38 |
| 2.2.1.1.4 | Procedure of an automated solid phase synthesis | 38 |
| 2.2.1.2 | Cleavage of oligomers and reagents | 39 |
| 2.2.1.2.1 | General cleavage of oligomers | 39 |
| 2.2.1.2.2 | Cleavage of oligomers containing oleic acid | 40 |
| 2.2.1.2.3 | Cleavage of NPys containing PEGylation reagents | 40 |
| 2.2.1.3 | Synthesis of oligomers | 40 |
| 2.2.1.3.1 | Synthesis of untargeted, PEGylated 2-arm oligomers | 40 |
| 2.2.1.3.2 | Synthesis of untargeted 2-arm oligomers containing Pro-Ala-Ser repeats | 41 |
| 2.2.1.3.3 | Synthesis of untargeted 3-arm oligomer | 42 |
| 2.2.1.3.4 | Synthesis of cmb containing two and 3-arm oligomers | 42 |
| 2.2.1.3.5 | Synthesis of PEGylated 2-arm oligomers with GE11 ligand and alanine | 43 |
| 2.2.1.3.6 | Synthesis of the T-shaped lipo-oligomer for post-modification ... | 44 |
| 2.2.1.3.7 | Synthesis of improved T-shaped lipo-oligomers | 44 |
| 2.2.1.4 | Synthesis of PEGylation reagents for polyplex post-modification ... | 45 |
| 2.2.1.4.1 | Synthesis of monovalent PEGylation reagents. | 46 |
| 2.2.1.4.2 | Synthesis of bivalent PEGylation reagents | 46 |
| 2.2.2 | pDNA polyplex formation | 46 |

| | | |
|---------|---|----|
| 2.2.2.1 | Post-modification with PEGylation reagents..... | 47 |
| 2.2.3 | pDNA binding assays | 47 |
| 2.2.4 | Particle size and zeta potential..... | 47 |
| 2.2.5 | Transmission electron microscopy (TEM) of polyplexes | 48 |
| 2.2.6 | Ethidium bromide compaction assay and polyanionic stress test..... | 48 |
| 2.2.7 | Stability of polyplexes in serum and media | 49 |
| 2.2.8 | Polyplex stability in the presence of salt..... | 49 |
| 2.2.9 | Polyplex adhesion to erythrocytes or serum..... | 49 |
| 2.2.10 | UV spectrometrical investigation of polyplex modification | 50 |
| 2.2.11 | Ellman's assay of oligomers..... | 50 |
| 2.2.12 | Ellman's assay of polyplexes | 50 |
| 2.2.13 | Release of 3-nitro-2-thiopyridone | 51 |
| 2.2.14 | EGF and HGF receptor measurement | 51 |
| 2.2.15 | <i>In vitro</i> pCMVLuc gene transfer and metabolic activity of transfected cells (MTT assay) | 52 |
| 2.2.16 | <i>In vitro</i> pCMVLuc gene transfer and metabolic activity of transfected cells (MTT assay) with addition of endosomolytic chloroquine or LPEI | 53 |
| 2.2.17 | Cellular association of pDNA polyplexes..... | 53 |
| 2.2.18 | Cellular internalization of pDNA polyplexes..... | 54 |
| 2.2.19 | <i>In vivo</i> gene transfer..... | 54 |
| 2.2.20 | Iodide uptake activity after hNIS gene delivery..... | 55 |
| 2.2.21 | MALDI-TOF mass spectrometry..... | 56 |
| 2.2.22 | Proton NMR spectroscopy..... | 56 |
| 2.2.23 | Analytical RP-HPLC | 56 |

| | | |
|----------|---|-----------|
| 2.2.24 | ESI mass spectrometry | 57 |
| 2.2.25 | Statistical analysis | 57 |
| 3 | Results | 58 |
| 3.1 | Influence of defined hydrophilic blocks within oligoaminoamide copolymers: compaction versus shielding of pDNA nanoparticles | 58 |
| 3.1.1 | Peptide and oligomer synthesis..... | 59 |
| 3.1.2 | Physicochemical polyplex characterization | 60 |
| 3.1.3 | Steric shielding..... | 63 |
| 3.1.4 | DNA compaction | 65 |
| 3.1.5 | Serum stability..... | 67 |
| 3.1.6 | Tumor cell interactions <i>in vitro</i> | 69 |
| 3.1.7 | Tumor cell interactions <i>in vitro</i> without and with targeting | 70 |
| 3.1.8 | Tumor cell interactions <i>in vivo</i> without and with targeting..... | 73 |
| 3.2 | EGFR targeting and shielding of pDNA lipopolyplexes via bivalent attachment of a sequence-defined PEG agent..... | 75 |
| 3.2.1 | pDNA nanoparticle design, peptide and oligomer syntheses | 76 |
| 3.2.2 | Physicochemical polyplex characterization | 81 |
| 3.2.3 | Luciferase gene transfections..... | 90 |
| 3.2.4 | Cellular binding and internalization of bivalent post-PEGylated polyplexes | 96 |
| 3.2.5 | Iodide uptake activity after hNIS gene delivery..... | 100 |
| 3.3 | Lipo-oligomers optimized towards enhanced lipopolyplex stability | 102 |
| 3.3.1 | Library design and oligomer synthesis | 102 |
| 3.3.2 | Physicochemical polyplex characterization | 105 |

| | | |
|----------|---|------------|
| 3.3.2.1 | Size and zeta potential of unmodified as well as post-modified lipopolyplexes | 105 |
| 3.3.2.2 | pDNA compaction in buffer and after polyanionic stress | 109 |
| 3.3.2.3 | Steric stability of unmodified as well as PEGylated lipopolyplexes under physiological salt conditions | 111 |
| 3.3.2.4 | Serum stability of unmodified as well as post-modified lipopolyplexes | 113 |
| 3.3.3 | Luciferase gene transfections..... | 115 |
| 3.3.4 | Ellman's assay to determine free thiols for polyplex post-modification | 117 |
| 3.3.5 | Cellular polyplex uptake | 119 |
| 3.3.6 | Gene transfer after enhanced endosomal escape..... | 121 |
| 4 | Discussion | 124 |
| 4.1 | Influence of defined hydrophilic blocks within oligoaminoamide copolymers: compaction versus shielding of pDNA nanoparticles..... | 124 |
| 4.2 | EGFR targeting and shielding of pDNA lipopolyplexes via bivalent attachment of a sequence-defined PEG agent..... | 127 |
| 4.3 | Lipo-oligomers optimized towards enhanced lipopolyplex stability | 130 |
| 5 | Summary | 136 |
| 6 | Appendix | 138 |
| 6.1 | Abbreviations..... | 138 |
| 6.2 | Serum stability of optimized T-shapes determined by DLS | 141 |
| 6.3 | Summary of SPS derived oligomers..... | 144 |
| 6.4 | Summary of SPS derived shielding reagents | 144 |
| 6.5 | Analytical data | 145 |
| 6.5.1 | MALDI-TOF MS of Dde-K-(S-A-P) ₈ -OH..... | 145 |

| | | |
|----------|---|------------|
| 6.5.2 | MALDI-TOF MS of the targeting peptides cmb and GE11 | 146 |
| 6.5.3 | ¹ H NMR spectra of oligomers | 147 |
| 6.5.4 | RP-HPLC of oligomers | 161 |
| 6.5.5 | Mass spectra of oligomers..... | 168 |
| 6.5.5.1 | Full mass spectra of oligomers..... | 169 |
| 6.5.6 | Mass spectra of shielding reagents | 176 |
| 6.5.6.1 | Full mass spectra of shielding reagents | 176 |
| 6.5.7 | RP-HPLC of shielding reagents..... | 178 |
| 7 | References | 181 |
| 8 | Publications | 196 |
| 9 | Acknowledgements..... | 199 |

1 Introduction

This chapter should give a brief introduction into the research field of bio-reducible polycationic carriers for nucleic acid delivery.

1.1 Non-viral gene therapy

This chapter gives a brief introduction into chemically designed, artificial vectors for nucleic acid delivery. It does not aim at giving a full review of the advances in polymer-based gene therapy since its invention in the 1960's. This, as well as an appropriate review of advances in viral gene therapy and a comparison of both would exceed the intended introduction of this Ph.D. thesis.

However, Lächelt and Wagner [1] as well as Herzog and colleagues [2] reviewed recent advances in detail.

So far, genetic disorders like mucoviscidosis [3], severe combined immunodeficiency (SCID) [4], haemophilia [5], β -thalassemia [6], as well as adrenoleukodystrophy (ALD) [7], metachromatic leukodystrophy [8], aromatic L-amino acid decarboxylase (AADC) deficiency [2] among others [9-11] have been tackled by classical, viral gene therapy. Thereby, classical gene therapy addresses these diseases by inserting functional DNA into the human genome in order to replace defect gene sections.

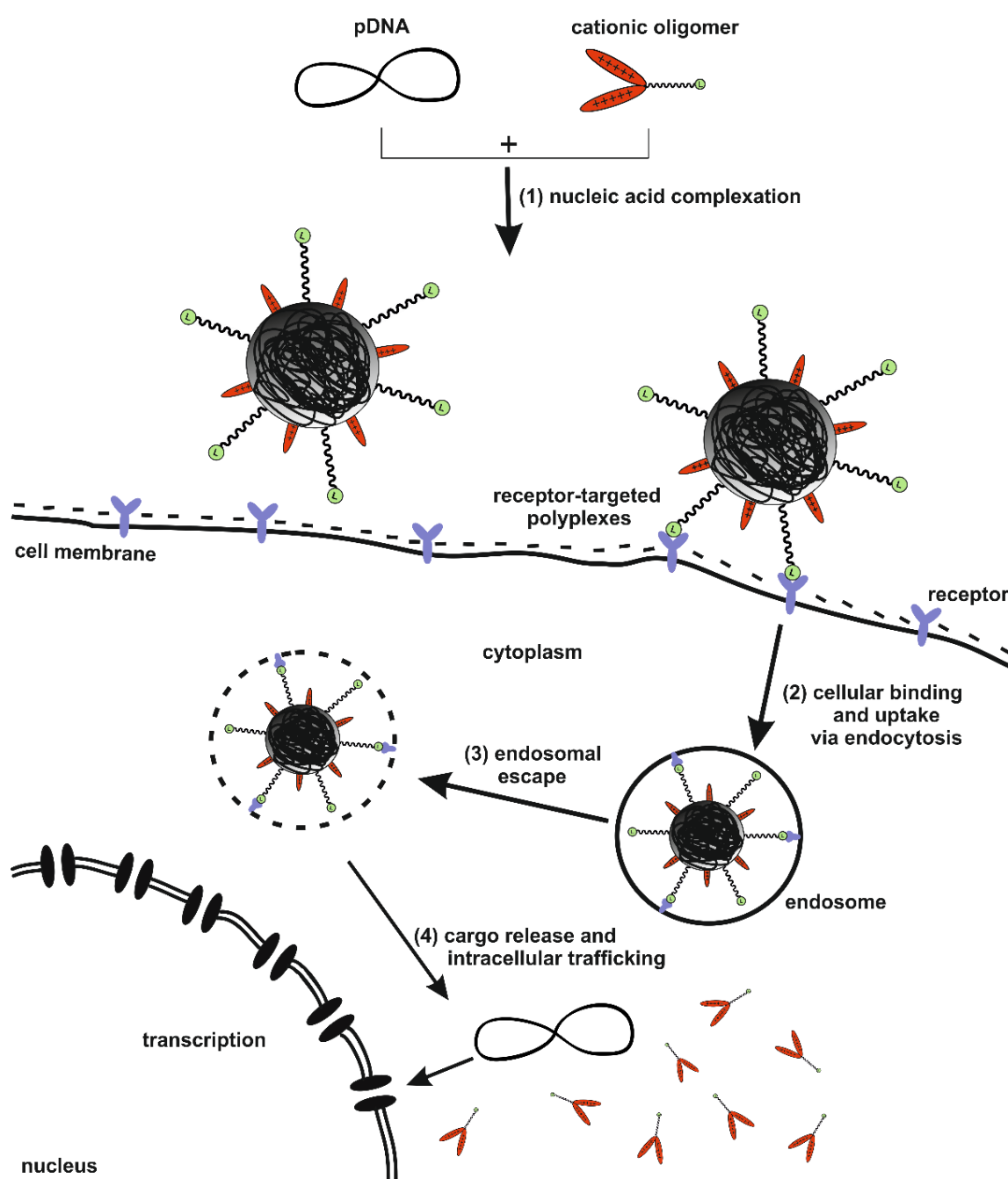
However, it took until 2012 until the first therapeutic product, Glybera, was approved by the European Medicines Agency (EMA) for the treatment of lipoprotein lipase deficiency (LPLD). Facing high therapy costs, the company will not extend the admission of Glybera® after its ended in October 2017. However, in the meantime Strimvelis®, for the treatment of adenosine deaminase (ADA)-deficient severe combined immunodeficiency (SCID), was approved on the European market [12].

The RNA interference (RNAi) discovered in 1998 by Fire et al. [13] also significantly increased therapeutic options within recent years. Specific gene silencing and hence the inhibition of cellular expression of a protein was since then widely explored for double stranded small (synthetic) interfering RNA (siRNA) as well as micro RNA

(miRNA) [14]. To investigate nucleic acid delivery, artificial vectors mimicking viruses have been considered since its discovery in the 1960's besides the established viral delivery [1]. Carriers, however, need to comprise several functionalities and overcome several barriers for a successful gene delivery *in vitro* as well as *in vivo*. These properties are addressed in the upcoming chapter.

1.1.1 The delivery pathway of non-viral nucleic acid carriers

Non-viral nucleic acid carriers face several obstacles prior to an efficient intracellular delivery. These barriers are schematically illustrated (cf. **Scheme 1**) to exhibit the very complex delivery pathway of polymer-based systems. The following chapter addresses the critical steps of nucleic acid complexation (1), cellular binding and uptake (2), endosomal escape (3), cargo release and intracellular trafficking (4) towards the compartment of further processing.



Scheme 1 The cellular delivery pathway of polymer-based nucleic acid carriers

A large size, anionic charge, as well as sensitivity towards degradation by nucleases are rather inefficient properties for the delivery of naked nucleic acids to their target location [15, 16], however, it rarely is possible [17, 18]. To overcome these issues, chemically engineered cationic polymers along with cationic lipids [19-21] were developed. By complexing nucleic acid, they were intended to shade the cargo in the extracellular environment and prevent them from degradation, but also facilitate the nucleic acid to be transported into the cytoplasm [22]. Within cationic polymers, polylysine (pLL) [23, 24], which was first evaluated clinically as a delivery vehicle for pDNA [25], the branched [26-29] and linear [30-33] versions of polyethylenimine (PEI) as well as dendritic polyamidoamine (PAMAM) [34-36] (cf. **Figure 1A-D**) represent the most prominent candidates besides many others [1].

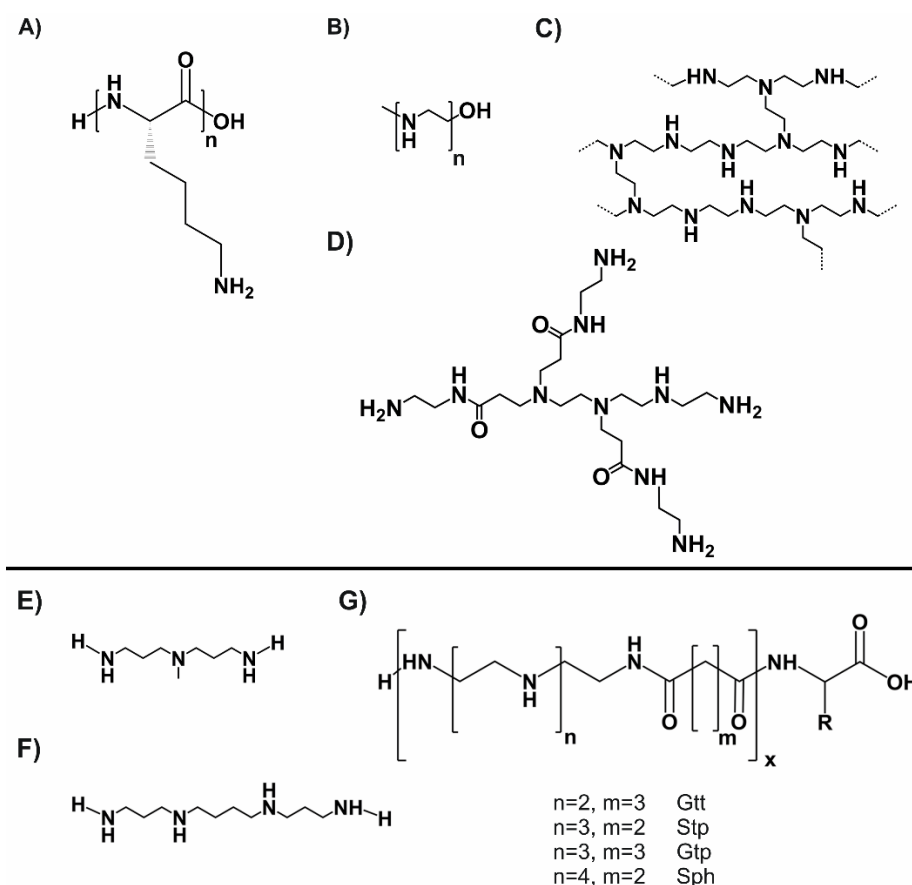


Figure 1 A) PLL, poly-L-lysine; B) LPEI, linear polyethylenimine prepared by hydrolysis of poly(2-ethyl-2-oxazoline); C) BPEI, branched polyethylenimine (partially); D) PAMAM, polyamidoamine dendrimer Generation 0; E) DAMP (3,3'-Diamino-N-methylpropylamine); F) Spermine (N,N-(butane-1,4-diyl)bis(propane-1,3-diamine)); G) Artificial amino acids derived from PEI repeat unit which are assembled by SPS to retrieve a nucleic acid binding domain within sequence-defined oligomers. Gtt represents glutaryl-triethylene tetramine, Stp succinyl tetraethylene pentamine, Gtp glutaryl-tetraethylene pentamine and Sph succinyl pentaethylene hexamine.

These cationic carriers, all comprise basic amines, are partially protonated at neutral pH and are thereby able to bind and compact negatively charged nucleic acids via electrostatic interaction. This complexation is entropy driven and leads to the formation of nano-sized complexes, so-called “polyplexes” [37, 38].

These polyplexes need to exhibit a certain size as well as stability for the successful delivery. Nanoparticles with a size of 5.5 nm or below suffer from rapid clearance by the kidney [39], while particles with a size between 20 and 400 nm can penetrate into highly vascularized solid tumors as a result of the enhanced permeability and retention (EPR) effect due to passage through leaky vessels of the tumor tissue [40-42]. However, the extent of passive tumor accumulation via EPR effect is strongly dependent on the size-threshold of the porous tumor vasculature which varies within different types of cancer [43-45].

As already mentioned before, also stability within the biological environment represents a crucial property for polyplex delivery. Here the positive surface charge of unshielded polyplexes can mediate interaction with proteins and electrolytes, causing polyplex dissociation or severe aggregation due to counterion exchange. This stability issue can be addressed by increased cationic charge or by the introduction of crosslinking domains (e.g. terminal cysteines) via formation of bio-reducible disulfide bonds [46-50], or the introduction of hydrophobic elements [51-53].

Cellular binding followed by endocytosis represents the next step towards gene delivery. By its nature, nanoparticles formed with cationic polymers exhibit a positive surface charge, due to a usual excess of amines per nucleic acid phosphate during polyplex formation. This can be beneficial for binding to the negatively charged cell surface via electrostatic interaction but represents a very unspecific and rather ineffective way compared to the receptor-mediated uptake route (cf. **Scheme 1(2)**) [54, 55]. Hence, the introduction of a targeting domain, exposed on the polyplex surface, is a convenient approach to enhance cellular uptake. The selection of the proper targeting domain is dependent of the receptor expression in the target tissue. Generally oncogenic transformation is accompanied by excessive proliferation and an elevated metabolic activity [56]. Therefore, transport proteins for the uptake of nutrients and cofactors, such as the folate receptor (FR) and transferrin receptor (TfR), growth factor receptors or integrins are often upregulated and represent auspicious targets

[55, 57-67]. As polyplex targeting represents a crucial part of this Ph.D. work, the two key targets (EGFR and HGFR) are described in more detail later on (cf. **1.1.2.3**).

Polyplex shielding, often impaired by the introduction of a targeting domain, represents another issue to be addressed as polyplexes with a positive surface charge can undergo aggregation or dissociation with electrolytes or proteins within the bloodstream. In addition, a positive surface charge can lead to the activation of the immune system. However, as polyplex shielding presents a key topic of this thesis, it is elucidated in more detail later on (cf. **1.1.2.2.1**).

When having reached the intracellular space by endocytosis [68], the next barrier within the delivery pathway is represented by endosomes. These intracellular vesicles are the major site for the sorting, trafficking and recycling of endocytosed material [69, 70]. To circumvent recycling to the cell membrane or degradation in late endo- and lysosomes, the entrapped polyplexes have to be released from the vesicles to reach the cytoplasm. This can be reached by different strategies. The so-called proton sponge effect, first described by J.P. Behr [71] represents the most common hypothesis on evasion from the endosome. Polymers with amines, becoming protonated under acidic pH, like LPEI, can increase osmotic pressure due to its buffer abilities, ultimately leading, due to endosomal swelling, to an endosomal burst [26, 72]. This effect can also be mediated by shorter diaminoethane motif containing chains. Here an even number of protonable amines is preferred [73]. Additionally, introduction of histidines (with a pK_a of the imidazole group of 6.5) enhance endosomal buffer capacity due to their favorable protonation at endosomal pH [50, 74, 75]. Alternatively, endosomal escape is mediated by interaction of peptides with a high content of basic amino acids [76], such as Tat [77], KALA [78, 79], GALA [80], influenza (Inf) virus-derived peptides [81, 82] and others [83-85] with the endosomal membrane. Also, lipids can contribute to the endosomal escape by lysing membranes in a favorable pH-dependent manner due to their amphiphilic character and cationization at endosomal pH [49]. As evaluated by Fröhlich et al., the unsaturated fatty acids oleic acid and linoleic acid emerged as the most potent candidates, balancing oligomer mediated siRNA delivery and cytotoxicity [51].

After having reached the cytoplasm, the delivered polyplexes now have to release the cargo. For this reason, particle stability needs to be well balanced between sufficient extracellular stability and fast nucleic acid release at the target site. Here, previously mentioned disulfide bonds can be reduced by cytosolic GSH, releasing the cargo and the single polymers, thereby reducing cytotoxicity due to an increased biodegradability of smaller units.

The released pDNA then needs to be transported into the nucleus for transcription towards mRNA. However, nuclear transport represents a critical hurdle within non-viral gene delivery [86]. This is achieved preferentially when the nuclear envelope dissolves during the cell division process [87]. After nuclear transcription [88], the mRNA needs to undergo ribosomal translation towards the protein of interest.

1.1.2 Cationic carriers: From polydisperse polymers towards sequence-defined oligomers

Artificial vectors as potent nucleic acid vehicles need to comprise different functionalities to be bioresponsive.

Previously, cationic vectors like pLL, PEI, PAMAM were generated by different kinds of polymerization techniques and resulted in polydisperse polymers. With improved chemistries, such as controlled radical polymer synthesis or specific ligation strategies, products with decreased polydispersity and more highly controlled architecture of carries were obtained [89-94].

Further development of cationic delivery systems requires clear-cut structure-activity relationships to be drawn. Therefore, a technique to obtain polymers with a precisely defined sequence is needed. A series of researchers have applied the well-established method of solid-phase assisted synthesis (SPS) to develop linear [84, 85, 95-103] and branched [75, 104-109] peptide-based as well as lipid-based [110-113] nucleic acid carriers. Recently, also artificial amino acids have been assembled to sequence-defined oligomers as shuttles for pDNA and siRNA (cf. **Figure 1E-G**) [49, 51, 64, 113-122].

Merrifield was the first to introduce SPS to assemble peptides in a non-liquid environment. Therefore, pre-activated polystyrene served as a solid support for synthesis [123]. The synthesis is initiated by loading the first protected amino acid onto these so-called resins. Orthogonally protected amino acids are coupled sequentially, with easy washing steps between coupling and removal of the protection group of the primary amine to constantly grow the macromolecule on the solid support. In comparison to solution-phase synthesis, solid-phase synthesis offers the following important advantages. Firstly, purification of intermediates is possible, due to the simple removal of unreacted reagents by washing during synthesis. Secondly, side products (produced by repeated couplings or capping) can be reduced, leading to increased product yields. And thirdly, due to the repetitive nature of the process, the whole assembly can be automated with the help of peptide synthesizers.

1.1.2.1 **SPS as a method to develop sequence-defined cationic vectors for structure activity relationships**

This chapter is partly based on:

Krhac Levacic A., Morys, S., Wagner E. *Solid-phase Supported Design of Carriers for Therapeutic Nucleic Acid Delivery. Bioscience Reports* **2017**, 37 (5).

Initially, tBoc chemistry was applied to protect the α -amino group of the amino acids. As mentioned previously, a solid support was introduced to assemble peptides sequentially [123]. The first amino acid with a tBoc α -amine (cf. **Figure 2A**) is linked to the solid support via the free, C-terminal carboxy group. Then, the resin-bound amino acid is treated with trifluoroacetic acid (TFA) to remove the tBoc protecting group and to free the α -amine. Now, the next tBoc protected α -amino acid can be coupled. For sequential amino acid coupling, the carboxylic acid group of each amino acids needs to be activated. Most commonly this is achieved by the addition of N,N'-dicyclohexylcarbodiimid (DCC). Dichloromethane (DCM) and dimethylformamide (DMF) are used as organic solvents, to create the required, non-aqueous environment for successful coupling, while facilitating swelling of the solid support during the reaction. After coupling the last amino acid, the resin is treated with hydrofluoric acid (HF) to cleave the peptide off the resin and to remove all side chain protecting groups. SPS advanced with more scientists facilitating this method of defined synthesis. Classical tBoc chemistry was soon replaced by introducing the base-labile protecting group Fmoc (N- α -9-fluorenylmethyloxycarbonyl) into SPS chemistry [124-127].

This approach no longer required the application of the hazardous HF as a cleavage reagent and thereby opened peptide manufacture to a wider range of operators. The use of resins with novel acid labile linkers, like the hydroxymethyl based Wang resin, the Rink amide resin or the trityl chloride (especially 2-chlorotrityl chloride) [127] enabled cleavage from the resin with TFA instead of HF. Instead of tBoc, Fmoc serves until today, as the state of the art protecting group of the amino acid's α -amines (e.g. **Figure 2B**). Easy removal by non-nucleophilic bases like piperidine or 1,8-Diazabicyclo[5.4.0]undec-7-en (DBU), maintained orthogonality to acid labile side chain protecting groups such as tBu, Trt, tBoc or Pbf [128]. Also, strategies for the synthesis of more highly sophisticated peptides, requiring orthogonality to Fmoc was

achieved by introduction of novel protecting groups [129].

A schematical cycle of SPS is given in **Figure 2D** pointing out the different, repetitive steps to obtain a fully deprotected peptide at the end of the synthesis.

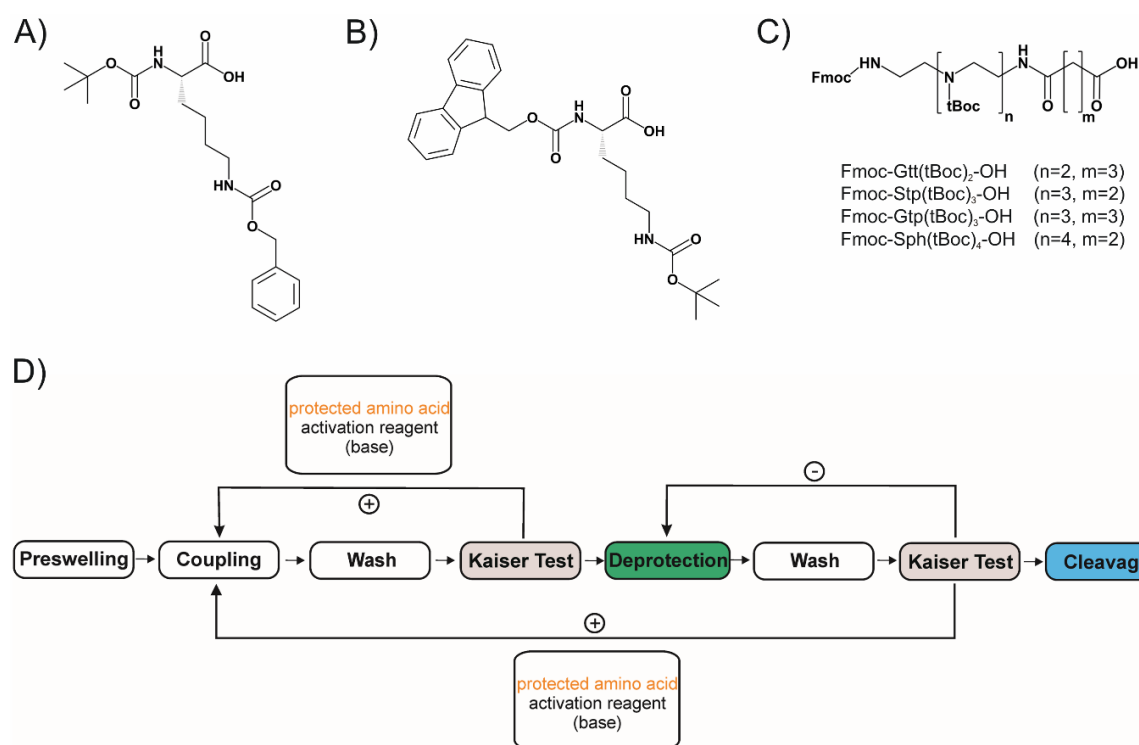


Figure 2 Protected lysine for A) tBoc (tBoc-L-Lys(Cbz)-OH) or B) Fmoc (Fmoc-L-Lys(tBoc)-OH) strategy. C) Fmoc, tBoc protected artificial oligoamino acids derived from PEI repeat units. tBoc represents tert-butyloxycarbonyl, Cbz Benzyloxycarbonyl, Fmoc N- α -9-fluorenylmethyloxycarbonyl, Gtt glutaryl-triethylene tetramine, Stp succinyl tetraethylene pentamine, Gtp glutaryl-tetraethylene pentamine and Sph succinyl pentaethylene hexamine D) Standard procedure of a solid phase peptide synthesis cycle. tBoc, as well as Fmoc strategy, follow the same procedure of a repetitive coupling cycle. Resins are commonly swollen in DCM. Coupling requires activation of the carboxylic function of the amino acid either by carbodiimides or by formation of activated esters with PyBOP, HBTU or HOBt and the addition of DIPEA or TEA. Washing steps are performed with non-aqueous, peptide grade DMF and DCM. A Kaiser test [130] for detection of unprotected amines via ninhydrine reaction is done to verify successful coupling and deprotection. Nevertheless, tBoc and Fmoc strategies differ significantly regarding protecting groups, their removal (deprotection) as well as the final cleavage from the solid support. In tBoc strategy α -amines of amino acids are tBoc protected, removal after coupling is performed with TFA and the final peptide cleavage is conducted with HF. In Fmoc strategy α -amines of amino acids are Fmoc protected, removal after coupling is performed with a mixture of piperidine/DMF and the final peptide cleavage is conducted with a cleavage cocktail mainly consisting of TFA. This figure is adapted from Krhac Levacic A., Morys, S., Wagner E. *Solid-phase Supported Design of Carriers for Therapeutic Nucleic Acid Delivery. Bioscience Reports 2017, 37 (5)*

Besides the previously mentioned, mostly lysine-based, oligomers [95, 96, 98, 100, 101, 104] the Fmoc peptide SPS strategy has been adopted for the synthesis of sequence-defined oligo(ethylenamino)amides (**Figure 2C**). Instead of natural amino acids, artificial oligoamino acids such as Stp (succinyl tetraethylene pentamine), Gtp (glutaroyl-tetraethylene pentamine) or Sph (succinyl pentaethylene hexamine) in Fmoc, tBoc-protected forms [49, 131, 132] can be used for manual as well as automated SPS, the latter requiring a peptide synthesizer [133]. These building blocks introduced the diaminoethane motif of LPEI, a well-established nucleic acid binding and endosomal buffering domain, for solid phase synthesis.

1.1.2.2 Tailoring topologies and functionalizing oligomers to improve nucleic acid delivery

With these artificial amino acids, a library of more than 1100 oligomers has been established and the oligomers have been tested for different nucleic acids (pDNA, siRNA, miRNA, mRNA) to evaluate the best suitable carriers. The choice of the artificial amino acids mentioned above, significantly influenced the nucleic acid binding and endosomal buffer ability of the first oligomers generated. Different topologies, including linear [134] as well as branched [49] structures, incorporating different artificial cationic building blocks were generated and evaluated [50, 132]. However, Stp (Fmoc-Stp(boc)₃-OH) was introduced into most of the later mentioned oligomers, as it can be obtained by a highly reproducible synthesis with good yield, nevertheless providing the required key features for a successful gene delivery. To achieve a more sophisticated multifunctionality, different topologies with the diamino acid lysine as a branching point were developed (cf. **Figure 3**).

Structures consisting of three Stp enriched cationic arms (3-arm) [49, 64, 133], as well as oligomers with PEG of a defined length instead of a third cationic arm (PEGylated 2-arm) were investigated (cf **Figure 3A,B**). The latter topology facilitated the introduction of a targeting domain like folic acid [135-137], as well as peptidic ligands like cmb, targeting the HGFR [64] or the GE11 peptide [138], targeting EGFR as well as other peptidic ligands [139, 140].

Also, oligomers with 4-arms [132] were built (cf. **Figure 3C**), and the effect of histidines as an endosomal buffering domain with its pK_a of 6.5, introduced between the artificial amino acids was evaluated [50]. The combined buffering capacity of alternately placed

histidines and cationic building blocks thereby led to a significantly improved buffer capacity at endosomal pH. Increased buffering enhanced cellular electrolyte influx, finally leading to endosomal burst due to osmotic swelling. In the 1990's Behr et al. already pointed out that this effect, also known as the proton sponge effect, importantly contributes to LPEI's intracellular performance [71]. Similar findings were made with highly branched HK rich peptides by Mixson et al. [105, 106], demonstrating that the proton sponge effect is also transferrable to sequence-defined vehicles, finally resulting in improved transduction efficacy *in vitro* as well as *in vivo*.

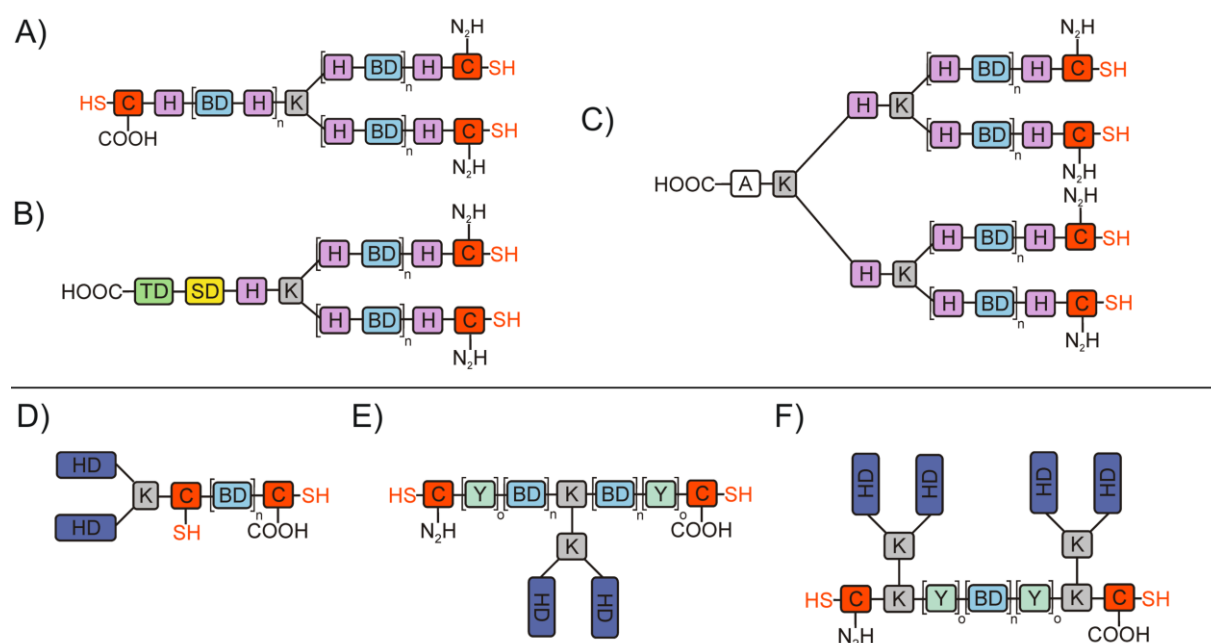


Figure 3 Common topologies of oligomers generated by SPS. A) histidine-rich 3-arm, B) histidine-rich shielded 2-arm, C) histidine-rich 4-arm. D)-F) represent fatty acid containing i-shape, T-shape and U-shapes, respectively. C represents cysteine, H histidine, K lysine and Y tyrosine. HD represents hydrophobic domains like aliphatic fatty acids or cholanic acid. TD represents a targeting domain such as peptides or small molecules targeting receptors overexpressed on tumor cell surfaces. SD represents shielding domains like PEG or (Pro-Ala-Ser) repeats. BD represents the cationic binding domain, in sequence-defined oligomers; Gtt glutaryl-triethylene tetramine, Stp succinyl tetraethylene pentamine, Gtp glutaryl-tetraethylene pentamine and Sph succinyl pentaethylene hexamine could be introduced, however, Stp was introduced mostly.

These findings then were transferred to the previously mentioned PEGylated 2-arm topology, resulting in significantly improved *in vitro* performance, not requiring the addition of the endosmolytic reagent chloroquine for successful gene delivery *in vitro* any further [64, 133, 137, 141]. In combination with a histidine-rich non-PEGylated 3-

arm oligomer these polyplexes even mediated sufficient stability for HGFR directed pDNA delivery *in vivo* [64, 65].

Within time, the existing histidine-rich 4-arm topology was further improved by the introduction of additional lysines between the cationic building blocks and the histidines, contributing to enhanced nucleic acid binding with its free ϵ - amine. This resulted in increased pDNA compaction and improved gene delivery *in vitro* as well as *in vivo* [142].

Besides the artificial amino acids and lysine all the above-mentioned topologies contained terminal cysteines. These were proven, within the evaluation of the first oligomers generated by SPS, to mediate significantly improved polyplex stability, resulting in enhanced nucleic acid delivery. An explanation for this is given due to the crosslinking abilities of cysteines by forming bioreducible disulfide bonds. Thereby, larger cationic chains exhibiting LPEI-like properties were generated within the polyplex [134]. The importance of disulfide formation and its characteristics is summarized in a review by Klein and Wagner [46], pointing out, that the general toxicity of LPEI [143] could be overcome by the assembly of shorter cationic oligomers to potent nucleic acid shuttles via disulfide crosslinking. Previous investigations on SPS derived oligolysine previously came to similar conclusions [95].

Fatty acids like oleic acid, myristic acid and other aliphatic acids were introduced to generate i-shaped, T-shaped or U-shaped structures (cf. **Figure 3D-F**) [49, 51, 52] for siRNA as well as pDNA delivery. For nucleic acids in general, but especially for siRNA delivery, these topologies mediated significantly improved gene delivery *in vitro* as well as *in vivo* [49]. So far, siRNA delivery with sequence-defined oligomers was only partially possible, as polyplexes suffered from the lack of suitable endosomal escape domains and instability *in vivo*. However, oligomers comprising fatty acids, with its highly hydrophobic aliphatic chain, mediated the required elevated polyplex stability - especially in combination with peripheral cysteines [49]. Also, oligomers equipped with fatty acids overcame the lack of endosomal escape, due to the enhanced endosomal membrane disruption facilitated by a pH-dependent lytic activity of the fatty acids at endosomal/lysosomal pH [49, 51]. Within these studies, T-shapes with central fatty acids, fulfilled the desired properties regarding nucleic acid binding, polyplex size (and particle dispersity), gene transfer efficacy and stability *in vivo* best. Therefore, this topology was further optimized by an introduction of a further hydrophobic domain, three sequentially coupled tyrosines (tyrosine trimers) at different positions of the

oligomer. In a series of experiments, it turned out, that also here, the combination of centrally placed fatty acids and terminal cysteines worked best in combination with peripheral tyrosine trimers. Nucleic acid delivery and polyplex stability could be further improved by increased hydrophobicity as well as π - π stacking between tyrosines of neighbored oligomers, resulting in extended polyplex circulation time and siRNA delivery *in vivo* [52]. The latter could be justified by an additional effect on endosomal buffering by the newly introduced tyrosines [52]. Consequently, tyrosine trimers were also incorporated into PEGylated 2-arm oligomers [137, 141], suffering from reduced polyplex stability mediated by PEGylation [133].

Recently, the introduction of cholanic acid into T-shaped oligomers mediated notable gene knockdown after siRNA delivery *in vitro* as well as *in vivo*, while not exhibiting lytic activity [111]. These oligomers also comprised a bioreducible disulfide building block to destabilize the polyplex after its uptake via GSH mediated endosomal cleavage of the central hydrophobic domain. This again resulted in enhanced siRNA release from the endosome and increased gene knockdown.

Besides the above-mentioned major topologies generated by SPS with the artificial amino acids, also comb-like oligomers were compared to linear oligomers to investigate structure-activity relationships for endosomal buffering, cellular uptake and pDNA transduction efficacy dependent on the positioning of the artificial building blocks [144].

1.1.2.2.1 Polyplex shielding

During nucleic acid delivery, an excess of the positively charged carrier is usually required for nucleic acid complexation. By mixing nucleic acid and cationic carrier, nanoparticles with positive surface potential are generated.

This positive charge offers advantages for the formed polyplexes, as it facilitates binding to negatively charged cell surfaces [145, 146] and contributes to endosomal escape after cellular uptake [147, 148].

Putting these positively charged nanoparticles into living organisms, these cationic carriers may mediate undesired interactions in the extracellular space. Positively charged polyplexes might lead to activation of the complement system, blood cells or other blood components [143, 149-151].

Polyplex surface shielding by introduction of a hydrophilic shielding domain into these artificial vectors has shown to reduce these interactions. Polyethylene glycol (PEG), with its hydrophilic properties, resulting in good solubility, is the most prominent and well-established shielding agent [152]. It has been successfully used for shielding of polyplexes in numerous instances, including solid-phase derived oligomers [59, 149, 153-158].

Due to reduced extracellular interaction of the polyplex, circulation time within the blood and biodistribution to the target tissue may greatly improve [152, 153]. However, its non-biodegradability, as well as recently reported formation of anti-PEG antibodies, gave reasons for the investigation of alternatives. Therefore, besides PEG, also poly(N-(2-hydroxypropyl)methacrylamide) (pHPMA) [142, 159, 160], hydroxyethyl starch (HES) [161] and polysarcosine [162] have been investigated as alternative hydrophilic shielding agents for polyplex shielding. Within this Ph.D. work, also a peptidic sequence composed of Pro-Ala-Ser (PAS) repeats has been examined [133] (cf. **Figure 4**).

Also, PEGylation may have negative effects on nucleic acid compaction, polyplex stability, cellular uptake and endosomal escape of nanoparticles [163-165]. The latter can be explained as cationic, PEI-like polyplexes, require a combined effect of osmotic endosomal eruption and direct phospholipid destabilization by the cationized vehicle for endosomal escape [1, 143, 166]. PEG can obviously interfere with this direct cationic membrane destabilization. These negative properties, coming along with the favorable effects of PEGylation are often referred to as the “PEG-Dilemma” [167].

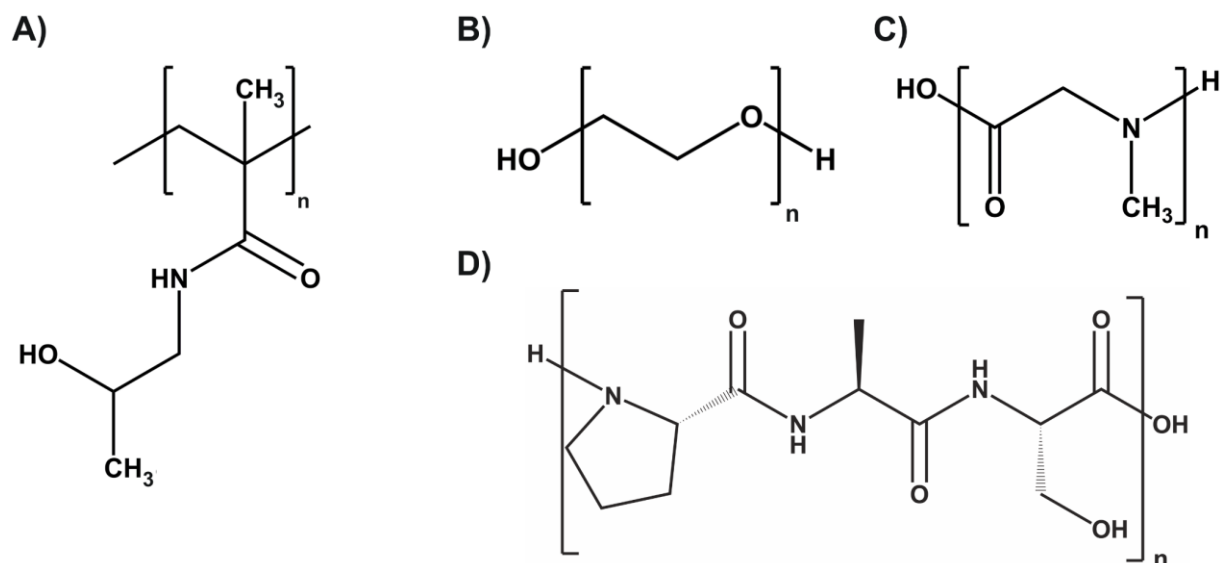


Figure 4 Chemical structures of selected reagents used for shielding. A) poly(N-(2-hydroxypropyl)methacrylamide) (HPMA), B) polyethylene glycol (PEG), C) polysarcosine, D) repetitive PAS blocks (Pro-Ala-Ser)

To overcome the disadvantages of PEGylation, several approaches of implementing PEG directly during synthesis of the cationic oligomers (referred to as pre-PEGylation) as well as after formation of PEG-free polyplexes (referred to as post-PEGylation), were investigated.

1.1.2.2.2 Approaches of pre-PEGylation, post-PEGylation

Pre-PEGylation of sequence-defined cationic vehicles was greatly improved by adaption of PEG in defined repetitions for SPS. Recently, a multifunctionalized polyplex, formed with a folate-targeted, pre-PEGylated two arm oligomer was reported to mediate siRNA delivery *in vivo* successfully [135]. However, the used PEG with exactly 24 ethylene oxide repetitions was not universally applicable for systemic delivery as pointed out by Kos et al. [64]. Here, an HGF directed pDNA polyplex composed of a pre-PEGylated, histidine-rich, 2-arm oligomer required an improved cation to PEG ratio by co-incubation of a PEG-free histidine-rich 3-arm oligomer to obtain pDNA delivery *in vivo* successfully. Recent studies [32, 133] point out that nucleic acid compaction, polyplex size and stability are greatly influenced by this ratio between the cationic domain and the hydrophilic shielding domain. These findings suggest that synthesis of sequence-defined carriers, directly incorporating PEG as a

shielding domain on the solid support, requires careful consideration of the right chain length of PEG.

In another approach, to avoid difficulties with nucleic acid compaction, non-PEGylated polyplexes were first formed and then PEG was introduced by receptor targeted PEGylation reagents via different chemical strategies. These approaches can be divided into thiol-dependent bioreducible and acid labile routes.

Post-modification of cationic vehicles with PEG via thiol chemistry was first investigated by Blessing et al. on LPEI [168]. The herein used thiol-maleimide chemistry was transferred to T-shaped oligomers containing terminal cysteines. By addition of folate [169], transferrin [170], or EGF [171] receptor targeted PEGylation reagents, polyplexes were successfully shielded and mediated tumor-specific siRNA delivery *in vitro* as well as *in vivo*.

Introducing acid labile hydrazone linked PEG onto cationic LPEI polyplexes via NHS chemistry was previously investigated by Fella et al. [156], also other pre-PEGylation of OEI polymers with acid labile PEG derivates depicted the improved endosomal release of polyplexes PEGylated with acid labile reagents [172-174].

The acid labile post-modification approach has recently been transferred onto pDNA polyplexes, composed of sequence-defined oligomers, via an acid labile AzMMan linker [142]. Here, post-modification with PEG and HPMA significantly improved polyplex stability with a fully recovered transfection efficacy *in vitro* as well as *in vivo* after cleavage in the acidic tumor environment.

1.1.2.3 Receptor targeting

Nanoparticles up to a size of 1 μm are taken up by cells via unspecific endocytosis [175, 176]. *In vivo* particles up to 400 nm can accumulate in solid tumors due to enhanced permeability and retention (EPR) effect. This is favored, as these cancers have a high vascular density and leaky blood vessels [40, 177]. However, an actively tumor-targeted nanoparticle delivery not only represents a more elegant but sometimes even decisive role in overcoming the PEG dilemma [54, 163, 167]. Targeting polyplexes towards tumors is facilitated as cancer cells often overexpress receptors, rarely occurring on vivid cells [178-182]. Incorporation of more than one targeting ligand can even enhance cellular uptake and thereby help to overcome the

previously mentioned PEG-Dilemma [183, 184]. In the following subchapters the two growth factor (EGF and HGF) receptors, targeted within different projects of this thesis are depicted in more detail.

1.1.2.3.1 HGFR targeting

The receptor tyrosine kinase HGFR/cMet is over-expressed in epithelial-derived tumors as well as in stromal and interstitial cell-derived tumors such as sarcomas [185]. When the natural ligand hepatocyte growth factor (HGF) binds to its receptor, cMet, it thereby stimulates cell motility and migration, triggers mitogenesis and morphogenesis and thus promotes oncogenesis and tumor progression. Therefore, cMet signaling has been addressed by different cancer treatment approaches: (1) Antagonists preventing binding of HGF to its receptor, (2) cytosolic active tyrosine kinase inhibitors (TKI) as well as (3) inhibitors of the downstream cascade after receptor activation have been investigated [186]. Therapeutic drug-antibody conjugates have been applied to target cMet over-expressing cancer tissues [187]. Also, *in vivo* imaging by application of HGFR specific antibodies [188-190] or two phage display-derived peptides is mentioned [181, 191]. Recently, in our laboratory, one of these peptides (KSLSRHDHIHHH) was introduced into PEGylated 2- and 4-arm oligomers, mediating HGFR specific cellular polyplex uptake as well as *in vivo* gene delivery of pCMV-Luc [64] and pCpG-hCMV-NIS [65]. The latter coding for the human NIS (Natrium Iodide Symporter) facilitated application of therapeutic ¹³¹I, leading to significantly reduced tumor growth and longed survival rate in Huh7 tumor-bearing mice.

1.1.2.3.2 EGFR targeting

The overexpression of epidermal growth factor receptor (EGFR) offers another well-established targeting strategy for the specific delivery of polyplexes [61-63, 68, 138, 192].

EGFR as a transmembrane receptor tyrosine kinase is involved in cell proliferation, survival, adhesion, migration and differentiation [193]. It is overexpressed in bladder, cervix, esophagus, head and neck, ovary, breast, endometrium, colon, lung and brain [194]. The EGFR has been a target of TKI (Erlotinib and gefitinib) reversibly inhibiting

its tyrosine kinase activity, as well as various monoclonal antibodies [180] (e.g. cetuximab and panitumumab) inhibiting ligand binding leading to enhanced receptor internalization and thereby promoted cytotoxicity [195]. EGFR represents an interesting target for the directed delivery of polyplexes. For polyplex targeting, murine EGF was successfully applied for LPEI polyplexes [55, 168, 196, 197]. Regarding the ratio of cation to targeting ligand, a short peptide offers advantages when used for oligomer targeting. Li et al. reported a phage display-derived peptide (GE11) exhibiting efficient and specific binding to the EGFR [198]. The hydrophobic GE11 peptide with a sequence of YHWYGYTPQNV I revealed less mitogenic activity compared to EGF, the original substrate of EGFR. GE11 as a targeting ligand for PEGylated LPEI conjugates has been widely explored [61, 62, 68, 192] without inducing receptor activation [62]. Mickler et al. investigated uptake mechanisms for EGF-PEG-PEI/pDNA and GE11-PEG-PEI/pDNA polyplexes, concluding that GE11 mediated uptake happens via more time consuming clathrin-mediated endocytosis, while EGF-PEG-PEI polyplexes are promptly taken up by EGFR activated endocytosis. However, the delayed, GE11 dependent uptake turned out to be as efficient as the faster EGFR activating pathway [68].

These findings led to the establishment of GE11 as a suitable targeting peptide within pre-PEGylated oligoaminoamides, used for a dual targeting approach for pDNA delivery [138] and lately as an EGFR targeted PEGylation reagent of bis-oleoyl-oligoethanamino amides [170] for siRNA delivery.

1.2 Aim of the thesis

The recent development of a solid-phase synthesis platform for the assembly of sequence-defined oligo(ethanamino)amides enables quick and easy synthesis of cationic oligomers complexing and delivering nucleic acids [131]. By introducing artificial amino acids [131], based on the diaminoethane motif of PEI which is well known for its nucleic acid binding and endosomal buffering abilities [26], differently shaped oligomers were synthesized. Into these oligomers, different functionalities, for shielding, polyplex stabilization and targeting can be introduced via SPS.

As the first aim of this thesis, the effect of different PEG lengths within 2-arm oligomers on biophysical properties and their biological performance *in vitro* as well as *in vivo* were to be investigated, incorporating pDNA as cargo. Also, an alternative to PEG, a more hydrophilic shielding motif sequentially *comprising* the natural amino acids proline-alanine-serine (PAS) was to be examined. 2-arm oligomers containing four and eight repetitions as shielding domain were to be compared in parallel to the PEGylated 2-arm oligomers equipped with 12, 24 or 48 EO units. The oligomers generated by SPS for this study should contain histidines for improved endosomal buffering [50], and cysteines for bio-reducible crosslinking via intermolecular disulfide formation. Also, a peptide (cmb), mediating HGF dependent polyplex uptake, was to be introduced in a set of oligomers.

The second aim of the thesis was to optimize pDNA delivery via post-modification of oligomers after polyplex formation. Firstly, this approach was introduced for pDNA polyplexes formed of PEI [168] and later applied for sequence-defined T-shaped oligomers for siRNA delivery [169, 170]. Within this study, targeted as well as untargeted PEGylation reagents, equipped with either 1 (monovalent) or 2 (bivalent) activated cysteines were to be synthesized. To target hepatocellular cancer, the well-established targeting peptide GE11 was to be chosen and be compared to alanine decorated PEGylation reagents. Within this *in vitro* study, like for siRNA delivery, the cysteine-rich T-shaped oligomer **454** turned out to be most promising, facilitating conjugation via disulfide exchange between oligomer and PEGylation reagent. Successful post-modification as well as EGF dependent delivery and stability of 454/pDNA polyplexes was to be investigated.

The last aim of the thesis, was to examine structure-activity relationship within T-shaped oligomers, leading to improved candidates for *in vivo* pDNA delivery of post-modified polyplexes. The generation of oligomers developed for this study was based on oligomer **454** and should address the effect of increased cationic charge (by applying 4, 6 or 8 Stp units), the stabilizing effect of peripheral tyrosines (Y₃ or Y₆) and the influence of the fatty compound either oleic acid or cholanic acid. Also, the effect of histidines within T-shaped oligomers was to be examined, by either alternating Stp and histidines or by generating oligomers with histidine blocks.

2 Materials and Methods

2.1 Materials

The solvents, reagents and buffers used for the experiments are summarized in **Table 1**, **Table 2** and **Table 3**.

Table 1 Solvents used for experimental procedures

| Solvent | CAS-No. | Supplier |
|---|-----------|--|
| Acetonitrile ^{1,11} | 75-05-8 | VWR Int. (Darmstadt, Germany) |
| Chloroform ^{2,11} | 67-66-3 | VWR Int. (Darmstadt, Germany) |
| Chloroform-d ^{3,11} | 865-49-6 | Euriso-Top (Saint-Aubin Cedex, France) |
| Deuterium oxide ³ | 7789-20-0 | Euriso-Top (Saint-Aubin Cedex, France) |
| Dichloromethane ⁴ | 75-09-2 | Bernd Kraft (Duisburg, Germany) |
| <i>N,N</i> -Dimethylformamide ⁵ | 68-12-2 | Iris Biotech (Marktredewitz, Germany) |
| Ethanol absolute ^{4,11} | 64-17-5 | VWR Int. (Darmstadt, Germany) |
| Ethyl acetate ^{7,11} | 141-78-6 | Staub & Co. (Nürnberg, Germany) |
| n-Heptane ^{8,11} | 142-82-5 | Grüssing (Filsum, Germany) |
| n-Hexane ⁸ | 110-54-3 | Brenntag (Mülheim/Ruhr, Germany) |
| Methanol ⁴ | 67-56-1 | Fisher Scientific (Schwerte, Germany) |
| Methyl- <i>tert</i> -butyl ether ⁹ | 1634-04-4 | Brenntag (Mülheim/Ruhr, Germany) |
| <i>N</i> -Methyl-2-pyrrolidone ⁵ | 872-50-4 | Iris Biotech (Marktredewitz, Germany) |
| Tetrahydrofuran ⁴ | 109-99-9 | Fisher Scientific (Schwerte, Germany) |
| Water ¹⁰ | 7732-18-5 | In-house purification |

¹ HPLC grade; ² DAB grade, distilled before use; ³ NMR grade (> 99.9 %); ⁴ analytical grade; ⁵ peptide grade; ⁶ BioReagent grade (> 99.9 %); ⁷ purum, distilled before use; ⁸ purissimum; ⁹ synthesis grade; ¹⁰ purified, deionized; ¹¹ only used within synthesis of Fmoc-Stp(boc)₃-OH

Table 2 Reagents used for experimental procedures

| Reagent | CAS-No. | Supplier |
|-------------------------------------|-------------|---------------------------------------|
| 1-Hydroxybenzotriazole hydrate | 123333-53-9 | Sigma-Aldrich (Munich, Germany) |
| 2-Chlorotriylchloride resin | 42074-68-0 | Iris Biotech (Marktredewitz, Germany) |
| 5,5'-Dithiobis(2-nitrobenzoic acid) | 69-78-3 | Sigma-Aldrich (Munich, Germany) |
| 5 β -Cholanic acid | 546-18-9 | Sigma-Aldrich (Munich, Germany) |
| Agarose NEEO Ultra | 9012-36-6 | Carl Roth (Karlsruhe, Germany) |
| Boc-L-Cys(NPys)-OH | 76880-29-0 | Bachem (Bubendorf, Switzerland) |
| Boc-L-Cys(Trt)-OH | 21947-98-8 | Iris Biotech (Marktredewitz, Germany) |
| Bromophenol blue | 115-39-9 | Sigma-Aldrich (Munich, Germany) |
| Chloroquine diphosphate | 50-63-5 | Sigma-Aldrich (Munich, Germany) |
| 4',6-Diamidin-2-phenylindol (DAPI) | 28718-90-3 | Sigma-Aldrich (Munich, Germany) |
| D-(+)-Glucose monohydrate | 14431-43-7 | Merck Millipore (Darmstadt, Germany) |
| DBU | 6674-22-2 | Sigma-Aldrich (Munich, Germany) |
| Dde-L-Lys(Fmoc)-OH | 156648-40-7 | Iris Biotech (Marktredewitz, Germany) |
| EDTA disodium salt dihydrate | 6381-92-6 | Sigma-Aldrich (Munich, Germany) |

| Reagent | CAS-No. | Supplier |
|--|-------------|--|
| Ethidium bromide | 1239-45-8 | Sigma-Aldrich (Munich, Germany) |
| Fmoc-L-Asn(Trt)-OH | 132388-59-1 | Iris Biotech (Marktredewitz, Germany) |
| Fmoc-L-Arg(Pbf)-OH | 154445-77-9 | Iris Biotech (Marktredewitz, Germany) |
| Fmoc-L-Cys(Trt)-OH | 103213-32-7 | Iris Biotech (Marktredewitz, Germany) |
| Fmoc-L-Gln(Trt)-OH | 132327-80-1 | Iris Biotech (Marktredewitz, Germany) |
| Fmoc-L-Gly-OH | 29022-11-5 | Iris Biotech (Marktredewitz, Germany) |
| Fmoc-L-His(Trt)-OH | 109425-51-6 | Iris Biotech (Marktredewitz, Germany) |
| Fmoc-L-Ile-OH | 71989-23-6 | Iris Biotech (Marktredewitz, Germany) |
| Fmoc-L-Leu-OH | 35661-60-0 | Iris Biotech (Marktredewitz, Germany) |
| Fmoc-L-Lys(Boc)-OH | 71989-26-9 | Iris Biotech (Marktredewitz, Germany) |
| Fmoc-L-Lys(Fmoc)-OH | 78081-87-5 | Iris Biotech (Marktredewitz, Germany) |
| Fmoc-L-Lys(Dde)-OH | 204777-78-6 | Iris Biotech (Marktredewitz, Germany) |
| Fmoc-L-Pro-OH | 71989-31-6 | Iris Biotech (Marktredewitz, Germany) |
| Fmoc-L-Ser(tBu)-OH | 71989-33-8 | Iris Biotech (Marktredewitz, Germany) |
| Fmoc-L-Thr-OH | 73731-37-0 | Iris Biotech (Marktredewitz, Germany) |
| Fmoc-L-Trp(Boc)-OH | 43824-78-6 | Iris Biotech (Marktredewitz, Germany) |
| Fmoc-L-Tyr(tBu)-OH | 71989-38-3 | Iris Biotech (Marktredewitz, Germany) |
| Fmoc-L-Val-OH | 68858-20-8 | Iris Biotech (Marktredewitz, Germany) |
| Fmoc- <i>N</i> -amido-dPEG ₁₂ -acid | 756526-01-9 | Quanta Biodesign (Powell, Ohio, USA) |
| Fmoc- <i>N</i> -amido-dPEG ₂₄ -acid | 756526-01-9 | Quanta Biodesign (Powell, Ohio, USA) |
| Fmoc-OSu | 82911-69-1 | Iris Biotech (Marktredewitz, Germany) |
| Fmoc-STODTA-OH | 172089-14-4 | Sigma-Aldrich (Munich, Germany) |
| Fmoc-Stp(Boc ₃)-OH | - | In-house synthesis [131, 199] |
| GelRed | - | Biotium Inc. (Hayward, CA, USA) |
| HBTU | 94790-37-1 | Multisynthetech (Witten, Germany) |
| Heparin sodium 5000 I.E./mL | 9041-08-1 | ratiopharm GmbH (Ulm, Germany) |
| HEPES | 7365-45-9 | Biomol (Hamburg, Germany) |
| Hydrazine monohydrate | 7803-57-8 | Merck Millipore (Darmstadt, Germany) |
| Hydrochloric acid solution (1 M) | 7647-01-0 | Sigma-Aldrich (Munich, Germany) |
| LPEI | 9002-98-6 | In-house synthesis [197] |
| MTT | 298-93-1 | Sigma-Aldrich (Munich, Germany) |
| <i>N,N</i> -Diisopropylethylamine | 7087-68-5 | Iris Biotech (Marktredewitz, Germany) |
| Ninhydrin | 485-47-2 | Sigma-Aldrich (Munich, Germany) |
| Oleic acid | 112-80-1 | Sigma-Aldrich (Munich, Germany) |
| Phenol | 108-95-2 | Sigma-Aldrich (Munich, Germany) |
| Piperidine | 110-89-4 | Iris Biotech (Marktredewitz, Germany) |
| Potassium cyanide | 151-50-8 | Sigma-Aldrich (Munich, Germany) |
| Propodium Iodide (PI) | 25535-16-4 | Sigma-Aldrich (Munich, Germany) |
| PyBOP® | 128625-52-5 | Multisynthetech GmbH (Witten, Germany) |
| Sephadex® G-10 | 9050-68-4 | GE Healthcare (Freiburg, Germany) |
| Sodium hydroxide (anhydrous) | 1310-73-2 | Sigma-Aldrich (Munich, Germany) |
| Succinic anhydride | 108-30-5 | Sigma-Aldrich (Munich, Germany) |
| Tetraethylene pentamine 5*HCl | 4961-41-5 | Sigma-Aldrich (Munich, Germany) |
| Triethylamine | 121-44-8 | Sigma-Aldrich (Munich, Germany) |
| Trifluoroacetic acid | 76-05-1 | Iris Biotech (Marktredewitz, Germany) |
| Triisopropylsilane | 6485-79-6 | Sigma-Aldrich (Munich, Germany) |
| Triton™ X-100 | 9002-93-1 | Sigma-Aldrich (Munich, Germany) |
| Trizma® base | 77-86-1 | Sigma-Aldrich (Munich, Germany) |

Table 3 Buffers used for experimental procedures

| Buffer | Composition |
|--------------------------------|--|
| 10 mM HCl SEC solvent | 693 mL water, 300 mL acetonitrile, 7 mL 1M HCl solution |
| Electrophoresis loading buffer | 6 mL glycerine, 1.2 mL 0.5 M EDTA solution (pH 8.0), 2.8 mL H ₂ O, 20 mg bromophenol blue |
| Ellman buffer | 0.1 M sodium phosphate buffer (pH 8.0), 1 mM EDTA |
| HBG | 20 mM HEPES, 5 % glucose, pH 7.4 |
| TBE buffer | 89 mM Trizma® base, 89 mM boric acid, 2 mM EDTA-Na ₂ |

Citrate-buffered erythrocytes for erythrocyte adhesion assays were kindly provided by Klinikum der Universität München, Großhadern (Munich, Germany).

2.1.1 Equipment for solid-phase synthesis

Automated parallel synthesis or synthesis supported with microwave irradiation was carried out using a Biotage Syro Wave (Biotage, Uppsala, Sweden) peptide synthesizer. Disposable polypropylene (PP) syringe microreactors with the volume sizes 2 mL, 5 mL, and 10 mL were purchased from Multisyntech (Witten, Germany). It was conducted with polytetrafluoroethylene (PTFE) filters. The recommended size of the reactors was chosen according to the amount of resin. For manual solid-phase synthesis microreactors with polyethylene filters (Multisyntech, Witten, Germany) were used. Reactions were carried out under steady shaking with an overhead shaker.

2.1.2 Plasmid DNA

The plasmid pCMVLuc (encoding for firefly luciferase under control of the CMV promoter) was purchased from Plasmid Factory (Bielefeld, Germany). The concentration of nucleic acid solutions was determined photometrically using an Eppendorf BioPhotometer (Eppendorf, Hamburg, Germany). Cy5-labeled nucleic acids were produced with a Cy5-labelling kit obtained from Mirus Bio (Madison, WI, USA).

The plasmid pCpG-hCMV-NIS (human NIS plasmid DNA driven by the human elongation factor 1 α promoter and human cytomegalovirus enhancer element) was prepared by Plasmid Factory (Bielefeld, Germany) as of a concentration of 1 mg/mL.

2.1.3 Cell culture

Cell culture work was carried out by Sarah Urnauer (Klinikum der Universität München, AG Spitzweg) and Ana Krhac Levacic, (Pharmaceutical Biotechnology, LMU). Cell culture media, antibiotics and fetal bovine serum (FBS) were purchased from Invitrogen (Karlsruhe, Germany) or Sigma Aldrich (Munich, Germany). The individual media used for the different cell cultures are summarized in **Table 4**. All media were supplemented with 10 % FBS, 4 mM stable glutamine, 100 U/mL penicillin and 100 µg/mL streptomycin. Cell lines were cultured at 37 °C and 5 % CO₂ in an incubator with a relative humidity of 95 %.

Exponentially growing cells were detached from the culture flasks using Millipore water, supplemented with 0.05 % trypsin-EDTA (Invitrogen, Karlsruhe, Germany), followed by resuspension in the required culture media. Cell suspensions were seeded at the desired density for each experiment. Luciferase cell culture lysis buffer and D-luciferin sodium salt were purchased from Promega (Mannheim, Germany).

Table 4 Overview of the used cell lines and corresponding culture media

| Cell line | Description | Medium |
|-----------|--|--------------------|
| Neuro2A | Mouse neuroblastoma cells | DMEM, low glucose |
| DU145 | Human prostate cancer cells | RPMI-1640 |
| Huh7 | Human hepatocellular carcinoma cells | DMEM, low glucose |
| MCF7 | Human breast cancer cells | DMEM, high glucose |
| FTC-133 | Human follicular thyroid carcinoma cells | DMEM/F12 (50:50) |

2.2 Methods

2.2.1 Synthesis of oligomers and PEGylation reagents via solid phase synthesis (SPS)

2.2.1.1 General procedure for solid phase synthesis (SPS)

2.2.1.1.1 Loading of a 2-chlorotrityl chloride resin with an Fmoc protected amino acid

After swelling 750 mg of a 2-chlorotrityl chloride resin (1.2 mmol chloride) in dry DCM for 10 min, the first Fmoc protected amino acid (T-shape: 0.3 eq. Fmoc-L-Cys(Trt)-OH; 3-arm: 0.3 eq. Fmoc-L-Cys(Trt)-OH or Fmoc-L-Lys(Dde)-OH; untargeted PEG/PAS shielded 2-arm: 0.4 eq. Dde-L-Lys(fmoc)-OH; targeted 2-arm: 0.2 eq. Fmoc-L-Lys(Dde)-OH (cmb) or 0.3 eq. Fmoc-L-Ile-OH (GE11); GE11 targeted PEGylation reagents: 0.3 eq. Fmoc-L-Ile-OH and a threefold molar excess of DIPEA over Fmoc protected amino acid were added to the resin for 1 h. The reaction solvent was drained and a mixture of DCM/MeOH/DIPEA (80/15/5) was added for at least 30 min. After the removal of the reaction mixture, the resin was washed with DMF and DCM 5 times each.

About 30 mg of the resin were removed and dried to determine the loading of the resin. Therefore, an exact amount of resin was treated with 1 mL deprotection solution (20 % piperidine in DMF) for 1 h. Afterwards, the solution was diluted and absorption was measured at 301 nm. The loading was then calculated according to the equation: resin load [mmol/g] = $(A \cdot 1000) / (m [\text{mg}] \cdot 7800 \cdot \text{df})$ with df as dilution factor.

The resin was treated twice with 20 % piperidine in DMF and twice with 20 % piperidine and 2 % DBU in DMF to remove the Fmoc protection group. Reaction progress was monitored by Kaiser test (cf. 2.2.1.1.3). Afterwards, the resin was washed with DMF, DCM and n-hexane and dried in vacuo.

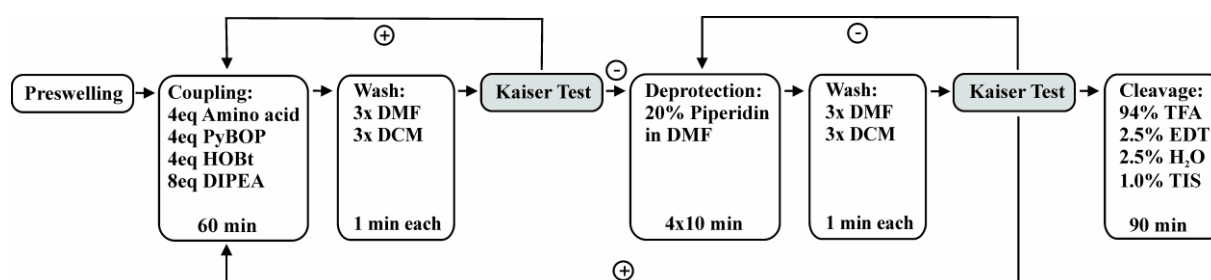
2.2.1.1.2 Procedure of a manually conducted solid phase synthesis

After amino acid (AA) loading and Fmoc removal (cf. 2.2.1.1.1), the synthesis was continued in a defined matter as a repetitive cycle to obtain the desired oligomer or PEGylation reagent. First the deprotected peptide resin is preswelled in 10 mL/g resin DCM. Then coupling of the Fmoc protected amino acids is performed with a fourfold

excess (based on the quantity of free amines) whilst an identical excess of HOBt and PyBOP was used for preactivation. DIPEA was added with an eightfold excess (also related to free amines). HOBt and PyBOP were dissolved in 5 mL of DMF/g of resin and the Fmoc protected amino acid was dissolved in 5 mL of DCM/g of resin. The corresponding amount of DIPEA was added, the solutions are mixed for preactivation and added to the resin. Routinely coupling time was chosen as 1 h, using an overhead shaker for steady shaking. After each coupling step (as well as after each step of deprotection), three washes with DMF and with DCM (10 mL/g of resin) were carried out. 20 % (v/v) piperidine/DMF was applied for Fmoc-removal four times per 10 min by default (10 mL/g resin). Coupling and deprotection were verified by testing for free amines qualitatively using Kaiser test (cf. **2.2.1.1.3**). If the result was unsatisfying the previous coupling or deprotection step was repeated. After a completed cycle (coupling and deprotection, with washing steps in between), the procedure was repeated until the desired oligomer is obtained. After the last coupling, the resin was dried and cleavage conducted (cf. **2.2.1.2**). Synthesis conditions for manual synthesis are summarized in **Table 5** and synthesis is displayed schematically in **Scheme 2**

Table 5 General steps of a manually conducted synthesis cycle

| Step | Description | Solvent | Volume | Time |
|------|-------------------|---------------------|---------------|----------------|
| 1 | Coupling | DCM/DMF 50/50 | 10 mL/g resin | 60 min |
| 2 | Wash | DMF and DCM | 10 mL/g resin | 3 x 1 min each |
| 3 | Kaiser test | - | - | - |
| 4 | Fmoc deprotection | 20 % piperidine/DMF | 10 mL/g resin | 4 x 10 min |
| 5 | Wash | DMF and DCM | 10 mL/g resin | 3 x 1 min each |
| 6 | Kaiser test | - | - | - |



Scheme 2 Illustration of a manually conducted SPS cycle

2.2.1.1.3 Kaiser test

Free amines of deprotected amino acids on the resin were determined qualitatively by the Kaiser test [130]. Therefore, a small sample of DCM washed resin was transferred into an Eppendorf reaction tube. One drop of each 80 % phenol in EtOH (w/v), 5 % ninhydrin in EtOH (w/v) and 20 μ M potassium cyanide (KCN) in pyridine (mixture of 1 mL aqueous 0.001 M KCN solution and 49 mL pyridine) were added. The tube was incubated at 99 °C for 4 min under shaking. A deep blue color indicated the presence of free amines.

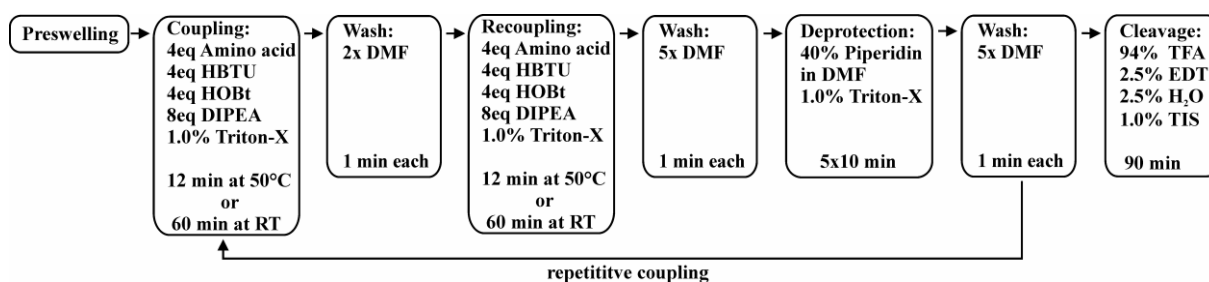
2.2.1.1.4 Procedure of an automated solid phase synthesis

After amino acid loading and Fmoc removal (cf. 2.2.1.1.1), automated synthesis also follows a repetitive cycle of coupling, washing, deprotection, washing after the deprotected resin is preswelled. Nevertheless, compared to manual synthesis, several steps required optimization. Firstly, during automated synthesis, all washing steps were conducted with the system liquid DMF (5 \times 1 min). Also, within automated synthesis, special reactors had to be used (cf. 2.1.1) and DCM, as a volatile solvent, was replaced by NMP. During coupling, PyBOP[®] was replaced by HBTU, providing improved stability of the activation reagent in solution within syntheses. Since the automated synthesis does not offer the opportunity to separate resin samples for the Kaiser test, improved coupling conditions and extended deprotection steps were applied. Briefly, during automated synthesis, coupling steps were conducted in double (tech. double couplings) prior to washing and Fmoc removal due to the lack of control. Within microwave assisted synthesis, thus the coupling solution was applied twice for 12°min at 50 °C and during automated parallel synthesis twice for 60 min at RT. Reagents were prepared as followed, calculated per AA on the resin: 4 eq. of amino acid, dissolved together with 4 eq. of HOBt in NMP, 4 eq. of activation reagent (HBTU) dissolved in DMF, and 8 eq. of DIPEA in NMP were set up in separate bottles. Also, the amino acid solutions were supplemented with Triton X-100, leading to a final concentration of 1 % (v/v), when applied to the resin. Double coupling of Boc-L-Cys(Trt)-OH was conducted at room temperature for 60 min in all synthesis to avoid racematization. Deprotection was carried out with 40 % piperidine/DMF, supplemented with 1 % Triton X-100, for 5 \times 10 min.

Synthesis conditions for automated synthesis are summarized in **Table 6** and are schematically displayed in **Scheme 3**.

Table 6 General steps of an automated synthesis cycle using the Biotage Syro Wave synthesizer

| Step | Description | Solvent | Volume | Time |
|------|-------------------|---------------------|--------------|---------------------------------------|
| 1 | Coupling | NMP/DMF | 5 mL/g resin | 60 min at RT or 12 min at 50 °C |
| | Wash | DMF | 8 mL/g resin | 2 x 1 min |
| | Recoupling | NMP/DMF | 5 mL/g resin | 60 min at RT or 12 min at 50 °C |
| 2 | Wash | DMF | 8 mL/g resin | 5 x 1 min |
| 3 | Fmoc deprotection | 40 % piperidine/DMF | 7 mL/g resin | 5 x 10 min |
| 4 | Wash | DMF | 8 mL/g resin | 5 x 1 min |



Scheme 3 Illustration of an automated synthesis using the Biotage Syro Wave synthesizer

2.2.1.2 Cleavage of oligomers and reagents

2.2.1.2.1 General cleavage of oligomers

This protocol was applied for all 2-arm, 3-arm oligomers and T-shaped oligomers containing cholanic acid. Oligomers were cleaved off the resin by incubation with TFA–EDT–H₂O–TIS (94 : 2.5 : 2.5 : 1.0; 10 mL g⁻¹ resin) for 90 min. The cleavage solution was concentrated by flushing nitrogen and oligomers were precipitated in 50 mL of pre-cooled MTBE–n-hexane (1 : 1). All oligomers were purified by size exclusion chromatography (SEC) using an Äkta purifier system (GE Healthcare Bio-Sciences AB, Uppsala, Sweden), a Sephadex G-10 column and 10 mM hydrochloric acid

solution–acetonitrile (7 : 3) as solvent. The relevant fractions were lyophilized, obtaining HCl salts of all oligomers.

2.2.1.2.2 Cleavage of oligomers containing oleic acid

The cleavage of t-shape oligomers containing oleic acid off the resin require an optimized protocol [200]. Therefore a mixture of TFA–EDT–H₂O–TIS (94 : 2.5 : 2.5 : 1.0; 10 mL g⁻¹ resin cooled to 4 °C prior to addition) was applied for 30 min, followed by immediate precipitation in 50 mL of pre-cooled MTBE–n-hexane (1 : 1). The oleic acid containing oligomers were then purified by SEC without further delay. A Äkta purifier system (GE Healthcare Bio-Sciences AB, Uppsala, Sweden), a Sephadex G-10 column and 10 mM hydrochloric acid solution–acetonitrile (7 : 3) as solvent were used. The relevant fractions were lyophilized, obtaining HCl salts of all oligomers.

2.2.1.2.3 Cleavage of NPys containing PEGylation reagents

The cleavage of the structures off the resin was performed by incubating the dried resin with TFA–TIS–H₂O (95 : 2.5 : 2.5) for 90 min followed by immediate precipitation in 50 mL of pre-cooled MTBE–n-hexane (1 : 1). Purification was conducted with SEC, using a Äkta purifier system (GE Healthcare Bio-Sciences AB, Uppsala, Sweden), a Sephadex G-10 column and 10 mM hydrochloric acid solution–acetonitrile (7 : 3) as solvent. The relevant fractions were lyophilized, obtaining HCl salts of all PEGylation reagents.

2.2.1.3 Synthesis of oligomers

Unless mentioned otherwise, oligomers were synthesized using a 2-chlorotrityl resin preloaded with the first C-terminal amino acid of the respective topology (cf. **2.2.1.1.1**) as solid support. All sequences and topologies of oligomers can be found in **Table 21**.

2.2.1.3.1 Synthesis of untargeted, PEGylated 2-arm oligomers

(Oligomers **1088, 1091, 1120**)

PEGylated two-arm oligomers with a C-terminal lysine, exhibiting a positive net charge and serving as a substitute for the targeting ligand cmb, were synthesized in 0.02 mmol

scale on a 2-chlorotrityl chloride resin, preloaded with Dde-L-Lys(Fmoc)-OH. Fmoc was removed, as described in **2.2.1.1.1**, prior to synthesis. To reduce costs, coupling of Fmoc-N-amido-dPEG_{12/24}-OH was carried out manually by adding the reagents dissolved in NMP/DMF and applying microwave irradiation for 50 °C for 12 min. After washing five times for one min, a Kaiser test has been performed. The peptides were placed separately into the automated peptide synthesizer, starting with a deprotection step. From now on synthesis was conducted with microwave irradiation as described in **2.2.1.1.4**. Fmoc-L-His(Trt)-OH, Fmoc-L-Lys(Fmoc)-OH, Fmoc-L-His(Trt)-OH, Fmoc-L-Lys(Fmoc)-OH, Fmoc-Stp(Boc)₃-OH [131, 199] and Boc-L-Cys(Trt)-OH were attached in the order as described in **Table 21**. Prior to cleavage, the Dde group protecting the α - amine of the C-terminal lysine was removed by 15 cycles of 4 % hydrazine in DMF (*v/v*) for 3 min each. After a final washing step, the resins, now containing the completed oligomers, were dried and cleavage was conducted as described in 2.2.1.2.1.

2.2.1.3.2 Synthesis of untargeted 2-arm oligomers containing Pro-Ala-Ser repeats

(Oligomers **1094**, **1097**)

Two-arm oligomers containing Pro-Ala-Ser repeats with a C-terminal lysine, exhibiting a positive net charge and serving as a substitute for the targeting ligand cmb, were synthesized in 0.02 mmol scale on a 2-chlorotrityl chloride resin, preloaded with Dde-L-Lys(Fmoc)-OH. Fmoc was removed, as described in **2.2.1.1.1**, prior to synthesis. Fmoc-Ser(*t*Bu)-OH, Fmoc-Ala-OH and Fmoc-Pro-OH (from now on called PAS) were attached sequentially, with four or eight triple sequence repeats (PAS₄, PAS₈) by automated, microwave assisted synthesis (cf. **2.2.1.1.4**). After an analytical cleavage, MALDI-TOF mass spectroscopy was carried out, verifying the correct sequence. Next, the peptides were placed separately into the automated peptide synthesizer, starting with a deprotection step. From now on synthesis was conducted with microwave irradiation as described in **2.2.1.1.4**. Fmoc-L-His(Trt)-OH, Fmoc-L-Lys(Fmoc)-OH, Fmoc-Stp(Boc)₃-OH [131, 199] and Boc-L-Cys(Trt)-OH were coupled in the order as described in **Table 21**. Prior to cleavage, the Dde group protecting the α - amine of the C-terminal lysine was removed by 15 cycles of 4 % hydrazine in DMF (*v/v*) for 3 min

each. After a final washing step, the resins, now containing the completed oligomers, were dried and cleavage was conducted as described in **2.2.1.2.1**.

2.2.1.3.3 Synthesis of untargeted 3-arm oligomer

(Oligomer **689**)

In the case of non-shielded three-arm oligomer, a Cys(Trt)-OH preloaded 2-chlorotrityl resin was used and automated microwave-assisted synthesis (cf. **2.2.1.1.4**) was carried out to obtain the sequence mentioned in **Table 21**.

2.2.1.3.4 Synthesis of cmb containing two and 3-arm oligomers

(Oligomers **442, 694, 901, 996, 1000, 1078**)

For hepatocyte growth factor (HGF) receptor/cMet targeted delivery, oligomers containing a cMet binding peptide (cmb) were synthesized. Chlorotrityl chloride resin preloaded with Fmoc-Lys(Dde)-OH was used for the synthesis of 2 x 0.1 mmol. After Fmoc removal with 5 times 20% piperidine, and a Kaiser test for verification of the deprotection, the cmb ligand (KSLSRHDHIIHHH) was synthesized with a Syro Wave (Biotage, Uppsala, Sweden), following the synthesis protocol as previously described in **2.2.1.1.4**. The terminal lysine was bocylated with 10 eq. Di-tert-butylidicarbonate and 20 eq DIPEA in NMP for 60 min to terminate synthesis at this arm of the lysine. After this coupling, an analytical cleavage (cf. **2.2.1.2.1**) of a small fraction for MALDI-TOF mass spectroscopy was done to verify the identity of the peptide (cf. 6.5.2).

Then Dde deprotection at the side chain was conducted with 15 cycles of 4 % hydrazine in DMF (v/v) for 3 min each. For the cmb targeted oligomers containing PEG₁₂, PEG₂₄, and PEG₄₈ either Fmoc-N-amido-dPEG₁₂-OH or Fmoc-N-amido-dPEG₂₄-OH was attached onto the previously freed ε- amine of the C-terminal lysine as described previously in **2.2.1.3.1**. PAS₄ or PAS₈ was attached onto the previously freed ε- amine of the C-terminal lysine by successive coupling of (Fmoc-L-Ser(tBu)-OH, Fmoc-L-Ala-OH and Fmoc-L-Pro-OH) repetitively four or eight times. Again, the Syro Wave, applying microwave irradiation (cf. **2.2.1.1.4**) was chosen due to complexity of the sequence. Afterwards, all resins were placed separately into the

microwave cavity of the Syro Wave automated synthesizer and the cationic backbone again was built with Fmoc-L-His(Trt)-OH, Fmoc-L-Lys(Fmoc)-OH, Fmoc-Stp(Boc)₃-OH performing double couplings. The sequence then was terminated with a double coupling of Boc-L-Cys(Trt)-OH for 1 h per coupling at room temperature. Instead of a hydrophilic shielding block, cmb-3-arm was built of three cationic arms containing alternating Fmoc-L-His(Trt)-OH, Fmoc-Stp(Boc)₃-OH, Fmoc-L-Lys(Fmoc)-OH, and was terminated by coupling Boc-L-Cys(Trt)-OH at room temperature. Synthesis followed the same coupling procedure as of the 3-arm (**689**), with the only difference that the C-terminal arm was not started with a Fmoc-L-Cys(Trt)-OH, but was attached to the H₂N-cmb-K, previously synthesized on the solid support. The exact sequences can be found in **Table 21** and deprotected oligomers were obtained after cleavage, following the standard protocol (cf. **2.2.1.2.1**).

2.2.1.3.5 Synthesis of PEGylated 2-arm oligomers with GE11 ligand and alanine (Oligomers **835** and **440**)

Synthesis of GE11 targeting peptide (YHWYGYTPQNVI) was carried out on a resin preloaded with Fmoc-L-Ile-OH. The peptide sequence was assembled with an automated Syro Wave peptide synthesizer equipped with a microwave cavity (cf. **2.2.1.1.4**) in 0.1 mmol scale size. After the last coupling cycle, an analytical cleavage (cf. **2.2.1.2.1**) of a small fraction for MALDI-TOF mass spectroscopy and HPLC was done to verify identity and purity of the peptide.

Then oligomer synthesis was carried out. In case of oligomer **440** 0.02 mmol of a commercially available Wang resin, preloaded with Fmoc-L-Ala-OH low-loaded (LL) was deprotected as described in **2.2.1.1.1**. In case of **835**, 0.02mmol of the GE11 peptide loaded resin (prepared as described above) was used. As coupling of Fmoc-N-amido-dPEG₂₄-OH represents a crucial step in synthesis, this step was conducted manually, and successful coupling and deprotection was monitored by Kaiser test (cf. **2.2.1.1.3**). Coupling was performed manually for 1 h under steady shaking with 4 eq of PyBOP, 8 eq of DIPEA, 4 eq of HOBt and 4 eq of Fmoc-N-amido-dPEG₂₄-acid dissolved in 50:50 (v/v) of DCM/DMF. Deprotection was performed as described before by addition of 40% piperidine in DMF (v/v) for 5 × 10 min (cf. **2.2.1.1.2**). Then both reactors were placed in the automated Syro Wave peptide synthesizer and cationic

backbones were synthesized in parallel. Reagents were prepared as for synthesis of GE11 and double couplings were performed at room temperature for 1 h each. First Fmoc-L-His(Trt)-OH, followed by Fmoc-L-Lys(Fmoc)-OH, was attached. Fmoc-L-His(Trt) and our novel building block Fmoc-Stp(boc)₃-OH were attached alternately four times, leading to five histidines and four Stp units. Synthesis was terminated by coupling of Boc-L-Cys(Trt)-OH. The exact sequences can be found in **Table 21** and deprotected oligomers were obtained after cleavage, following the standard protocol (cf. **2.2.1.2.1**).

2.2.1.3.6 Synthesis of the T-shaped lipo-oligomer for post-modification

(Oligomer **454**)

Oligomer **454** was synthesized on a 2-chlorotrityl chloride resin preloaded with Fmoc-L-Cys(Trt)-OH. The resin was placed in the microwave cavity of the Syro Wave peptide synthesizer. The cationic backbone, was attached using the protocol described in 2.2.1.1.4. First Fmoc-L-Tyr(tBu)-OH was coupled three times, then the artificial amino acid Fmoc-Stp(boc)₃-OH was coupled twice. Fmoc-L-Lys(Dde)-OH served as a mirror axis so again two Fmoc-Stp(boc)₃-OH and three times Fmoc-L-Tyr(tBu)-OH were coupled. Coupling of Boc-L-Cys(Trt)-OH at room temperature for 2 x 1 h terminated the cationic backbone. To introduce the hydrophobic domains, Dde removal was conducted with 4 % hydrazine in DMF (v/v) for 15 cycles lasting 3 min each. Then Fmoc-L-Lys(Fmoc)-OH was coupled for symmetrical branching prior to attaching oleic acid on both arms. The deprotected oligomer was obtained after cleavage, following the protocol for oleic acids (cf. **2.2.1.2.2**).

2.2.1.3.7 Synthesis of improved T-shaped lipo-oligomers

(Oligomers **1021-1024**, **1026**, **1173-1180**)

All oligomers were synthesized on a 2-chlorotrityl chloride resin preloaded with Fmoc-L-Cys(Trt)-OH. After Fmoc deprotection, the cationic backbones C-Y₃-Stp₂-K(Dde)-Stp₂-Y₃-C (**1021**), C-Y₆-Stp₂-K(Dde)-Stp₂-Y₆-C (**1173**, **1174**), C-Y₃-Stp₃-K(Dde)-Stp₃-Y₃-C (**1022**, **1023**), C-Y₃-Stp₄-K(Dde)-Stp₄-Y₃-C (**1175**, **1176**), C-Y₃-(H-Stp)₂-H-K(Dde)-H-(Stp-H)₂-Y₃-C (**1024**), C-Y₃-H₃-Stp₂-K(Dde)-Stp₂-H₃-Y₃-C (**1026**) were

synthesized in a scale size of 0.04 mmol each, within the parallel block of the Syro Wave automated synthesizer. Double couplings at room temperature, following the protocol described in **2.2.1.1.2**, were conducted to obtain the cationic backbones. Small amounts of resin were separated and cleaved of the resin for analysis with MALDI-TOF mass spectroscopy. For synthesis of the more complex backbones C-Y₆-Stp₄-K(Dde)-Stp₄-Y₆-C (**1177, 1178**), C-Y₃-(H-Stp)₄-H-K(Dde)-H-(Stp-H)₄-Y₃-C (**1179**) and C-Y₃-H₅-Stp₄-K(Dde)-Stp₄-H₅-Y₃-C (**1180**) 0.04 mmol of a deprotected 2-chlorotrityl chloride resin, preloaded with Fmoc-L-Cys(Trt)-OH, were each placed separately into the microwave cavity of the Syro wave synthesizer and double couplings were performed according to **2.2.1.1.4**. Also here, small amounts of resin were separated and the backbones were cleaved of the resin for analysis of MALDI-TOF mass spectroscopy.

Then all reactors were placed in the parallel block of the Syro Wave peptide synthesizer and automated Dde removal was conducted with 4 % hydrazine in DMF (v/v) for 15 cycles lasting 3 min each. Next, Fmoc-L-Lys(Fmoc)-OH was coupled for symmetrical branching at room temperature applying double couplings and Fmoc was removed with 40 % piperidine in DMF (v/v), followed by a Kaiser test (cf. **2.2.1.1.3**) after washing each resin with DMF for 5 × 1 min. At this point, resins were split into two. Reactors for manual synthesis (containing 0.02 mmol each) were chosen and either oleic acid or cholanic acid (4 eq. per free amine) was attached, applying conditions for manual coupling (cf. **2.2.1.1.2**). A negative Kaiser test verified successful coupling and termination of the syntheses. The resins were dried and either general cleavage conditions for cholanic acid containing oligomers (**1021, 1023, 1174, 1176, 1178**) or optimized cleavage conditions for oleic acid containing oligomers (**1022, 1024, 1026, 1173, 1175, 1177, 1179, 1180**), followed by SEC, were applied. For more details see **2.2.1.2.1** or **2.2.1.2.2** respectively.

2.2.1.4 Synthesis of PEGylation reagents for polyplex post-modification

All sequences of PEGylation reagents can be found in **Table 22**, unless stated otherwise. Coupling steps were carried out manually using 4 eq. Fmoc-amino acid, 4 eq. HOBt, 4 eq. PyBOP[®] and 8 eq. DIPEA (10 mL g⁻¹ resin) per free amine for 60 min at room temperature under steady shaking. General steps within manual synthesis are summarized in **Table 5** and explained in detail in **2.2.1.1.2**.

2.2.1.4.1 Synthesis of monovalent PEGylation reagents.

Monovalent PEGylation reagents were either synthesized on a deprotected, commercially available, preloaded Ala-Wang resin (for the Ala control reagent) or were attached to GE11 previously assembled on the solid support as described above (cf. **2.2.1.3.5**). Reaction scale size was chosen as 0.02 mmol. First Fmoc-*N*-amido-dPEG₂₄-acid was coupled onto both resins followed by Boc-L-Cys(Npys). The resins were dried under high vacuum and then cleavage was conducted following the cleavage protocol for NPys containing PEGylation reagents (cf. **2.2.1.2.3**).

2.2.1.4.2 Synthesis of bivalent PEGylation reagents

As described for the monovalent PEGylation reagents, either a commercially available, preloaded Ala-Wang resin (for the Ala control reagent) or a 2-chlorotriethyl chloride resin, containing the previously synthesized GE11 ligand was used. Scale size was here chosen between 0.02 and 0.035 mmol. First Fmoc-*N*-amido-dPEG₂₄-acid was coupled onto both resins followed by Fmoc-L-Lys(Fmoc)-OH was attached onto the resins manually. After Fmoc deprotection, STOTDA was introduced as a short spacer before terminating the sequence by coupling of Boc-L-Cys(NPys)-OH. Finally, resins were dried under high vacuum and cleavage was conducted following the cleavage protocol for NPys containing PEGylation reagents (cf. **2.2.1.2.3**).

2.2.2 pDNA polyplex formation

Nucleic acid and oligomers were dissolved at concentrated stock solutions in water, and diluted with 20 mM HEPES buffered 5 % glucose pH 7.4 (HBG). pDNA and oligomer were prepared in separate tubes. According to the indicated nitrogen/phosphate (N/P) ratio, oligomer solutions were prepared and the same volume of diluted pDNA was added to the oligomer. Only protonatable nitrogens were considered in the N/P calculations (cf. **Table 21**). The mixture was rapidly pipetted 15 × and incubated for at least 30 min at room temperature (RT).

2.2.2.1 Post-modification with PEGylation reagents

For post-modifying pDNA polyplexes with mono- or bivalent PEGylation reagents, pDNA and oligomers were mixed at N/P 12 (unless stated elsewhere) and incubated for 30 min to form the core polyplex. Then PEGylation reagents were added, the polyplex solution was gently mixed and further incubated for 15 min. Amounts of PEGylation reagents were calculated as molar eq per –SH in the T-shaped lipo-oligomers.

2.2.3 pDNA binding assays

A 1 % agarose gel for pDNA analyses was prepared by dissolving agarose in TBE buffer (Trizma base 10.8 g, boric acid 5.5 g, disodium EDTA 0.75 g, and 1 L of water) and boiled up to 100 °C. After cooling down to about 50 °C and addition of GelRed™ (Biotum, Hayward, U.S.A.), the agarose gel was casted in the electrophoresis unit. Polyplexes prepared with 200 ng pDNA were formed as described at indicated N/P ratios and placed into the sample pockets after addition of 4 µL of loading buffer (prepared from 6 mL of glycerine, 1.2 mL of 0.5 M EDTA, 2.8 mL of H₂O, 0.02 g of bromophenol blue). Electrophoresis was performed at 120 V for 80 min.

2.2.4 Particle size and zeta potential

Particle size and zeta potential of polyplexes were measured by dynamic laser-light scattering (DLS) using a Zetasizer Nano ZS (Malvern Instruments, Worcestershire, UK). 2 µg pDNA was diluted to 30 µL in HBG and was added to an amount of oligomers corresponding to N/P 12 prepared in 30 µL HBG. After rapid mixing, polyplexes were incubated for 30 min at RT. In case of post-modification, 0.5 or 1.0 eq of PEGylation reagents were added and further incubated at RT for 15 min. Then 740 µL of 10 mM sodium chloride solution (pH 7.4) was added to all samples and particle size and zeta potential was measured. Results were plotted as Z-Average (D_H in nm) and SD out of three runs with 12 sub-runs each. Zeta potential (ZP) is displayed as average (mV) of three runs with up to 15 sub-runs each. For size measurements, the equilibration time was 0 min, the temperature was 25 °C and an automatic attenuator was used. The refractive index of the solvent was 1.330 and the viscosity was 0.8872 mPa•s. Every

sample was measured 3 times with at least 6 sub runs each. Zeta potentials were calculated by the Smoluchowski equation. Ten to fifteen sub runs lasting 10 s each at 25 °C (n = 3) were determined.

2.2.5 Transmission electron microscopy (TEM) of polyplexes

Samples were prepared as follows. The formvar/carbon-coated 300 mesh copper grids (Ted Pella Inc., Redding, CA, USA) were activated by mild plasma cleaning. Afterwards, the grids were incubated with 20 μ L of the polyplex solution at N/P 12 for 2.5 min. Polyplexes were previously prepared in water with 1 μ g pDNA / 0.1 ml and, if indicated, post-modified with 1.0 eq. of PEGylation reagent. Excess liquid was blotted off using filter paper until the grid was almost dry. Prior to staining, the grids were washed with 5 μ L of staining solution for 5 s. Then, the copper grids were incubated with 5 μ L of a 2% aqueous uranylformate solution for 5 s, excess liquid was blotted off using filter paper, followed by air-drying for 30 min. Samples were then analyzed at 80 kV using a JEM 1011 (Jeol, Freising, Germany) by Susanne Kempter or Caroline Hartl (LMU Munich, Department of Physics).

2.2.6 Ethidium bromide compaction assay and polyanionic stress test

Polyplexes containing 2 μ g pDNA were formed at N/P ratio of 12 in a total volume of 200 μ L HBG. LPEI polyplexes formed at N/P 12 served as positive control. If indicated, PEG agents were added at indicated ratios. HBG buffer (200 μ L) served as blank and 2 μ g pDNA in 200 μ L HBG buffer was considered as maximum ethidium bromide (EtBr) fluorescence intensity (100% value). These samples were prepared in parallel to the polyplexes. After incubation at room temperature, 700 μ L of a EtBr solution (c = 0.5 μ g/mL) was added. The fluorescence intensity of EtBr was measured after an additional 3 min incubation using a Cary Eclipse spectrophotometer (Varian, Germany) at the excitation wavelength $\lambda_{\text{ex}} = 510$ nm and emission wavelength $\lambda_{\text{em}} = 590$ nm. The fluorescence intensity of EtBr was determined in relation to free pDNA. As a further experiment, 250 IU of heparin (Ratiopharm, Ulm, Germany) was added to the samples after EtBr addition to investigate polyplex stability against polyanionic stress and the samples were remeasured.

2.2.7 Stability of polyplexes in serum and media

Polyplex stability in full serum (FBS) or in DMEM supplemented with 10% serum was determined by DLS. Polyplexes were prepared as described previously with 8 µg pDNA and oligomers at N/P 12 in a total volume of 50 µL HBG. After incubation for 30 min, if indicated, polyplexes were PEGylated for 15 min, then 30 µL of HBG and 720 µL FBS (or DMEM) were added to reach a final concentration of 90% serum or DMEM. For measurement 60 µL were placed in a DTS1070 cuvette and t=0 min was determined. Polyplexes in serum or media were incubated under steady shaking at 37 °C and aliquots were taken for further measurements at indicated time points. Each time point represents one measurement averaged from 6 sub runs.

2.2.8 Polyplex stability in the presence of salt

Polyplexes were prepared with oligomers at N/P 12 and 2 µg pCMVLuc in a total volume of 60 µL deionized water. After 30 min and, if indicated, post-modification with 1.0 eq of the bivalent PEGylation reagents for 15 min, 500 µL of phosphate-buffered saline (PBS) was added and a dynamic laser-light scattering (DLS) measurement with three runs (including six sub-runs each) was performed immediately. Samples were incubated at room temperature, and further measurements were conducted. In case of investigation within **3.1.5** samples were taken after 5, 30, 60, 180 min as well as after 24 h (if indicated). In **3.3.2.3** polyplex stability was investigated after 30 min, 60 min, 180 min and if indicated after 24 h.

2.2.9 Polyplex adhesion to erythrocytes or serum

Polyplexes were prepared at N/P 12 and 2 µg pDNA (20% Cy5 labeled) in a total volume of 60 µL HBG. After 30 min, three groups were treated differently. Either HBG, 3×10^6 erythrocytes in HBG, or serum (to a final concentration of 90%) were added. After further 30 min of incubation at 37 °C, erythrocytes containing polyplexes were sedimented by centrifugation (1500 rpm for 10 min at room temperature) and the supernatant was taken. Then, 3500 IU of heparin sulfate was added to dissociate the polyplex and determine the remaining amount of pDNA via Cy5 excitation/emission

($\lambda_{\text{ex}} = 649 \text{ nm}$ and emission wavelength $\lambda_{\text{em}} = 670 \text{ nm}$). Data were calculated in comparison to equally treated free pDNA.

2.2.10 UV spectrometrical investigation of polyplex modification

Polyplexes consisting of 8 μg pDNA and **454** at N/P 12 in 50 μL HBG were prepared. After 30 min samples were either diluted to 100 μL HBG or post-modified with 1.0 eq of Ala-PEG₂₄-Cys(NPys)₂ for 15 min prior to dilution. HBG served as blank; 8 μg pDNA in HBG, its correlating amount of **454** at N/P 12 and 1.0 eq of Ala-PEG₂₄-K-(STOTDA-(Cys(NPys))₂) were treated as controls. For all samples UV/Vis spectra from 200-700 nm were recorded with a Genesys 10S UV-VIS spectrophotometer (Thermo Scientific, Schwerte, Germany).

2.2.11 Ellman's assay of oligomers

Oligomer stock solutions (10 mg/mL) were diluted to a theoretical amount of approximately 0.4 mM free thiols in water. DTNB dissolved in MeOH (4 mg/mL) was diluted 1:40 with Ellman's buffer obtaining an Ellman's working solution. 30 μL of the diluted oligomer solution and 170 μL of the Ellman's working solution were mixed and incubated for 15 min at 37 °C under steady shaking. Absorbance at A_{412} was determined against a mixture of 30 μL of Water and 170 μL of Ellman's working solution. The theoretical used concentration of free thiols was set as 100% per oligomer and related to the concentration determined by a correlation curve of cysteine.

2.2.12 Ellman's assay of polyplexes

Polyplexes were formed in 50 μL HBG (containing 8 μg pDNA and **454** at N/P 12). Solutions containing unmodified **454**/pDNA polyplexes as well as post-modified polyplexes (15 min with 1.0 eq (Cys)₂-PEG₂₄-Ala), were diluted with 275 μL Ellman's Buffer (0,2M Na₂HPO₄, 1mM EDTA, pH 8,0) and eight μL of a DTNB solution (4mg/ml dissolved in MeOH). After addition of DTNB, both solutions were incubated for 15 min at 37 °C and absorbance at 412 nm was measured. Post-modified polyplex absorption was measured at 412 nm prior and after DTNB addition in order to exclude distortion

mediated by 3-nitro-2-thiopyridone, released during post-modification. A Genesys 10S UV-VIS spectrophotometer (Thermo Scientific, Schwerte, Germany) was used for measurement. A_{412} of PEGylated polyplexes then was calculated according to the following formula: $A_{412}(\text{Sample}) = A_{412}(\text{+DTNB}) - A_{412}(\text{-DTNB})$. The percentage of free mercapto groups is based on the theoretical amount (100%) of thiols.

2.2.13 Release of 3-nitro-2-thiopyridone

The amount of (Cys)₂-PEG₂₄-Ala corresponding to 1.0 molar eq of **454** was diluted with HBG (pH 7.4) to 300 μL and 33 μL of a 1M DTT (dithiothreitol) solution was added to the solution. The maximum absorbance of 3-nitro-2-thiopyridone was determined at 324 nm. Absorbance, then was consequently measured at A_{324} and compared to the amount released from the PEGylated polyplex. Therefore 50 μL of polyplex solution (containing 8 μg of pDNA, and **454** at N/P 12) was post-modified with 1.0 eq (Cys)₂-PEG₂₄-Ala for 15 min and the polyplex solution was diluted with 275 μL of Ellman's Buffer prior to measurement. Absorbance of (Cys)₂-PEG₂₄-Ala reduced with 1M DTT was considered as 100% and was put in relation to 3-nitro-2-thiopyridone release after PEGylation.

2.2.14 EGF and HGF receptor measurement

Huh7 and DU145 cells for HGFR measurement and Huh7, MCF-7 and FTC-133 cells for EGFR measurement were detached with trypsin. Then 8×10^5 in case of HGFR receptor screening and 1×10^6 cells in case of EGFR screening were washed with PBS (supplemented with 10% FBS) and incubated with either an HGFR specific antibody (1:100; monoclonal mouse IgG1, R&D Systems, Minneapolis, MN, USA) or an EGFR specific antibody (1:100; monoclonal mouse IgG1 - Dako, Glostrup, Denmark). In both cases similar cells counts incubated with an IgG-anti-mouse antibody (BD Bioscience, Franklin Lakes, USA) served as control. Cells were treated for 1 h on ice and were subsequently washed with buffer (10% FBS in PBS) twice. Next, cells were washed with PBS supplemented with 10% FBS and incubated with an AlexaFluor 488 labeled goat anti-mouse secondary antibody (1:400 - Invitrogen, Langenselbold, Germany) for 1 h on ice. After a final washing step, cells were resuspended in PBS (supplemented with 10% FBS) and flow cytometry analysis was performed on a Cyan™ ADP flow Cytometer (Dako, Hamburg, Germany) using

Summit™ acquisition software (Summit, Jamesville, NY, USA) in case of HGF receptor measurement and on a BD Accuri C6 flow cytometer (BD Bioscience, Franklin Lakes, USA) in case of EGF receptor measurement. Cells were gated by forward/sideward scatter and pulse width for exclusion of doublets. In case of HGF measurement cells were counterstained with DAPI in case of HGFR measurement and with propidium iodide (PI) in case of EGFR measurement to discriminate between viable and dead cells. Experiments were carried out by Ana Krhac Levacic (PhD study, Department of Pharmaceutical Biotechnology, LMU) for c-Met receptor measurements and by Sarah Urnauer (PhD study, University Hospital of LMU, Department of Internal Medicine IV) of EGF receptor measurements on Huh7, MCF-7 and FTC-133. Wei Zhang, PhD (Department of Pharmaceutical Biotechnology, LMU) performed receptor level measurements on KB cells.

2.2.15 *In vitro* pCMVLuc gene transfer and metabolic activity of transfected cells (MTT assay)

For determining luciferase activity, cells were seeded 24 h prior to pDNA delivery. 10,000 cells/well were added into 96-well plates for all used cell lines. Transfection efficiency of oligomers at indicated N/P ratios was determined. 200 ng pCMVLuc per well were used for polyplex formation (cf. 2.2.2). If indicated, lipopolyplexes were PEGylated according to 2.2.2.1. Before treatment, cells received 80 µL of fresh medium containing 10% FBS. Polyplex solution (20 µL) was added to each well and incubated on cells at 37 °C for either 45 min or 24 h. In the first case, medium was replaced 45 min after transfection by fresh medium. In the second case, cells were incubated with polyplex solution for 24 h after initial transfection. All experiments were performed in quintuplicate. LPEI or LPEI-PEG_{2k}-GE11 (N/P 6) was used as a positive control and HBG buffer served as negative control. Luciferase activity of cells was determined after lysis with 100 µL lysis buffer using a Centro LB 960 plate reader luminometer (Berthold Technologies, Bad Wildbad, Germany) and LAR buffer supplemented with 1 mM luciferin. Transfection efficiency was evaluated as relative light units (RLU) per well.

For metabolic activity, cells, plated as 10,000 per well, were also transfected with polyplexes, as described above. 24 h after initial transfection, 10 µL of MTT (3-(4,5-

dimethylthiazol-2-yl)-2,5-diphenyltetrazolium bromide) was added to each well reaching a final concentration of 0.5 mg/mL. Medium with unreacted dye was removed after an incubation time of 2 h at 37 °C. The 96-well plates were stored at -80 °C for at least one hour and afterwards the purple formazan product was dissolved in 100 µL DMSO per well. The absorbance was determined by using a microplate reader at 530 nm with background correction at 630 nm. The relative cell viability (%) related to the buffer treated control cells was calculated as $([A]_{\text{test}}/[A]_{\text{control}}) \times 100 \%$. Experiments were carried out by Ana Krhac Levacic (PhD study, Department of Pharmaceutical Biotechnolgy, LMU) and Sarah Urnauer (PhD study, University Hospital of LMU, Department of Internal Medicine IV).

2.2.16 *In vitro* pCMVLuc gene transfer and metabolic activity of transfected cells (MTT assay) with addition of endosomolytic chloroquine or LPEI

Cells were seeded 24 h prior to pDNA delivery. 10,000 Huh7 cells/well were added into 96-well plates. Transfection efficiency of the novel lipo-oligomers (**454**, **1026**, **1176-1178**) at N/P 12 was determined. Therefore 200 ng pCMVLuc per well were used for polyplex formation (cf. **2.2.2**). If indicated, lipopolyplexes were PEGylated according to **2.2.2.1**. Before treatment, cells received 80 µL of fresh medium containing 10% FBS. Polyplex solution (20 µL) was added to each well and either incubated on cells at 37 °C for 45 min, followed by addition of endosomolytic chloroquine for 4 h prior to an additional media change, or lipopolyplexes were incubated for 2 h and media was replaced by a media enriched with LPEI, another endosomolytic reagent, corresponding to N/P 9 per well. In both types of experiments, total incubation time was 24 h and a MTT assay to investigate polyplex toxicity was performed in parallel in quintuplicate. Calculations were performed as mentioned previously (cf. **2.2.15**), and experiments were performed by Ana Krhac Levacic (PhD study, Department of Pharmaceutical Biotechnolgy, LMU).

2.2.17 Cellular association of pDNA polyplexes

Cells were seeded 24 h prior to transfection into 24-well plates at a density of 50,000 cells per well. Culture medium was replaced with 400 µL fresh growth medium 24 h after seeding the cells. pDNA polyplexes were formed with oligomers (N/P 12) and 1 µg pCMVLuc (20% of Cy5-labeled pCMVLuc) and incubated for 30 min in 100 µL HBG

on ice. PEGylation reagents were, if indicated, co-incubated for further 15 min prior to addition onto the cells. Subsequently, cells were washed twice with 500 μ L PBS, detached with trypsin/EDTA and resuspended in PBS supplemented with 10% FBS. Cellular association of the polyplexes was measured by excitation of Cy5 at 635 nm and detection of emission at 665 nm. DAPI (4',6-diamidino-2-phenylindole) or PI (propidium iodine) staining was used to discriminate between viable and dead cells. Cells were properly gated by forward/sideward scatter and pulse width for exclusion of doublets. Experiments were carried out by Ana Krhac Levacic (PhD study, Department of Pharmaceutical Biotechnology, LMU) and Sarah Urnauer (PhD study, University Hospital of LMU, Department of Internal Medicine IV).

2.2.18 Cellular internalization of pDNA polyplexes

Cells were seeded 24 h prior to transfection into 24-well plates at a density of 50 000 cells/well. Culture medium was replaced with 400 μ L fresh growth medium 24 h after seeding the cells. pDNA polyplexes, formed at N/P ratio 12 in 100 μ L HBG, containing 1 μ g pCMVLuc (20 % of Cy5-labeled pCMVLuc) were added to each well and incubated at 37 °C for 45 min. PEGylation reagents were, if indicated, co-incubated for further 15 min prior to addition to cells. Subsequently, cells were washed once with 500 μ L PBS containing 1000 IU heparin for 15 min on ice to remove any polyplexes sticking to the cell surface and again washed once with 500 μ L PBS only. Cells were detached with trypsin/EDTA and resuspended in PBS supplemented with 10 % FBS. Cellular internalization of the polyplexes was measured by excitation of Cy5 at 635 nm and detection of emission at 665 nm. DAPI (4',6-diamidino-2-phenylindole) or PI (propidium iodine) staining was used to discriminate between viable and dead cells. Cells were properly gated by forward/sideward scatter and pulse width for exclusion of doublets. Experiments were carried out by Ana Krhac Levacic (PhD study, Department of Pharmaceutical Biotechnology, LMU) and Sarah Urnauer (PhD study, University Hospital of LMU, Department of Internal Medicine IV).

2.2.19 *In vivo* gene transfer

Animal experiments were performed in female 6-week-old nude mice, Rj: NMR1-nu (nu/nu) (Janvier, Le-Genest-St-Isle, France) which were housed in isolated ventilated

cages with a 12 h day/night interval and food and water *ad libitum*. Huh7 (5×10^6 cells) suspended in 150 μ L PBS were injected subcutaneously into the left flank. After injection, tumor size was monitored with a caliper and determined by formula $a \times b^2 / 2$ (a = longest side of the tumor; b = widest side vertical to a). When tumors reached a size of approximately 1200 mm³, the experiments started by intratumoral injection of 60 μ L polyplex solution containing 50 μ g pCMVLuc at N/P 12 in HBG. For each polymer, a group of 5 mice (n=5) was treated. Mice were euthanized 48 hours later, and tumors were collected to assess luciferase activity via *ex vivo* luciferase assay. Tumors were homogenized in 500 μ L cell lysis buffer using a tissue and cell homogenizer (FastPrep®-24). To separate insoluble cell components, the samples were centrifuged at 3000 g at 4 °C for 10 min. Luciferase activity was measured in the supernatant using a Centro LB 960 luminometer. All animal experiments were performed according to the guidelines of the German law for the protection of animal life and were approved by the local animal ethics committee. Experiments were performed by Sarah Kern and Jasmin Kuhn (Doctoral studies, Pharmaceutical Biotechnology, LMU).

2.2.20 Iodide uptake activity after hNIS gene delivery

For determining iodide uptake activity after NIS gene delivery, 200,000 cells/well were plated in 6-well plates. Transfection efficiency of (post-modified) polyplexes formed at N/P 12 was evaluated using 2 μ g hNIS pDNA. After 24 h incubation with polyplexes, cells were washed with HBSS (Hank's Balanced Salt Solution; Thermo Fisher Scientific, Waltham, USA) and then incubated with HBSS supplemented with 10 μ M NaI, 0.1 μ Ci of Na¹²⁵I / ml and 10 mM HEPES at pH 7.3 for 45 min at 37°C. Sodium perchlorate (NaClO₄; 100 μ M) as NIS-specific inhibitor was added to control wells. After incubation with iodide, cells were washed with HBSS and trapped iodide was removed from cells by a 20 min incubation in 1 M NaOH and measured by γ -counting and expressed as counts per minute (cpm).

Metabolic activity of transfected cells was determined as described in 0. Here, 200 μ L of MTT reagent was added to each well, reaching a final concentration of 0.5 mg/mL. Medium with unreacted dye was removed after incubation for 2 h at 37 °C and washed with PBS (phosphate-buffered saline) and measurement and calculation was

conducted as mentioned before. Experiments were performed by Sarah Urnauer (PhD study, University Hospital of LMU, Department of Internal Medicine IV).

2.2.21 MALDI-TOF mass spectrometry

One μL matrix consisting of a saturated solution of Super-DHB (mixture of 2,5-dihydroxybenzoic acid and 2-hydroxy-5-methoxybenzoic acid) in acetonitrile / water (1:1) containing 0.1% (v/v) trifluoroacetic acid was applied on a MTP AnchorChip (Bruker Daltonics, Bremen, Germany). After the Super-DHB matrix dried and crystalized, one μL of the sample solution (10 mg/mL in water) was added to the matrix spot. Samples were analyzed using an Autoflex II mass spectrometer (Bruker Daltonics, Bremen, Germany). Spectra were recorded after positive or negative ionization.

2.2.22 Proton NMR spectroscopy

^1H -NMR spectra were recorded using an AVANCE III HD500 (500 MHz) by Bruker with a 5 mm CPPBBO probe. Spectra were recorded without TMS as internal standard and therefore all signals were calibrated to the residual proton signal of the deuterium oxide (D_2O) solvent. Chemical shifts are reported in ppm and refer to the solvent as internal standard (D_2O at 4.79). Integration was performed manually. The spectra were analyzed using MestreNova (Ver.9.0 by MestReLab Research). Integrals were normalized to the succinic acid peaks.

2.2.23 Analytical RP-HPLC

Reversed-phase HPLC (RP-HPLC) was carried out with a VWR-Hitachi Chromaster 5160 Pump System (VWR, Darmstadt, Germany), VWR-Hitachi Chromaster 5260 Autosampler (VWR, Darmstadt, Germany) and a Diode Array Detector (VWR-Hitachi Chromaster 5430; VWR, Darmstadt, Germany) at 214 nm detection wavelength. As a column either a YMC Hydrosphere 302 C_{18} (YMC Europe, Dinslaken, Germany) or a Waters Sunfire C_{18} (Waters, Saint-Quentin en Yvelines Cedex, France) was used. A gradient starting at 95:5 (water / acetonitrile) to 0:100 within 20 min was applied. All solvents were supplemented with 0.1% trifluoroacetic acid.

2.2.24 ESI mass spectrometry

Electrospray ionization (ESI) mass spectrometry was carried out using a ThermoScientific LTQ FT Ultra Fourier transform ion cyclotron and an IonMax source. Samples were dissolved in water containing 1% formic acid to a concentration of 1 mg/ml. Data is shown after positive ionization as (M+X). Samples were kindly processed by Dr. Werner Spahl from the analytical core facility at the Department of Chemistry, LMU Munich.

2.2.25 Statistical analysis

The results are presented as mean values of experiments performed in at least triplicates. Unless stated otherwise, error bars display standard deviation (SD). Statistical analysis of the results (mean \pm SD) was evaluated by unpaired t test: *p < 0.05; **p < 0.01; ***p < 0.001; ****p < 0.0001. Calculations and graphical presentation were performed with Prism 6 (GraphPad Software Inc.).

3 Results

3.1 Influence of defined hydrophilic blocks within oligoaminoamide copolymers: compaction versus shielding of pDNA nanoparticles

This chapter has been adapted from:

Morys, S.; Krhac Levacic, A.; Urnauer, S.; Kempter, S.; Kern, S.; Rädler, J.O.; Spitzweg, C.; Lächelt, U.; Wagner, E. *Influence of Defined Hydrophilic Blocks within Oligoaminoamide Copolymers: Compaction versus Shielding of pDNA Nanoparticles*. *Polymers* **2017**, *9*, 142.

Cationic sequence-defined oligoaminoamides equipped with polyethylene glycole polymers as non-viral vectors for nucleic acid delivery need to comprise several functionalities. Besides a nucleic acid (NA) binding element, also a shielding block and a tumor-specific targeting domain is required for a successful *in vitro* as well as *in vivo* delivery of the NA. Recently solid phase synthesis (SPS) derived oligomers were successfully applied as pDNA shuttles for receptor targeted gene delivery *in vitro* and *in vivo* [64, 65], investigating the capabilities (PEG) of a defined length and a HGF (**h**epatocyte **g**rowth **f**actor) binding peptide (cmb), targeting hepatocellular cancer. This work focuses on the modification of histidine-rich oligoaminoamide [50] carriers with hydrophilic shielding blocks mediating receptor specific gene delivery due to the nanoparticle's shielding potential and introduction of a targeting domain [64, 65, 137, 201]. It was described earlier that polyplex shielding is necessary to prevent aggregation or dissociation of NA polyplexes *in vitro* [202], and hinder opsonization [153] with blood components *in vivo*.

Herein, the oligomers equipped with either the shielding agent PEG, in three defined lengths (12, 24, or 48 oxyethylene repeats) or with peptidic shielding blocks composed of four or eight repeats of sequential proline-alanine-serine (PAS) are compared.

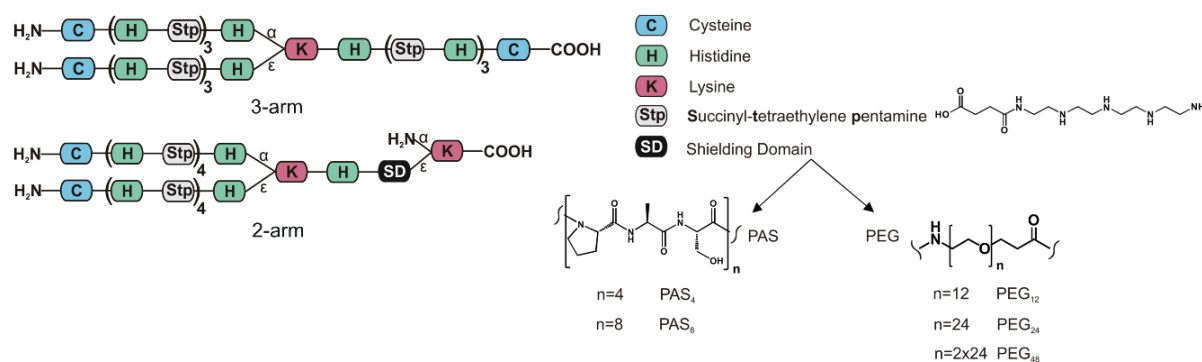
3.1.1 Peptide and oligomer synthesis

The objective of this study was to examine different hydrophilic blocks—PAS and PEG—with varying length in combination with a cationic oligoaminoamide backbone for their “shielding abilities” in pDNA polyplexes. The cationic oligomers can mainly be divided into two subgroups: a three-arm cationic topology without shielding domain [49] for control carriers, or shielded two-arm structures comprising certain PEG or PAS repetitions—topologies are described in **Scheme 4**. PAS represents the three neutral amino acids proline, alanine, and serine, ordered from N to C terminus. Solid phase assisted synthesis (SPS) was used for the assembly of the oligomers listed in **Table 7**. This method allowed oligomers to be easily tailored to our needs. The non-shielded positive control with three-arm topology had a similar number of charge-bearing units (9 Stp, 12 histidines) as the shielded two-arm oligomers (8 Stp, 11 histidines). A two-arm structure without shielding agent might have been considered as a suitable control, but previous studies [134] revealed a lower efficacy of short cationic two-arm oligomers. Moreover, a shielded two-arm in fact presents a three-arm topology (with the shielding polymer block arm representing the third arm). The length of shielding blocks used in this study were chosen along the commercially available, precise PEG derivatives of 12 or 24 ethylenoxide (EO) units and analogous PAS peptides. So PAS₄ consisting of four PAS repeats (4 × 3 = 12 amino acids) was considered as backbone analog to 12 EO units (PEG₁₂), and PAS₈ (8 × 3 = 24 amino acids) as analog to 24 EO units (PEG₂₄). Due to the amino acid side groups, the molecular weight of a PAS tri-amino acid block is substantially higher (273 g/mol) than the analogous EO trimer block (3 × 44 g/mol = 132 g/mol).

Table 7 List of oligomers included in this study. Internal polymer numbers, structures from N to C terminus, as well as abbreviations used within the paper.

| ID # | Structure | Abbreviation |
|------|--|-------------------|
| 689 | $[C-(H-Stp)_3-H]_{\alpha,\epsilon}-K-H-(Stp-H)_3-C$ | 3-arm |
| 1088 | $\{[C-(H-Stp)_4-H]_{\alpha,\epsilon}-K-H-dPEG_{12}\}_{\epsilon}-K$ | PEG ₁₂ |
| 1091 | $\{[C-(H-Stp)_4-H]_{\alpha,\epsilon}-K-H-dPEG_{24}\}_{\epsilon}-K$ | PEG ₂₄ |
| 1120 | $\{[C-(H-Stp)_4-H]_{\alpha,\epsilon}-K-H-dPEG_{24}-dPEG_{24}\}_{\epsilon}-K$ | PEG ₄₈ |
| 1094 | $\{[C-(H-Stp)_4-H]_{\alpha,\epsilon}-K-H-(PAS)_4\}_{\epsilon}-K$ | PAS ₄ |
| 1097 | $\{[C-(H-Stp)_4-H]_{\alpha,\epsilon}-K-H-(PAS)_8\}_{\epsilon}-K$ | PAS ₈ |

In case of shielded two-arm structures, first a Dde-L-Lysine-(Fmoc) was loaded on a 2-chlorotrityl resin. Consequently, the shielding domain was attached to the ϵ -amine after successful Fmoc deprotection. It consisted of either monodisperse polyethylene glycol (PEG) of 12, 24, or 2×24 units, or of four or eight repetitive Ser–Ala–Pro units. The cationic backbone consists of histidines, the artificial amino acid Stp (succinyl-tetraethylene pentamine) [131, 199], lysine, and cysteine. Histidines were introduced for enhanced endosomal buffering [50, 64, 203]. Stp was used for nucleic acid packaging, endosomal buffering, and endosomal escape [49, 132]. The diamino acid lysine served as a branching point, and N-terminal cysteines were introduced for polyplex stabilization via disulfide-crosslinking [49, 52, 134]. Each oligomer was characterized by $^1\text{H-NMR}$ and RP-HPLC and can be found in the appendix (cf. 6.5)



Scheme 4 Schematic structures of the oligomer topologies evaluated in this paper. PAS: proline-alanine-serine; PEG: polyethylene glycol.

3.1.2 Physicochemical polyplex characterization

Oligomer/pDNA interaction was examined in different assays, focusing on pDNA binding abilities, stability, and compaction. First, pDNA binding potency of the oligomers was investigated by agarose gel electrophoresis shift assays. Here polyplexes were formed with different ratios of oligomer to pDNA. This ratio is displayed as N/P, with varying amount of oligomer but constant amount of 200 ng pDNA (cf. **Figure 5** and **Figure 6**) This assay revealed that all tested oligomers efficiently complex pDNA at an N/P ratio between 2 and 2.5. We already reported similar findings with oligomers composed of the same cationic backbone [64, 137]. Importantly, the presence and nature of shielding elements did not influence the pDNA binding of the cationic backbone in this assay for shielding agents with the length up to PEG₂₄. Only

the oligomer with longest PEG₄₈ shielding domain exhibited slightly decreased binding potency, since certain fractions of free pDNA could still be observed at N/P 3 and 6. Notably, pDNA binding does not necessarily correlate with its degree of compaction or polyplex shape. Polyplex properties regarding DNA compaction were therefore investigated with alternative techniques (cf. **Figure 7**).

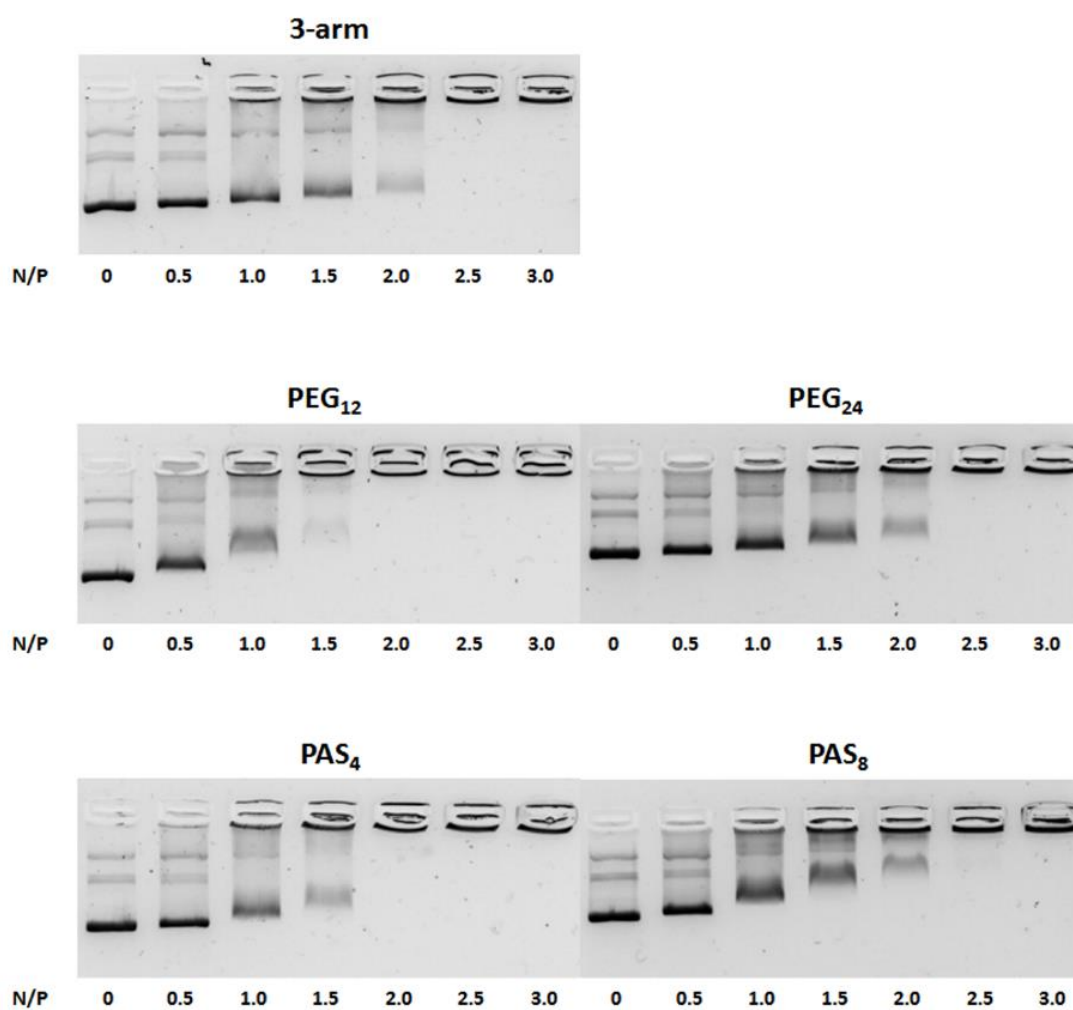


Figure 5 Retardation of formed pDNA complexes in agarose gel of untargeted polyplexes between N/P of 0 (free pDNA) and 3 in an agarose gel shift assay.

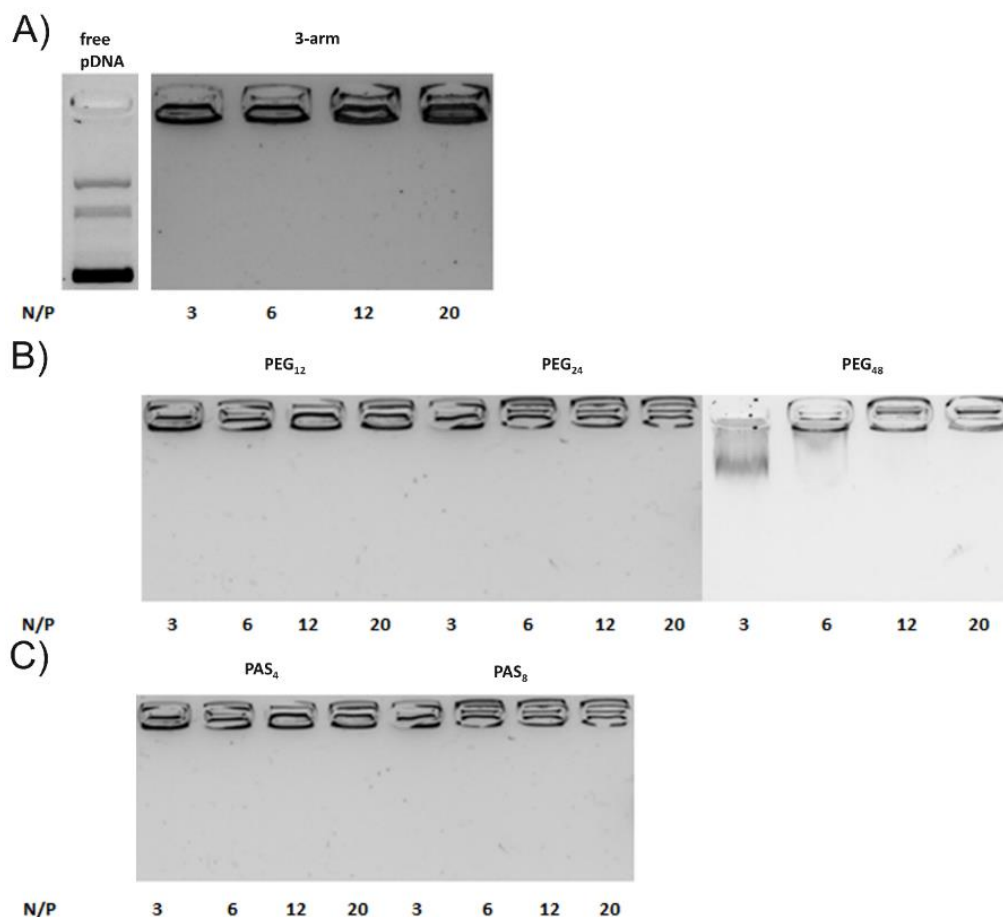


Figure 6 Retardation of formed pDNA complexes in agarose gel at N/P 3 to 20 with non-shielded 3-arm (A) PEGylated (B) and PASylated (C) oligomers. Left lane: free pDNA.

After pDNA binding was confirmed, particle sizes and zeta potential were determined by dynamic light scattering at N/P 12. Results revealed very homogenous particles with a polydispersity index (PDI) between 0.04 and 0.33, where 1.0 represents the highest polydispersity (cf. **Table 8**). All polyplexes show D_H values (displayed as Z-Average in nm) in the range between 98 nm and 147 nm. It has been reported that particles up to 200 nm can be taken up via a clathrin-dependent pathway [175], indicating that subsequent uptake into cells should be possible via endocytosis. DLS data provide a hint that particles with shorter shielding agents (PEG₁₂ or PAS₄) exhibit smaller particle sizes than longer shielding agents. This could be explained by more compact and condensed particles. Also increased length of the shielding agents resulted in decreased zeta potential, indicating improved surface shielding.

Table 8 Particle size (Z-average), polydispersity index (PDI), and zeta potential of plasmid DNA (pDNA) polyplexes formed in HEPES-buffered 5% glucose (HBG) buffer determined with dynamic laser-light scattering (DLS). Mean of three measurements of the same sample is indicated. Polymer at nitrogen-to-phosphate ratio (N/P) 12 and 2 μg plasmid DNA (pDNA) were separately diluted with HBG pH 7.4 to 30 μL each. Then solutions were mixed and incubated for 30 min. Polyplexes were diluted to 800 μL with 10 mM NaCl pH 7.4 prior to measurement. # indicates internal library compound IDs.

| ID # | Abbreviation | Z-average [nm] | Mean PDI | Mean zeta potential [mV] |
|-------------|-------------------|-----------------|-----------------|--------------------------|
| 689 | 3-arm | 126.8 \pm 2.7 | 0.15 \pm 0.02 | 32.0 \pm 3.5 |
| 1088 | PEG ₁₂ | 97.9 \pm 1.1 | 0.14 \pm 0.02 | 6.7 \pm 2.3 |
| 1091 | PEG ₂₄ | 111.6 \pm 0.9 | 0.16 \pm 0.01 | 3.1 \pm 0.6 |
| 1120 | PEG ₄₈ | 87.2 \pm 1.4 | 0.33 \pm 0.05 | 1.6 \pm 0.5 |
| 1094 | PAS ₄ | 127.7 \pm 0.8 | 0.12 \pm 0.01 | 7.1 \pm 1.5 |
| 1097 | PAS ₈ | 147.0 \pm 1.8 | 0.15 \pm 0.01 | 3.4 \pm 0.8 |

PDI: Polydispersity index.

3.1.3 Steric shielding

As a next step to characterize polyplexes, a stress assay was performed with salt to evaluate the behavior in isotonic salt concentration. Therefore, PBS buffered at pH 7.4 was added to the polyplexes after 30 min of incubation in deionized water. DLS measurements were performed immediately after addition, and at 5, 30, 60, and 180 min. In case of polyplexes stable for 180 min, also a measurement after 24h was conducted. As displayed in **Figure 7A**, the unshielded three-arm started to aggregate within 5 min after addition of PBS. Along with the three-arm, PAS₄ and PEG₁₂ also underwent colloidal aggregation. Meanwhile PEG₂₄-, PEG₄₈-, and PAS₈-decorated polyplexes showed colloidal stability over 24 h without any significant aggregation. This indicates that longer PEG or PAS chains provide improved colloidal stability with lower risk for aggregation, while polyplexes with shorter PEG length or lack of shielding agent show immediate aggregation after salt addition. These findings (together with the DNA binding studies) are in accordance with previously published work where PEG shielding of PEI polyplexes increased the colloidal stability of polyplexes against salt-induced stress, however at the expense of reduced pDNA binding [29, 204].

The next experiment was designed to investigate the interaction of polyplexes with erythrocytes. Results are displayed in **Figure 7B**. Polyplexes in HBG and polyplexes after incubation with erythrocytes were dissociated by heparin addition, and Cy5

emission of released labeled pDNA was detected. pDNA can be fully released by heparin (**Figure 7B**, dark bars) within the range of experimental accuracy. The data reveal a reduced pDNA recovery due to erythrocyte binding (grey bars); they also reveal that interaction with erythrocytes decreases with ascending length of the shielding agents. PEGylation is known to reduce the interaction of polyplexes with erythrocytes [29], which is in accordance with our findings.

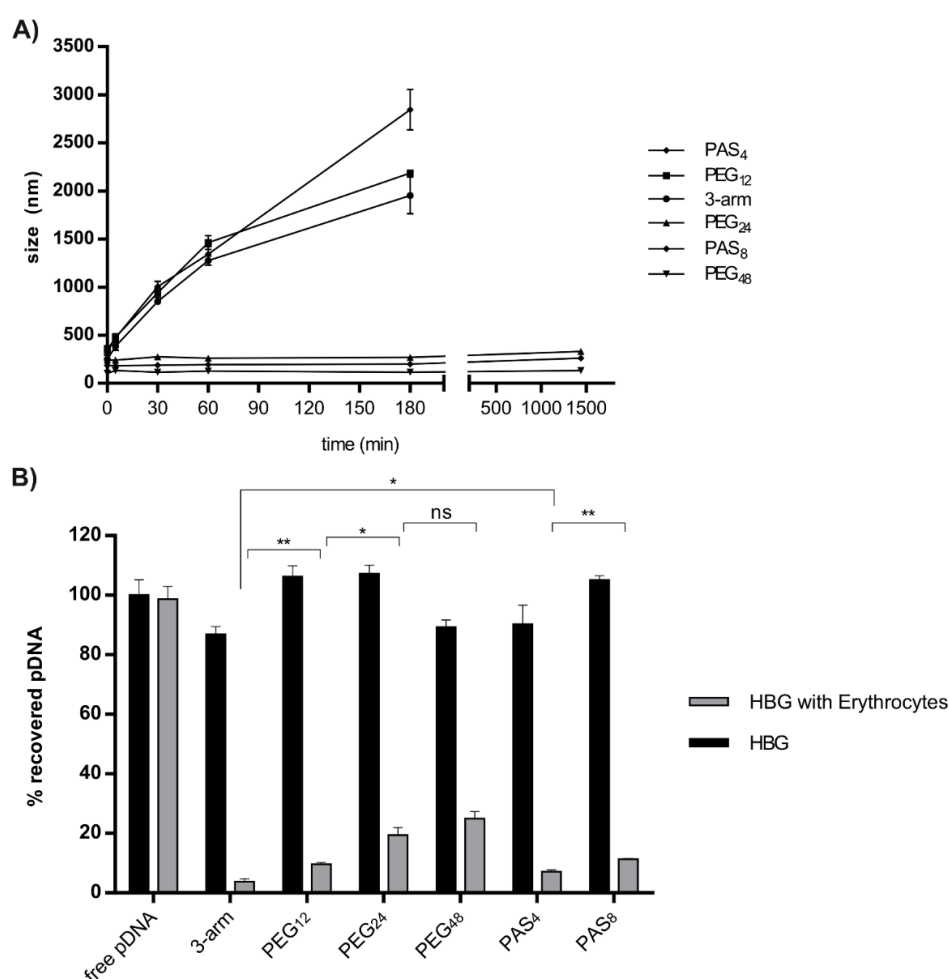


Figure 7 (A) Stability testing of untargeted polyplexes against phosphate-buffered saline (PBS). After 30 min of polyplex incubation (2 μ g pDNA; N/P 12) in deionized water and addition of 500 μ L PBS, DLS measurement was performed. Time points 0, 5, 30, 60, and 180 min were displayed. In case of colloiddally-stable polyplexes of PEG₂₄, PEG₄₈, and PAS₈, a measurement after 24 h is also displayed. Data are presented as mean value (\pm SD) out of triplets; **(B)** Polyplexes (2 μ g pDNA; N/P 12) were incubated in HBG with or without 3×10^6 erythrocytes. After centrifugation, the supernatant was taken, and 3500 IU of heparin were added to release pDNA of the polyplexes. Cy5 fluorescence was compared to uncomplexed (free) pDNA. Statistical analysis (Student's t-test): ns $p > 0.05$, * $p \leq 0.05$; ** $p \leq 0.01$; *** $p \leq 0.001$, **** $p \leq 0.0001$

3.1.4 DNA compaction

Transmission electron microscopy (TEM) was performed to investigate polyplex size and shape. While differences between shielding agents could not be observed by TEM, we observed a clear difference compared to D_H in general, but more unexpected between polyplexes decorated with shorter or longer shielding agents (cf. **Figure 8A**). Particles formed out of oligomers with shorter shielding agents tend to be not only smaller, but also more condensed regarding their structure compared to polyplexes shielded with longer shielding agents. Polyplexes with PEG₁₂ or PAS₄ exhibited sizes of around 50 nm and a more condensed “rod-like” structure, while PEG₂₄ or PAS₈ decorated polyplexes revealed sizes of approximately 80–100 nm in a “doughnut-like” state. PEG₄₈ decorated polyplexes revealed the lowest level of compaction and a very erratic shape of around 100 nm in size. Polyplexes including no shielding agent displayed the most condensed population with sizes around 40–50 nm in a very compact globular shape. However, polyplexes tend to aggregate due to their charged surface; this effect is not visible in case of polyplexes decorated with short shielding agents. These findings are in accordance with recent observations [205], where particle morphology changed from long rods to globular condensed polyplexes with decreasing amounts of conjugated PEG. To further investigate the ability to compact pDNA depending on the shielding agent used, pDNA compaction was determined with an ethidium bromide (EtBr) exclusion assay (cf. **Figure 8B**). Therefore, 2 µg of pDNA was mixed with oligomers at either N/P 6 or 12, incubated for 30 min, and then measured after the addition of EtBr. As reference, linear PEI (LPEI) was included in this study. The intensity of EtBr fluorescence normalized to uncomplexed pDNA is displayed in **Figure 8B** (left). These data support the findings from previous agarose gel shifts and confirm the findings from TEM images. All oligomers complex pDNA well, but with increased length of shielding agent, pDNA compaction decreased, which can be seen most pronounced in the case of the longest shielding element PEG₄₈. In the right part of **Figure 8B**, fluorescence of the released pDNA of polyplexes is displayed after the addition of 250 IU of heparin sulfate to cause anionic dissociative stress.

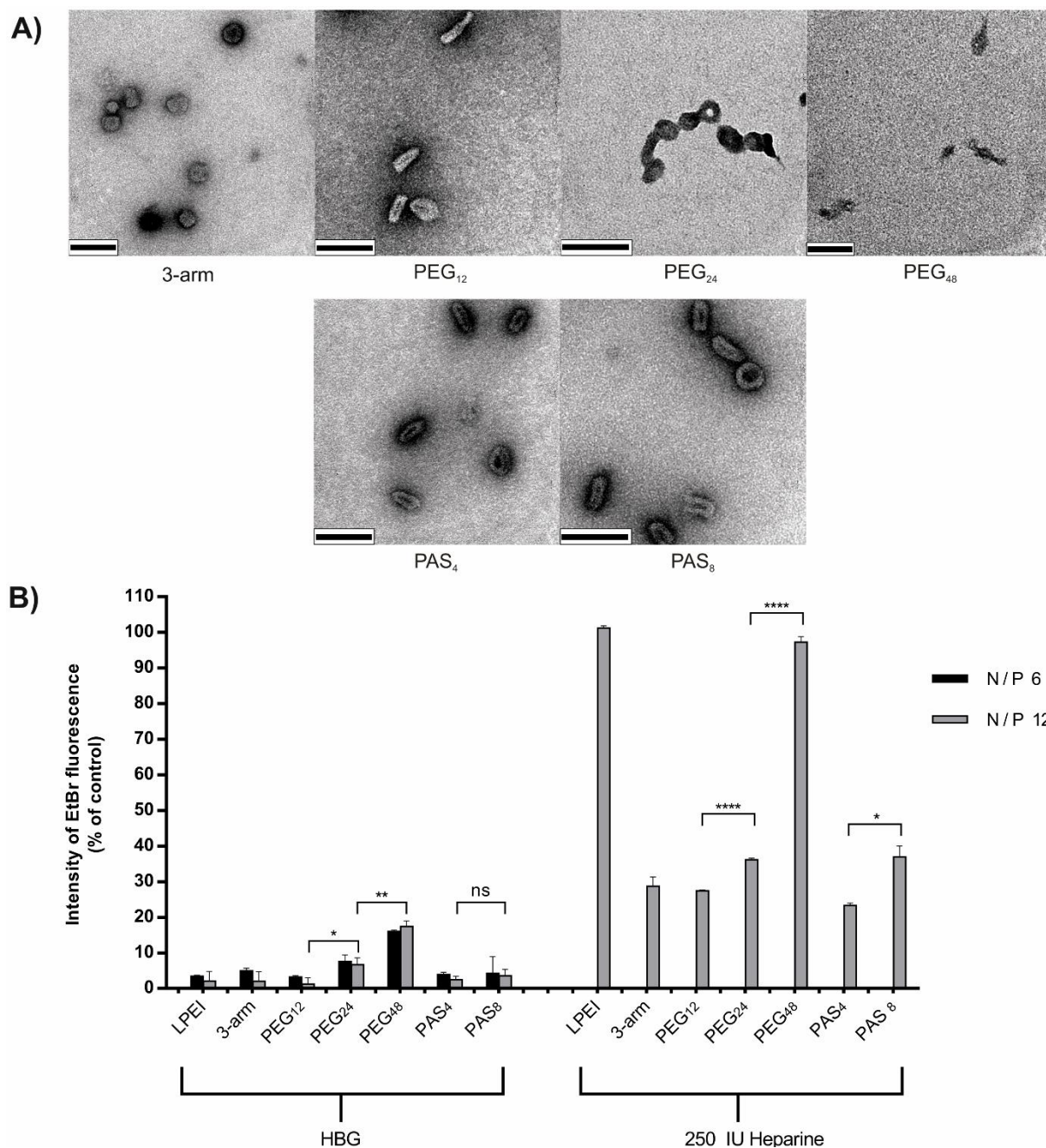


Figure 8 Transmission electron microscopy images of polyplexes formed at N/P 12 in deionized water and stained with uranylformate. Scale bar represents 100 nm; **(B) Left:** pDNA compaction, correlating with the remaining fluorescence of ethidium bromide (EtBr). Results are calculated against free pDNA. **Right:** Polyplexes at N/P 12 after addition of 250 IU of heparin. Statistical analysis (Student's t-test): ns $p > 0.05$, * $p \leq 0.05$; ** $p \leq 0.01$; *** $p \leq 0.001$, **** $p \leq 0.0001$. TEM was performed by Susanne Kempter (Faculty of Physics, LMU).

Here it can be seen that polyplexes formed with LPEI and polyplexes decorated with PEG₄₈ completely release pDNA and cause full EtBr fluorescence, while all other polyplexes are at least partly resistant to the applied heparin stress. Most interestingly,

the shorter the PEG respectively PAS shield, the more resistant the polyplexes were towards heparin stress. In other words, long PEG (24 or 48 units) or eight PAS repeats tend to destabilize the polyplex. These results suggest that the cationic charge density of the backbone is just one critical point for nucleic acid interaction, but the length of the shielding agent also plays a certain role. These findings from EtBr exclusion assay confirm our results from TEM. They are also in accordance with a most recent report on LPEI polyplexes [32], where PEGylation caused more sensitivity towards heparin stress as well as lower compaction in general.

3.1.5 Serum stability

Stability of polyplexes in the blood protein environment presents a most relevant and critical issue, as interaction with proteins can cause aggregation or partial to complete dissociation of the polyplex. Thus, further experiments were designed to investigate polyplex stability in serum. We applied an assay to measure polyplex size in 90% FBS with DLS. This method offered the possibility to monitor polyplex behavior over a long-time period from the point of serum addition up to 24 h. Time points $t = 0, 2, 4, 24$ h are displayed in **Figure 9B–G**. Firstly, the size of all polyplexes increased in serum, from 100–150 nm in 10 mM NaCl to 250–300 nm immediately after addition of FBS. From here on, a decay (loss of intensity and increase in size) of the polyplexes was observed over time in the case of the longer shielding agents PEG₂₄ and PAS₈, with a tendency towards a higher colloidal stability of PAS₈. PEG₁₂ and PAS₄ were the most promising candidates, with almost no decay over time. While polyplexes shielded with PEG₄₈ underwent immediate decay and aggregation, unshielded three-arm underwent no additional changes after the initial size increase within the following 24 h. An explanation for the elevated stability of three-arm, PAS₄, and PEG₁₂ might be the formation of a serum corona around the polyplexes (which also explains the increased size), and due to the higher compaction, the ionic complexes remain stable despite serum interaction. Serum corona - especially when attached to PEGylated nanostructures - has been demonstrated to mediate favorable shielding properties [206]. In **Figure 9H**, the behavior of polyplexes after 30 min of incubation with 90% FBS is compared to polyplexes maintained for the same time in HBG. The amount of released Cy5-labeled pDNA after addition of heparin was determined. In all cases, pDNA release was lower after polyplex incubation with FBS. In the case of PEGylated

polyplexes, a trend towards less pDNA release could be observed with increasing PEG length. At least at this early time point, the formation of a serum corona seems to mediate increased resistance towards polyanionic stress. However, this protective effect seems to reverse when polyplexes are incubated over a long time in serum, maybe due to the lack of compaction (cf. **Figure 9C,F,G**).

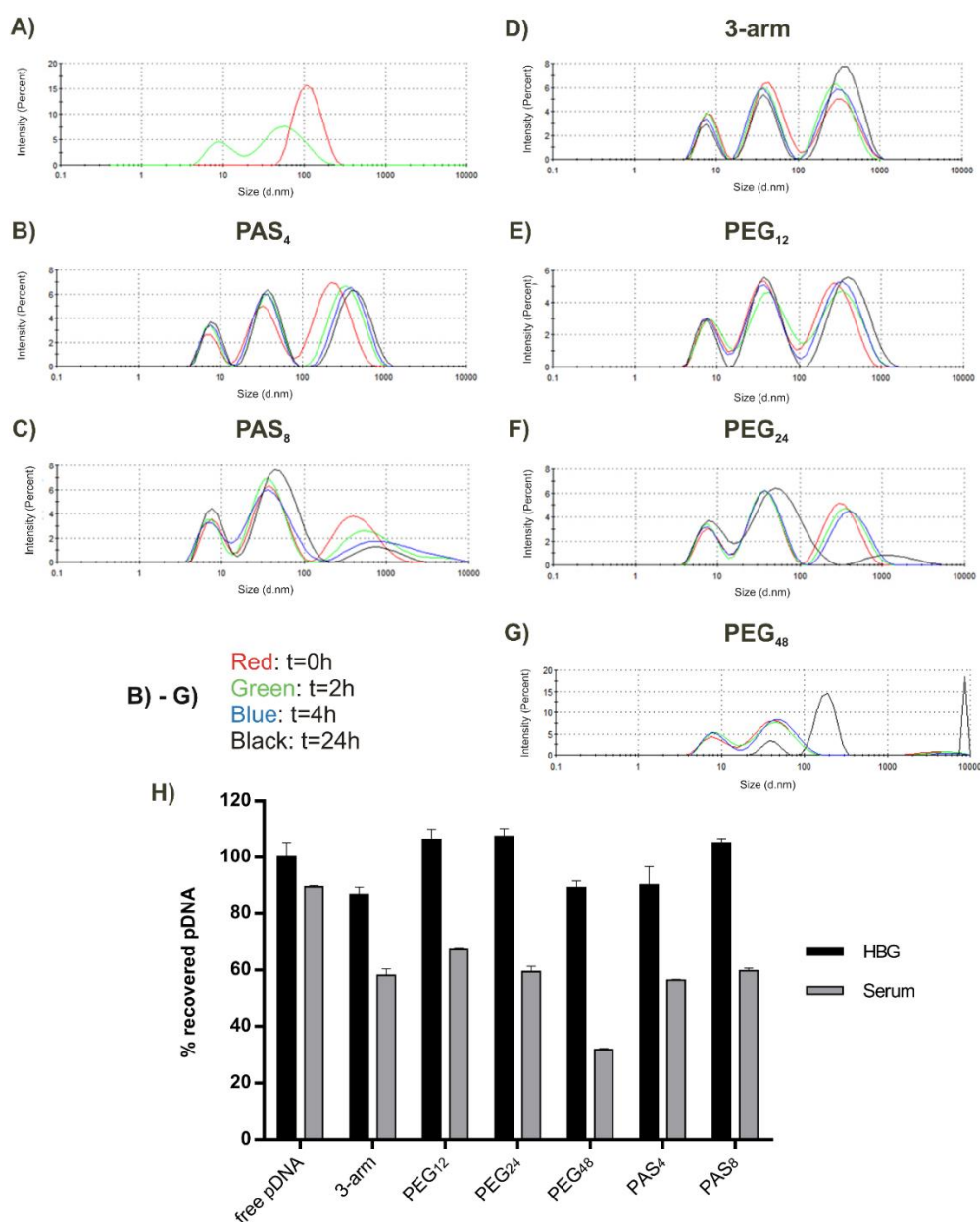


Figure 9 (A) DLS measurements of 90% fetal bovine serum (FBS, green) and pDNA polyplexes of the three-arm oligomer in HBG (red) as references to discriminate polyplex and serum peaks; (B–G) Display behavior of polyplexes with indicated oligomers in 90% FBS over time. In (H), the amount of recovered pDNA of polyplexes containing Cy5-labeled pDNA after treatment with 3500 IU heparin is displayed after incubation with FBS for 30 min; HBG-treated polyplexes served as control.

3.1.6 Tumor cell interactions *in vitro*

Different interactions of our polyplexes were investigated on N2a (mouse neuroblastoma) cells. In **Figure 10A,B** cellular binding is shown. Only polyplexes decorated with PEG₄₈ showed strong shielding against unspecific binding within 30 min of interaction with cells.

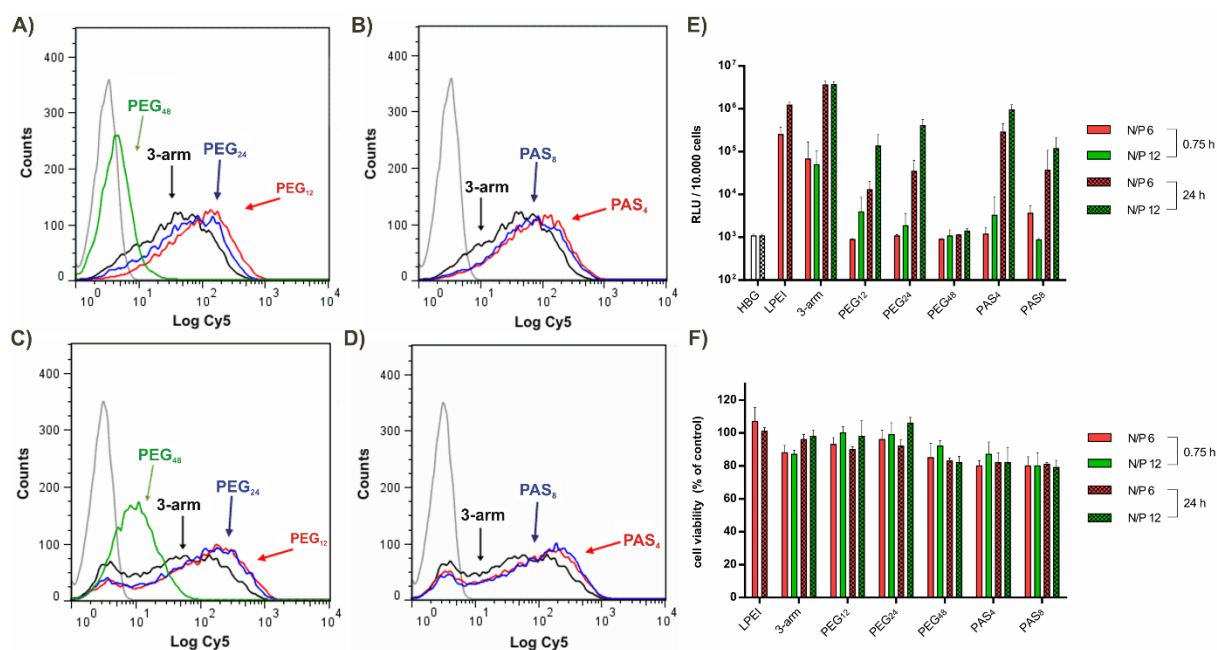


Figure 10 In (A,B) cellular association of polyplexes with N2a cells after 30 min incubation at 4 °C as determined by flow cytometry is plotted; In (C,D) cellular internalization of polyplexes after 45 min incubation at 37 °C followed by removal of extracellularly-bound polyplexes is displayed; Logarithmic X-scale in (A–D) represents Cy5 fluorescence of polyplexes; (E) Luciferase reporter gene expression in N2a cells after 0.75 h (**without pattern**) and after 24 h (**with pattern**). Transfections were performed at two different ratios: N/P = 6 (**red**) and N/P = 12 (**green**). (F) Cell viability assay was performed in parallel. Assays were performed by Ana Krhac Levacic (PhD study, Pharmaceutical Biotechnology, LMU).

Figure 10C,D displays cellular uptake within 45 min of incubation on cells. Again, only PEG₄₈ polyplexes did not interact with cells and did not mediate significant uptake. In **Figure 10E**, gene transfer activity is shown after 0.75 h and 24 h at N/P ratios 6 and 12. After the early 0.75 h time point, only unshielded three-arm and LPEI polyplexes caused notable gene transfer, while after 24 h of incubation, all polyplexes showed similar transfection efficacy; it is noteworthy that they were as efficient as LPEI. None of the polyplexes mediated cytotoxicity at any time point (cf. **Figure 10F**). These results

suggest that rapid binding and cellular uptake takes place only in case of unshielded cationic polyplexes (three-arm, LPEI) with sufficient critical endosomal amount of cationic proton sponge carrier required for efficient endosomal escape and transfection [26, 71, 202]. In case of oligoaminoamide carriers with short shielding elements, the internalized amounts of polyplexes increases over time, reaching sufficient levels for endosomal escape. Only for PEG₄₈ polyplexes, notable transfection is not even reached after 24 h. Either the critical amount for endosomal escape is not reached, or the longer PEG domain hampers the endosomal membrane disruption. The widely known effect that introduction of PEG into cationic transfection complexes can reduce transfection efficacy has been referred to as the “PEG dilemma” [163]. For PEI-type polyplexes, it has been assumed that a combined effect of osmotic endosomal burst and direct phospholipid destabilization by the cationized carrier is required for endosomal escape [1, 143, 147, 166]; obviously, PEGylation can hinder the direct cationic membrane destabilization. Consistently, bioreversible PEGylation was demonstrated to resolve this dilemma [163, 165, 172].

3.1.7 Tumor cell interactions *in vitro* without and with targeting

For this study, a phage-derived peptide (cmb) binding specifically to the HGF receptor cMet [191, 201] was introduced into our oligomers via modification at the α -amine of the c-terminal lysine. A complete list of cmb-containing oligomers can be found in **Table 9**. cMet is widely overexpressed in epithelial-derived tumors as well as stromal and interstitial cell-derived tumors (e.g., sarcomas) [185], and was pointed out previously as a suitable target for tumor targeting [65, 181, 201]; introduction of cmb into sequence-defined oligomers improved transfection efficacy over untargeted controls *in vitro* and *in vivo* [64, 65].

In the current work, transfections of two cMet–overexpressing cell lines, the prostate cancer cell line DU145 (cf. **Figure 12A**) and the hepatocellular cancer cell line Huh7 (cf. **Figure 12B**) - were carried out with polyplexes without or with a cMet targeted ligand. Receptor levels of both cell lines are displayed in **Figure 11**.

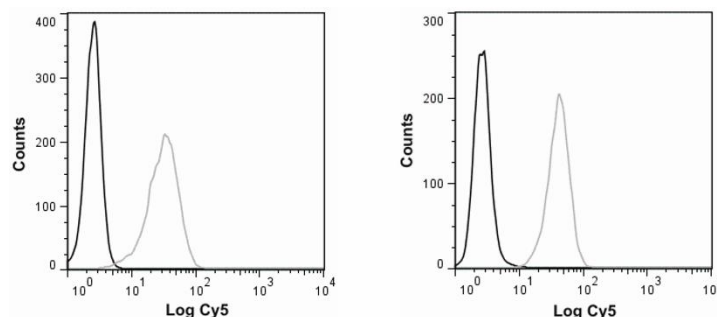


Figure 11 HGFR expression of HGFR/cMet positive DU145 (left) and Huh7 (right) cell lines are displayed, obtained with a monoclonal mouse anti-human HGFR antibody and IgG control. Alexa 488-labeled goat anti-mouse secondary antibody was used for the detection of receptor expression by flow cytometry. Control cells are presented in black, HGFR positive cells are presented in grey. Receptor levels were determined by Ana Krhac Levacic (PhD study, Pharmaceutical Biotechnology, LMU).

Table 9 List of cMet targeted oligomers. cmb represents cMet binding peptide, structures from N to C terminus, as well as an abbreviation used within the paper. # indicates internal library compound IDs

| ID # | Structure | Abbreviation |
|------|--|-----------------------|
| 1078 | cmb-[(C-(H-Stp) ₃ -H) _{α,ε} -K-H-(Stp-H) ₃] _ε K | cmb-3-arm |
| 996 | cmb-[(C-(H-Stp) ₄ -H) _{α,ε} -K-H-dPEG ₁₂] _ε K | cmb-PEG ₁₂ |
| 442 | cmb-[(C-(H-Stp) ₄ -H) _{α,ε} -K-H-dPEG ₂₄] _ε K | cmb-PEG ₂₄ |
| 694 | cmb-[(C-(H-Stp) ₄ -H) _{α,ε} -K-H-dPEG ₂₄ -dPEG ₂₄] _ε K | cmb-PEG ₄₈ |
| 1000 | cmb-[(C-(H-Stp) ₄ -H) _{α,ε} -K-H-(PAS) ₄] _ε K | cmb-PAS ₄ |
| 901 | cmb-[(C-(H-Stp) ₄ -H) _{α,ε} -K-H-(PAS) ₈] _ε K | cmb-PAS ₈ |

With both cell lines, results were consistent with the previous N2a transfections; short-term incubations with polyplexes for 45 min only mediated moderate gene transfer, while higher gene expression was observed after a longer transfection time of 24 h. Transfection of Huh7 with cmb-PAS₈ (no increase with time) presents an exemption from this rule. In case of the PEG₁₂ containing polymer, we observed an elevating effect of the introduction of the cmb targeting peptide on transfection efficacy. Further on, transfection efficacy of PEG₁₂ decorated polyplexes tended to be higher than with PEG₂₄-decorated polyplexes. This increased transfection efficacy could be affiliated with the beneficial compact, rod-like structure of PEG₁₂-containing polyplexes [207]. MTT assays for both cell lines were also performed in parallel to transfections, and did not show notable cytotoxicity at any time point (cf. **Figure 13**). In addition to the

transfections of cMet-positive cell lines, transfections of receptor negative N2a cells (for 0.75 h and 24 h) with targeted polyplexes can be found in **Figure 14A**. No significant gene transfer was observed after 0.75 h. After 24 h, polyplexes had been taken up unspecifically and caused notable gene transfer in the case of cmb-3-arm, cmb-PEG₁₂, and cmb-PEG₂₄. cmb-PAS₄ and cmb-PAS₈ hardly mediated any gene transfer. Cytotoxicity was not observed (cf. **Figure 14B**).

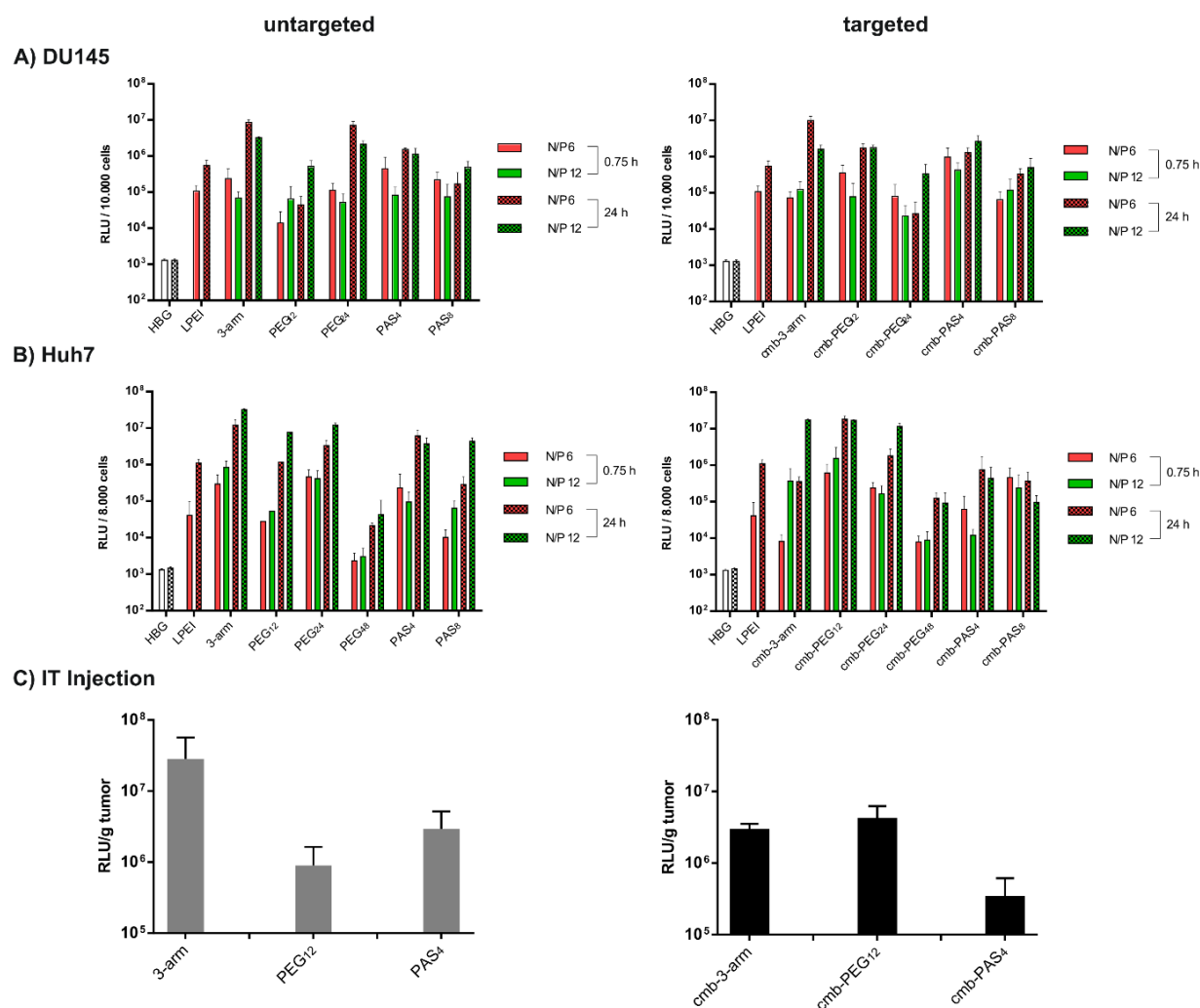


Figure 12 (A) Luciferase reporter gene expression in human prostate cancer cell line DU145 as well as in **(B)** human hepatocellular cancer cells Huh7 after 0.75 h (without pattern), and after 24 h (with pattern). Transfections were performed at two different ratios: N/P = 6 (red) and N/P = 12 (green); **(C)** Luciferase gene expression at 48 h after intratumoral administration of pCMVLuc polyplexes at N/P = 12 into Huh7 tumor-bearing mice. Luciferase gene expression is presented as relative light units per gram tumor (RLU/g tumor; n = 5, mean ± SEM). Lysis buffer RLU values were subtracted. Transfections on DU145 cell line and ex vivo Luc assay were performed by Ana Krhac Levacic (PhD study, Pharmaceutical Biotechnology, LMU), transfections on Huh7 were performed by Sarah Urnauer (PhD study, University Hospital of LMU, Department of Internal Medicine IV) and animal experiments were carried out by Sarah Kern and Jasmin Kuhn (PhD studies, Pharmaceutical Biotechnology, LMU).

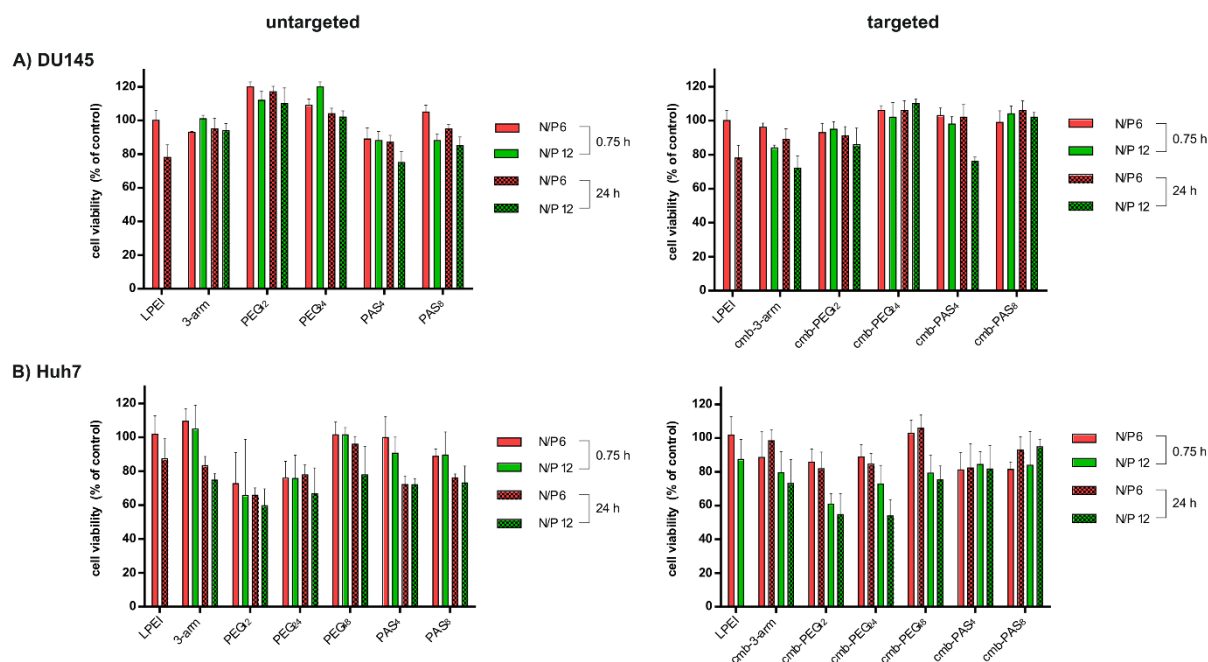


Figure 13 Cell viability assay of (A) DU145 and (B) Huh7 was performed in parallel to luciferase transfection. An MTT assay was performed after 0.75 h (without pattern), and after 24h (with pattern) at two different N/P ratios, N/P = 6 (red) and N/P = 12 (green). MTT Assays were performed by Ana Krhac Levacic (PhD study, Pharmaceutical Biotechnology, LMU) for DU145 cells and by Sarah Urnauer (PhD study, University Hospital of LMU, Department of Internal Medicine IV) for Huh7 cells.

3.1.8 Tumor cell interactions *in vivo* without and with targeting

An *in vivo* experiment was the next logical step to further evaluate the potency of our oligomers. As a first step, intratumoral application into a subcutaneous Huh7 mouse model was chosen. Kos et al. [64] pointed out in the same model that polyplexes formed with cmb-PEG₂₄ were superior to cmb-PEG₄₈ in gene transfer. Therefore, in the current experiments, untargeted as well as targeted polyplexes of 3-arm, PEG₁₂, and PAS₄ were intratumorally injected into mice. Untargeted, unshielded 3-arm mediated the highest gene transfer, as already observed *in vitro* (see **Figure 10E** and **Figure 12A,B**). This might be explained by the local stickiness of unshielded surface and in the tumor. At the same time, polyplexes with PEG₁₂ mediated decreased transgene expression, indicating a successful shielding *in vivo*. By introduction of targeting peptide cmb into PEG₁₂-shielded polyplexes, transfection efficacy was recovered again. Overall, luciferase gene expression was also increased as compared to cmb-PEG₂₄ [64], which extends the already previously observed trend of increasing gene transfer activity with decreasing PEG length (PEG₄₈ < PEG₂₄ < PEG₁₂).

Interestingly, recent work with LPEI polyplexes [32] also reported favorable properties for incorporating targeting peptides via a 500–700 Da PEG molecule, which has similar size as PEG₁₂.

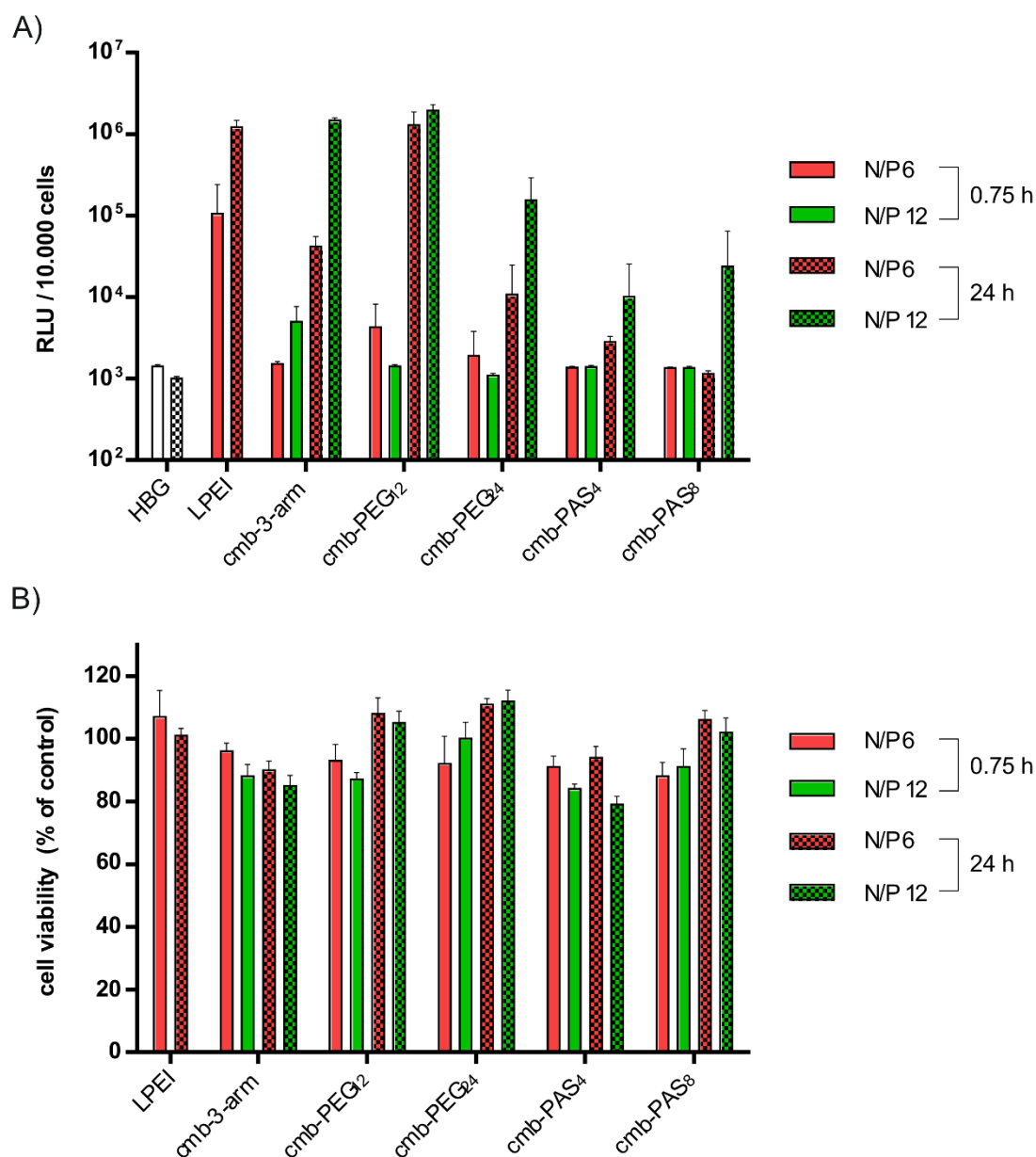


Figure 14 (A) Luciferase reporter gene expression in cMet negative cell line N2a after 0.75 h (without pattern) and after 24 h (with pattern). Transfections were performed at two different N/P ratios, N/P = 6 (red) and N/P = 12 (green). **(B)** An MTT assay was performed after 0.75 h (without pattern) in parallel after 24 h (with pattern) at two different N/P ratios, N/P = 6 (red) and N/P = 12 (green). Assays were performed by Ana Krhac Levacic (PhD study, Pharmaceutical Biotechnology, LMU).

3.2 EGFR targeting and shielding of pDNA lipopolyplexes via bivalent attachment of a sequence-defined PEG agent

This chapter has been adapted from:

Morys S.*, Urnauer S.*, Spitzweg C., Wagner E., *EGFR Targeting and Shielding of pDNA Lipopolyplexes via Bivalent Attachment of a Sequence-Defined PEG Agent*, *Macromol. Biosci.* **2017**. (* indicates that authors contributed equally to this work)

Stephan Morys thereby designed the study, developed and synthesized the oligomers and PEGylation reagents, and carried out biophysical experiments (e.g. DLS, EtBr compaction assay, Ellman's assay, NPys release assay, polyplex stability assays), while Sarah Urnauer conducted all cell related experiments (association and uptake assays via FACS, receptor screening, transfections and iodide uptake assay). The draft manuscript was written together.

For successful non-viral gene delivery, cationic oligomers are promising DNA carriers which need to comprise several functionalities. Shielding and directing polyplexes specifically towards the tumor by introduction of a specific targeting molecule or peptide represents two important characteristics for gene delivery. Therefore, the cationic oligomers can be either pre-PEGylated and a targeting ligand can be introduced during synthesis, or polyplexes can be post-modified with PEG reagents comprising a targeting domain. The latter was recently successfully applied for siRNA lipopolyplexes by introduction of an EGFR targeted GE11-PEG reagent via cysteine dependent maleimide chemistry [170]. Within this chapter, this approach has been transferred to pDNA/lipopolyplexes and further optimized in regards of chemistry. Here, the bis-oleoyl-oligoaminoethanamide **454** containing tyrosine trimer - cysteine ends was applied for complex formation with pDNA coding for luciferase or sodium iodine symporter (NIS). In a second step, the lipopolyplexes were modified via disulfide formation with sequence-defined monovalent or bivalent PEGylation reagents containing one or two 3-nitro-2-pyridinesulfenyl (NPys)-activated cysteines, respectively. For targeting, the PEG reagents comprise the EGFR targeting peptide GE11. Polyplexes were investigated for their biophysical properties as well as EGFR specificity on different cell lines *in vitro*.

3.2.1 pDNA nanoparticle design, peptide and oligomer syntheses

As published in 2001 by Blessing et al [168], EGF-PEG-PEI pDNA polyplexes were successfully generated by two different methods; either via pre-conjugation of PEI (25 kDa) with EGF before pDNA complex formation, or by post-modification of previously formed PEI/pDNA polyplexes. Also in the current study, the pre- and post-modification strategy was compared for generation of EGFR-targeted polyplexes. Instead of PEI 25kDa, in the novel investigation shorter sequence-defined oligomers were applied as pDNA carriers, with far higher biocompatibility and chemical precision (cf. **Table 10**). Instead of EGF as targeting ligand, the phage-display derived EGFR targeting peptide GE11 (YHWYGYTPQNVI) [198] was applied; and instead of polydisperse PEG linkers, a precise monodisperse PEG of exactly 24 ethylenoxide repeats (dPEG₂₄) was used. Like all other components, also the PEG reagents required for the post-modification strategy (cf. **Table 11**) were synthesized in precise fashion by solid-phase synthesis as described in **2.2.1.4**. Analytical data can be found in the appendix (cf. **6.5**).

Table 10 List of oligomers as pDNA carriers used in this study. An internal ID, an abbreviation as well as its sequence (N to C terminus) are displayed. Detailed chemical structures can be found in **Figure 15**

| ID # | Structure | Abbreviation |
|------------|---|-----------------------------------|
| 440 | (C-(H-Stp) ₄ -H) _{α,ε} -K-dPEG ₂₄ -A | 2-arm-PEG ₂₄ -His-Ala |
| 454 | C-Y ₃ -Stp ₂ -K-(K(OleA) _{α,ε})-Stp ₂ -Y ₃ -C | T-shape |
| 835 | (C-(H-Stp) ₄ -H) _{α,ε} -K-dPEG ₂₄ -YHWYGYTPQNVI | 2-arm-PEG ₂₄ -His-GE11 |

The pre-conjugation strategy is based on a 2-arm oligomer topology of ligand-PEG-Stp/His, which had already proven as effective for receptor targeted gene transfer *in vitro* as well as *in vivo* for several receptor/ligand combinations [50, 64, 65, 137]. Four cationizable alternating Stp/histidine repeats provide effective nucleic acid binding and endosomal buffering [50, 203], a lysine as symmetrical branching point links the dPEG₂₄ molecule, which is end-modified with the targeting ligand. In the current case, the EGFR targeted oligomer **835** contains GE11, whereas the analogous control structure **440** contains alanine instead (cf. **Table 10** and **Figure 15**). These oligomers also contain terminal cysteines for polyplex-stabilizing disulfide cross-link formation.

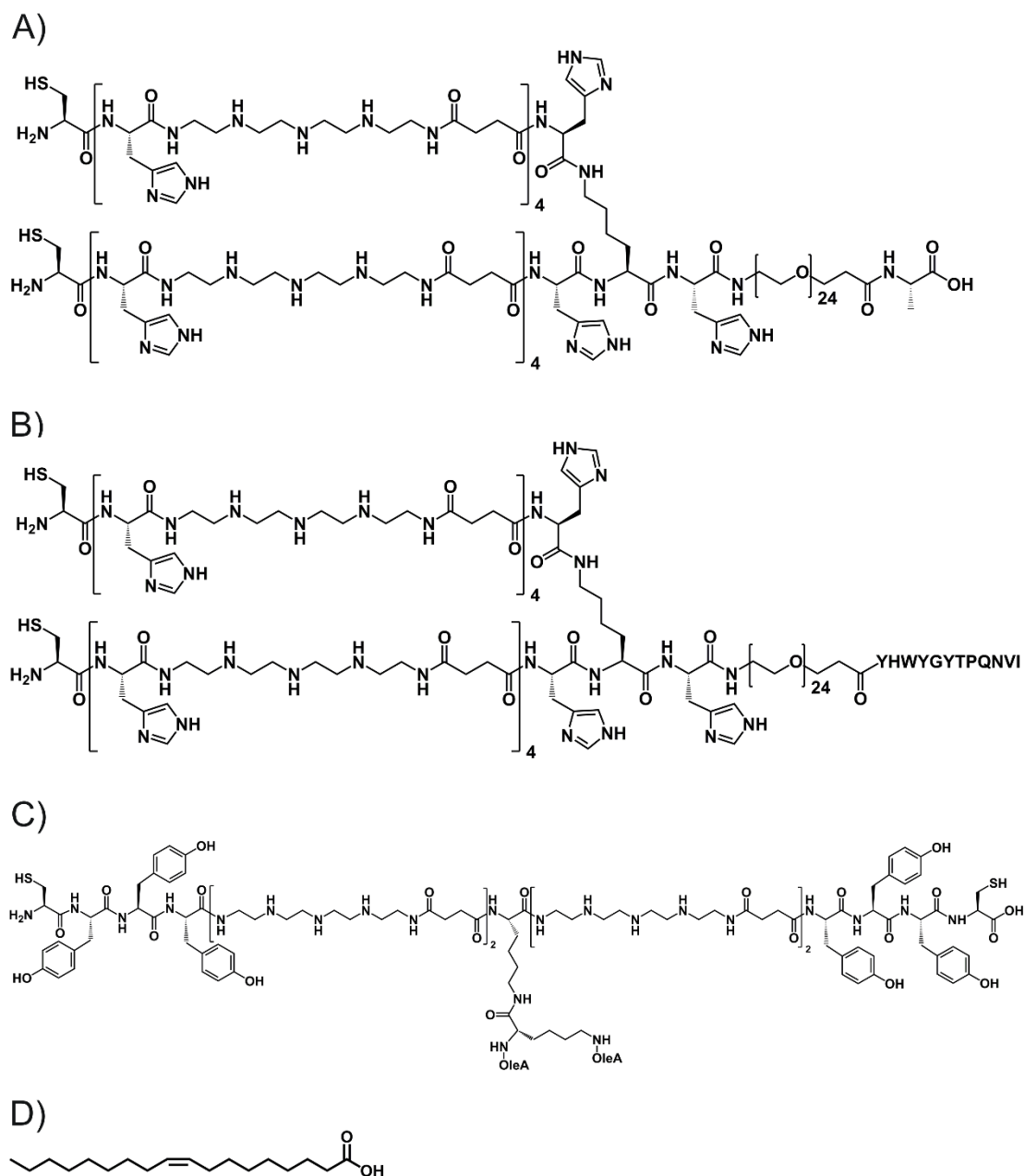
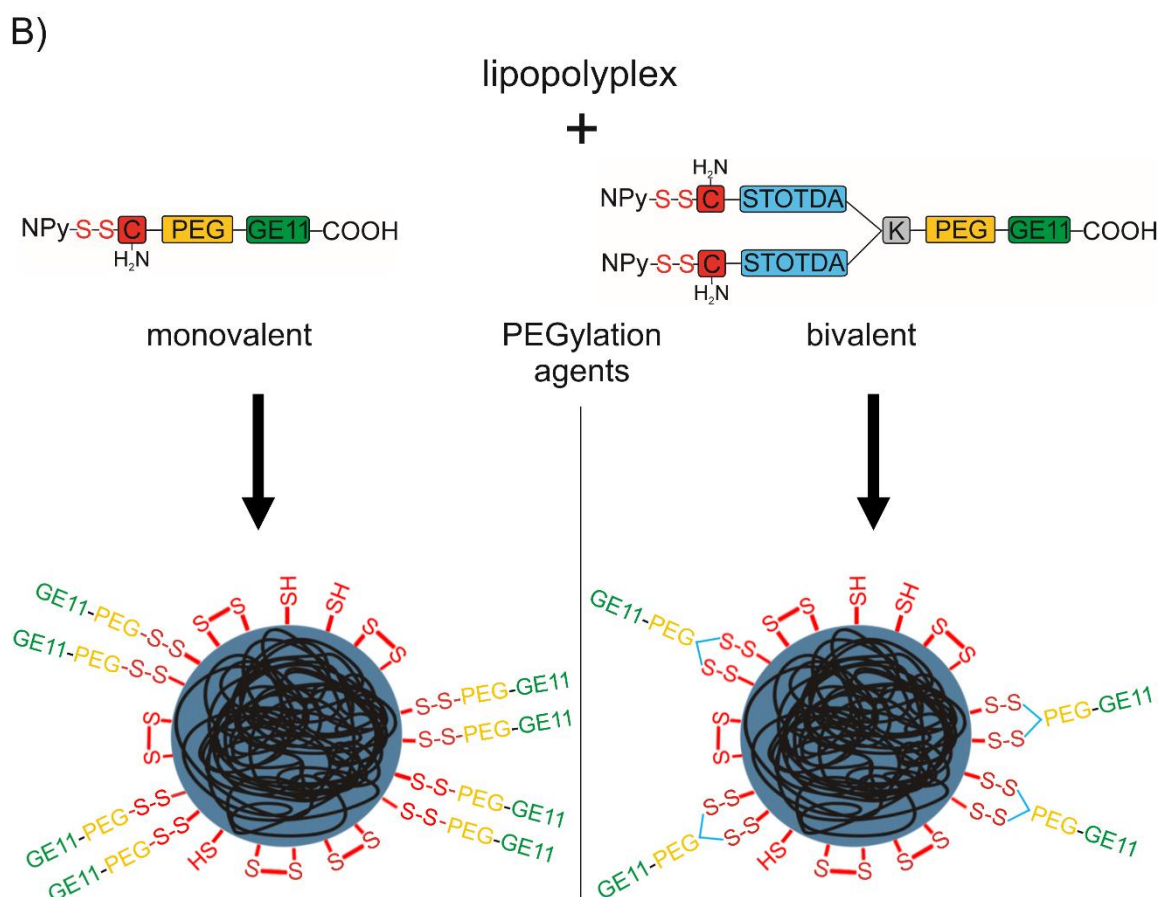
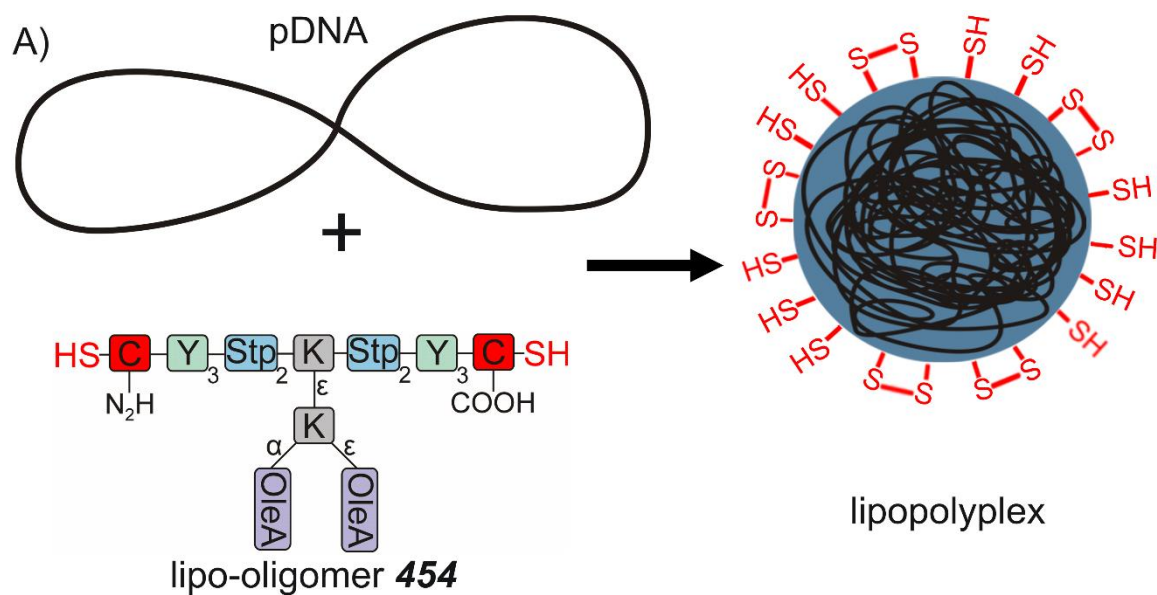


Figure 15 Chemical structures from N- to C- terminus of oligomers **440** (A), **835** (B) and **454** (C). Oleic acid (OleA) is shown in (D).

In the novel post-modification strategy (cf. **Scheme 5**), activated disulfide exchange chemistry was used for introduction of the targeted PEG reagents. Core pDNA lipopolyplexes were formed using the T-shaped lipo-oligomer **454**, which had been designed to mediate efficient siRNA knockdown due to its optimized structure [52].



Scheme 5 EGFR-targeted pDNA lipopolyplexes designed by post-modification of **454** (Table 10) core complexes with mono- or bi-valent PEG reagents (Table 11). (A) Lipopolyplex formation. (B) Post-PEGylation via disulfide exchange chemistry.

Four units of the cationizable artificial amino acid Stp (12 protonatable nitrogens in total) provide nucleic acid binding and endosomal buffering [50, 131, 134], two centrally

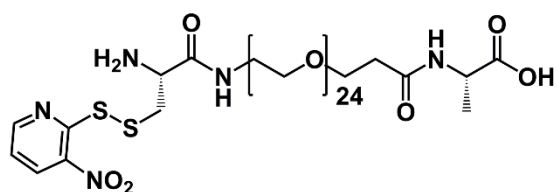
placed oleic acids contribute to hydrophobic polyplex stability and have lytic potential upon acidification within the endosome [49, 51, 52]. Peripheral tyrosine trimers (Y₃) increase polyplex stability via inter-oligomeral $\pi - \pi$ stacking of aromatic rings [208]; C-terminal as well as N-terminal cysteine residues provide additional, disulfide triggered polyplex stabilization [134] as well as anchors for the subsequent post-PEGylation. This oligomer has been extensively investigated as core oligomer for receptor dependent siRNA delivery *in vitro* as well as *in vivo*, e.g. via folate receptor [169], transferrin receptor [170] as well as EGFR [170], but has never been used as core carrier for receptor targeted pDNA delivery. Pre-PEGylation of **454** before polyplex formation was unsuccessful, resulting in polyplex aggregation (unpublished data).

For modification of **454**/pDNA polyplexes via activated disulfide exchange, monovalent or bivalent PEGylation reagents, comprising precise dPEG₂₄ with GE11 or alanine as control, were synthesized by SPS with introduction of Boc-L-Cys(NPys)-OH as terminal coupling. In case of the bivalent reagent, the diamino acid Fmoc-L-lysine(Fmoc)-OH was inserted for symmetrical branching following the PEG domain, and a short PEG spacer (STOTDA) was introduced for increasing flexibility of the reagent. The sequence was terminated by introduction of Boc-L-Cys(NPys)-OH on both branches.

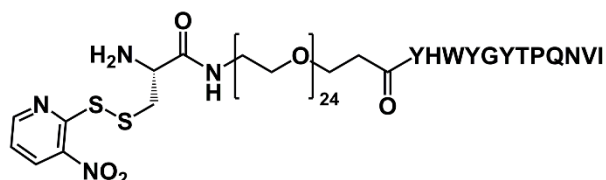
Table 11 Sequences of PEGylation reagents (N to C terminus) as well as used abbreviation are displayed. Detailed chemical structures can be found in **Figure 16**.

| ID # | Structure | Abbreviation |
|-------------|---|---|
| 1059 | Cys(NPys)-dPEG ₂₄ -A | Cys-PEG ₂₄ -Ala |
| 999 | Cys(NPys)-dPEG ₂₄ -YHWYGYTPQNV | Cys-PEG ₂₄ -GE11 |
| 1060 | (Cys(NPys)-STOTDA) _{α,ϵ} -K-dPEG ₂₄ -A | (Cys) ₂ -PEG ₂₄ -Ala |
| 1056 | (Cys(NPys)-STOTDA) _{α,ϵ} -K-dPEG ₂₄ -YHWYGYTPQNV | (Cys) ₂ -PEG ₂₄ -GE11 |

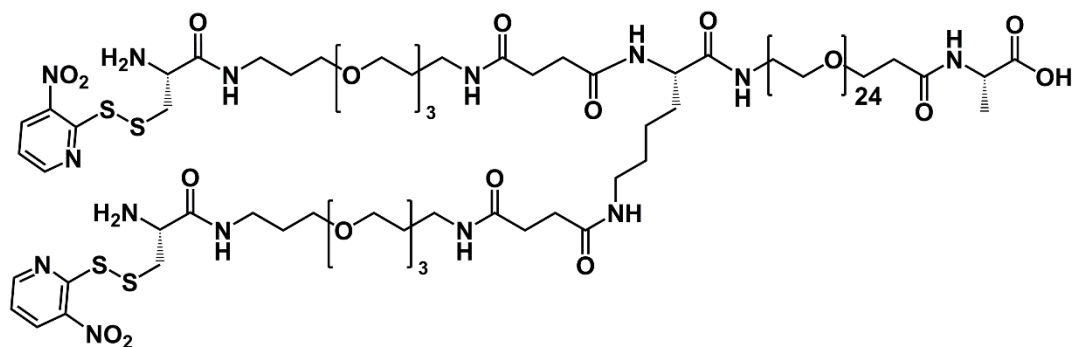
A)



B)



C)



D)

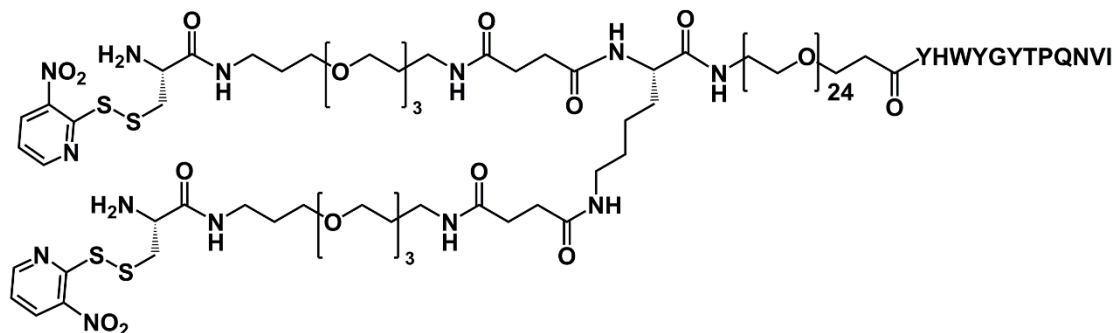
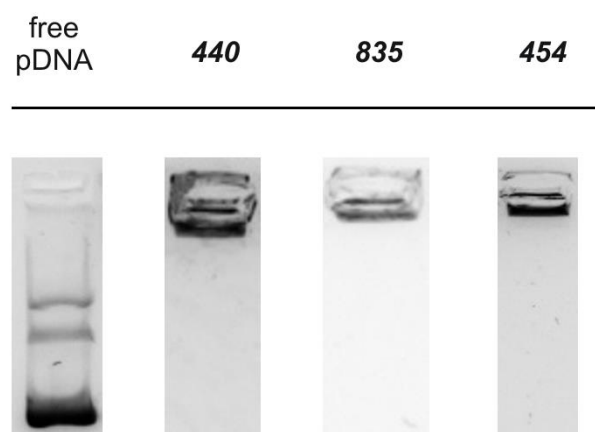


Figure 16 Chemical structures from N- to C- terminus of Cys(NPys)-dPEG₂₄-Ala (A), Cys(NPys)-dPEG₂₄-GE11 (B), (Cys(NPys)-STOTDA)_{α,ε}-K-dPEG₂₄-Ala (C) and (Cys(NPys)-STOTDA)_{α,ε}-K-dPEG₂₄-GE11 (D).

3.2.2 Physicochemical polyplex characterization

Oligomer/pDNA interaction was examined in different assays, focusing on pDNA binding ability, stability and compaction. Polyplexes with and without post-PEGylation were evaluated. First, complete binding of 200 ng of pDNA by oligomers at N/P 12 was verified by agarose gel electrophoresis shift assays (**Figure 17A**). N/P 12 was previously determined as the required ratio for complete pDNA binding of **454** and therefore was chosen for all further experiments [52]. Most important, it is to note that post-modification of **454** polyplexes did not influence pDNA binding, independent of the amounts attached to the core particle (**Figure 17B**).

A)



B)

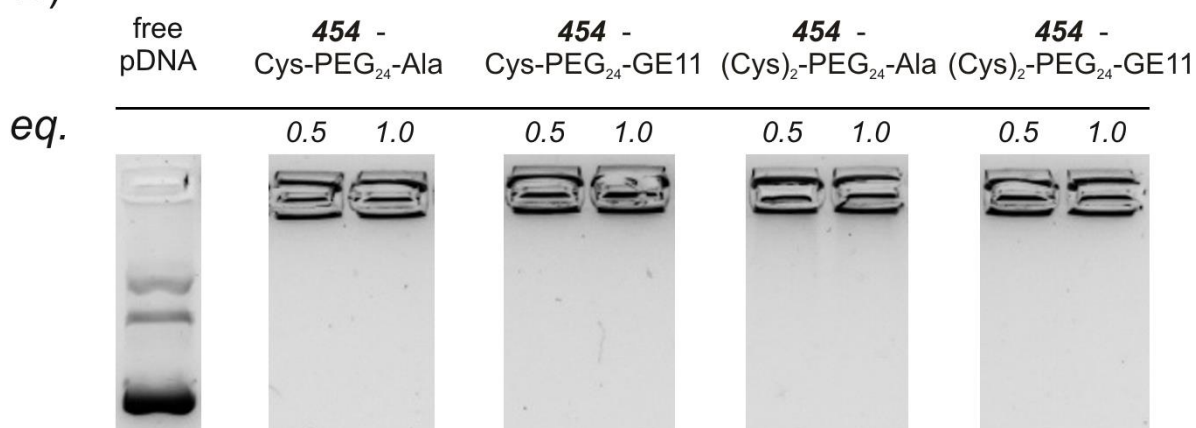


Figure 17 Retardation of formed pDNA complexes in agarose gel at N/P 12. (A) Pre-conjugated 2-arm-His-PEG₂₄ (**440** and **835**) as well as unmodified **454**. (B) Post-PEGylated **454** polyplexes with indicated PEGylation reagents.

Also, pre-PEGylated polyplexes, consisting of targeted or untargeted 2-arm-His-PEG₂₄ and 200 ng of pDNA, showed complete pDNA retention (**Figure 17A**) at N/P 12. It was reported that lower N/P ratios for these kinds of carriers were sufficient to completely bind pDNA [64, 133]. For reasons of comparability between post-PEGylated lipopolyplexes and pre-PEGylated 2-arm polyplexes, all further experiments were conducted with N/P 12. After pDNA binding was confirmed, particle sizes and zeta potential were determined by dynamic light scattering. Results of **454** (post-PEGylated) polyplexes revealed very homogenous particles with a polydispersity index (PDI) between 0.11 and 0.20, where 1.0 represents the highest polydispersity (cf. **Table 12**).

Table 12 Particle size (Z-average), PDI and zeta potential of pDNA polyplexes formed in HBG buffer determined with DLS. Mean of three measurements of the same sample is indicated. Polymer at N/P 12 and 2 µg pDNA were separately diluted with HBG pH 7.4 to 30 µL each. Then solutions were mixed and incubated for 30 min. If indicated, PEGylation was carried out with 0.5 eq or 1.0 eq for further 15 min. Polyplexes then were diluted to 800 µl with 10 mM NaCl pH 7.4 prior to measurement.

| ID # | Z-Average [nm] | Mean PDI | Mean zeta potential [mV] |
|---|----------------|-------------|--------------------------|
| 440 | 1367 ± 134.0 | 0.39 ± 0.11 | 1.2 ± 0.2 |
| 835 | 1947 ± 211.7 | 0.51 ± 0.04 | 4.5 ± 0.1 |
| 454 | 81.4 ± 5.2 | 0.18 ± 0.02 | 29.9 ± 1.3 |
| 454 - 0.5 eq Cys-PEG ₂₄ -Ala | 85.1 ± 1.3 | 0.13 ± 0.01 | 17.8 ± 0.3 |
| 454 - 1.0 eq Cys-PEG ₂₄ -Ala | 82.4 ± 0.4 | 0.15 ± 0.01 | 14.7 ± 0.9 |
| 454 - 0.5 eq Cys-PEG ₂₄ -GE11 | 95.2 ± 0.3 | 0.11 ± 0.01 | 20.8 ± 1.4 |
| 454 - 1.0 eq Cys-PEG ₂₄ -GE11 | 121.1 ± 0.8 | 0.12 ± 0.01 | 16.9 ± 1.3 |
| 454 - 0.5 eq (Cys) ₂ -PEG ₂₄ -Ala | 79.3 ± 0.5 | 0.18 ± 0.01 | 14.7 ± 0.8 |
| 454 - 1.0 eq (Cys) ₂ -PEG ₂₄ -Ala | 83.8 ± 0.8 | 0.12 ± 0.02 | 15.6 ± 0.9 |
| 454 - 0.5 eq (Cys) ₂ -PEG ₂₄ -GE11 | 189.0 ± 1.4 | 0.20 ± 0.02 | 22.0 ± 1.5 |
| 454 - 1.0 eq (Cys) ₂ -PEG ₂₄ -GE11 | 283.8 ± 0.4 | 0.17 ± 0.01 | 17.7 ± 2.0 |

PDI: Polydispersity index.

At the same time polyplexes formed with 2-arm PEG-oligomers **440** and **835** showed very inhomogeneous particle populations with a PDI between 0.4 and 0.5. This non-homogeneity resulted in D_H values (displayed as Z-Average in nm) of more than 1000 nm (cf. **Table 12**) for pre-PEGylated polyplexes. This could be explained by the high degree of PEGylation in comparison to a rather small cationizable pDNA compacting domain and the associated large amount of hydrophobic GE11 peptide; it is known that hydrophobic peptides tend to cause aggregation [209, 210].

Unmodified **454** polyplexes exhibited a size of approximately 80 nm. It is to note that the polyplex size increased after post-modification with the monovalent GE11 reagent up to 121 nm and with the bidentate reagent up to 284 nm (1.0 eq each). In contrast, post-PEGylation with alanine containing reagents (independent of its topology or amount up to 1.0 eq) did not influence polyplex size. Similar findings of increasing polyplex size after post-PEGylation were observed for **454**/siRNA polyplexes post-modified with GE11-PEG₂₈-maleimide [170]. In sum, these data indicate a special property of the hydrophobic GE11 ligand which can be better handled by the post-modification strategy. At the same time the zeta potential of post-shielded polyplexes was reduced from 30 mV (unmodified **454**) as far as 15 mV, thereby indicating the successful post-modification. To validate post-PEGylation, UV spectra of a **454** polyplex before and after addition of 1.0 eq of (Cys)₂-PEG₂₄-Ala was recorded and compared to the reagents solely. A change in absorbance around 350-400 nm compared to the unconjugated PEGylation agent demonstrates the successful release of NPys. Data can be found in **Figure 18**.

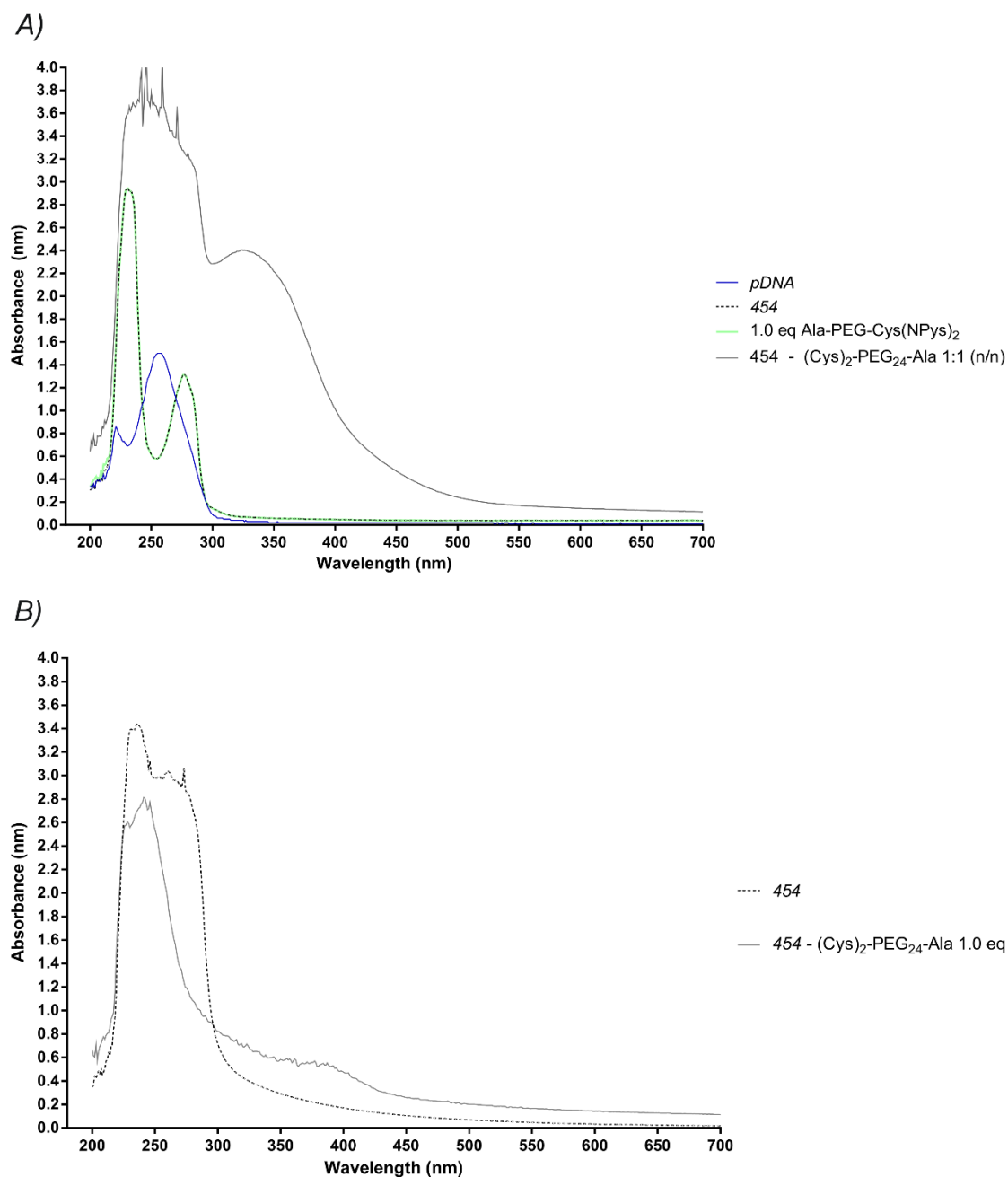


Figure 18 UV/Vis detection of PEGylation reaction. (A) 8 μg of pDNA, corresponding amount of **454** at N/P 12 and 1.0 eq of Ala-PEG₂₄-K-(STOTDA-Cys(NPys))₂ were used. **454** - (Cys(NPys)-STOTDA)₂-K-PEG₂₄-Ala mixed without pDNA served as positive control (mol Cys **454** / mol Cys(Npys)). (B) The same reagents were used to form polyplexes. **454**/pDNA, as well as **454**/pDNA PEGylated with 1.0 eq of (Cys)₂-PEG₂₄-Ala indicated successful reaction.

Further on, quantitative evidence of successful PEGylation of the **454**/pDNA lipopolyplexes is provided by determination of free lipo-oligomer thiols (**Figure 19A**) as well as release of 3-nitro-2-thiopyridone from the PEGylation reagent (**Figure 19B**).

Significant reduction of free thiols (100% in free oligomers) to approximately 80% after polyplex formation and to 15% after PEGylation was observed.

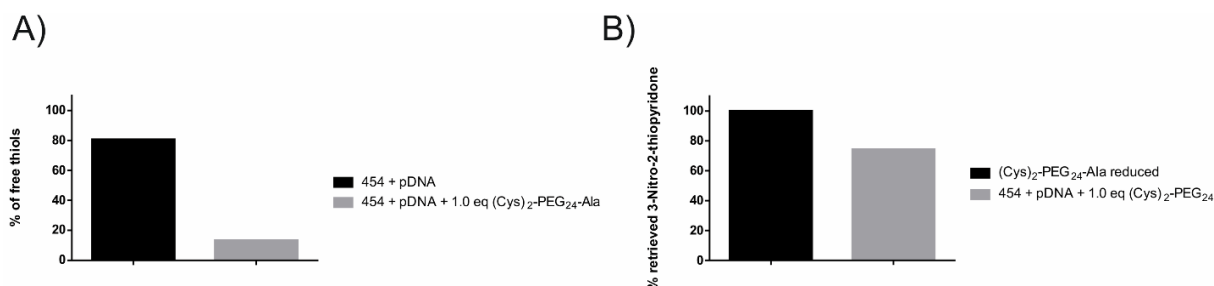


Figure 19 (A) Percentage of residual cysteine mercapto (SH) groups as determined with Ellman's assay for **454** polyplexes before (black) and after (grey) modification with 1.0 molar eq of (Cys)₂-PEG₂₄-Ala. The percentage of free mercapto groups is based on the theoretical amount (100%) of cysteines (two molar eq in Oligomer **454**) applied in the polyplex formation. (B) Release of 3-nitro-2-thiopyridone (detected at 324 nm) from 1.0 molar eq (Cys)₂-PEG₂₄-Ala after reduction. Complete 3-nitro-2-thiopyridone release after addition of 1M DTT solution (black bar) and after addition to a **454**/pDNA polyplex for further 15 min (grey bar) is displayed.

Next, transmission electron microscopy (TEM) was performed to investigate polyplex size and shape. In **Figure 20A** and **Figure 21A** TEM images of pre- as well as post-PEGylated polyplexes are shown. Polyplexes of **835** and **440** exhibited a homogeneous size of around 50 nm, appearing in short rods, while aggregation as determined by DLS, could not be seen. These findings indicate that bigger particles can either not be detected by TEM, or that they only occurred in minor extent, influencing size distribution by intensity in a severe manner.

At the same time, non-PEGylated **454** polyplexes form globules of around 40 nm, not undergoing significant changes due to post-modification, regardless of the topology of applied reagents (monovalent or bivalent). These findings suggest that the mean particle size could be much smaller as determined by dynamic light scattering, facilitating cellular uptake by standard pathways [175].

Next, the ability of the oligomers to compact pDNA was investigated by an ethidium bromide (EtBr) compaction assay. Interestingly, a significant difference between 2-arm-PEG₂₄-His and post-PEGylated **454** polyplexes was found (cf. **Figure 20B**). Within the first group, the remaining EtBr fluorescence was determined as more than 20%

(compared to untreated pDNA). In comparison to polyplexes formed with **440** and **835**, EtBr compaction of polyplexes formed with **454** was decreased by 50% to approximately 10% in total, even in case of post-functionalization with 1.0 eq.

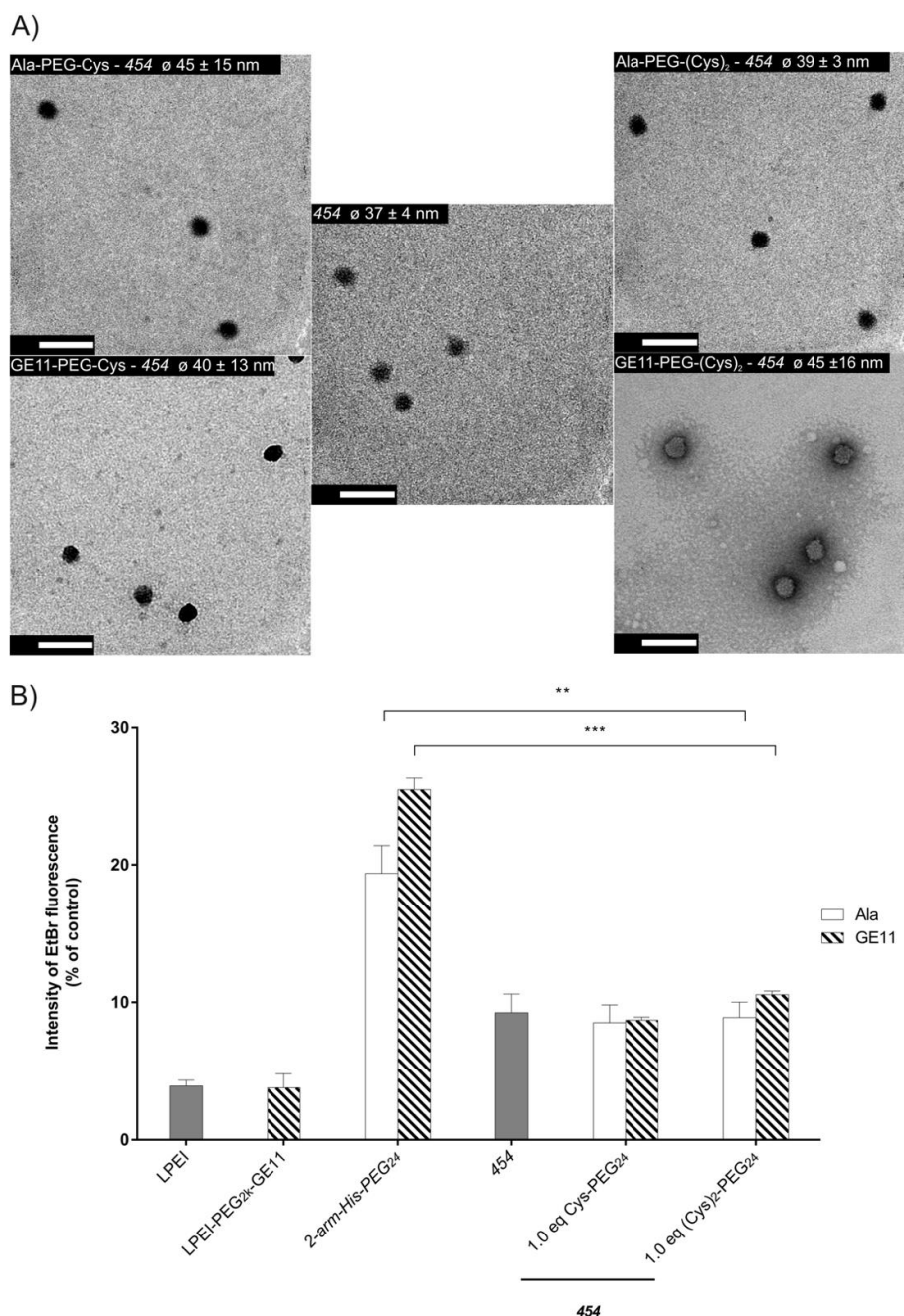


Figure 20 (A) Transmission electron microscopy images (TEM) of polyplexes formed with 1 μ g of pDNA at N/P 12. Average diameters (nm) of polyplexes ($n=5$) \pm SD are displayed. Scale bar represents 100 nm. (B) pDNA compaction of polyplexes determined with an EtBr assay. Untargeted controls are displayed in white, while polyplexes targeted with GE11 peptide are marked with pattern. For post PEGylation 1.0 eq was used, additional EtBr data can be found in **Figure 21**. TEM was performed by Susanne Kempter and Caroline Hartl (Faculty of Physics, LMU).

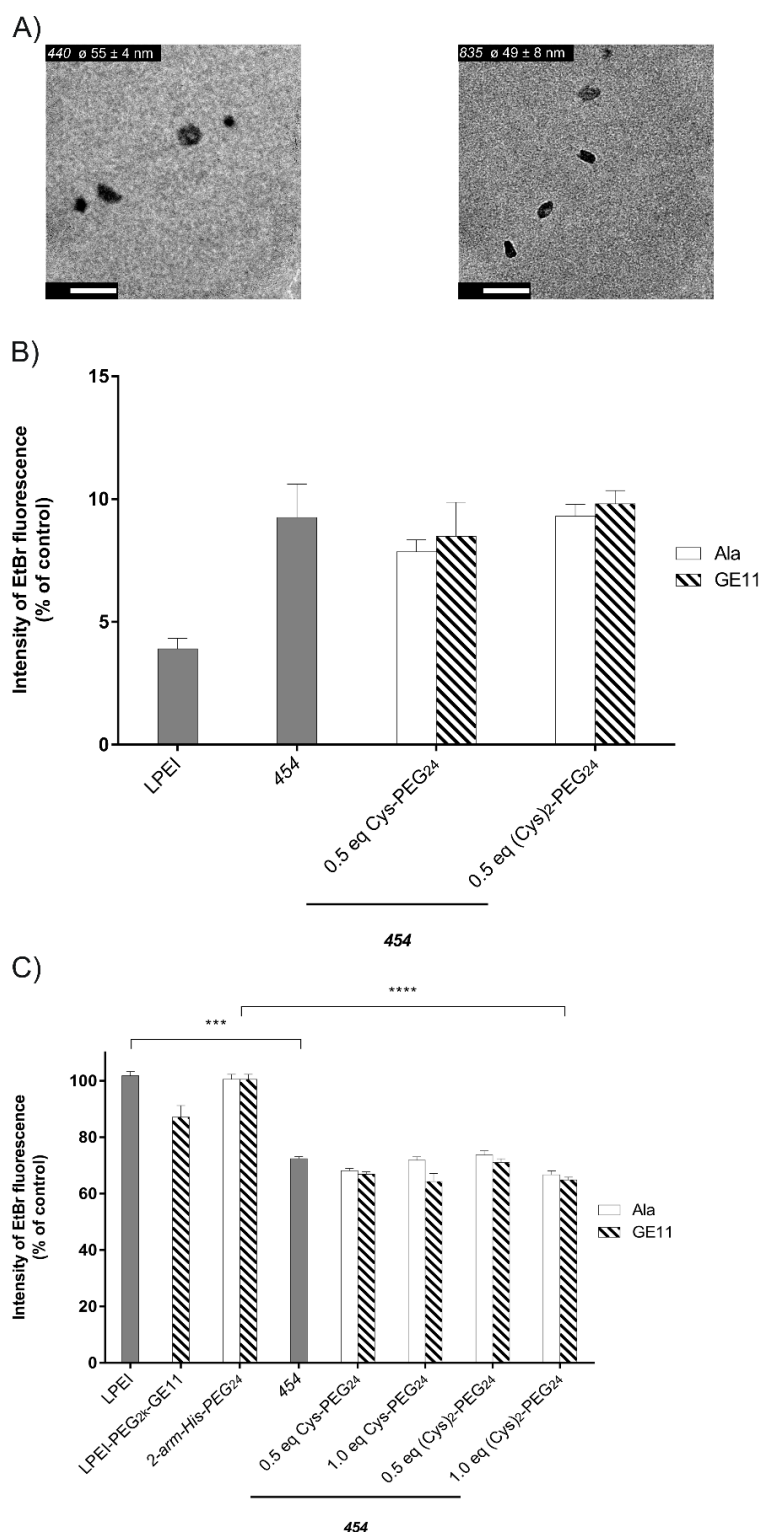


Figure 21 (A) Transmission electron microscopy images (TEM) of pre-conjugated polyplexes **440** and **835** formed with 1 μ g of pDNA at N/P 12. Average diameters (nm) of polyplexes ($n=5$) \pm SD are displayed. Scale bar represents 100 nm. (B) pDNA compaction of polyplexes post-PEGylated with 0.5 eq of reagents determined with EtBr assay. (C) Polyplex stability in presence of 250 IU heparin determined with EtBr assay. Untargeted controls are displayed in white, while polyplexes targeted with GE11 peptide are marked with pattern. TEM was performed by Susanne Kempter and Caroline Hartl (Faculty of Physics, LMU).

No difference between modified (data for 0.5 eq can be found in **Figure 21B**) and unmodified **454** polyplex was observed, indicating that post-PEGylation does not have an influence on pDNA compaction of the core particle. Also, no difference between C-terminal alanine or the GE11 peptide was found. The highest pDNA compaction nevertheless can be achieved by LPEI, a far larger polycation, with a remaining EtBr fluorescence of less than 5%. To the same samples 250 IU of heparin sulfate was added to determine anionic stress tolerance (**Figure 21C**). Here we found, as reported previously [133], that LPEI polyplexes are very sensitive, leading to 100% EtBr fluorescence corresponding to full pDNA release. These effects were minor pronounced for LPEI-PEG_{2k}-GE11, retaining approximately 13% pDNA, nevertheless they were notably increased in comparison to **454** based polyplexes, where only 70% could be released. By increasing the cationic charge, even better pDNA retention could be achieved. While no difference between unmodified **454**/pDNA polyplexes and post-PEGylated could be observed, pre-PEGylated polyplexes were also very prone to heparin stress and fully released pDNA. This could be explained by the increased size, also leading to looser polyplexes.

Stability of polyplexes in the protein environment presents a most critical issue. Therefore, polyplexes have been investigated by DLS after incubation with 10% FBS supplemented cell culture media or full serum (FBS). Pre-PEGylated polyplexes formed with **440** and **835** underwent immediate aggregation under both conditions (**Figure 22C-F**). Non-modified **454** polyplexes increased from 80 nm to 250 nm with no further changes over time. **454** polyplexes post-modified with the monovalent structures showed immediate size increase from 100 nm in 10 mM NaCl to approximately 200 nm in both conditions. Between 4 h and 24 h these polyplexes aggregated to particles >800 nm (**Figure 22I-L**). For **454** post-modified with 1.0 eq (Cys)₂-PEG₂₄-GE11 a size of 280 nm in 10 mM NaCl was determined that changed to approximately 300 nm after addition of full serum or cell culture media. Between 4 h and 24 h these polyplexes underwent no changes in full serum (**Figure 22O**). As in **454** polyplexes post-modified with the bivalent structures (Cys)₂-PEG₂₄-Ala/GE11 the aggregation was less profound, higher stability is suggested.

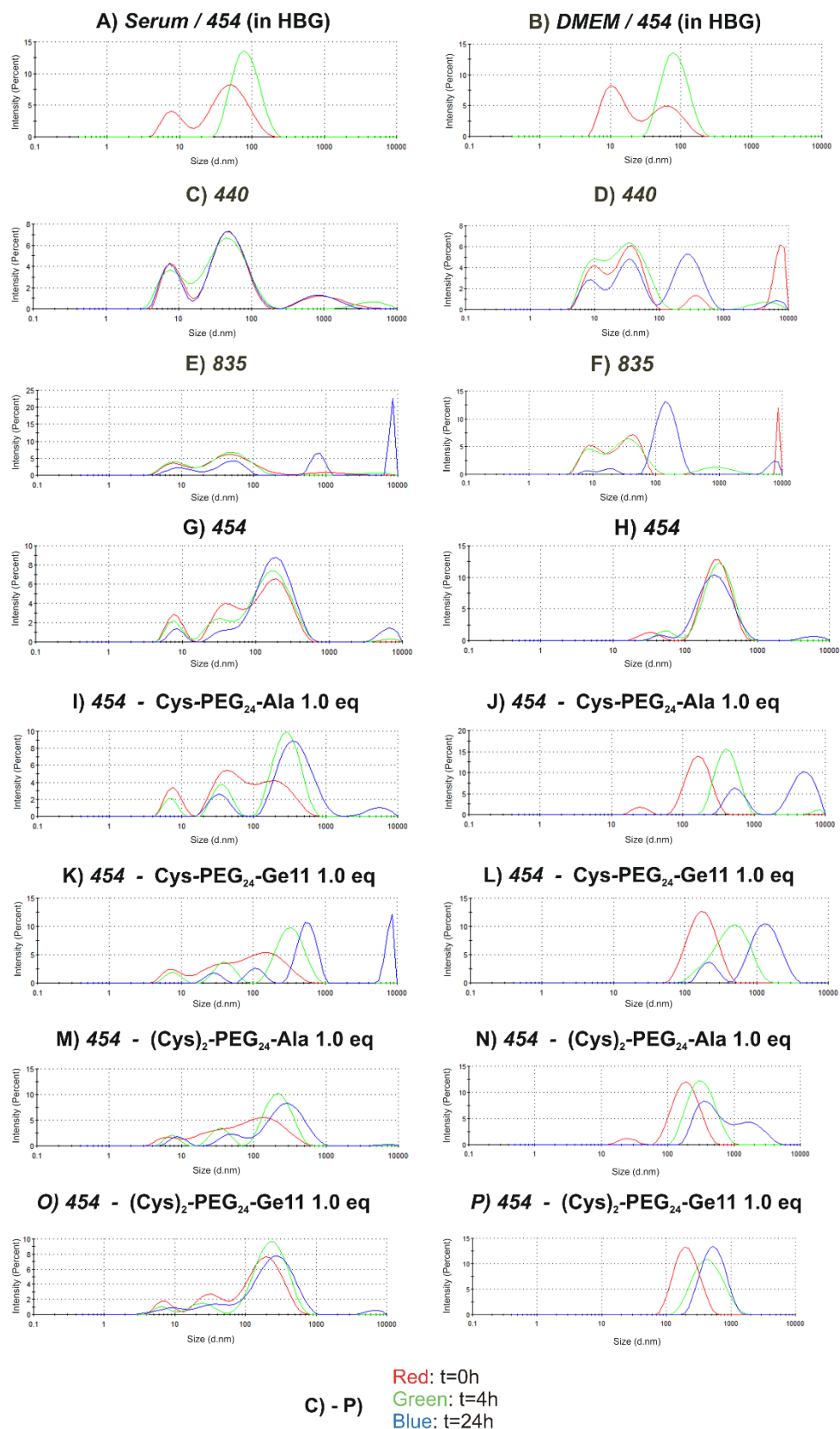


Figure 22 Intensity mean curves maintained by DLS. Full serum (A) or DMEM (supplemented with 10% FBS) (B) are displayed in green and polyplexes of the **454**/pDNA in 10 mM NaCl in red. These references should help to discriminate between polyplex and serum (left column) /media (right column) peaks. (C) - (P) Polyplexes with indicated oligomers in FBS (left) / DMEM (right) over time.

3.2.3 Luciferase gene transfections

Prior to pDNA transfections, EGFR expression levels of the three chosen cell lines were determined (cf. **2.2.14**). While the hepatocellular cell line Huh7 and the breast cancer cell line MCF-7 both showed high EGFR cell surface expression, the FTC-133 exhibited low EGFR cell surface expression (cf. **Figure 23**). For the subsequent luciferase gene transfections, cells were either incubated for 45 min or 24 h with pDNA complexes and luciferase intensity was determined after 24 h for Huh7 (cf. **Figure 24A**), MCF-7 (cf. **Figure 24B**) as well as FTC-133. Polyplexes post-PEGylated (with monovalent or bivalent polymers) were compared to PEG-free core particle complexes (**454**) and 2-arm histidine-containing pre-PEGylated polymers. LPEI-PEG_{2k}-GE11, which already has shown high transduction efficacy and EGFR specificity *in vitro* and *in vivo*, was used as positive control [63, 138, 192].

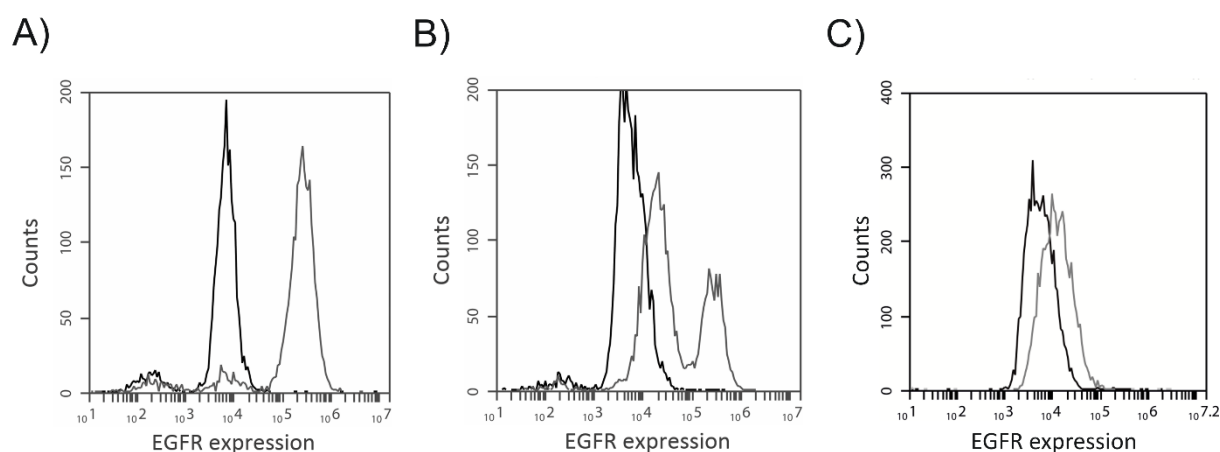


Figure 23 EGFR expression of EGFR positive cell lines Huh7 (A), MCF-7 (B) as well as low EGFR expressing cell line FTC-133 (C) are displayed, obtained with a monoclonal mouse anti-human EGFR antibody and IgG control. Alexa 488-labeled goat anti-mouse secondary antibody was used for the detection of receptor expression by flow cytometry. Control cells are presented in black, EGFR positive cells are presented in grey. Receptor screening was performed by Sarah Urnauer (PhD study, University Hospital of LMU, Department of Internal Medicine IV).

The EGFR-targeted bivalent structure (Cys)₂-PEG₂₄-GE11 coupled to **454** core polyplexes at a molar ratio of 1.0 eq demonstrated a strong EGFR-targeting effect, in contrast to the alanine containing structure on both receptor positive cell lines. Moreover, significantly higher expression levels compared to all other polymers were

detected. The pre-PEGylated polyplexes (**835** and **440 control**) revealed similar transfection level as LPEI-PEG_{2k}-GE11 in Huh7 cells and even lower results in MCF-7 cells. Based on sizes measured by DLS, which showed sizes over 1 μm for both pre-PEGylated polymers, transfection efficacy might be attributed to high aggregation and not due to specific uptake. Transfection of non-PEGylated **454** demonstrated equal (in Huh7) or slightly higher (MCF-7) expression level compared to LPEI-PEG_{2k}-GE11. None of the polyplexes mediated cytotoxicity after 45 min and 24 h of incubation (**Figure 25**).

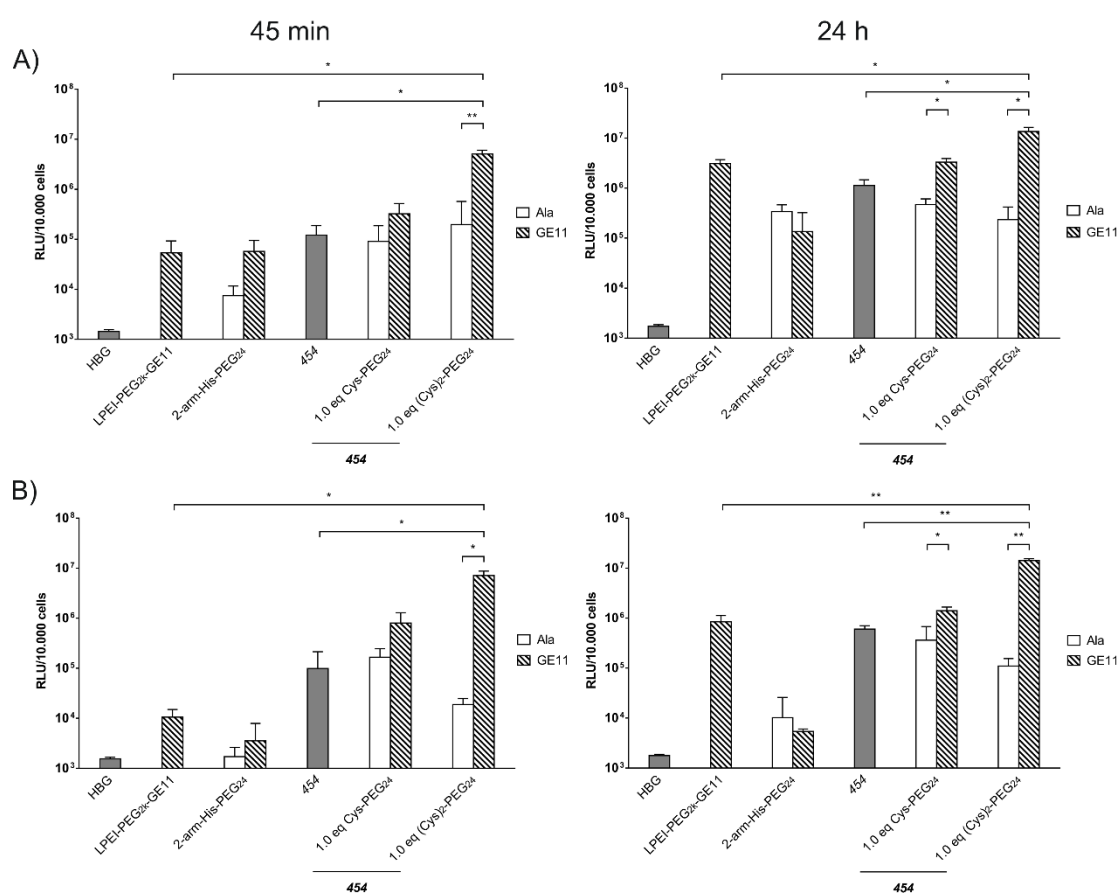


Figure 24 Luciferase reporter gene expression in two EGFR positive human cancer cell lines. (A) Human hepatocellular cancer cells Huh7 and (B) human breast cancer cell line MCF-7. pCMVLuc polyplexes were incubated on cells for 45 min (left) or 24 h (right). Untargeted controls are displayed in white, while polyplexes targeted with GE11 peptide are marked with pattern. Transfections were performed by Sarah Urnauer (PhD study, University Hospital of LMU, Department of Internal Medicine IV).

The EGFR-targeted bivalent structure (Cys)₂-PEG₂₄-GE11 coupled to **454** core polyplexes at a molar ratio of 1.0 eq demonstrated a strong EGFR-targeting effect in both cell lines, in contrast to the alanine containing structure. Moreover, significantly higher expression levels compared to all other polymers were detected. The pre-PEGylated polyplexes (**835** and **440 control**) revealed similar transfection level as LPEI-PEG_{2k}-GE11 in Huh7 cells and even lower results in MCF-7 cells. Based on sizes measured by DLS, which showed sizes over 1 μm for both pre-PEGylated polymers, transfection efficacy might be attributed to high aggregation and not due to specific uptake. Transfection of non-PEGylated **454** demonstrated equal (in Huh7) or slightly higher (MCF-7) expression level compared to LPEI-PEG_{2k}-GE11. None of the polyplexes mediated cytotoxicity after 45 min and 24 h of incubation (**Figure 25**).

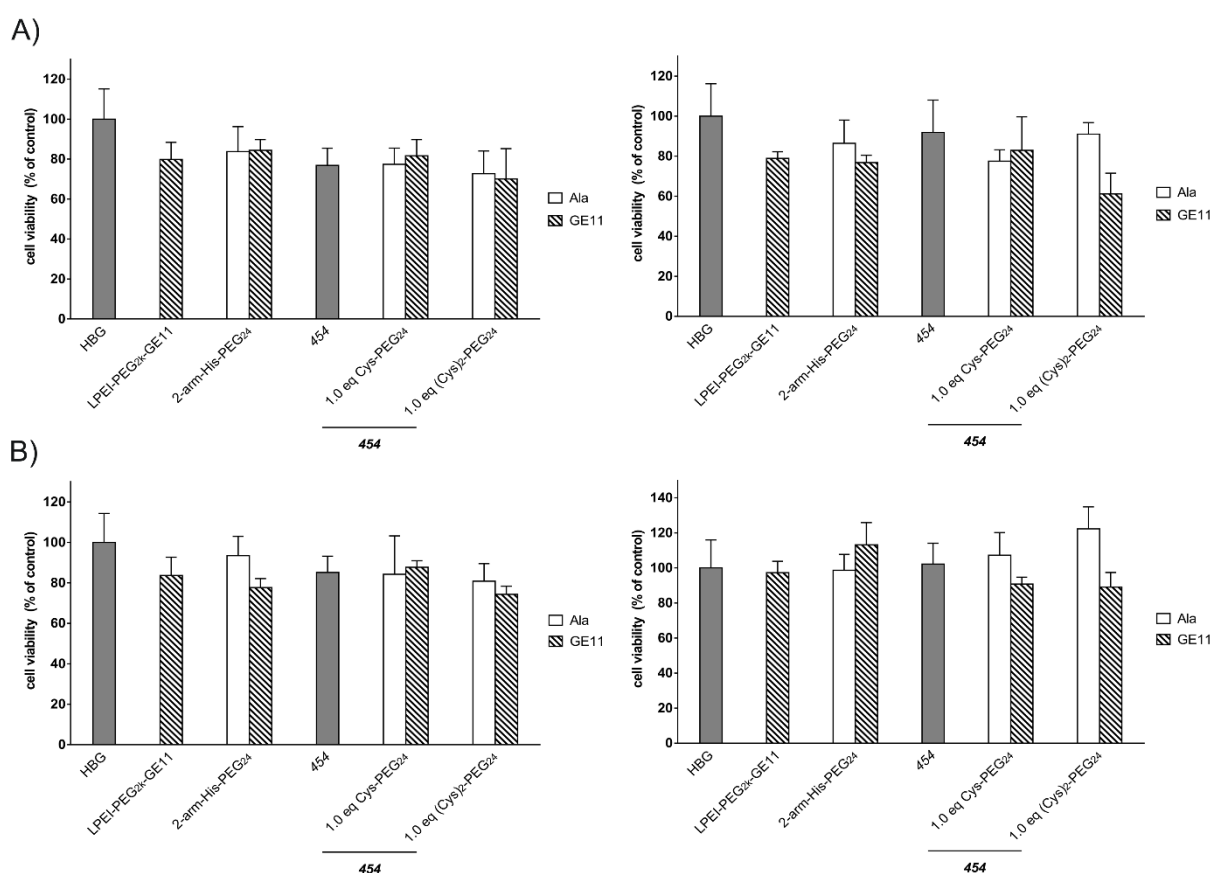


Figure 25 Cell viability assay of (A) Huh7 and (B) MCF-7 was performed in parallel to luciferase transfection. MTT was performed after 45 min (left), and after 24 h (right). Viability assays were performed by Sarah Urnauer (PhD study, University Hospital of LMU, Department of Internal Medicine IV).

For post-integration of PEG onto core polyplexes, monovalent and bivalent structures were compared at two different molar ratios. One eq proved to be more efficient than 0.5 eq. Results for 0.5 eq are displayed in **Figure 26A-B**, with no occurring cytotoxicity (cf. **Figure 26C-D**). Interestingly, transduction efficacy was not influenced by post-modification of **454** polyplexes with up to 1.0 eq of (Cys)₂-PEG₂₄-Ala in comparison to the unshielded core polyplexes, thereby highlighting this approach as possibility to circumvent the so-called “PEG-dilemma” of pre-PEGylated structures [163]. It is widely accepted that PEI-like polyplexes require a combined effect of osmotic endosomal eruption and direct phospholipid destabilization by the cationized vehicle for endosomal escape [1, 143, 166]. PEG obviously can interfere with this direct cationic membrane destabilization. Consistently, bioreversible PEGylation was introduced to resolve this dilemma [61, 62, 64] and also the disulfide conjugation of oligomer and PEG used in the present work could possibly be cleaved off by intracellular glutathion (GSH) as demonstrated in other work [111, 211, 212].

In comparison to Huh7 and MCF-7 cells that demonstrated strong EGFR dependency of transfection rates, this was not detected in low EGFR expressing FTC-133 cells. FTC-133 cells demonstrated no differences in transfection rates of post-PEGylated monovalent and bivalent structures coupled to either GE11 or Ala after 45 min incubation time. This further indicates the beneficial EGFR targeting strategy of polyplexes post-modified with GE11 targeted PEGylation reagents (cf. **Figure 27A**). At the same time, no polyplex mediated cytotoxicity was observed after 45 min of incubation (cf. **Figure 27B**).

After 24 h of polyplex incubation, an overall increased transduction efficacy was measurable due to unspecific uptake mechanisms that occur after long-time incubation. Due to residual positive charge polyplexes tend to adhere unspecifically to the negatively charged cell membrane and particles get taken up unspecifically over time, leading to a diminished targeting effect. Nevertheless, the advantageous bivalent conjugation of EGFR-targeted PEG to **454** is still evident after 24 h of incubation.

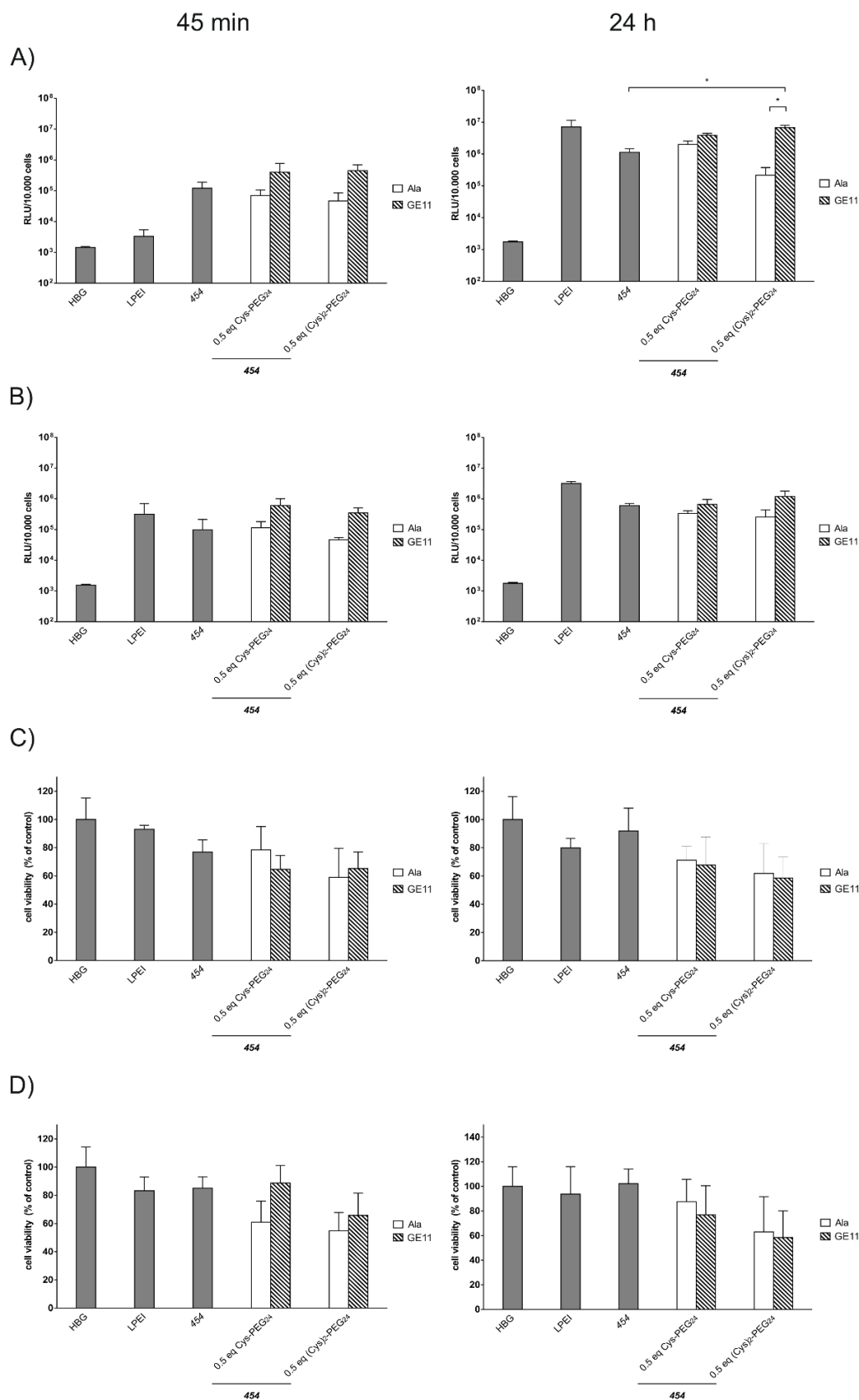


Figure 26 Transfection of **454** polyplexes PEGylated with 0.5 eq after 45 min (left) and 24 h (right). Luciferase gene expression determined in Huh7 (A) and MCF-7 (B). Corresponding MTT assays performed in parallel as displayed in (C) and (D) respectively. Assays were performed by Sarah Urnauer (PhD study, University Hospital of LMU, Department of Internal Medicine IV).

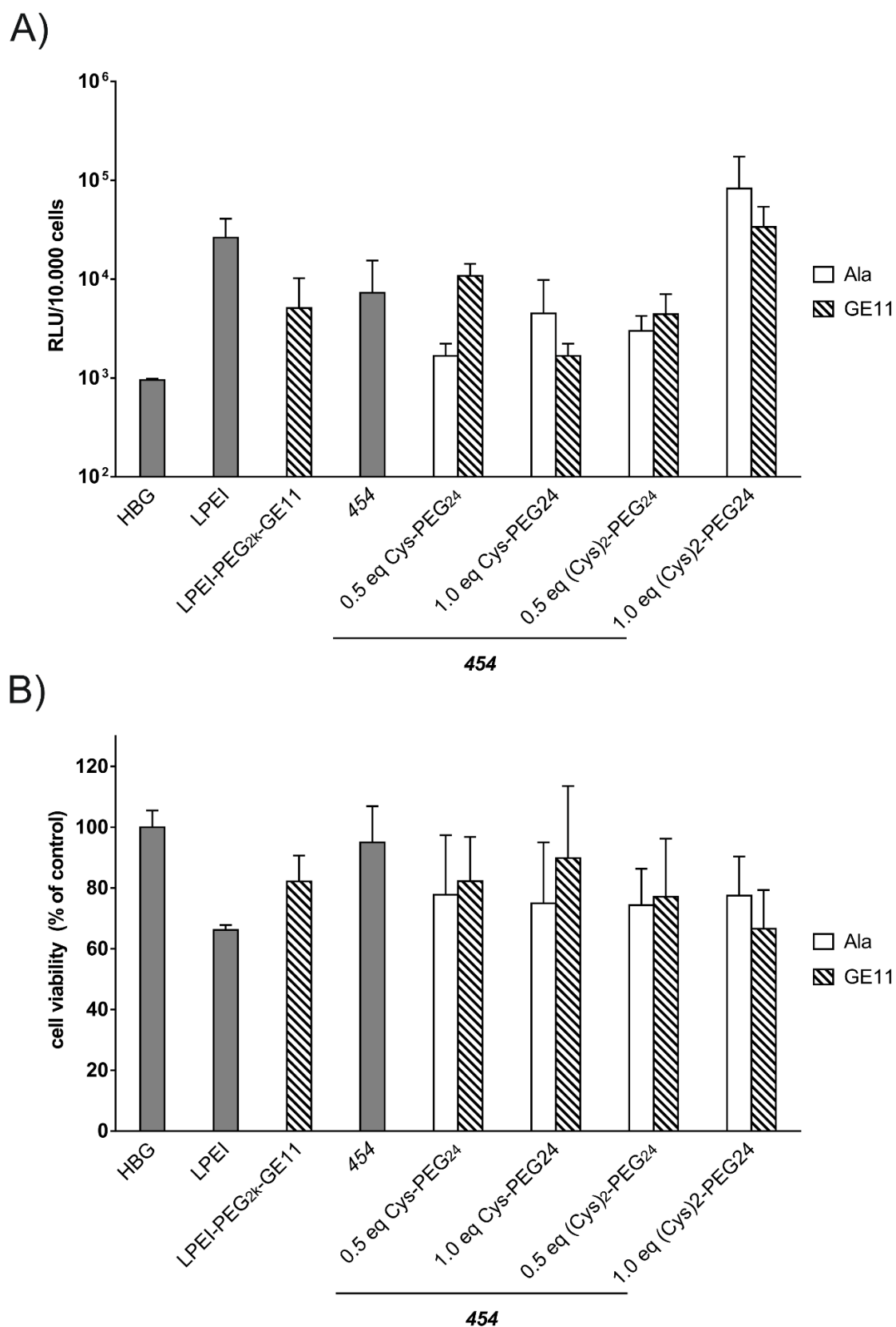


Figure 27 Luciferase gene expression in the low EGFR expressing cell line FTC-133 (A). Transfection results after 45 min of polyplex incubation. The corresponding MTT assay was performed in parallel (B). Assays were performed by Sarah Urnauer (PhD study, University Hospital of LMU, Department of Internal Medicine IV).

3.2.4 Cellular binding and internalization of bivalent post-PEGylated polyplexes

For a more detailed investigation, cellular association and uptake of Cy5 labeled pDNA complexes were determined by flow cytometry. Best-performing condition (1.0 eq) was used. Binding efficiency of bivalent post-PEGylated (EGFR-targeted and untargeted) lipopolyplexes in comparison to unshielded lipopolyplexes (**454**) was examined (**Figure 28**). All three lipopolyplexes showed efficient binding after 30 min incubation on ice. Far higher Cy5 fluorescence intensity was measured in cells transfected with the post-PEGylated EGFR-targeted bidentate structure. This emphasizes the suitability of GE11 as EGFR specific ligand and at the same time demonstrates that the bidentate structure represents the most promising post-PEGylation reagent. Shielding with PEG did not result in diminished interaction with cell surface, as can be seen by comparing fluorescence activity between non-shielded **454** and bivalent post-PEGylated alanine control (cf. **Figure 28A-B**). Experiments were also performed with monovalent PEGylation reagents, which did not result in any enhancement of binding in comparison to **454** and the alanine control in Huh7 and MCF-7 (cf. **Figure 29A,C**). Complementary binding results of LPEI-PEG_{2k}-GE11 and 2-arm pre-PEGylated structures are shown in **Figure 30A,C**.

Results of uptake studies were consistent with binding studies, showing highest intracellular uptake after transfection with the bivalent post-PEGylated structure in comparison to unshielded **454** and alanine control (**Figure 28 C-D**) and lower uptake was obtained after transfection with monovalent post-PEGylation complexes (cf. **Figure 29B,D**), LPEI-PEG_{2k}-GE11 and pre-PEGylated structures (cf. **Figure 30B,D**).

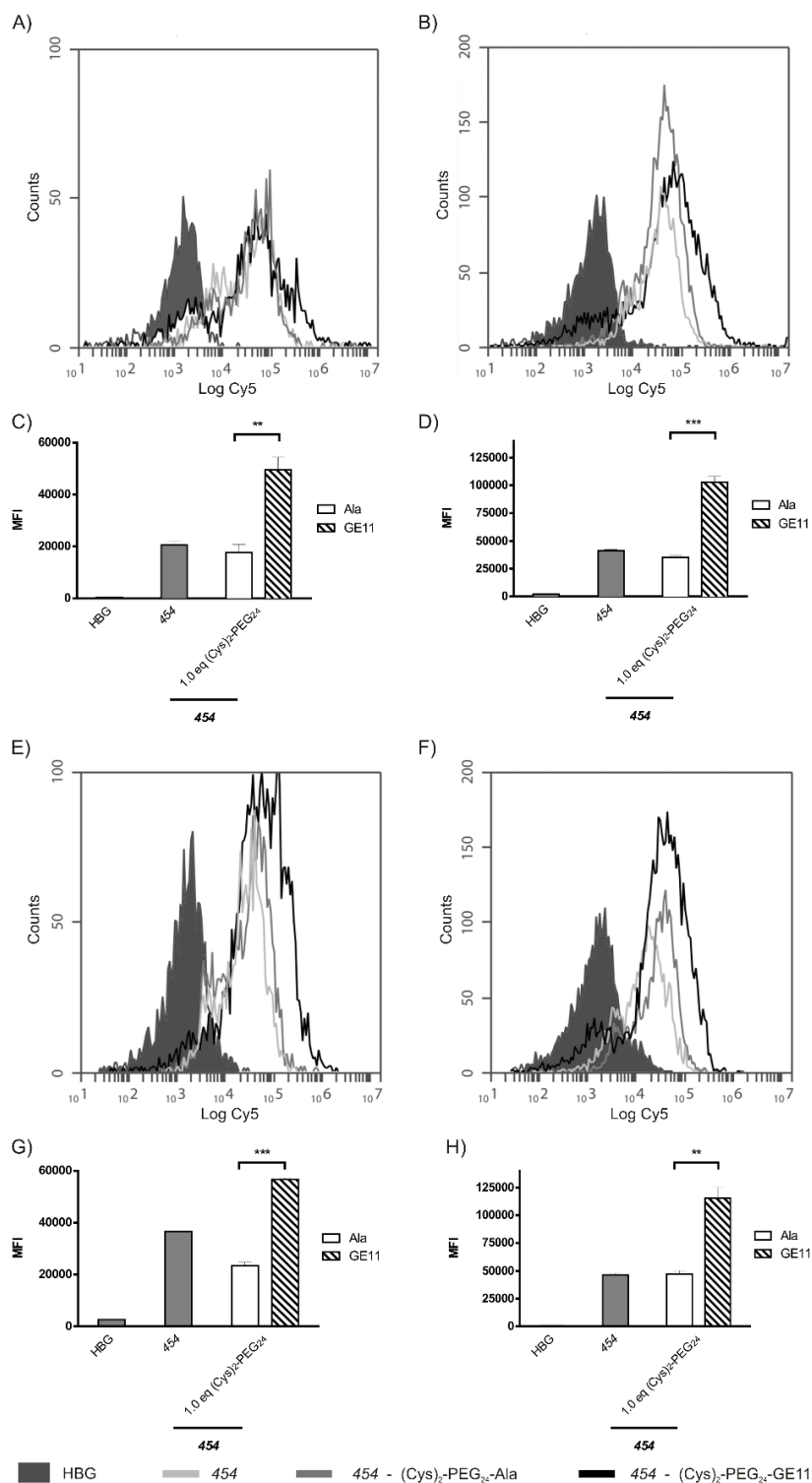


Figure 28 Cellular association of **454** polyplexes post-PEGylated with 1.0 eq of bidentate reagents on Huh7 (A) and MCF-7 (B) after 30 min incubation at 4 °C as determined by flow cytometry. (C) and (D) represent corresponding mean fluorescence intensity (MFI) values. Cellular internalization of polyplexes after 45 min of incubation at 37 °C followed by removal of extracellularly bound polyplexes is displayed in (E) and (F). Corresponding MFI values can be found in (G) and (H). Logarithmic X-scale in (A) and (B) as well as (E) and (F) represents Cy5 fluorescence of polyplexes. Assays were performed by Sarah Urnauer (PhD study, University Hospital of LMU, Department of Internal Medicine IV).

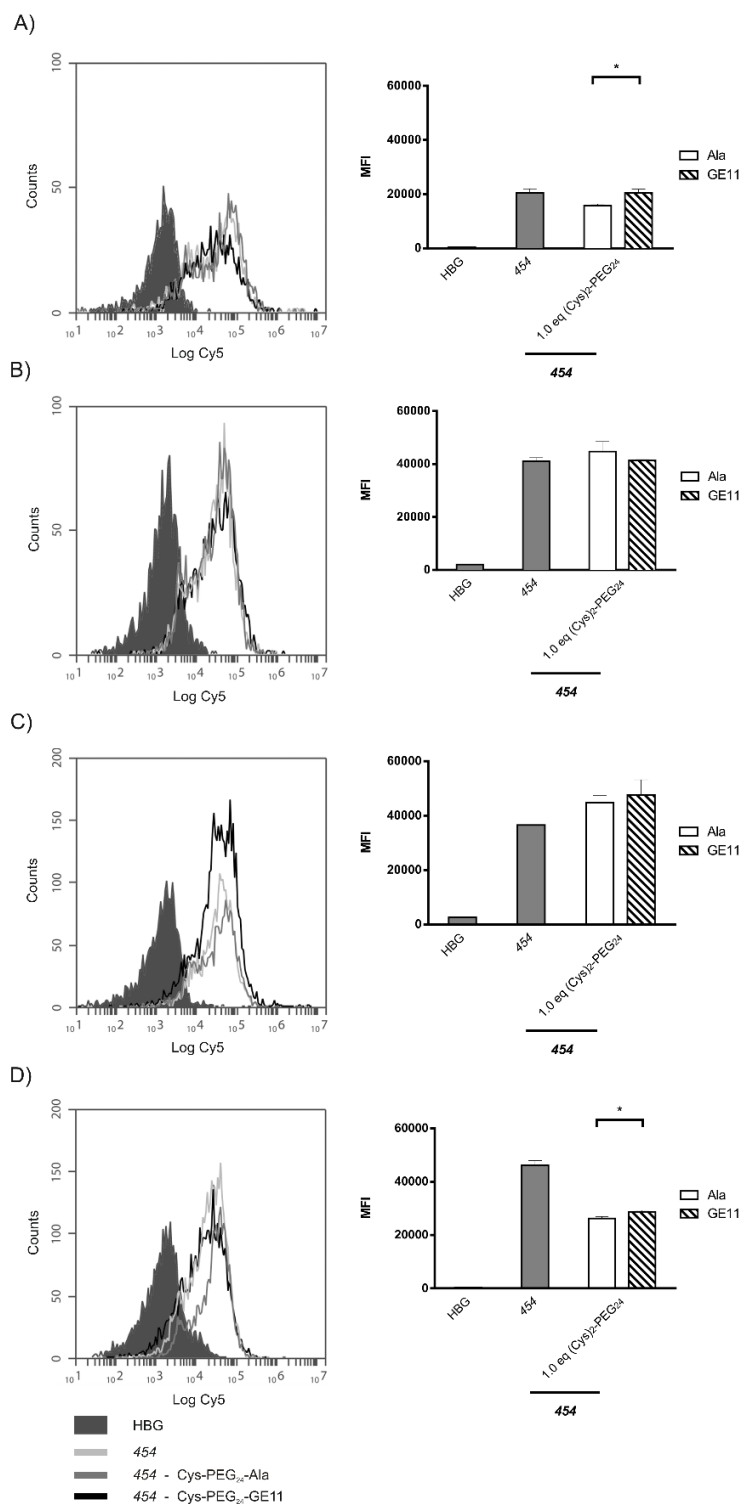


Figure 29 Flow cytometry results of **454** polyplexes PEGylated with 1.0 eq of monovalent reagents as well as corresponding mean fluorescence intensities. Cellular association of polyplexes on Huh7 (A) and MCF-7 (C) after 30 min incubation at 4 °C determined by flow cytometry. (B) and (D) cellular internalization of polyplexes after 45 min of incubation at 37 °C followed by removal of extracellularly bound polyplexes. Logarithmic X-scale in (A) - (D) represents Cy5 fluorescence of polyplexes. Assays were performed by Sarah Urnauer (PhD study, University Hospital of LMU, Department of Internal Medicine IV).

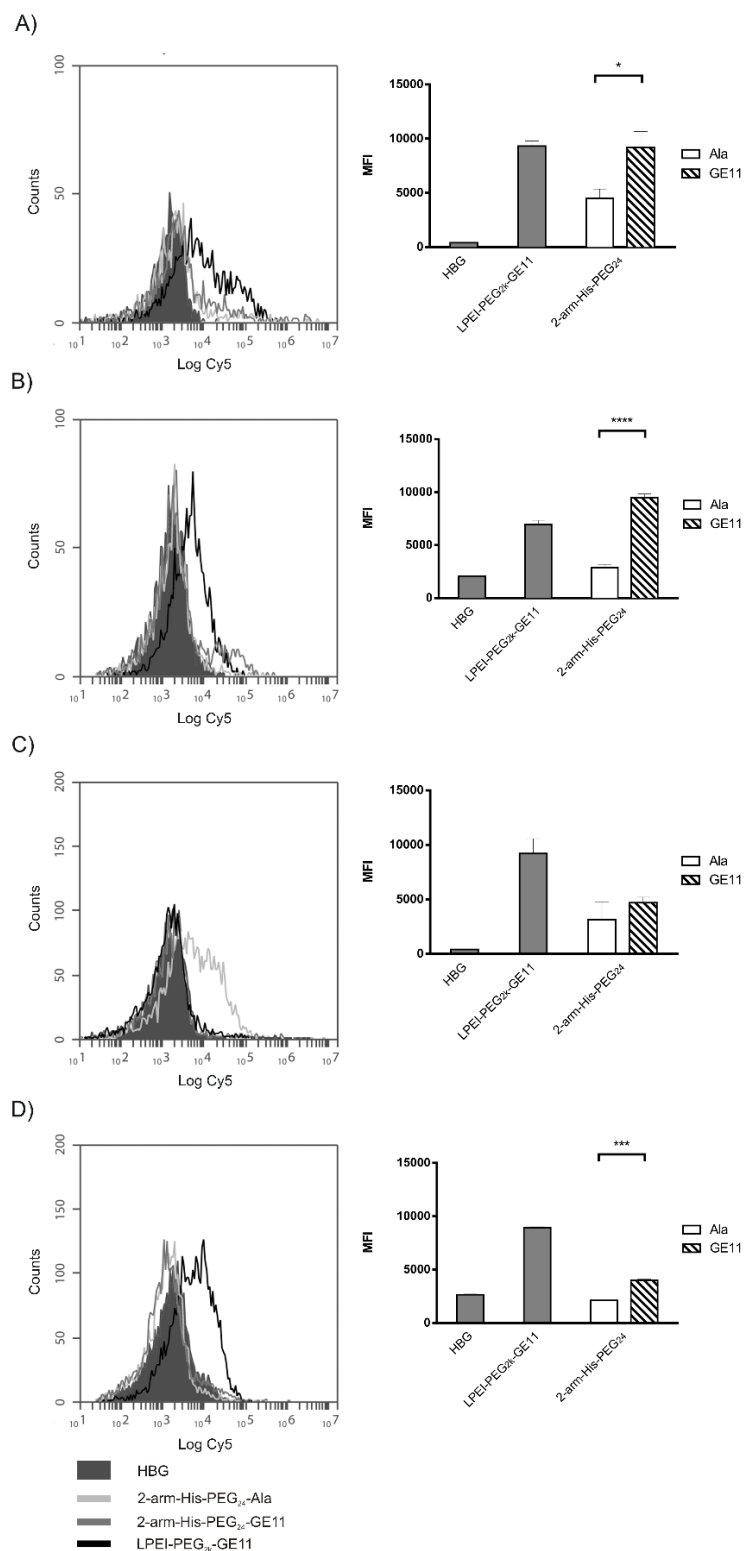


Figure 30 Flow cytometry results of pre-conjugated polyplexes, as well as corresponding mean fluorescence intensity. Cellular association of polyplexes on Huh7 (A) and MCF-7 (C) after 30 min incubation at 4 °C. In (B) and (D) cellular internalization of polyplexes after 45 min of incubation at 37 °C followed by removal of extracellularly bound polyplexes. Logarithmic X-scale in (A) - (D) represents Cy5 fluorescence of polyplexes. Assays were performed by Sarah Urnauer (PhD study, University Hospital of LMU, Department of Internal Medicine IV).

For nanoparticles, different uptake pathways are described depending on cell type, nanoparticle formulation, nanoparticle size and incorporation of ligands for active targeting. Various studies have been performed to rule out the exact mechanisms. Size-dependent uptake studies determined that particles up to 500 nm were internalized into cells by energy based processes [175, 176]. A clathrin-dependent uptake mechanism, as well as caveolae-assisted uptake, was detected for particles up to 200 nm. For lipopolyplexes, the clathrin dependent way is the major mechanism, whereas for polyplexes, both ways are possible [176].

The lipopolyplexes used in this study exhibited a size of approximately 200 nm or smaller, which suggests a clathrin depend uptake. However, uptake is not only size dependent, but also ligand dependent. Referring to this point, a study comparing the ligand GE11 and EGF for receptor mediated uptake revealed following that GE11 targeted polyplexes were taken up into the cell via clathrin-mediated endocytosis. This GE11-mediated uptake showed no activation of EGFR with constant EGFR levels after transfection and demonstrated an alternative actin-dependent pathway [68].

In conclusion, EGFR-targeted lipopolyplexes in this study are designed to achieve characteristics for an active targeted, clathrin-dependent uptake mechanism, which was proved to be the process of lipopolyplexes and polyplexes with the GE11 ligand [68].

After the successful uptake into endosomes, the endosomal buffer capacity of the Stp units in the oligomer backbone of the lipopolyplexes leads to protonation. The cationic function as well as the hydrophobic domains lead to enhanced interaction with the lysosomal membrane followed by destabilization of the membrane and degradation of the lipopolyplex and hence release of the pDNA in the cytosol.

3.2.5 Iodide uptake activity after hNIS gene delivery

After the proof of concept using the sensitive luciferase reporter capability for quantifying transduction efficacy, the sodium iodide symporter (NIS) was used as a clinically more relevant target gene. NIS features the beneficial dual characteristic as diagnostic and therapeutic gene [213, 214].

This theranostic function gives the possibility of exact determination of tumoral NIS gene expression *in vivo* by non-invasive imaging modalities as well as therapeutic investigation by application of cytotoxic radionuclides [63, 65, 192, 215-223].

In cell culture studies, NIS gene expression after lipopolyplex mediated delivery can be detected by measuring iodide (^{125}I) uptake activity of transfected cells by gamma-counter analysis. To verify NIS-dependent ^{125}I cell uptake, cells were pretreated with the NIS-specific inhibitor perchlorate (NaClO_4) that results in a blockade of NIS mediated iodide uptake.

As already observed in transfection, binding and uptake studies with the luciferase reporter gene, superiority of the post-integration approach of EGFR-targeted bidentate structures over non- and pre-PEGylated structures as well as untargeted complexes were confirmed (**Figure 31A**). Measured iodide uptake was perchlorate-sensitive verifying NIS mediated uptake. No effects on cell viability were observed after transfection (**Figure 31B**). The advantageous new EGFR specific delivery vehicles combine high transduction efficacy, high biocompatibility, ideal size along with optimal shielding that was introduced by post-integration of the bivalent $(\text{Cys}(\text{NPys})\text{-STOTDA})_{\alpha,\varepsilon}\text{-K-dPEG}_{24}$ via disulfide exchange reaction.

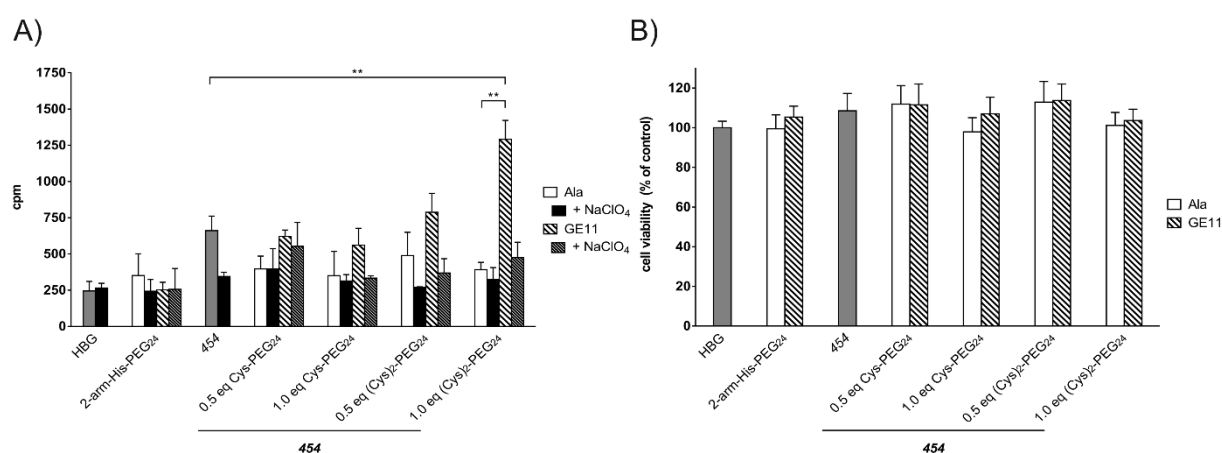


Figure 31 (A) Transfection of polyplexes on Huh7 cells. A sodium iodide symporter (NIS) coding pDNA was used. After ^{125}I application, iodide uptake was determined as counts per minute (cpm). Results are displayed with (black) and without (white) blockade of NIS by application of NaClO_4 prior to measurement. (B) MTT performed in parallel to transfections. Untargeted controls are displayed in white, while polyplexes targeted with GE11 peptide are marked with pattern. Assays were performed by Sarah Urnauer (PhD study, University Hospital of LMU, Department of Internal Medicine IV).

3.3 Lipo-oligomers optimized towards enhanced lipopolyplex stability

In chapter 3.2 polyplex post-modification was pointed out to be a promising tool to enhance EGFR dependent gene transfer *in vitro*. Within this study, pDNA lipopolyplexes formed with T-shaped **454** were PEGylated via mono- and bivalent EGFR targeted reagents. Lipopolyplexes modified with 1.0 eq of (Cys)₂-PEG₂₄-GE11 (cf. **Table 11**) displayed the highest tumor cell uptake and gene transfer. Considering that polyplex stability represents a critical step within *in vivo* gene delivery, a new library of oligomers was designed to increase lipopolyplex stability. The T-shaped oligomer **454** served as a starting point for this study.

3.3.1 Library design and oligomer synthesis

Oligomers were generated by SPS. Synthesis was mainly carried out by automated peptide synthesis as described in 2.2.1.3.7. For all oligomers synthesis started with a 2-chlorotriyl chloride resin preloaded with Fmoc-L-Cys(Trt)-OH. After loading determination, Fmoc was removed and synthesis was conducted to obtain the sequences listed in **Table 13**. Besides terminal cysteines, introduced for triggered polyplex stabilization via bioreducible crosslinking [134] and serving as anchors for the PEGylation reagents, all oligomers contained tyrosine blocks for hydrophobic stabilization via inter-oligomeral π - π stacking [208]. For nucleic acid binding and endosomal buffering all oligomers were equipped with Stp units and centrally placed L-Lys(Dde) facilitated orthogonal attachment of two hydrophobic fatty acids after the introduction of a Fmoc-L-Lys(Fmoc)-OH for symmetrical branching. These inserted oleic or cholanic acids contribute to hydrophobic polyplex stabilization [49, 51, 52, 111]; oleic acid is also known to enhance endosomal escape due to a pH-dependent lytic potential.

The library can be divided into three different approaches to enhance oligomer mediated lipopolyplex stability.

Within the first approach, the number of Stp units was increased from 4 to 6 or 8 respectively. As noted in 3.2.2 an increase of intra-oligomeral cationic charge density is known to enhance polyplex compaction and endosomal buffering [224]. Within this set also cholanic acid, which was mentioned to improve lipopolyplex stability [111] was

introduced alternatively to oleic acid. Thereby the set of oligomers consisted of **454** and **1021**, **1022** and **1023**, **1175** and **1176** (firstly mentioned oligomers contain oleic acid, followed by cholanic acid containing oligomers, with Stp units increasing from 4 to 6 to 8 – peripheral Y₃ were kept in all oligomers).

Another approach aimed at the increase of hydrophobic stabilization by introduction of peripheral Y₆ instead of Y₃. As investigated previously, tyrosines have additionally been found to stabilize polyplexes via π - π stacking [52]. Therefore, oligomers containing 4 and 8 Stp units and peripheral tyrosine hexamers with centrally placed oleic as well as cholanic acid were generated. **1173** and **1174** as well as **1177** and **1178** thereby were generated (again oleic acid containing structures are mentioned first, followed by cholanic acid containing oligomers).

The last set of oligomers aimed to investigate the effect of histidines within sequence-defined oligomers. Introduction of histidines significantly enhanced endosomal buffering and thereby endosomal escape within sequence-defined oligomers [50, 64]. For this study, also another characteristic was taken into account; Histidines, with a pK_a of 6.5 are only marginally protonated at neutral pH, and thereby exhibit hydrophobic properties. The aromatic imidazole ring is therefore thought to contribute to stability via π - π stacking [225]. To investigate the effect on positioning, cationic oligomers were built with either 4 or 8 Stp units and histidines were either introduced alternately between the Stp units (H-(Stp-H)_x) or blockwise (H_Y-Stp_x) between Y₃ and Stp. X was either considered as 2 or 4 while Y at the same time is considered as 3 or 5 respectively, thereby leading to oligomers **1026** and **1024** or **1179** and **1180**. Centrally placed oleic acid should maintain the fundamental level of stability within all of these oligomers.

To provide an overview of this study, all oligomers are illustrated in **Scheme 6** and summarized in **Table 13**. Abbreviations instead of internal ID # are introduced for a better understanding.

PEGylation of lipopolyplexes was conducted with 1.0 eq of the bivalent reagents. Synthesis was conducted as described in **2.2.1.4.2** and was discussed previously (cf. **3.2.1**). They are summarized in **Table 14**.

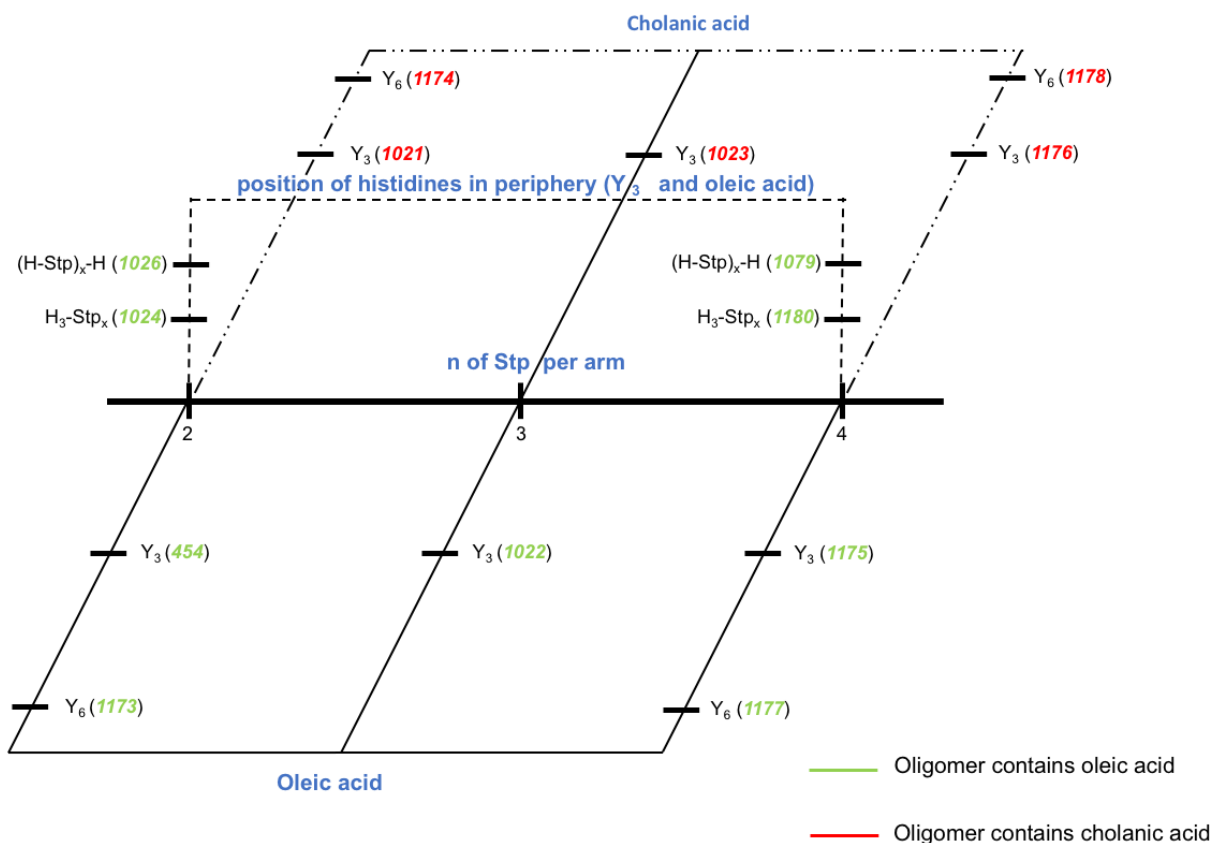
Table 13 List of oligomers generated for this study. Internal ID, chemical structure from C to N terminus and an abbreviation for each oligomer is given.

| ID # | Structure | Abbreviation |
|------|--|--|
| 454 | C-Y ₃ -Stp ₂ -K-[K-(OleA) _{α,ε}] _ε -Stp ₂ -Y ₃ -C | Stp ₂ -Y ₃ -OleA |
| 1021 | C-Y ₃ -Stp ₂ -K-[K-(CholA) _{α,ε}] _ε -Stp ₂ -Y ₃ -C | Stp ₂ -Y ₃ -CholA |
| 1022 | C-Y ₃ -Stp ₃ -K-[K-(OleA) _{α,ε}] _ε -Stp ₃ -Y ₃ -C | Stp ₃ -Y ₃ -OleA |
| 1023 | C-Y ₃ -Stp ₃ -K-[K-(CholA) _{α,ε}] _ε -Stp ₃ -Y ₃ -C | Stp ₃ -Y ₃ -CholA |
| 1024 | C-Y ₃ -H ₃ -Stp ₂ -K-[K-(OleA) _{α,ε}] _ε -Stp ₂ -H ₃ -Y ₃ -C | Stp ₂ -H ₃ -Y ₃ -OleA |
| 1026 | C-Y ₃ -(H-Stp) ₂ -H-K-[K-(OleA) _{α,ε}] _ε -H-(Stp-H) ₂ -Y ₃ -C | (Stp-H) ₂ -H-Y ₃ -OleA |
| 1173 | C-Y ₆ -Stp ₂ -K-[K-(OleA) _{α,ε}] _ε -Stp ₂ -Y ₆ -C | Stp ₂ -Y ₆ -OleA |
| 1174 | C-Y ₆ -Stp ₂ -K-[K-(CholA) _{α,ε}] _ε -Stp ₂ -Y ₆ -C | Stp ₂ -Y ₆ -CholA |
| 1175 | C-Y ₃ -Stp ₄ -K-[K-(OleA) _{α,ε}] _ε -Stp ₄ -Y ₃ -C | Stp ₄ -Y ₃ -OleA |
| 1176 | C-Y ₃ -Stp ₄ -K-[K-(CholA) _{α,ε}] _ε -Stp ₄ -Y ₃ -C | Stp ₄ -Y ₃ -CholA |
| 1177 | C-Y ₆ -Stp ₄ -K-[K-(OleA) _{α,ε}] _ε -Stp ₄ -Y ₆ -C | Stp ₄ -Y ₆ -OleA |
| 1178 | C-Y ₆ -Stp ₄ -K-[K-(CholA) _{α,ε}] _ε -Stp ₄ -Y ₆ -C | Stp ₄ -Y ₆ -CholA |
| 1179 | C-Y ₃ -(H-Stp) ₄ -H-K-[K-(OleA) _{α,ε}] _ε -H-(Stp-H) ₄ -Y ₃ -C | (Stp-H) ₄ -H-Y ₃ -OleA |
| 1180 | C-Y ₃ -H ₅ -Stp ₄ -K-[K-(OleA) _{α,ε}] _ε -Stp ₄ -H ₅ -Y ₃ -C | Stp ₄ -H ₅ -Y ₃ -OleA |

Analytical data (MALDI-MS) of the oligomers can be found in **6.5.5**.

Table 14 Sequences of PEGylation reagents (N to C terminus) as well as used abbreviation are displayed. Detailed chemical structures can be found in **Figure 16C,D**.

| ID # | Structure | Abbreviation |
|------|--|---|
| 1060 | (Cys(NPys)-STOTDA) _{α,ε} -K-dPEG ₂₄ -A | (Cys) ₂ -PEG ₂₄ -Ala |
| 1056 | (Cys(NPys)-STOTDA) _{α,ε} -K-dPEG ₂₄ -YHWYGYTPQNV | (Cys) ₂ -PEG ₂₄ -GE11 |



Scheme 6 Oligomers generated within this study

3.3.2 Physicochemical polyplex characterization

3.3.2.1 Size and zeta potential of unmodified as well as post-modified lipopolyplexes

After synthesis, oligomers were investigated biophysically by formation of pDNA polyplexes. Thereby, mean particle size (displayed as Z-average), mean PDI and mean zeta potential (mV) was determined at N/P 12 with 2 μ g pDNA. Within particle distribution, a PDI of 1.0 represents the highest polydispersity. All polyplexes displayed a size between 68 and 102 nm prior to PEGylation, while the PDI revealed a low polydispersity between 0.11 and 0.26 (cf. **Table 15**). All polyplexes exhibited a positive zeta potential between 17 and 30 mV.

Table 15 Particle size (Z-average), PDI and zeta potential of pDNA polyplexes formed in HBG buffer determined with DLS. Mean of three measurements of the same sample is indicated. Polymer at N/P 12 and 2 μg pDNA were separately diluted with HBG pH 7.4 to 30 μL each. Then solutions were mixed and incubated for 30 min. Polyplexes then were diluted to 800 μL with 10 mM NaCl pH 7.4 prior to measurement.

| Compound | Z-Average | Mean PDI | Mean zeta potential |
|--|-----------------|-----------------|---------------------|
| Stp ₂ -Y ₃ -OleA (454) | 81.5 \pm 5.2 | 0.18 \pm 0.02 | 29.9 \pm 1.3 |
| Stp ₂ -Y ₃ -CholA (1021) | 69.9 \pm 0.6 | 0.14 \pm 0.02 | 22.4 \pm 2.5 |
| Stp ₃ -Y ₃ -OleA (1022) | 76.3 \pm 0.4 | 0.15 \pm 0.01 | 22.8 \pm 2.1 |
| Stp ₃ -Y ₃ -CholA (1023) | 73.5 \pm 0.7 | 0.17 \pm 0.02 | 22.5 \pm 1.3 |
| Stp ₂ -H ₃ -Y ₃ -OleA (1024) | 79.8 \pm 0.9 | 0.15 \pm 0.01 | 22.5 \pm 0.7 |
| (Stp-H) ₂ -H-Y ₃ -OleA (1026) | 75.4 \pm 0.8 | 0.11 \pm 0.01 | 24.8 \pm 1.2 |
| Stp ₂ -Y ₆ -OleA (1173) | 99.5 \pm 2.1 | 0.26 \pm 0.05 | 27.1 \pm 1.9 |
| Stp ₂ -Y ₆ -CholA (1174) | 101.6 \pm 0.5 | 0.17 \pm 0.01 | 27.4 \pm 1.7 |
| Stp ₄ -Y ₃ -OleA (1175) | 71.8 \pm 0.3 | 0.19 \pm 0.01 | 19.2 \pm 1.7 |
| Stp ₄ -Y ₃ -CholA (1176) | 67.6 \pm 1.5 | 0.17 \pm 0.01 | 16.7 \pm 1.6 |
| Stp ₄ -Y ₆ -OleA (1177) | 80.2 \pm 0.5 | 0.18 \pm 0.01 | 26.7 \pm 1.2 |
| Stp ₄ -Y ₆ -CholA (1178) | 75.6 \pm 0.6 | 0.17 \pm 0.01 | 22.6 \pm 2.4 |
| (Stp-H) ₄ -H-Y ₃ -OleA (1179) | 78.6 \pm 0.3 | 0.20 \pm 0.01 | 19.5 \pm 4.2 |
| Stp ₄ -H ₅ -Y ₃ -OleA (1180) | 72.7 \pm 2.0 | 0.18 \pm 0.02 | 18.8 \pm 3.2 |

PDI: Polydispersity index. Z-average is displayed in nm and mean zeta potential in mV

With increasing amounts of incorporated Stp, polyplexes containing oleic acids and Y₃ exhibited a decrease between 82 nm (Stp₂) and 68 nm (Stp₄). This indicates that the cargo is compacted better due to elevated cationic charge, resulting in smaller nanoparticles. Within the same set of cholanic acid containing oligomers, no notable differences were observed. The increase of tyrosines from Y₃ to Y₆ in oligomers containing 4 and 8 Stp units generally led to an increase in size compared to oligomers with only Y₃. The introduction of histidines, independent of the positioning, did not significantly affect polyplex size.

While post-modification with 1.0 eq (Cys)₂-PEG₂₄-Ala did not significantly influence polyplex size, all polyplexes exhibit a size below 90 nm. Addition of 1.0 eq (Cys)₂-PEG₂₄-GE11 resulted in increased polyplex sizes. Reduction of zeta potential indicates a successful PEGylation (cf. **Table 16**, **Table 17** and **Table 18**) compared to non-PEGylated polyplexes can be observed in all cases (cf. **Table 15**). While polyplexes formed with Y₃-Stp₂/Stp₃ (**454** and **1021**, **1022** and **1023**) increased size to more than

160 nm, this could not be observed for Y₃-Stp₄ (**1175** and **1176**) post-modified with GE11, where polyplex size was only increased by approximately 25 nm to below 95 nm.

Table 16 Polyplexes were post-modified with 1.0 eq (Cys)₂-PEG₂₄-Ala or GE11. Within the cationic backbone, the number of Stp units was increased from 4 to 6 or 8, while peripheral tyrosine trimers (Y₃) was preserved. Oleic acid or cholanic acids were incorporated as central hydrophobic stabilization domains.

| Compound - 1.0 eq (Cys)₂-PEG₂₄-Ala/GE11 | Z-Average | Mean PDI | Mean zeta potential |
|---|------------------|-----------------|----------------------------|
| Stp ₂ -Y ₃ -OleA (454) - Ala | 83.8 ± 0.8 | 0.12 ± 0.02 | 15.6 ± 0.9 |
| Stp ₂ -Y ₃ -OleA (454) - GE11 | 283.8 ± 0.4 | 0.17 ± 0.01 | 17.7 ± 2.0 |
| Stp ₂ -Y ₃ -CholA (1021) - Ala | 89.3 ± 0.4 | 0.15 ± 0.01 | 9.3 ± 1.0 |
| Stp ₂ -Y ₃ -CholA (1021) - GE11 | 166.1 ± 0.7 | 0.09 ± 0.01 | 21.6 ± 1.0 |
| Stp ₃ -Y ₃ -OleA (1022) - Ala | 85.3 ± 0.5 | 0.18 ± 0.01 | 13.3 ± 2.0 |
| Stp ₃ -Y ₃ -OleA (1022) - GE11 | 336.0 ± 11.5 | 0.34 ± 0.05 | 19.2 ± 1.0 |
| Stp ₃ -Y ₃ -CholA (1023) - Ala | 80.1 ± 1.4 | 0.21 ± 0.01 | 8.6 ± 0.8 |
| Stp ₃ -Y ₃ -CholA (1023) - GE11 | 168.2 ± 0.9 | 0.17 ± 0.02 | 20.6 ± 0.2 |
| Stp ₄ -Y ₃ -OleA (1175) - Ala | 72.2 ± 0.6 | 0.18 ± 0.01 | 9.1 ± 1.3 |
| Stp ₄ -Y ₃ -OleA (1175) - GE11 | 82.8 ± 0.9 | 0.19 ± 0.01 | 16.7 ± 1.2 |
| Stp ₄ -Y ₃ -CholA (1176) - Ala | 72.8 ± 0.9 | 0.17 ± 0.01 | 8.6 ± 1.3 |
| Stp ₄ -Y ₃ -CholA (1176) - GE11 | 93.6 ± 0.4 | 0.17 ± 0.02 | 16.6 ± 1.7 |

PDI: Polydispersity index. Z-average is displayed in nm and mean zeta potential in mV

Table 17 Polyplexes were post-modified with 1.0 eq (Cys)₂-PEG₂₄-Ala or GE11. Within the cationic backbone, the number of peripheral tyrosines was increased from trimers (Y₃) to hexamers (Y₆). The number of Stp units was increased from 4 to 8. Oleic acid or cholanic acids were incorporated as central hydrophobic stabilization domains.

| Compound - 1.0 eq (Cys)₂-PEG₂₄-Ala/GE11 | Z-Average | Mean PDI | Mean zeta potential |
|---|------------------|-----------------|----------------------------|
| Stp ₂ -Y ₆ -OleA (1173) - Ala | 214.2 ± 9.6 | 0.44 ± 0.03 | 2.8 ± 0.3 |
| Stp ₂ -Y ₆ -OleA (1173) - GE11 | 8778 ± 595 | 0.46 ± 0.47 | 13.8 ± 0.6 |
| Stp ₂ -Y ₆ -CholA (1174) - Ala | 105.8 ± 0.8 | 0.18 ± 0.01 | 4.5 ± 0.6 |
| Stp ₂ -Y ₆ -CholA (1174) - GE11 | 6152 ± 189 | 0.22 ± 0.12 | 17.5 ± 0.6 |
| Stp ₄ -Y ₆ -OleA (1177) - Ala | 84.8 ± 0.8 | 0.16 ± 0.02 | 11.1 ± 1.6 |
| Stp ₄ -Y ₆ -OleA (1177) - GE11 | 101.9 ± 0.6 | 0.13 ± 0.02 | 20.2 ± 0.3 |
| Stp ₄ -Y ₆ -CholA (1178) - Ala | 81.7 ± 0.4 | 0.17 ± 0.02 | 10.7 ± 2.4 |
| Stp ₄ -Y ₆ -CholA (1178) - GE11 | 96.3 ± 0.4 | 0.16 ± 0.01 | 18.8 ± 1.0 |

PDI: Polydispersity index. Z-average is displayed in nm and mean zeta potential in mV

At the same time, introduction of Y₆ resulted for oligomers **1173** and **1174** (4 Stp units) in severe aggregation of more than 5000 nm (cf. **Table 17**), this could not be observed for **1177** and **1178** (8 Stp units), pointing out that an increased cationic charge is beneficial to overcome the risk of aggregation during lipopolyplex PEGylation with GE11.

As observed previously during PEGylation of **454** with GE11 [226], the potential of aggregation is linked to an unbalanced ratio between PEG-GE11 and the cationizable domain within the oligomer – which was improved by the introduction of additional Stp units. It is also known that hydrophobic peptides tend to cause aggregation [209, 210].

Introduction of histidines notably increased nanoparticle size within polyplexes formed with oligomers containing only 4 Stp units (cf. **Table 18**). At the same time, this could not be observed for oligomers with 8 Stp units. A clear conclusion on the positioning of histidines could not be drawn, as for **1024** and **1026** (4 Stp units), the blockwise positioning exhibited sizes of ~ 850 nm while alternating histidines resulted in ~ 200 nm particles. For oligomers containing 8 Stp units, only an increase of 30 nm (71 nm alternating and 100 nm for blockwise positioning) could be observed, displaying contrary effects. However, regarding size control after PEGylation with the bivalent GE11 reagent, all oligomers containing 8 Stp units (**1175-1180**) showed the best properties. Comparing oleic acid and cholic acid as centrally placed hydrophobic stabilization domains, polyplexes after post-modification tended to be slightly smaller when cholic acid was incorporated instead of oleic acid.

Table 18 Polyplexes were post-modified with 1.0 eq (Cys)₂-PEG₂₄-Ala or GE11. Histidines, either alternately or blockwise, were introduced into oligomers consisting of 4 or 8 Stp units. Tyrosine trimers (Y₃) and centrally placed oleic acid are intended to maintain polyplex stability due to hydrophobic stabilization.

| Compound - 1.0 eq (Cys) ₂ -PEG ₂₄ -Ala/GE11 | Z-Average | Mean PDI | Mean zeta potential |
|---|--------------|-------------|---------------------|
| Stp ₂ -H ₃ -Y ₃ -OleA (1024) - Ala | 124.8 ± 1.0 | 0.26 ± 0.01 | 1.4 ± 0.1 |
| Stp ₂ -H ₃ -Y ₃ -OleA (1024) - GE11 | 854.0 ± 26.8 | 0.68 ± 0.05 | 21.0 ± 0.5 |
| (Stp-H) ₂ -H-Y ₃ -OleA (1026) - Ala | 86.6 ± 0.7 | 0.11 ± 0.01 | 3.2 ± 0.3 |
| (Stp-H) ₂ -H-Y ₃ -OleA (1026) - GE11 | 196.4 ± 2.7 | 0.12 ± 0.02 | 22.2 ± 1.0 |
| (Stp-H) ₄ -H-Y ₃ -OleA (1179) - Ala | 83.7 ± 0.5 | 0.15 ± 0.01 | 12.0 ± 1.0 |
| (Stp-H) ₄ -H-Y ₃ -OleA (1179) - GE11 | 99.8 ± 1.0 | 0.19 ± 0.01 | 17.0 ± 1.2 |
| Stp ₄ -H ₅ -Y ₃ -OleA (1180) - Ala | 70.5 ± 0.1 | 0.13 ± 0.01 | 11.5 ± 2.9 |
| Stp ₄ -H ₅ -Y ₃ -OleA (1180) - GE11 | 70.8 ± 0.2 | 0.14 ± 0.01 | 18.3 ± 1.7 |

PDI: Polydispersity index. Z-average is displayed in nm and mean zeta potential in mV

3.3.2.2 pDNA compaction in buffer and after polyanionic stress

pDNA compaction was examined with EtBr exclusion assay. However, none of the polyplexes compacted pDNA as good as LPEI, which served as control (~ 5% remaining EtBr fluorescence). Remaining EtBr fluorescence related to uncomplexed pDNA for all tested oligomers was between 7 and 17% for non-PEGylated polyplexes (cf. **Figure 32**). Again, polyplexes formed with Stp₄-Y₃ oligomers exhibited the highest compaction, although differences are not significant. The increase of tyrosines did not affect pDNA compaction significantly. Introduction of histidines resulted in the least compact particles. These findings are in accordance with previous findings, where it was pointed out, that dependent on the used artificial amino acid, pDNA compaction was reduced in case of Stp [50]. Comparing oligomers with 4 and 8 Stp units, within all settings (Y₃ to Y₆ and introduction of histidines) pDNA compaction was slightly improved for oligomers with increased numbers of Stp units. PEGylation with 1.0 eq of the Ala or GE11 containing reagent did not notably affect nucleic acid compaction.

As a next experiment, pDNA compaction after addition of 250 IU heparin, mediating polyanionic stress to the polyplex, was observed. Here, clearly LPEI was most prone to releasing 96% of its cargo. Comparing the three groups (only increased cationic charge density, increase of tyrosines, and introduction of histidines), polyplex resistance towards polyanionic stress can be summarized as follows: Stp₂-Y₆ > Stp₂-H₃ ≈ (H-Stp)₂-H > Stp₄-H₅ ≈ (H-Stp)₄-H ≈ Stp₄-Y₆ > Stp₄-Y₃ ≈ Stp₃-Y₃ > Stp₂-Y₃ (cf. **Figure 32D-F**). These findings correlate with the hypothesis of additional lipopolyplex stabilization via hydrophobic domains (such as tyrosines and histidines). PEGylation did not clearly influence lipopolyplex stability, in some cases, even an increased resistance is observed (cf. **Figure 32D**).

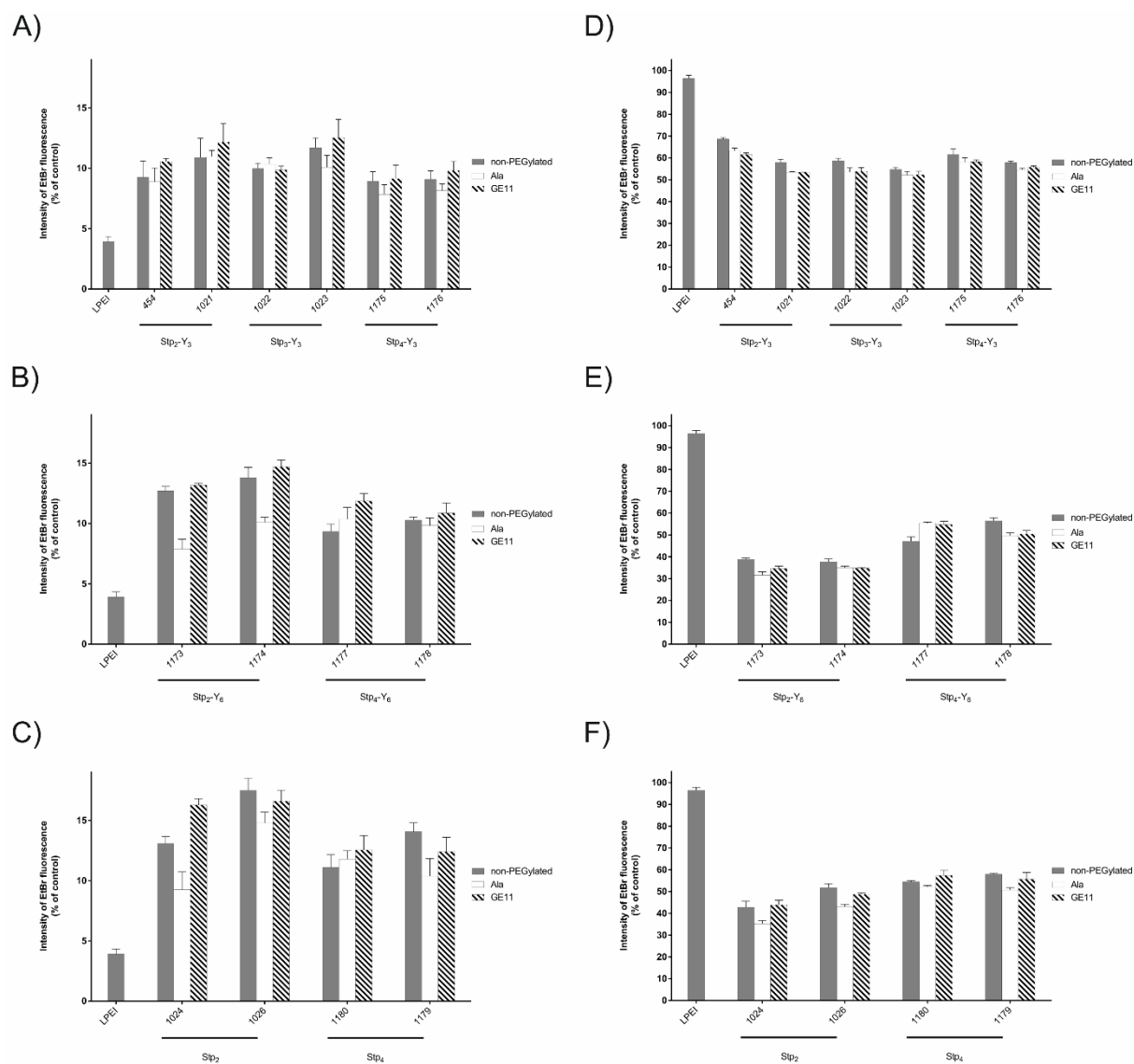


Figure 32 pDNA compaction of oligomers was determined by EtBr assay. After lipopolyplex formation (grey bars), followed by post-modification with 1.0 eq of bivalent Ala (white bars) or GE11 (patterned bars) the remaining EtBr fluorescence was determined and related to uncomplexed pDNA. (A) Oligomers with ascending Stp units. (B) Introduction of tyrosine hexamers into oligomers containing 4 and 8 Stp units. (C) Alternating or blockwise introduction of histidines into oligomers containing 4 and 8 Stp units. (D)- (F) Corresponding pDNA compaction after addition of 250 IU of heparin.

3.3.2.3 Steric stability of unmodified as well as PEGylated lipopolyplexes under physiological salt conditions

Lipopolyplex stability was further investigated by addition of PBS and nanoparticle sizes were determined immediately after addition, after 0.5, 3 and if indicated 24 h. This test for colloidal stability under physiological salt conditions exhibit again the influence of cationic charge, and thereby pDNA compaction, as lipopolyplexes composed of oligomers with 4 or 6 Stp units underwent aggregation within 30 minutes (cf. **Figure 33A**) exhibiting particle sizes of more than 1000 nm. At the same time, polyplexes formed with oligomers **1175** or **1176** (Stp₄-Y₃) increased in size within 30 min but remained stable for 24h with a particle size of approximately 400 or 200 nm respectively. The size difference within these two polyplexes could be explained by the enhanced stability mediated by cholanic acid [111]. Introduction of further tyrosines into oligomers containing 4 or 8 Stp units was in accordance with results mentioned above. Here, an increase of tyrosines weakened lipopolyplex stability, resulting in immediate aggregation of polyplexes formed with **1173** and **1174** to particles >800 nm, while size only increased from ~ 100 nm to 260 nm in case of **1177** and **1178**. Also, again within the latter two, cholanic acid (incorporated in **1178**), tends to retard particle aggregation and thereby increases stability up to 3 h. Compared to oligomers with Stp₄-Y₃ (**1175** & **1176**), introduction of histidines seemed to be beneficial independent of the positioning. Here, sizes only increased up to 200 nm, interestingly this effect was less pronounced for oligomers with alternating H-Stp repeats than with blockwise introduction of histidines (cf **Figure 33C**).

In parallel, lipopolyplexes were post-PEGylated with 1.0 eq of (Cys)₂-PEG₂₄-Ala and treated similarly to non-PEGylated nanoparticles (cf. **Figure 33D-F**). Here, lipopolyplexes remained stable for 24 h. Also, no difference in particle stability could be observed for oligomers with 4, 6 or 8 Stp units, nor did the introduction of tyrosines or histidines impact polyplex stability. This indicates the strength of this post-modification approach, enhancing polyplex stability after PEGylation due to the steric stabilization as observed for PEGylated PEI complexes [29] as well as pDNA/oligomer polyplexes [133]. However, post-modification with 1.0 eq of (Cys)₂-PEG₂₄-GE11 resulted for all lipopolyplexes in immediate aggregation for all polyplexes (cf. **Figure 34**). For reasons of control, LPEI-PEG_{2k}-GE11 which was previously found to reliably mediate pDNA delivery *in vivo* [62, 192], was compared to the sequence-defined

oligomers, resulting in polyplex aggregation to the same extent as lipopolyplexes most-modified with 1.0 eq of the bivalent GE11 reagent. Aggregation of PEI was previously mentioned to be overcome after addition of PEG [29].

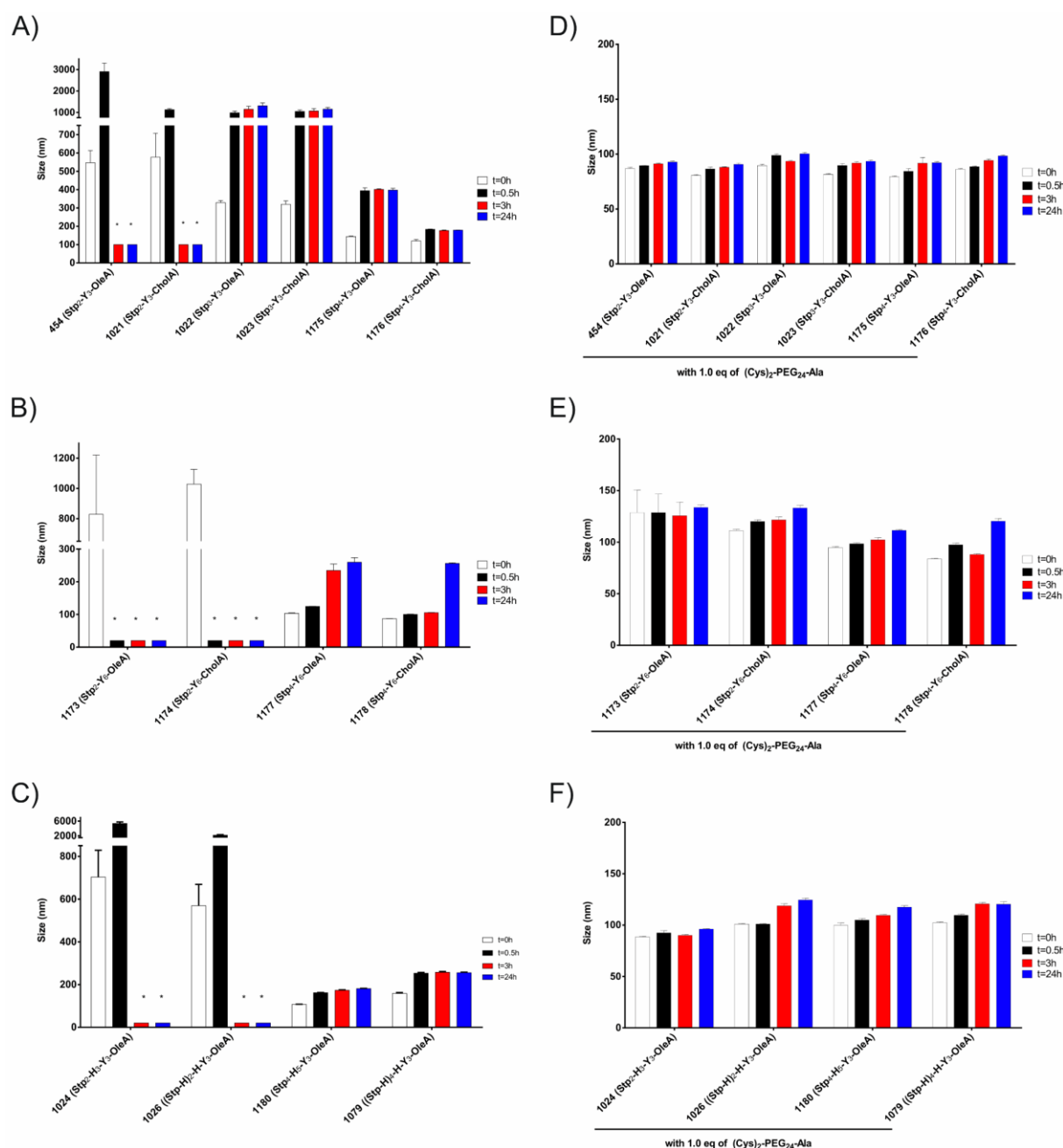


Figure 33 Lipopolyplexes after incubation in PBS 7.4 mimicking physiological salt conditions. Polyplex size was determined immediately after PBS addition (t=0), after 0.5, 3 and if indicated after 24h. In case of aggregation, the samples were not further incubated under steady shaking. No determinable particles (as a result of severe aggregation or dissociation over time – resulting in a low count rate at an attenuator of 11 or sizes >8000 nm) were marked with *. (A)-(C) displays non-PEGylated lipopolyplexes, while (D)-(F) displays polyplexes after PEGylation with 1.0 eq (Cys)₂-PEG₂₄-Ala.

This again pronounces the special behavior of the hydrophobic GE11 within polyplexes. However, also aggregation for HGFR targeted polyplexes formed with sequence-defined cmb containing oligomers was observed (SM, unpublished data).

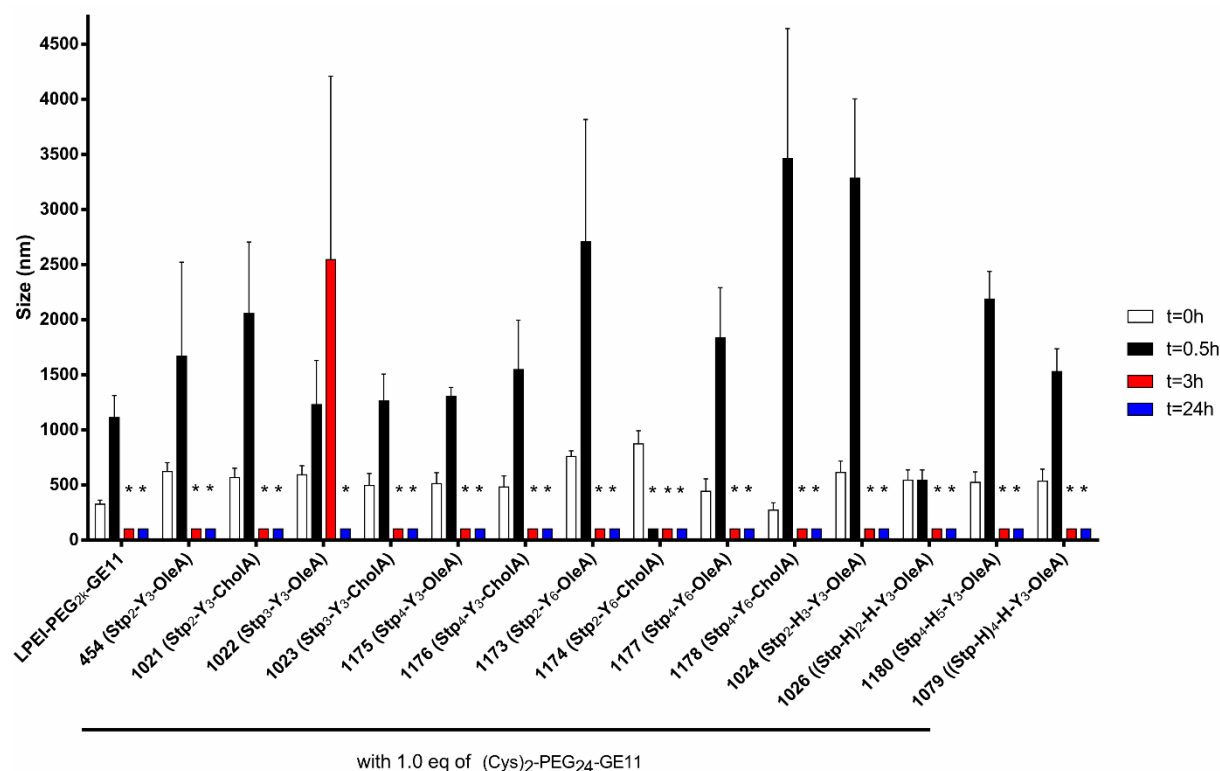


Figure 34 Lipopolyplexes PEGylated with 1.0 eq of (Cys)₂-PEG₂₄-GE11 after addition of PBS 7.4. Polyplex size was determined immediately after PBS addition (t=0), after 0.5, 3 and after 24h LPEI-PEG_{2k}-GE11 was included as control. No determinable particles (as a result of severe aggregation or dissociation over time – resulting in a low count rate at an attenuator of 11 or sizes >8000 nm) were marked with *.

3.3.2.4 Serum stability of unmodified as well as post-modified lipopolyplexes

In a last experiment to investigate polyplex stability, (PEGylated) lipopolyplexes were incubated in 90% FBS. Changes in size were examined by DLS. In general, all polyplexes underwent immediate interaction with the serum, leading to increased polyplex sizes, resulting in nanoparticle sizes, determined as intensity mean values of 250-300 nm. Generally, the majority underwent no further change within 24h, however also an additional time point of 4h was investigated. While non-PEGylated polyplexes maintained their size without significant changes (apart from **1173** and **1178**),

polyplexes post-PEGylated with 1.0 eq (Cys)₂-PEG₂₄-Ala underwent partial aggregation (**1026**, **1173**, **1175** and **1177**). Non-PEGylated polyplexes might benefit from the formation of a serum corona around the polyplexes (which would also explain the increased lipopolyplex size), and remain stable despite the serum interaction. However, the formation of a serum corona - especially when attached to PEGylated nanostructures - has been demonstrated to also mediate favorable shielding properties [206]. Aggregation of polyplexes PEGylated with Ala could be affiliated with a decreased surface charge (cf. **Table 16**, **Table 17** and **Table 18**).

Lipopolyplexes PEGylated with 1.0 eq (Cys)₂-PEG₂₄-GE11 mostly maintained stability over 24h, but **1173**, **1175** and **1177** (Stp₂-Y₆-OleA, Stp₄-Y₃-OleA and Stp₄-Y₆-OleA) underwent severe aggregation, observed by DLS. However, within intensity based size distribution, which was required for detection besides serum proteins, small particle populations are over pronounced compared to smaller particles, which still could be detected as the main populations. Overall polyplexes exhibit a high stability in the presence of serum, which was already demonstrated previously [133, 226].

Results are summarized in **Table 19** and detailed intensity mean curves can be found in the Appendix (cf. **6.2**) due to the large data set.

Table 19 Summary table of polyplex stability in the presence of 90% serum determined after 24h with DLS. Colors represent: No significant change over time, partial population shift within time, total aggregation, as far as detectable by DLS.

| ID # | non-PEGylated | PEGylated with Ala | PEGylated with GE11 |
|-------------|---------------|--------------------|---------------------|
| 454 | | | |
| 1021 | | | |
| 1022 | | | |
| 1023 | | | |
| 1024 | | | |
| 1026 | | | |
| 1173 | | | |
| 1174 | | | |
| 1175 | | | |
| 1176 | | | |
| 1177 | | | |
| 1178 | | | |
| 1179 | | | |
| 1180 | | | |

3.3.3 Luciferase gene transfections

After biophysical evaluation, transfection efficacy of the post-modified lipopolyplexes was examined on two different cell lines. KB, a cervical adenocarcinoma cell line as well as the previously used hepatocellular carcinoma cell line Huh7 were both found to be EGFR positive (cf. **Figure 23A** and **Figure 35**).

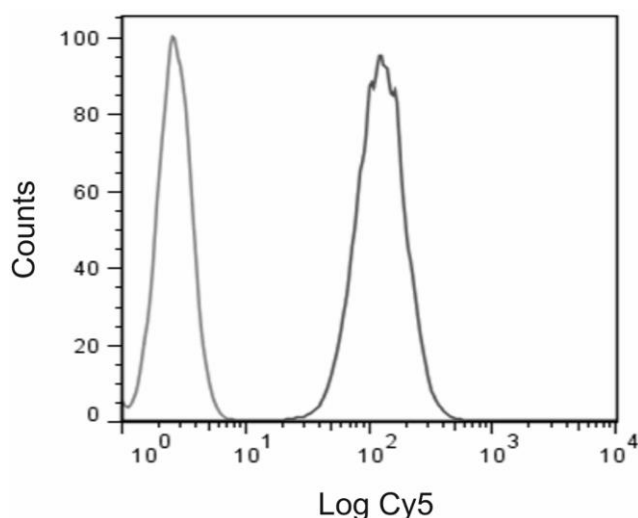


Figure 35 EGFR expression of the EGFR positive cell line KB, obtained with a monoclonal mouse anti-human EGFR antibody and IgG control. Alexa 488-labeled goat anti-mouse secondary antibody was used for the detection of receptor expression by flow cytometry. Control cells are presented in light grey, EGFR positive cells are presented in grey. Receptor screening was performed by Wei Zhang (postdoctoral study, Pharmaceutical Biotechnology, LMU).

The most stable oligomers were chosen for pDNA transfections. Besides LPEI, **454** served as control, while the histidine-rich oligomer **1026**, also containing 4 Stp but additional alternating histidines was investigated. All oligomers containing 8 Stp units were evaluated as well, to determine differences in transfection efficacy mediated by a variation of Y₃ or Y₆, differences between oleic acid and cholanic acid and also to investigate, if introduction and positioning of histidines influence endosomal escape. Lipopolyplexes were formed and post-modified with 1.0 eq of the bivalent reagents to investigate EGFR dependent gene delivery.

However, on both cell lines, after 24 h of incubation, only **454** mediated significant gene transfer (cf. **Figure 36A and B**). This gene transfer is in accordance with previous findings [226], but the lack of gene transfer of the newly generated oligomers needed

to be evaluated. At the same time, polyplexes did not mediate significant cytotoxicity (cf. **Figure 36C and D**).

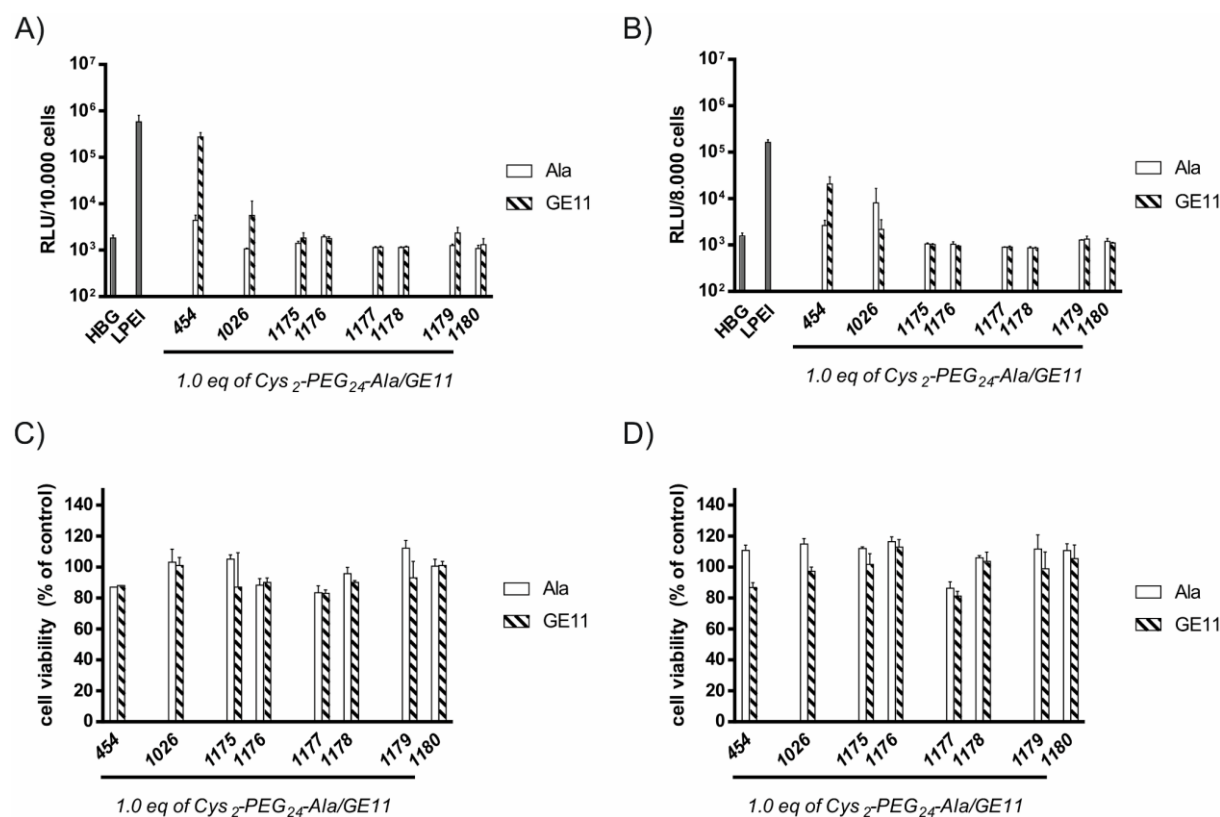


Figure 36 Luciferase gene expression was determined on the EGFR expressing cell lines Huh 7 (A) and KB (B). Transfection results after 24 h of polyplex incubation are shown. The corresponding MTT assays were performed in parallel and are displayed in (C) and (D). Assays were performed Ana Krhac Levacic (PhD study, Pharmaceutical Biotechnology, LMU).

As pointed out in the previous chapters (cf. **3.3.2.3** and **3.3.2.4**), additional introduction of Stp into the T-shaped oligomers improved lipopolyplex stability and thereby might hinder gene transfer *in vitro*.

Generally, when comparing gene transfer of the oligomer **454** in the previous chapter (cf. **3.2.3**) and in the results shown above, a notable difference was observed. During previous work, the influence of a proper cleavage, to prevent hydroxylation of the oleic acid's double bond [200], was not explored and therefore, oligomer cleavage was performed with much harsher conditions (90 min of TFA cleavage) than for the oligomer used for the current study. The impact of this different cleavage (30 min with

a thiol specific scavenger (EDT)) was not prominent for siRNA delivery [200], but it might explain the difference observed for pDNA delivery (cf. **Figure 37**). Further future investigations of the influence of hydroxylation of the double bond could be conducted by quantitative hydroxylation of the double bond. Gene transfer of the generated hydroxyl-stearic acid derivate could be compared to the non-hydroxylated oleic acid used for this study (cf. spectrum of **454** in **6.5.5.1**.)

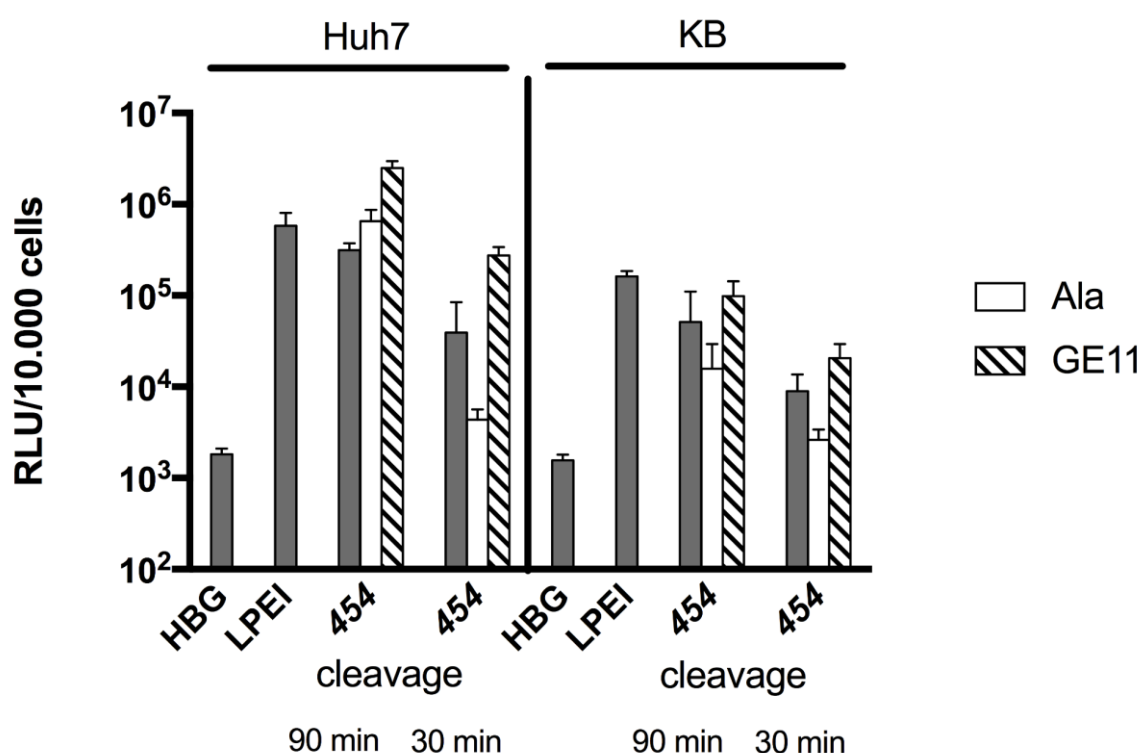


Figure 37 Comparison of gene transfer of two **454** syntheses, followed by either TFA treatment for 90 min or for 30 min. Gene transfer of non-PEGylated as well as post-modified polyplexes (with 1.0 eq of the bivalent reagents) was performed on Huh7 and KB cells by Ana Krhac Levacic (PhD study, Department of Pharmaceutical Biotechnology, LMU).

3.3.4 Ellman's assay to determine free thiols for polyplex post-modification

The shorter cleavage time (cf. **2.2.1.2.2**), applied for the **454** used in this chapter as well as all other oleic acid containing oligomers used for this chapter (cf. **Table 13**) could influence removal of certain sidechain protecting groups. Especially the Trt-protected thiols within the oligomers' cysteines are prone to side reactions or

uncomplete cleavage. This could later on influence the degree of post-modification during polyplex formation and thereby hinder receptor-specific tumor targeting. Consequently, an Ellman's assay for quantification of free thiols was conducted for oligomers **454**, **1026**, **1175-1180**. During storage, a certain number of thiols can oxidize and form disulfides, and are thereby not available for determination by this colorimetric, DTNB based reaction. Generally, 80% or more of the theoretically available thiols are considered as acceptable. Within the tested oligomers, only **1180** exhibited a reduced number of free thiols (cf. **Figure 38**). Oleic acid containing oligomers (like **1180**) could suffer from incomplete removal of the thiol protecting Trt group within 30 min of cleavage. Additionally, the excess of reactive triphenylmethyl carbenium ions, released during cleavage from the side chains of histidines and cysteines, bear a high potential of side reactions during cleavage as they can react with deprotected thiols via an nucleophilic addition.

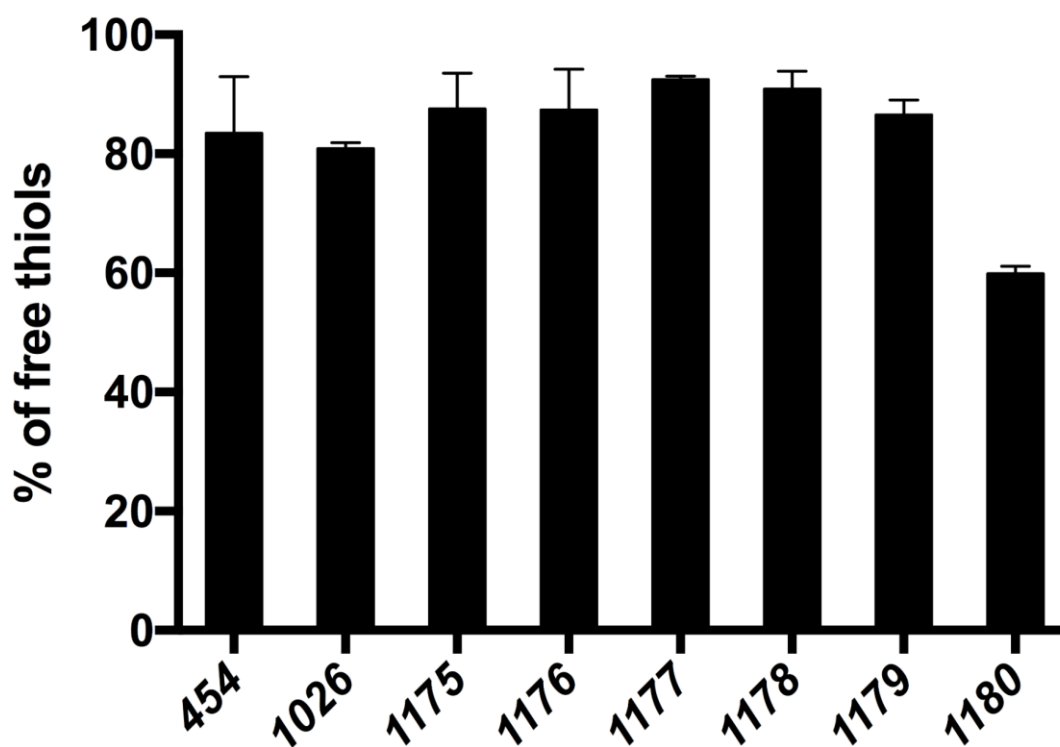


Figure 38 Ellman's assay of the displayed oligomers. % of free thiols are related to the theoretical amount of thiols in each sample. All oligomers containing oleic acid (**454**, **1026**, **1175**, **1177**, **1179**, **1180**), were cleaved for 30 min, while oligomers with cholanic acid (**1176**, **1178**) were cleaved for 90 min. Addition of EDT to the cleavage solution was supposed to prevent thiols from side reactions.

3.3.5 Cellular polyplex uptake

To investigate if polyplexes are taken up in an EGFR specific manner, but remain in the endosome, and thereby do not mediate gene transfer, FACS analysis with Cy5 labeled pDNA was carried out. Therefore, non-PEGylated lipopolyplexes, as well as polyplexes PEGylated with 1.0 eq of (Cys)₂-PEG₂₄-Ala and -GE11 were incubated with Huh7 cells for 45 min. A heparin wash was conducted to distinguish between internalized and associated lipopolyplexes and Cy5 intensity was investigated (cf. **Figure 39**).

After 45 min, all cells incubated with lipopolyplexes showed notable uptake compared to control cells, indicating that polyplexes are successfully internalized independently of the PEGylation. All polyplexes post-modified with the bivalent GE11 reagent exhibit a significantly improved uptake compared to lipopolyplexes post-modified with Ala. The latter in contrast showed hampered uptake compared to non-PEGylated lipopolyplexes within all polyplexes formed with oligomers containing 8 Stp units. This data thereby suggests that un-modified polyplexes are taken up unspecifically, via electrostatic interaction of the positively charged polyplexes and the negatively charged cell-surface, which could be reduced by PEGylation with Ala. Introduction of the EGFR specific binding peptide GE11 again increased uptake in a tumor-specific manner, resulting in a polyplex internalization at least as good as for non-modified lipopolyplexes.

Internalization of the tested lipopolyplexes can be summarized as followed: **454, 1026, 1077 > 1076, 1178 > 1175, 1179, 1180**. The lipo-oligomers with 4 Stp units (**454** and **1026**) tended to be internalized to a greater extent than lipo-oligomers consisting of 8 Stp units, however, also exhibited an increased polyplex size determined by DLS (cf. **3.3.2.1**). Overall all, oligomers in this study confirmed previous findings, that lipopolyplex post-modification with bivalent PEGylation reagents exhibits an effective tool to mediate EGFR dependent polyplex targeting [226]. GE11 mediated cellular uptake is summarized in **Figure 40**. The optimization of T-shaped oligomers significantly improved polyplex stability compared to the well-established oligomer **454**, however this increased stability could be a limitation regarding gene transfer efficacy. Previous results on PEI pointed out two important findings. Firstly, comparing pDNA/LPEI complexes and pDNA/BPEI complexes, both complexes quickly facilitated endosomal escape, however, the more compact pDNA/BPEI complexes remained stable for up to 24h inside the cell and only mediated gene transfer to a minor extent.

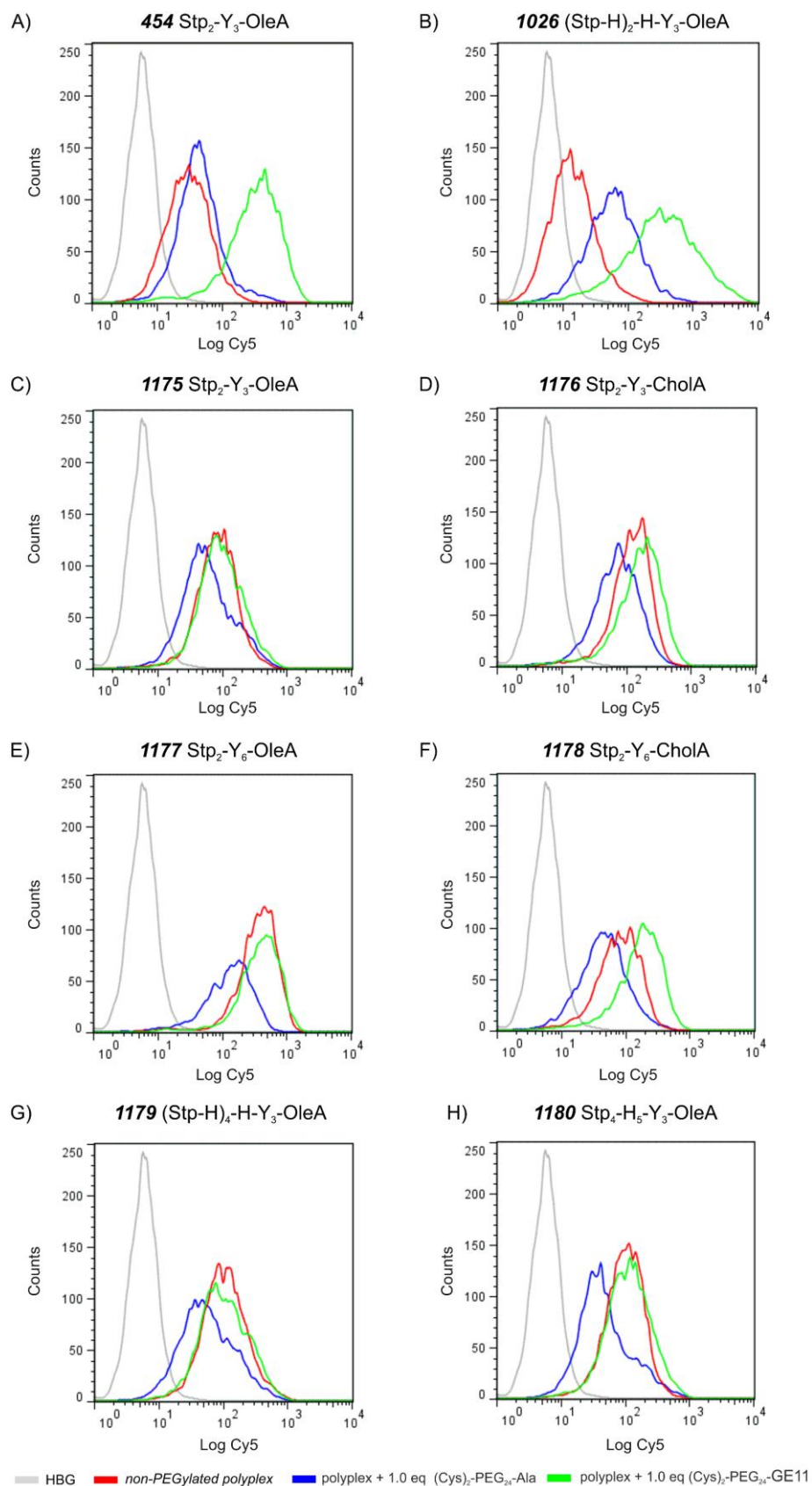


Figure 39 polyplex internalization of non-PEGylated (red), polyplexes post-modified with (Cys)₂-PEG₂₄-Ala as well as (Cys)₂-PEG₂₄-GE11 after 45 min of incubation into Huh7 cells. Lipopolyplexes formed with **454** served as control and were compared to lipopolyplexes formed with the novel lipo-oligomers.

At the same time, LPEI complexes dissociate rather quickly and thereby mediated gene transfer [227]. Also, within this study LPEI polyplexes dissociated rather quickly in the presence of heparin, and they are known to be prone to colloidal aggregation [29] while polyplexes formed with these novel lipo-oligomers remained stable within these environments.

Also, Ogris and colleagues pointed out, that LPEI polyplexes exhibiting an enhanced size due to increased colloidal aggregation, mediated significantly enhanced gene transfer in comparison to non-aggregated pDNA/PEI polyplexes [202]. However, lipopolyplexes formed with these novel lipo-oligomers exhibit in these regards both disadvantages; pDNA compaction as well as colloidal stability is improved, when compared to the previously examined **454** or LPEI.

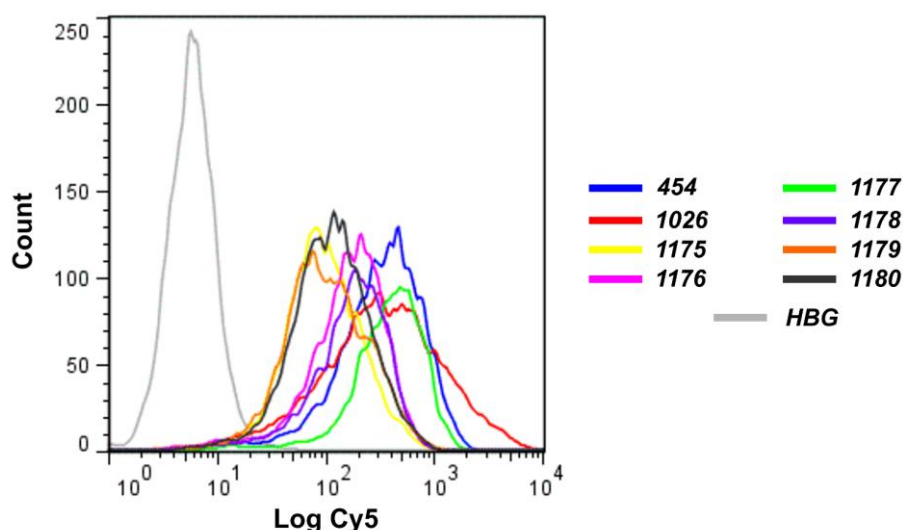


Figure 40 Summary of cellular uptake into Huh7 after lipopolyplex post-modification with 1.0 eq of (Cys)₂-PEG₂₄-GE11.

3.3.6 Gene transfer after enhanced endosomal escape

Besides the already mentioned increased polyplex stability, the lack of gene transfer of these novel oligomers could also be mediated by a hampered release from the endosome intracellularly. Therefore, two further experiments have been carried out. Chloroquine, as a well established endosomolytic reagent [57, 228], was added to Huh7 cells after pDNA lipopolyplex transfection for 45 min. Thereby we wanted to investigate, if the limited transfection efficacy is mediated by endosomal entrapment.

Cells treated with chloroquine for 4 hours neither showed any cytotoxicity nor significantly enhanced gene transfer apart from **454** (cf. **Figure 41**). However, **1026** and **1176** tended to mediate slightly improved gene transfer after chloroquine addition compared to HBG.

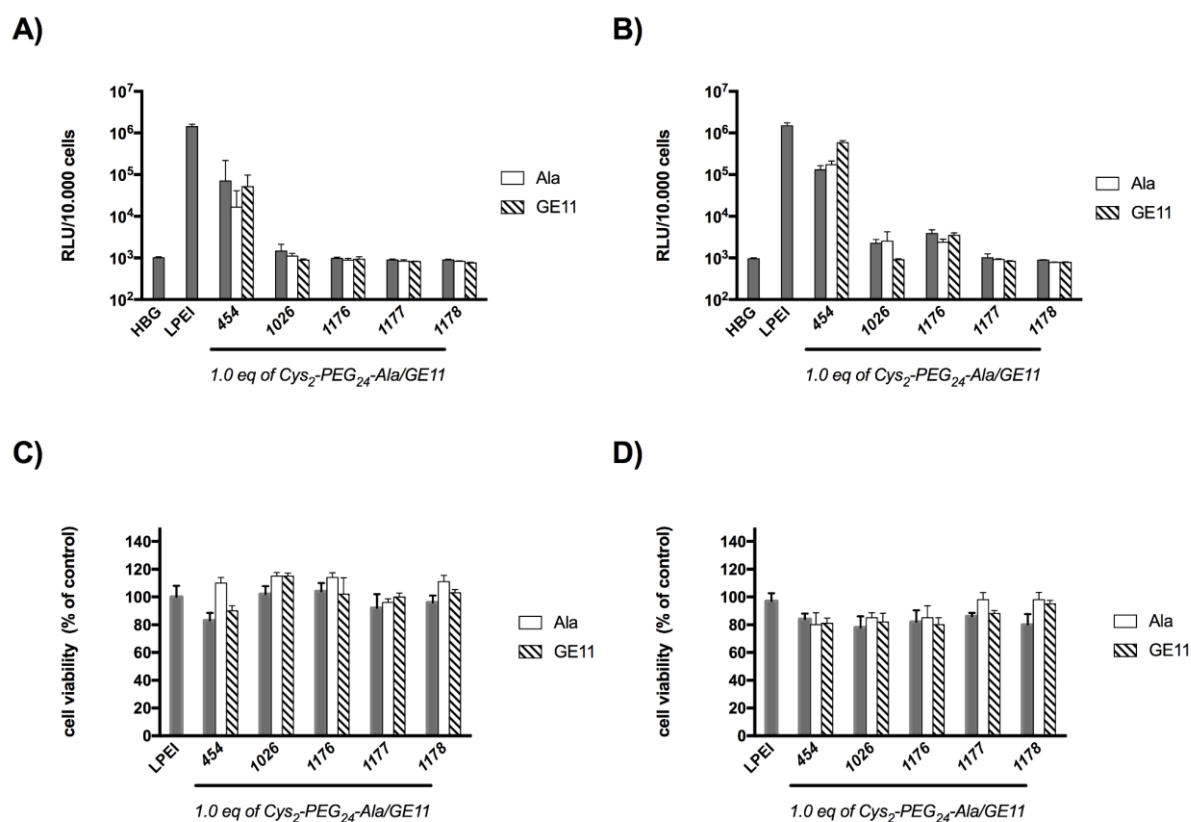


Figure 41 Gene transfer of the lipopolyplexes which mediated the best cellular uptake without (A) and with chloroquine addition (B). (PEGylated) lipopolyplexes at N/P 12 were incubated for 45 min and then were treated with chloroquine for 4h, prior to a media change and further incubation for 24 h in total. (C) and (D) represent the corresponding MTT assays performed in parallel.

As a next experiment, (post-modified) lipopolyplexes were incubated for 2 h on Huh7 cells, followed by a change towards LPEI (corresponding to N/P 9 per well) enriched culture media. Cells were then further cultured for up to 24 h. Previously, Boeckle and colleagues [229] as well as Yue and colleagues [230] pointed out that addition of free LPEI, with its diaminoethane motif buffering at endosomal pH, onto cells incubated with pDNA polyplexes significantly led to increased transfection efficacy.

However, within this experiment (cf. **Figure 42**), transfection efficacy tended to be only

slightly and unspecifically improved after LPEI addition. But also here, **454** lipopolyplexes exhibited the highest gene transfer, indicating that endosomal escape does not represent the only bottleneck for successful gene transfer of the novel lipopolyplexes and enhanced lipopolyplex stability still could contribute to the reduced gene transfer in comparison to the less stable **454** lipopolyplexes.

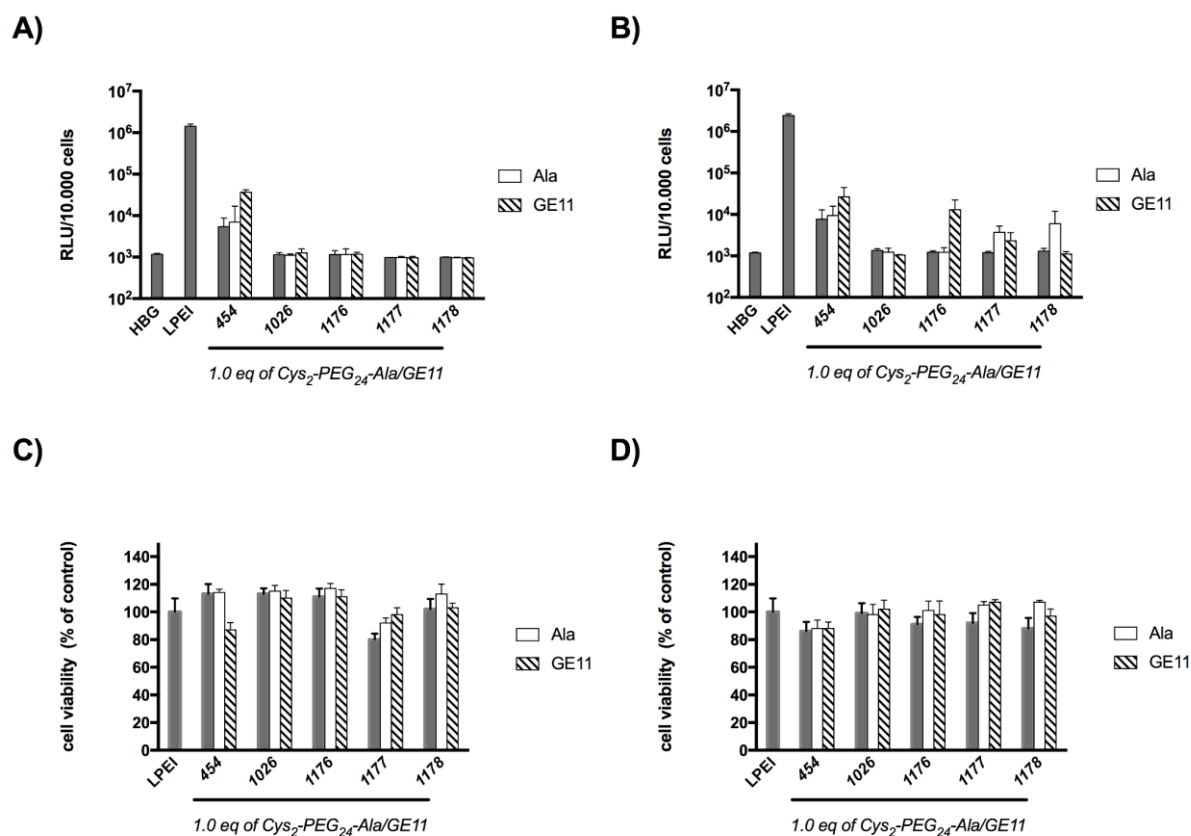


Figure 42 Gene transfer of the lipopolyplexes which mediated the best cellular uptake without (A) and with addition of LPEI (B). (PEGylated) lipopolyplexes were incubated for 2 h and then were treated with cell culture media supplemented with LPEI (corresponding to N/P 9 per well) in case of (B) while cell culture media was replaced with normal media for (A). Cells were then further incubated for 24 h in total. (C) and (D) represent the corresponding MTT assays performed in parallel.

4 Discussion

4.1 Influence of defined hydrophilic blocks within oligoaminoamide copolymers: compaction versus shielding of pDNA nanoparticles

This chapter is based on:

Morys, S.; Krhac Levacic, A.; Urnauer, S.; Kempter, S.; Kern, S.; Rädler, J.O.; Spitzweg, C.; Lächelt, U.; Wagner, E. *Influence of Defined Hydrophilic Blocks within Oligoaminoamide Copolymers: Compaction versus Shielding of pDNA Nanoparticles*. *Polymers* **2017**, *9*, 142.

Shielding of polyplexes represents an important characteristic required for a successful gene delivery [153]. Unshielded polyplexes exhibiting a positive surface charge may challenge interaction with blood components, colloidal aggregation due to electrostatic interaction or in the worst case an immune response [149].

Therefore, histidine-rich 2-arm oligomers, decorated with either PEG or peptidic PAS as a surface shielding domain were synthesized. This topology was previously shown, due to enhanced endosomal buffering [50], to be most suitable for pDNA delivery *in vitro* as well as *in vivo* [64, 65, 137]. These SPS derived oligomers were decorated with highly defined PEG as well as PAS repetitions to determine the optimal ratio of hydrophilic shielding blocks and cationic artificial amino acids. They were compared side-by-side and with an unshielded control oligomer. Besides a shielding domain, the cationic core of these oligomers consisted of the artificial amino acid Stp for nucleic acid binding [131], histidines for enhanced endosomal buffering [50], lysine for symmetrical branching as well as cysteines for bio-reducible crosslinking [131, 134].

During extensive biophysical evaluation, oligomers consisting of 12 repetitions of PEG were compared to oligomers with 4 PAS repetitions, while 24 PEG repetitions were considered equivalent to 8 PAS repetitions. Due to a sophisticated synthesis of PAS shielded oligomers, no control oligomer compared to oligomers equipped with PEG₄₈ was generated. TEM, as well as EtBr compaction, exhibited decreased pDNA compaction and a less firm (rod- to worm-like) particle shape with increasing amounts of PEG. Similar findings have been made previously for pLL and LPEI/pDNA polyplexes decorated with PEG [32, 205]. Within the performed *in vitro* structure-activity relationship studies, polyplexes shielded with PEG and PAS of comparable

length exhibited similar properties. At the same time, unshielded polyplexes provided the highest degree of pDNA compaction as well as the most compact (globule) nanoparticle shape determined by TEM. During this study, polyplex stability was challenged in the presence of physiological electrolyte concentrations (PBS), in the presence of 90% FBS, as well as adhesion to erythrocytes was examined. Here a contrary effect could be shown. Unshielded polyplex as well as polyplexes decorated with short shielding blocks (PEG₁₂ or PAS₄) suffered from immediate colloidal instability, while polyplexes decorated with PEG₂₄ or PEG₄₈ as well as PAS₈ remained size stable for at least 24 h. These results are in accordance with previous findings published by Ogris et al. [29].

Investigating erythrocyte adhesion of Cy5-labeled polyplexes findings similar to the previous experiment were observed. Unshielded polyplexes adhered to erythrocytes in a very high manner (>95%), while >20% pDNA could be recovered from polyplexes incubated with PEG₄₈ decorated oligomers. During incubation with 90% FBS, firstly all polyplexes underwent an initial interaction with serum, leading to polyplex sizes approximately increased about 200 nm compared to HBG both measured by DLS. In this experiment, polyplexes decorated with PEG₂₄, PEG₄₈ or PAS₈ revealed the highest potential towards aggregation and polyplex dissociation, which was confirmed by another serum assay after incubation with Cy5-labeled pDNA. These findings indicate that unshielded polyplexes, exhibiting the highest potential of electrostatic interaction with negatively charged serum proteins, could be more stabilized by the formation of a serum corona than shielded polyplexes [206].

Treatment of N2a tumor cells showed significant transfection efficacy for all polyplexes apart from polyplexes decorated with PEG₄₈ after long-term incubation for 24 h. However, in the short term, sufficient shielding and thereby no significant transfection was yet achieved by PEG₁₂ and PAS₄.

To determine tumor-specific delivery, a cMet targeting peptide (cmb) was introduced into all oligomers. After treatment to cMet positive Huh7 cells (and DU145 cells), untargeted polyplexes decorated with PEG₄₈ demonstrated reduced transfection efficacy which could be partially recovered by the introduction of the cmb peptide. These findings are in accordance with previous findings [64]. Nevertheless, these results highlight the difficulties of polyplex shielding leading to the so-called PEG dilemma [167]. Transfection efficacy of cMet targeted polyplexes incorporating PEG₄₈ as a shielding agent was significantly reduced in comparison to polyplexes shielded with

shorter shielding agents or unshielded polyplexes, leading to a higher specificity of the polyplexes due to an improved surface shielding, but a reduced transfection efficacy overall.

In sum, it is evident that opposing requirements have to be dealt with balanced measures; both extremes (no shielding or very long shielding) come along with disadvantages. The oligomer characteristics are summarized in **Table 20**. In different *in vitro* experiments, it was pointed out that within two-arm oligoaminoamide pDNA polyplexes, the shorter PEG₁₂ domain represents the best compromise. Similar results have been recently reported both for shielded LPEI polyplexes [32] and liposomes [231]. Polymers containing the targeting peptide cmb also confirmed these findings. Within the c-Met targeted polymers, polyplexes shielded with PEG₁₂ showed the most pronounced targeting effect and mediated gene transfer *in vitro* as well as *in vivo* most efficiently.

Table 20 Summary of oligomer characteristics

| Experiment | Oligomers | | | | | |
|---------------------------|-----------|-------------------|---------------------|-------------------|------------------|------------------|
| | 3-arm | PEG ₁₂ | PEG ₂₄ | PEG ₄₈ | PAS ₄ | PAS ₈ |
| PBS resistance | - | - | + | + | - | + |
| Erythrocyte adhesion | - | ++ | ++ | +++ | + | + |
| Particle compaction | +++ | ++ | + | - | ++ | + |
| Polyplex shape | globule | rod-like | doughnut aggregates | cord-like | rod-like | doughnut |
| Heparin resistance | + | + | - | - | + | + |
| Serum stability | + | + | - | - | + | - |
| Shielding | - | + | ++ | +++ | + | ++ |
| Transfection (short term) | + | - | - | - | - | - |
| Transfection (long term) | + | + | + | - | + | + |

PBS resistance: +/- indicates Yes/No; Erythrocyte adhesion: +++ lowest adhesion, ++ low adhesion, + increased adhesion, - complete adhesion; Particle compaction: +++ highest compaction, ++ mediate compaction, + compaction, - no sufficient compaction (evaluated by EtBr exclusion assay and TEM images); Heparin resistance against 250 IU: +/- indicates Yes/No; Serum stability: +/- indicates Yes/No; Shielding: +++ zeta potential (ZP) < 2 mV, ++ ZP < 5 mV, + ZP < 10 mV, - ZP > 10 mV; Transfection efficacy of polyplexes on N2a cells (short as well as long-term): + significant transfection efficacy compared to untransfected cells, - no transfection signal compared to untreated cells.

4.2 EGFR targeting and shielding of pDNA lipopolyplexes via bivalent attachment of a sequence-defined PEG agent

This chapter is based on:

Morys S. , Urnauer S.* , Spitzweg C., Wagner E., EGFR Targeting and Shielding of pDNA Lipopolyplexes via Bivalent Attachment of a Sequence-Defined PEG Agent, Macromol. Biosci. 2017. (* indicates that authors contributed equally to this work)*

pDNA polyplexes can be functionalized with shielding and targeting domains either by pre-conjugation or by post-modification strategies. However, as mentioned previously, shielding of polyplexes represents an important characteristic required for a successful gene delivery to avoid aggregation with blood components, colloidal aggregation due to electrostatic interaction or in the worst case an immune response [149, 153]. To overcome the emerging disadvantages of PEGylation, tumor cell specific binding can be increased by introduction of a targeting domain, consisting of either small molecules [122, 135], peptides [50, 61, 62, 65, 139, 140] or proteins [57, 178, 197].

The current study aimed at the design of EGFR-targeted pDNA delivery shuttles. EGFR targeted polyplexes formed of PEG-Stp/His 2-arm oligomers were compared with T-shaped lipopolyplexes that were post-modified with mono- or bivalent EGFR targeted PEGylation reagents. In a previous approach, pDNA/LPEI polyplexes pre- and post-modified with EGF-PEG were already compared side by side, pointing out the advantageous strategy of a polyplex post-modification [168]. Within this study, GE11 (YHWYGYTPQNVI), a phage-derived peptide, served as a specific ligand for the EGFR within sequence-defined oligomers. Pre-PEGylated oligomers consisted of the GE11 peptide or alanine, a PEG of exactly 24 repetitions, while the cationic core was composed of the artificial amino acid Stp, histidines for enhanced endosomal buffering, lysine for symmetrical branching as well as cysteines for bioreducible crosslinking. T-shaped oligomer **454** was built with tyrosines for hydrophobic stabilization via $\pi - \pi$ stacking, cysteines for bioreducible crosslinking as well as it served as anchors for the PEGylation reagents. Stp was introduced for nucleic acid binding, lysine for symmetrical branching and two oleic acids as central stabilizing, pH-dependent lytic domains. All reagents used in this study were sequentially generated via SPS.

Polyplexes assembled via pre- and post-modification strategy were examined to understand the biophysical behavior as well as incubated on different cancer cell lines to investigate tumor-specific binding, uptake and finally gene transfer of luciferase marker gene and sodium iodide symporter (NIS) *in vitro*.

Polyplex size, determined by DLS, exhibited aggregation of polyplexes formed with the pre-PEGylated GE11-PEG-Stp/His 2-arm oligomer as well as its alanine equipped control oligomer. This could be explained by the high degree of PEGylation in comparison to a rather small cationizable pDNA compacting domain and the associated large amount of hydrophobic GE11 peptide; it is known that hydrophobic peptides tend to cause aggregation [209, 210].

The size of polyplexes formed with the T-shaped lipo-oligomer **454** and pDNA only increased from 81.4 nm (non-PEGylated) to a maximum size of 283.8 nm after addition of the bivalent Cys₂-PEG₂₄-GE11 PEGylation reagent. Besides a reduced zeta potential, also release of NPys and a significant reduction of free thiols proved the successful post-modification approach. An EtBr compaction assay reproduced the findings of size measurement. Pre-PEGylated oligomers compacted pDNA to a lower extent (20-25%) than unmodified (8%) or post-modified lipopolyplexes (8-10%). Next, polyplex stability was investigated in the presence of 90% FBS and cell culture media (supplemented with 10% FBS) via DLS. Within both solvents, pre-PEGylated polyplexes underwent aggregation after 24 h or particle dissociation which is in accordance with previous results [64, 133]. At the same time, **454**/pDNA polyplexes underwent immediate interaction with the solvents, leading to increased sizes of approximately 250 nm but underwent no further changes over a time of 24 h. Lipopolyplexes post-modified with 1.0 eq of monovalent PEGylation reagents revealed a lower stability than lipopolyplexes PEGylated with 1.0 eq of the bivalent PEGylation reagents. In the latter case, only minor size increase occurred, while the monovalent PEGylation reagents tended to destabilize the polyplexes, leading to partially aggregation within time.

Cell experiments were carried out on the EGFR positive cell lines Huh7 and MCF-7 as well as the low EGFR expressing cell line FTC-133.

Firstly, transfection efficacy was investigated by determination of luciferase expression. Here, gene transfer was highly enhanced in an EGFR dependent manner by lipopolyplexes modified with the bivalent Cys₂-PEG₂₄-GE11 reagent after 45 min. But also, lipopolyplexes PEGylated with the monovalent Cys-PEG₂₄-GE11 exhibited a

target specificity compared to unmodified lipopolyplexes. Pre-PEGylated polyplexes, as well as LPEI-PEG_{2k}-GE11, mediated gene transfer less efficiently than the unmodified lipopolyplexes. Incubation of the polyplexes on cells for 24 h led to generally increased transfection efficacy, while the trend remained unaffected. Transfections on the EGFR low expressing cell line FTC-133 pointed out the EGFR dependency of the transfections on Huh7 and MCF-7 as no enhanced gene transfer could be investigated by the GE11 targeted polyplexes. Within all transfections, no cytotoxicity could be observed.

Secondly, cellular binding and uptake of the polyplexes was investigated on Huh7 and MCF-7 cells. Here, the polyplexes post-modified with 1.0 eq of the bivalent EGFR targeted PEGylation reagent mediated a significantly higher cellular binding than polyplexes PEGylated with 1.0 eq of the monovalent reagent, while both reagents were superior to unmodified lipopolyplexes. However, all polyplexes showed a higher specificity than polyplexes formed with LPEI-PEG_{2k}-GE11 and pre-PEGylated polyplexes. In the latter case, a GE11 mediated targeting effect was observed, but this might be due to the previously mentioned severe aggregation of GE11-PEG₂₄-Stp/His polyplexes.

As a last experiment, polyplexes were formed with a NIS (sodium iodide symporter) expressing pDNA and incubated on Huh7 cells. The NIS gene can be introduced to achieve a tumor-specific iodide uptake for theranostic as well as therapeutic use [213, 214]. Here the theranostic ¹²⁵I was chosen to demonstrate the capabilities of the system. Also within these transfections, the lipopolyplexes post-modified with the 1.0 eq of the bivalent EGFR targeted PEGylation reagent mediated the highest gene transfer, corresponding with the highest iodide uptake.

Overall, this work is very consistent with previous work pointing out that post-modification offers an auspicious tool for shielding and targeting of pDNA [29, 142, 156, 160, 168, 232-234] as well as of siRNA polyplexes [169, 170]. The superior effect of the bivalent over monovalent PEGylation reagents is well consistent with similar findings applying multivalent coatings of nucleic acid nanoparticles [160, 232, 233]. Also, this approach offers a possibility to overcome GE11 mediated polyplex aggregation, and diminishes negative side-effects of PEGylation, such as reduced cellular binding. Also, reduced endosomal escape due to the introduction of a targeting ligand and a very effective lipo-oligomer based polyplex core could be overcome with this post-modification approach.

4.3 Lipo-oligomers optimized towards enhanced lipopolyplex stability

Within this chapter, oligomers for an *in vivo* translation of the lipopolyplex PEGylation approach were designed. Lipo-oligomer **454** served as a starting point and was stepwise modified. Nucleic acid compaction (1), hydrophobic stabilization (2) and enhanced endosomal escape (3) was to be improved by varying the relevant functional groups. The main aim of this study was the optimization of lipopolyplex stability after PEGylation with the previously investigated bivalent shielding reagents (cf **3.2**). Oligomers generated for this study can be subdivided into three groups.

Within the first group, the effect of prolonging the positively charged binding domain within the carrier (Stp domain) was investigated. Stp, which is known, to mediate nucleic acid compaction and endosomal buffering [131, 134] was increased from 4 Stp units (within **454**) up to 6 and 8 units respectively. Also, the stabilizing effect of tyrosine from peripherally placed trimers (Y_3) [52] to hexamers was investigated, as they are known to stabilize via inter-oligomeral π - π stacking of the aromatic rings [208]. Additional stabilization within **454** was obtained by two centrally placed oleic acids. These hydrophobic domains, also facilitating endosomal release via pH-dependent lytic activity [51], were compared to cholanic acid, which previously elevated stability within siRNA lipopolyplexes [111]. Within the last group of oligomers, histidines were introduced alternately between the Stp units, as well as blockwise between tyrosines and Stp. Histidine is known to improve endosomal escape via enhanced endosomal buffering due to its imidazole side chain ($pK_a=6.5$) [50, 105], but it is also hypothesized to interact inter-molecularly via π - π stacking [225, 235].

These oligomers were evaluated within different assays for lipopolyplex stability before and after PEGylation with 1.0 eq Cys₂-PEG₂₄-Ala and GE11.

First, size of non-PEGylated polyplexes was investigated. All polyplexes exhibited a particle size between 70 and 102 nm, a PDI (whereas 1.0 represents the highest polydispersity) between 0.12 and 0.26 and a positive surface potential between 17 and 30 mV. These results are in accordance with previous findings, pointing out that, non-PEGylated lipopolyplexes exhibit a positive zeta potential [226]. Polyplex size and polydispersity also meet criteria for a PEGylation approach for *in vivo* gene delivery, where sizes between 20 and 400 nm were found to be best suitable for gene delivery into solid tumors [41, 236]. PEGylation with 1.0 eq of the bivalent Cys₂-PEG₂₄-Ala resulted for all lipopolyplexes in only minor increased particle sizes between 72 and 90

nm, but a highly decreased zeta potential (between 1.5 and 12 mV), indicating the successful PEGylation reaction. However, introduction of 1.0 eq of the bivalent Cys₂-PEG₂₄-GE11 reagent resulted in partial aggregation. As reported previously, the hydrophobic GE11 peptide is known to promote aggregation within pre-PEGylated polyplexes and enhanced particles sizes in case of **454** [226]. An increase in size was identified for all oligomers containing only 4 Stp units, whereas sizes ranged from 284 nm (**454**) to >5000 nm in case of oligomers containing Y₆ (**1173** and **1174**). An increase to 6 Stp units (**1022** and **1023**) did not completely help to overcome this aggregation, however with size decreased to a lower extent in case of cholanic acid bearing polyplexes. Lipopolyplexes formed with oligomers containing 8 Stp units exhibited nanoparticle sizes between 71 and 102 nm, and thereby just an increase of approximately 25 nm during PEGylation with Cys₂-PEG₂₄-GE11. Polyplexes formed with cholanic acid containing oligomers tended to maintain smaller particle sizes than oleic acid containing polyplexes. Summarizing these findings, we conclude, that the elevated cationic charge is helping to overcome the aggregation potential of hydrophobic peptides [209, 210] such as GE11 by increased nucleic acid compaction. Consequently, an EtBr compaction assay was carried out to investigate if increased cationic chain-length comes along with improved cargo compaction. For non-PEGylated lipopolyplexes, a remaining EtBr fluorescence was determined between 8 and 17%, while LPEI, which was used as a control exhibited less than 5 % free EtBr fluorescence. PEGylation with 1.0 eq of the bivalent reagents, independent if Ala or GE11 was spiked, did not significantly influence nucleic acid compaction. No differences between oleic acid and cholanic acid could be observed, but oligomers with 8 Stp units generally tended to mediate a slightly improved pDNA compaction compared to oligomers containing only 4 Stp units.

250 IU heparin was added to the same samples, and nucleic acid compaction after polyanionic stress was determined. Here, all lipopolyplexes mediated higher resistance, leading to a maximum of 60% EtBr fluorescence, than LPEI complexes, which released nucleic acid almost completely (>95%). Interestingly, within this experiment polyplexes with Stp₂-Y₆ (**1173** and **1174**) retained 60% of pDNA. All other polyplexes maintained pDNA compaction between 40 and 50%, which was already shown for **454** previously [226]. Generally, no notable differences between polyplexes comprising oleic or cholanic acid as stability inducing domains could be observed.

PEGylation of lipopolyplexes did not negatively influence pDNA compaction after polyanionic stress as observed previously for pre-PEGylated polyplexes [133].

As a next experiment, after polyplex formation, stability within physiological salt concentrations, mediated by PBS solution buffered at pH 7.4, was investigated. Here, non-PEGylated polyplexes formed with oligomers consisting of 6 or less Stp units underwent colloidal aggregation with sizes more than 1000 nm. After three hours, all polyplexes apart from polyplexes formed with oligomers containing 8 Stp units were either dissociated or exhibited a size of several 1000 nm. Oligomers **1175-1180** comprising 8 Stp units increased to a maximum size of 370 nm, however, mostly exhibited a size below 250 nm, indicating that the combination of hydrophobic stabilization via peripheral tyrosines (at least trimers) as well as fatty acids (independent if cholanic or oleic acid was introduced) and 8 Stp units per oligomer significantly increased polyplex stability against colloidal stress. Stability of these non-PEGylated lipopolyplexes was maintained for 24 h. PEGylation with 1.0 eq bivalent reagents resulted in different findings. While all polyplexes PEGylated with Ala underwent no aggregation within 24 h, giving proof of the successful PEGylation of these polyplexes, lipopolyplexes PEGylated with GE11 underwent immediate aggregation, latest after 30 min of incubation with PBS. To point out that the behavior of GE11 is linked to lipopolyplexes solely, the well-established LPEI-PEG_{2k}-GE11 [62, 192] was additionally included in this study, however also underwent aggregation 30 min after addition of PBS. This again points out the special behavior of GE11 within polyplexes. Nevertheless, this GE11 mediated aggregation is only an indicator for a reduced stability compared to polyplexes PEGylated with the less hydrophobic Ala, as LPEI-PEG_{2k}-GE11 is well known to mediate EGFR specific gene transfer *in-vivo* [192, 237].

In a last experiment evaluating biophysical properties, polyplex stability in the presence of serum was investigated. Therefore, polyplexes were formed and incubated in 90% FBS. In general, as mentioned previously [226], polyplexes remained stable for 24h. All lipopolyplexes underwent immediate interaction with serum, displayed in an increased size of around 300 nm. This is most likely due to the formation of a serum corona. This interaction is known to facilitate stability, especially for PEGylated polyplexes, and thereby significantly contributes to their stability over time [206]. However, polyplexes PEGylated with Ala tended to (partially) aggregate to a greater

extent than lipopolyplexes PEGylated with GE11, indicating that lipopolyplexes post-modified with GE11 form a more stable serum corona.

Overall these data suggest, that PEGylation is beneficial for lipopolyplex stability and emphasizes that an increased cationic charge density, is required to overcome GE11 mediated polyplex aggregation and to enhance polyplex stability compared to polyplexes formed with oligomers of 4 or 6 Stp units.

Next, lipopolyplexes were post-modified with 1.0 eq of Cys₂-PEG₂₄-Ala/GE11 and gene transfer was investigated on the two EGFR positive cell lines Huh7 and KB. After 24 h of incubation on the cells, only the PEGylated **454**/pDNA polyplex mediated notable gene transfer in an EGFR specific manner. All other tested oligomers mediated no gene transfer compared to buffer-treated cells, but also none of the polyplexes mediated cytotoxicity within 24 h on the cells. A reason for this could be the enhanced stability of the lipopolyplexes generated from the novel oligomers as investigated by different stress-inducing stability assays. An increased cationic charge density as well as hydrophobic domains (Y₆ or cholanic acid), mediated a significantly enhanced lipopolyplex stability *in vitro* and thereby could hinder DNA release.

Consequently, cellular internalization was investigated. FACS analysis revealed significant intracellular uptake for all Cy5-labeled pDNA/oligomer complexes. A reduced cellular uptake of the lipopolyplexes PEGylated with 1.0 eq of the bivalent Ala control reagent was observed, pointing out that polyplex shielding hinders unspecific cellular uptake in comparison to unmodified lipopolyplexes. Similar findings have been made previously for PEGylated PEI complexes [164]. At the same time, post-modification with 1.0 eq of the bivalent EGFR targeted GE11 PEGylation reagent facilitated cellular uptake at least as good as non-PEGylated core lipopolyplexes. Ogris et al. previously already pointed out in a PEI based work that EGFR-targeting is only affected to a minor extent by PEGylation [54].

Overall, lipopolyplexes formed with oligomers containing 4 Stp units (**454** and **1026**) mediated a higher uptake than polyplexes formed with oligomers containing 8 Stp units (**1175-1180**).

Polyplexes with the highest uptake (**454**, **1026**, **1176**, **1177**, **1178**) were transfected again but within these transfections endosomolytic LPEI and chloroquine was added afterwards to reduce the possible lack of endosomal escape during gene delivery. This experiment was conducted as polyplexes formed with the novel lipo-oligomers were successfully taken up in a EGFR specific manner, but could not mediate gene transfer.

Although chloroquine is also known to facilitate polyplex dissociation intracellularly [238, 239], significantly improved transfection efficacy was only found for polyplexes formed with **454**. Endosomal escape could be enhanced for parts of the novel oligomers (**1026**, **1176**), although only in a minor extent. Thereby, it still could be considered that the herein generated lipopolyplexes suffer from their enhanced polyplex stability in comparison to the more labile **454**/pDNA polyplexes as all polyplexes were internalized facilitating gene transfer theoretically.

However, polyplexes formed with the newly generated lipo-oligomers might retain their cargo in subsequent steps preventing transformation of the pDNA towards its protein. This question could only be addressed by time consuming microscopy techniques requiring high expertise and labeling of pDNA as well as the oligomers for determination of cellular trafficking.

In general, for all experiments, an equimolar amount of PEG per cysteine within all oligomers was used. This not only resulted in a two-fold excess of PEG per oligomer (as all oligomers contain two cysteines) but also in a two-fold excess of NPys (due to its bivalency) per cysteine of the oligomer. Although this excess mediated the best gene transfer (data not shown) for **454**/pDNA polyplexes PEGylated with these bivalent reagents, the excess of reactive PEGylation reagents might reduce uptake to a certain extent, referring to the previously mentioned PEG dilemma [163]. Sizes of (PEGylated) lipopolyplexes were approximately 100 nm for oligomers containing 8 Stp units (**1175-1180**), with an enhanced stability in the presence of physiological salt concentrations. At the same time (post-modified) **454** and **1026** pDNA polyplexes exhibited particle sizes of at least 200 nm. This increased size could at least partially help to compensate cellular uptake reduced by the excess of PEGylation reagents as larger particles might be taken up more efficiently [240, 241]. Ogris and colleagues [202] previously showed that polyplex size also plays a critical role for gene transfer itself, pointing out that larger polyplexes lead to at least 10x increased gene transfer due to improved endosomal escape.

The excess of NPys during PEGylation in this surrounding could hinder oligomer crosslinking, theoretically leading to mono-functionalized oligomer-PEG constructs and not oligomer-oligomer constructs crosslinked by a bivalent linker. Although this mechanism is not clearly described, it was previously [242, 243] pointed out that pLL/pDNA polyplexes modified with pHMPA equipped with multiple attachment sites

mediated superior stability over linear (semitelechelic) pHMPA structures, considerably because of intermolecular cross-linking. However, for this shielding with enhanced stability, a slower reaction kinetic is described, suggesting that further experiments could be carried out after an elongated PEGylation reaction with a lower amount of PEGylation reagent.

5 Summary

Non-viral gene delivery depicts a promising alternative to the classical, established method of viral gene delivery [1]. However, for a successful gene delivery by artificial vectors, these carriers need to display several functionalities. Besides the ability to bind and compact the cargo, they are also required to shield the nucleic acid from degradation. During formulation of the nanoparticles (so-called polyplexes), the particles need to exhibit a suitable size between 50 and 400 nm to accumulate within the tissue of interest [39, 40]. To tailor these vehicles to its needs, such as preventing the nucleic acid from degradation, or to reduce interaction with blood components [153], solid phase synthesis (SPS) was recently introduced [95, 98, 117, 131, 134]. Thereby, oligomers could be generated to draw clear-cut structure-activity relationships.

This first part of the study focuses on the optimization of shielding domains within sequence-defined oligomers (oligoaminoamides), which were generated by incorporation of novel artificial polyamino acids [131] for nucleic acid binding and compaction. Hereby, the strategy of pre-PEGylation, implying that a hydrophilic block of defined ethylene oxide repetitions was incorporated during oligomer synthesis, was applied to optimize pDNA delivery. To overcome the hampered transfection efficacy mediated by PEG [167], a hepatocyte growth factor receptor (HGFR) binding peptide (cmb) [181], that was previously found to mediate tumor-specific gene delivery *in vitro* as well as *in vivo* [64, 65], was introduced. Opposing requirements had to be dealt with while comparing shielding agents (PEG and peptidic Pro-Ala-Ser repeats) of different repetitions; both extremes (no shielding or very long shielding) have their drawbacks within two-arm oligoaminoamide pDNA polyplexes. However, it is concluded that a shorter shielding domain consisting of 12 PEG repetitions displays the best compromise for HGFR targeted gene delivery - this could also be shown by intratumoral delivery *in vivo*.

Besides pre-PEGylation, also the introduction of a targeted PEGylation reagent after polyplex formation facilitates tumor-specific gene delivery [169, 170]. This approach was explored within the second part of this thesis for EGFR (epidermal growth factor receptor) targeted pDNA polyplexes, complexed by a cysteine-containing sequence-

defined lipo-oligomer (**454** [52]). Therefore, the EGFR specific peptide GE11 (YHWYGYTPQNVI) was linked to PEG of 24 repetitions and activated terminal cysteines (one or two respectively) which were assembled as mono- or bivalent PEGylation reagents via SPS. During biophysical evaluation and *in vitro* testing on different EGFR positive or low expressing tumor cells, pDNA lipopolyplexes post-modified with the bivalent PEGylation reagent via disulfide exchange chemistry, exhibited the highest EGFR dependent tumor uptake and gene expression, while circumventing polyplex aggregation observed for pre-PEGylated GE11 targeted 2-arm oligomers, which were evaluated side by side within this study.

Lipopolyplexes are described to mediate increased polyplex stability, which is known to be of high importance for *in vivo* gene delivery. However, post-modified **454**/pDNA polyplexes lack stability. Therefore new oligomers with increased cationic charge (mediated by increased Stp units from 4 to 6 or 8), improved hydrophobic stabilization (due to introduction of Y₆ and/ or cholanic acid instead of oleic acid) as well as additional histidines (for endosomal buffering as well as potential stabilization via imidazole mediated π - π stacking [225, 235]) were introduced and then carefully evaluated via biophysical experiments to determine polyplex behavior in the presence of (poly)anionic stress and in the presence of serum. Here the novel oligomers **1175-1180** exhibited a significantly improved polyplex stability compared to **454**. While *in vitro* transfections of the post-modified lipopolyplexes could not mediate gene delivery within 24 h, significant receptor-dependent cellular polyplex uptake was observed after 45 min for oligomers **1026**, **1177** as well as **1176** and **1178** as well as **454**. Transfections of these post-modified polyplexes followed by addition of endosomolytic LPEI or chloroquine pointed out the functionality of this assay, as gene transfer could be significantly improved for **454**/pDNA polyplexes. However, gene transfer was not notably enhanced for all other lipopolyplexes. This indicates that polyplexes formed with the newly generated lipo-oligomers might retain their cargo in subsequent steps preventing transformation of the pDNA towards its protein. Future *in vivo* experiments could show if stability was sufficiently improved to resist effects occurring *in vivo* and lipopolyplexes can overcome the intracellular barriers towards successful gene delivery.

6 Appendix

6.1 Abbreviations

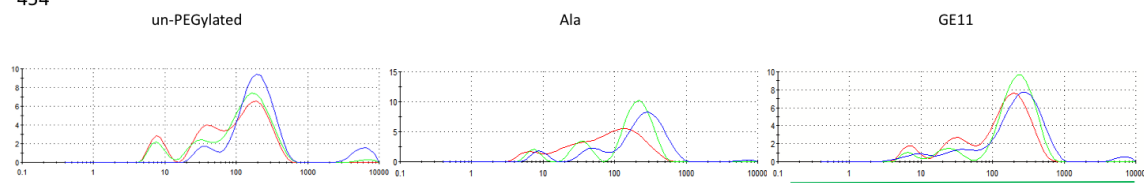
| | |
|----------|---|
| Boc | <i>tert</i> -Butoxycarbonyl protecting group |
| CholA | 5 β -Cholanic acid |
| DAMP | 3,3'-Diamino-N-methyldipropylamine; |
| DCM | Dichloromethane |
| DIPEA | <i>N,N</i> -Diisopropylethylamine |
| DLS | Dynamic light scattering |
| DMEM | Dulbecco's modified Eagle's medium |
| DMF | <i>N,N</i> -Dimethylformamide |
| DNA | Desoxyribonucleic acid |
| EDTA | Ethylendiaminetetraacetic acid |
| EGF/EGFR | Epidermal growth factor (receptor) |
| EtBr | Ethidium bromide |
| FBS | Fetal bovine serum |
| Fmoc | Fluorenylmethoxycarbonyl protecting group |
| FoIA | Folic acid |
| FR | Folate receptor |
| GSH | Glutathione |
| Gtt | Glutaroyl triethylene tetramine |
| HBG | Hepes-buffered glucose |
| HBTU | 2-(1H-benzotriazole-1-yl)-1,1,3,3-tetramethyluronium hexafluorophosphate |
| HEPES | <i>N</i> -(2-hydroxyethyl) piperazine- <i>N'</i> -(2-ethansulfonic acid) |
| HGF/HGFR | Hepatocyte growth factor (receptor) |
| HOBt | 1-Hydroxybenzotriazole |
| Inf7 | An endosomolytic influenza virus derived peptide |
| kDa | Kilodalton |
| LMW | Low molecular weight |
| LPEI | Linear polyethylenimine |
| mM | Millimolar |

| | |
|----------|--|
| mRNA | Messenger RNA |
| MTBE | Methyl <i>tert</i> -butyl ether |
| MTT | 3-(4,5-dimethylthiazol-2-yl)-2,5-diphenyltetrazolium bromide |
| mV | Millivolt |
| MWCO | Molecular weight cut-off |
| N/P | Nitrogen to phosphates ratio |
| NEM | N-ethylmaleimide |
| NHS | <i>N</i> -Hydroxysuccinimide |
| nm | Nanometer |
| NMP | <i>N</i> -Methyl-2-pyrrolidone |
| NMR | Nuclear magnetic resonance |
| OEI | Oligoethylenimine |
| OleA | Oleic acid |
| PAA | Polyamino acid |
| pCMVLuc | Plasmid encoding for firefly luciferase under the control of the cytomegaly virus (CMV) promoter |
| pHPMA | Poly- <i>N</i> -(2-hydroxypropyl)methacrylamide |
| PDI | Polydispersity index |
| pDNA | Plasmid DNA |
| PEG | Polyethylene glycol |
| BPEI | Branched polyethylenimine |
| LPEI | Linear Polyethylenimine |
| PAMAM | Poly(amidoamine) |
| pKa | $-\log_{10} K_a$ (acid dissociation constant) |
| pLL | Polylysine |
| PyBOP | Benzotriazol-1-yloxy-tripyrrolidinophosphonium hexafluorophosphate |
| RLU | Relative light units |
| RNA | Ribonucleic acid |
| RP-HPLC | Reversed-phase high-performance liquid chromatography |
| RT | Room temperature |
| SEC | Size-exclusion chromatography |
| siRNA | Small interfering RNA |
| Spermine | <i>N,N</i> -(butane-1,4-diyl)bis(propane-1,3-diamine) |
| Sph | Succinyl-pentaethylene hexamine |

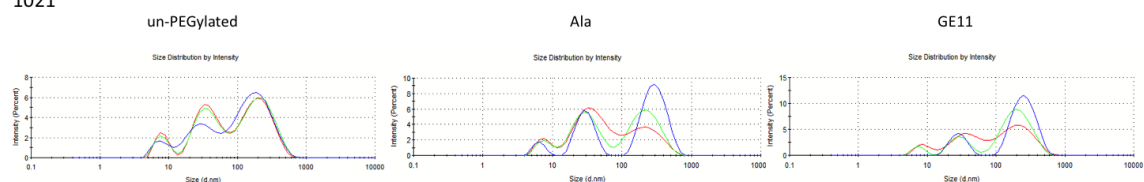
| | |
|--------|---|
| SPS | Solid-phase synthesis |
| Stp | Succinyl-tetraethylene pentamine |
| STOTDA | <i>N</i> -Fmoc- <i>N</i> '-succinyl-4,7,10-trioxa-1,13-tridecanediamine |
| Tat | Transactivator of Transcription |
| TBE | Tris-boric acid-EDTA buffer |
| TEPA | Tetraethylene pentamine |
| TETA | Triethylene tetramine |
| TFA | Trifluoroacetic acid |
| THF | Tetrahydrofuran |
| TIS | Triisopropylsilane |
| TKI | Tyrosine kinase inhibitor |

6.2 Serum stability of optimized T-shapes determined by DLS

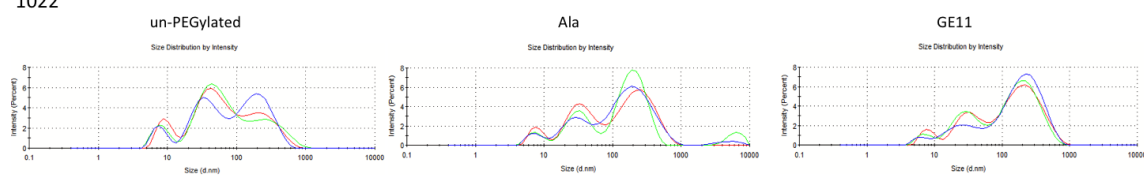
454



1021

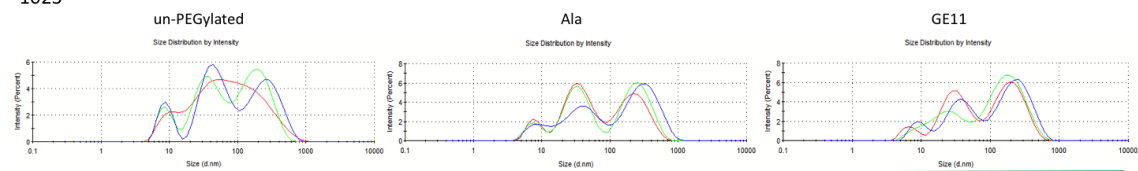


1022

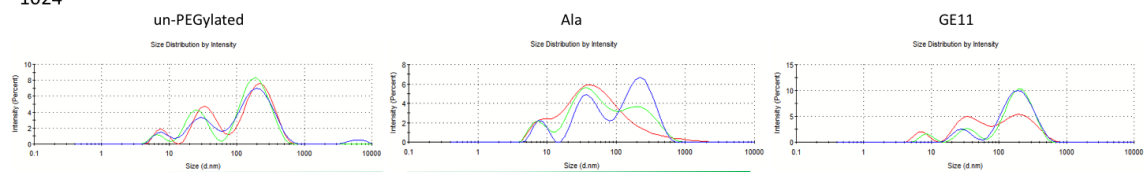


Intensity mean curves of oligomers **454**, **1021** and **1022** un-PEGylated, PEGylated with 1.0 eq (Cys)₂-PEG24-Ala and GE11 as determined by DLS measurement. Red curve: t=0 h, green curve t=4 h and blue after 24 h. Color of bars below the graphs indicate classification according to **Table 19**.

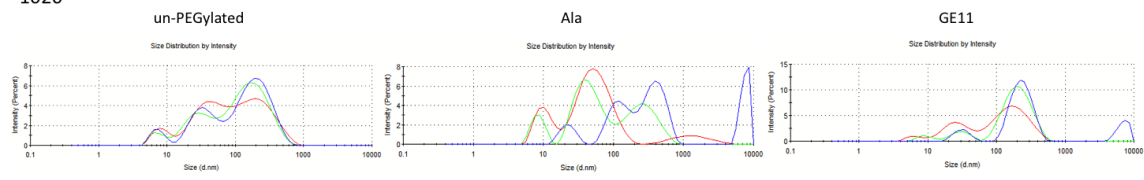
1023



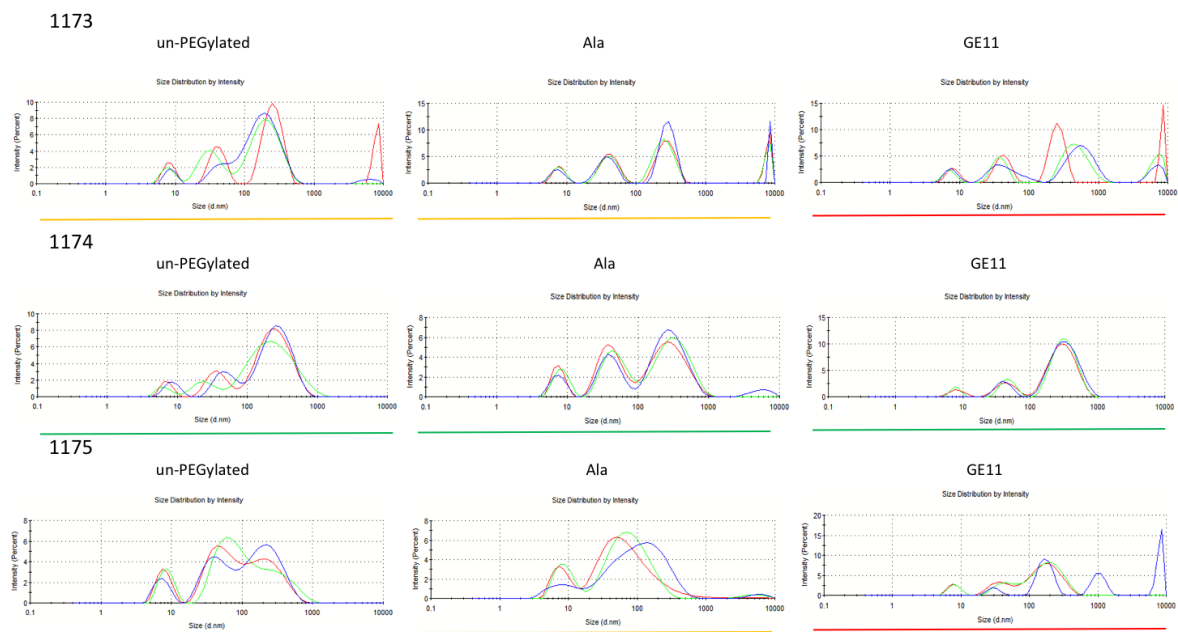
1024



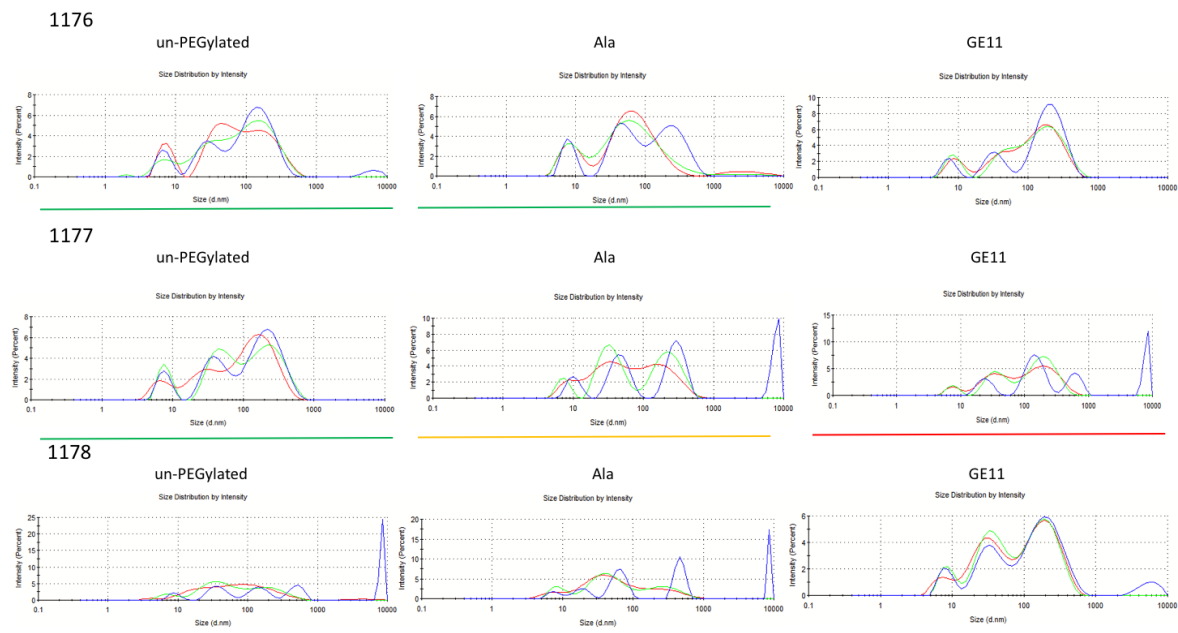
1026



Intensity mean curves of oligomers **1023**, **1024** and **1026** un-PEGylated, PEGylated with 1.0 eq (Cys)₂-PEG24-Ala and GE11 as determined by DLS measurement. Red curve: t=0 h, green curve t=4 h and blue after 24 h. Color of bars below the graphs indicate classification according to **Table 19**.

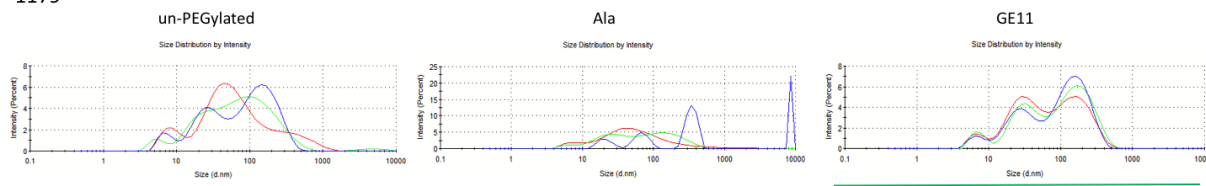


Intensity mean curves of oligomers **1173**, **1174** and **1175** un-PEGylated, PEGylated with 1.0 eq (Cys)₂-PEG24-Ala and GE11 as determined by DLS measurement. Red curve: t=0 h, green curve t=4 h and blue after 24 h. Color of bars below the graphs indicate classification according to **Table 19**.

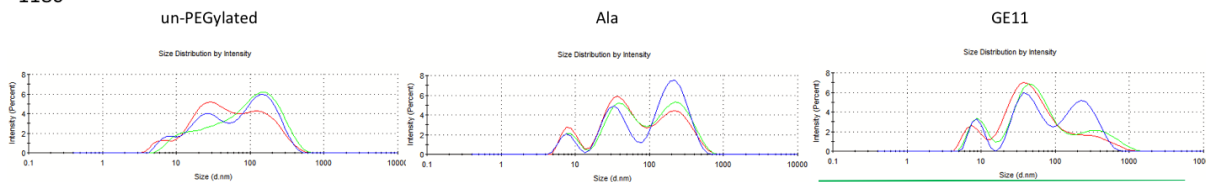


Intensity mean curves of oligomers **1176**, **1177** and **1178** un-PEGylated, PEGylated with 1.0 eq (Cys)₂-PEG24-Ala and GE11 as determined by DLS measurement. Red curve: t=0 h, green curve t=4 h and blue after 24 h. Color of bars below the graphs indicate classification according to **Table 19**.

1179



1180



Intensity mean curves of oligomers **1179** and **1180** un-PEGylated, PEGylated with 1.0 eq (Cys)₂-PEG24-Ala and GE11 as determined by DLS measurement. Red curve: t=0 h, green curve t=4 h and blue after 24 h. Color of bars below the graphs indicate classification according to **Table 19**.

6.3 Summary of SPS derived oligomers

Table 21 Summary of SPS derived oligomers

| Oligomer ID | Topology | Sequence (N→C) | Proton. amines | Chapter |
|-------------|-----------------|--|----------------|----------|
| 440 | PEGylated 2-arm | [C-(H-Stp) ₄ -H] _{α,ε} -K-dPEG ₂₄ -A | 26 | 3.2 |
| 442 | PEGylated 2-arm | KLSLRHDHIIHHH-[[C-(H-Stp) ₄ -H] _{α,ε} -K-H-dPEG ₂₄] _ε -K | 26 | 3.1 |
| 454 | T-Shape | C-Y ₃ -Stp ₂ -K-[K(OleA) _{α,ε}] _ε -Stp ₂ -Y ₃ -C | 13 | 3.2, 3.3 |
| 689 | 3-arm | [C-(H-Stp) ₃ -H] _{α,ε} -K-H-(Stp-H) ₃ -C | 29 | 3.1 |
| 694 | PEGylated 2-arm | KLSLRHDHIIHHH-[[C-(H-Stp) ₄ -H] _{α,ε} -K-H-dPEG ₂₄ -dPEG ₂₄] _ε -K | 26 | 3.1 |
| 835 | PEGylated 2-arm | [C-(H-Stp) ₄ -H] _{α,ε} -K-dPEG ₂₄ -YHWYGYTPQNV | 26 | 3.2 |
| 901 | PASylated 2-arm | KLSLRHDHIIHHH-[[C-(H-Stp) ₄ -H] _{α,ε} -K-H-(PAS) ₈] _ε -K | 26 | 3.1 |
| 996 | PEGylated 2-arm | KLSLRHDHIIHHH-[[C-(H-Stp) ₄ -H] _{α,ε} -K-H-dPEG ₁₂] _ε -K | 26 | 3.1 |
| 1000 | PASylated 2-arm | KLSLRHDHIIHHH-[[C-(H-Stp) ₄ -H] _{α,ε} -K-H-(PAS) ₄] _ε -K | 26 | 3.1 |
| 1021 | T-Shape | C-Y ₃ -Stp ₂ -K-[K-(CholA) _{α,ε}] _ε -Stp ₂ -Y ₃ -C | 13 | 3.3 |
| 1022 | T-Shape | C-Y ₃ -Stp ₃ -K-[K-(OleA) _{α,ε}] _ε -Stp ₃ -Y ₃ -C | 25 | 3.3 |
| 1023 | T-Shape | C-Y ₃ -Stp ₃ -K-[K-(CholA) _{α,ε}] _ε -Stp ₃ -Y ₃ -C | 25 | 3.3 |
| 1024 | T-Shape | C-Y ₃ -H ₃ -Stp ₂ -K-[K-(OleA) _{α,ε}] _ε -Stp ₂ -H ₃ -Y ₃ -C | 13 | 3.3 |
| 1026 | T-Shape | C-Y ₃ -(H-Stp) ₂ -H-K-[K-(OleA) _{α,ε}] _ε -H-(Stp-H) ₂ -Y ₃ -C | 13 | 3.3 |
| 1078 | 3-arm | KLSLRHDHIIHHH-[[C-(H-Stp) ₃ -H] _{α,ε} -K-H-(Stp-H) ₃] _ε -K | 29 | 3.1 |
| 1088 | PEGylated 2-arm | [[C-(H-Stp) ₄ -H] _{α,ε} -K-H-dPEG ₁₂] _ε -K | 26 | 3.1 |
| 1091 | PEGylated 2-arm | [[C-(H-Stp) ₄ -H] _{α,ε} -K-H-dPEG ₂₄] _ε -K | 26 | 3.1 |
| 1094 | PASylated 2-arm | [[C-(H-Stp) ₄ -H] _{α,ε} -K-H-(PAS) ₄] _ε -K | 26 | 3.1 |
| 1097 | PASylated 2-arm | [[C-(H-Stp) ₄ -H] _{α,ε} -K-H-(PAS) ₈] _ε -K | 26 | 3.1 |
| 1120 | PEGylated 2-arm | [[C-(H-Stp) ₄ -H] _{α,ε} -K-H-dPEG ₂₄ -dPEG ₂₄] _ε -K | 26 | 3.1 |
| 1173 | T-Shape | C-Y ₆ -Stp ₂ -K-[K-(OleA) _{α,ε}] _ε -Stp ₂ -Y ₆ -C | 13 | 3.3 |
| 1174 | T-Shape | C-Y ₆ -Stp ₂ -K-[K-(CholA) _{α,ε}] _ε -Stp ₂ -Y ₆ -C | 13 | 3.3 |
| 1175 | T-Shape | C-Y ₃ -Stp ₄ -K-[K-(OleA) _{α,ε}] _ε -Stp ₄ -Y ₃ -C | 25 | 3.3 |
| 1176 | T-Shape | C-Y ₃ -Stp ₄ -K-[K-(CholA) _{α,ε}] _ε -Stp ₄ -Y ₃ -C | 25 | 3.3 |
| 1177 | T-Shape | C-Y ₆ -Stp ₄ -K-[K-(OleA) _{α,ε}] _ε -Stp ₄ -Y ₆ -C | 25 | 3.3 |
| 1178 | T-Shape | C-Y ₆ -Stp ₄ -K-[K-(CholA) _{α,ε}] _ε -Stp ₄ -Y ₆ -C | 25 | 3.3 |
| 1179 | T-Shape | C-Y ₃ -(H-Stp) ₄ -H-K-[K-(OleA) _{α,ε}] _ε -H-(Stp-H) ₄ -Y ₃ -C | 25 | 3.3 |
| 1180 | T-Shape | C-Y ₃ -H ₅ -Stp ₄ -K-[K-(OleA) _{α,ε}] _ε -Stp ₄ -H ₅ -Y ₃ -C | 25 | 3.3 |

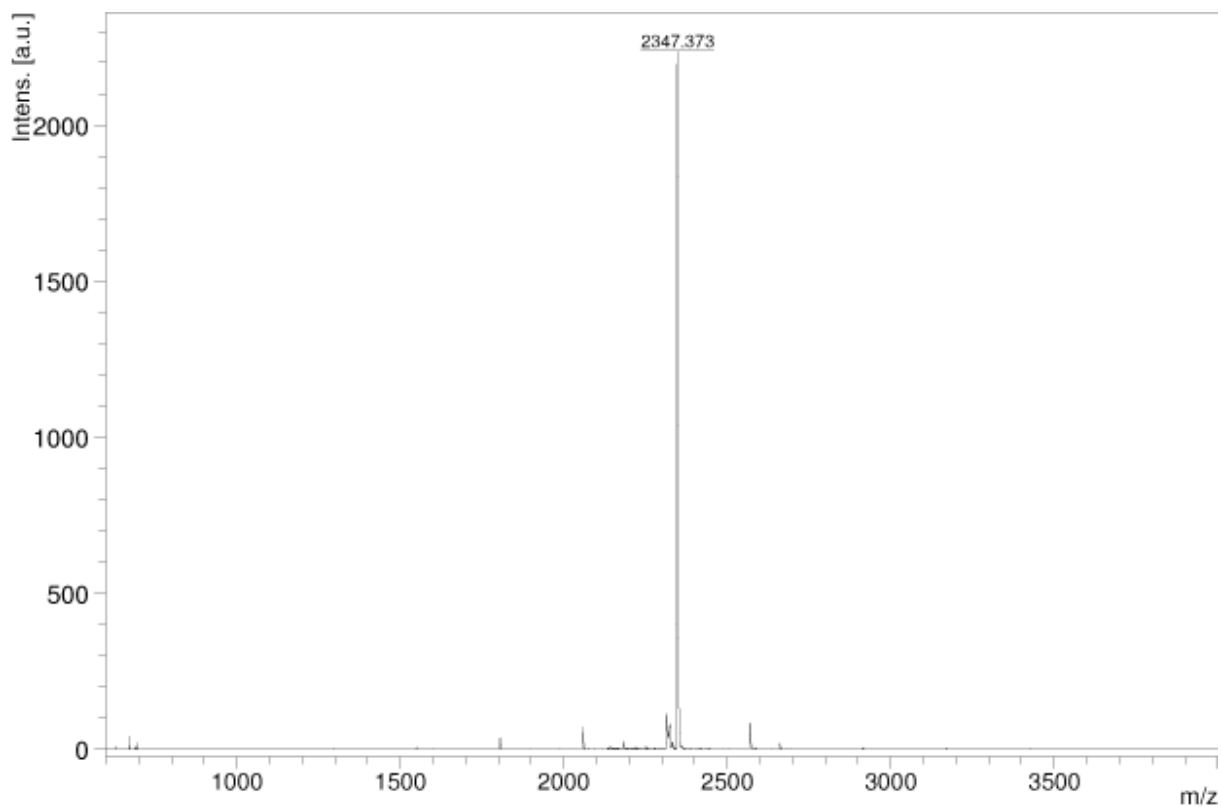
6.4 Summary of SPS derived shielding reagents

Table 22 Summary of SPS derived shielding reagents

| ID | Name | Sequence (C→N) | Chapter |
|------|---|--|----------|
| 1059 | Cys-PEG ₂₄ -Ala | Cys(NPys)-dPEG ₂₄ -A | 3.2, 3.3 |
| 999 | Cys-PEG ₂₄ -GE11 | Cys(NPys)-dPEG ₂₄ -YHWYGYTPQNV | 3.2, 3.3 |
| 1060 | (Cys) ₂ -PEG ₂₄ -Ala | (Cys(NPys)-STOTDA) _{α,ε} -K-dPEG ₂₄ -A | 3.2, 3.3 |
| 1056 | (Cys) ₂ -PEG ₂₄ -GE11 | (Cys(NPys)-STOTDA) _{α,ε} -K-dPEG ₂₄ -YHWYGYTPQNV | 3.2, 3.3 |

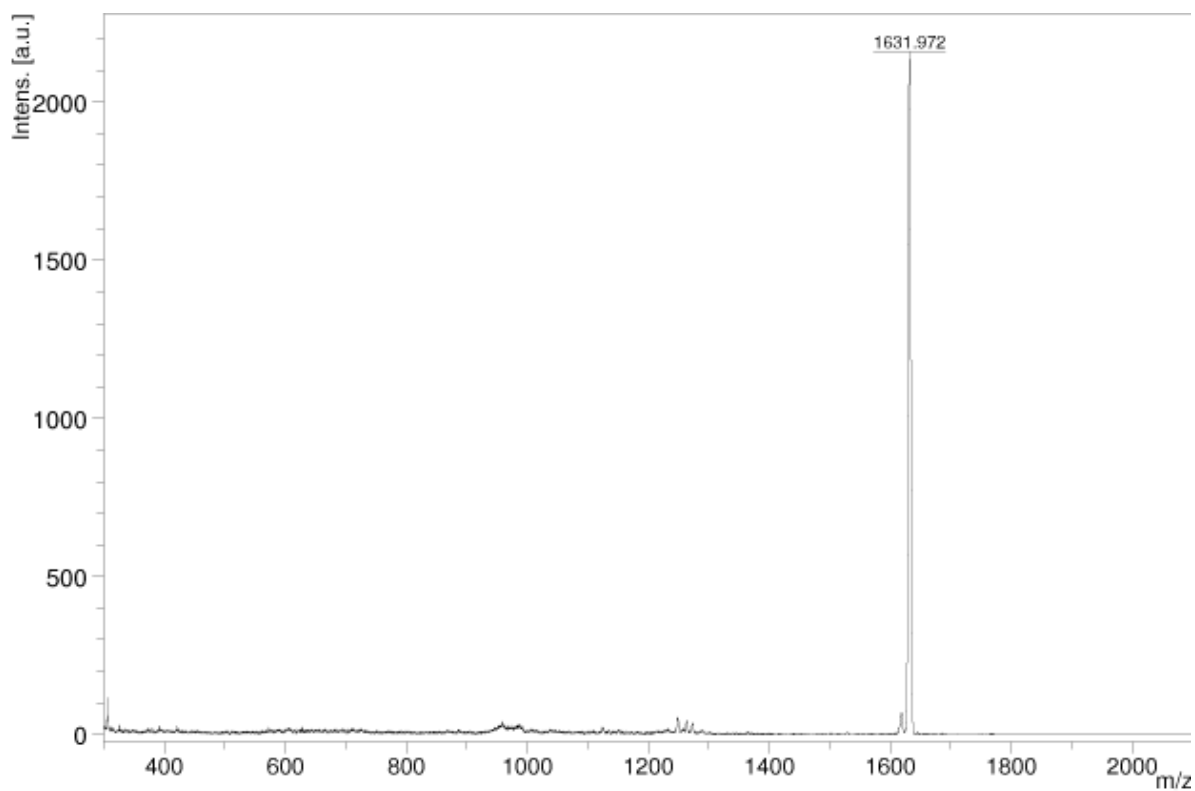
6.5 Analytical data

6.5.1 MALDI-TOF MS of Dde-K-(S-A-P)₈-OH

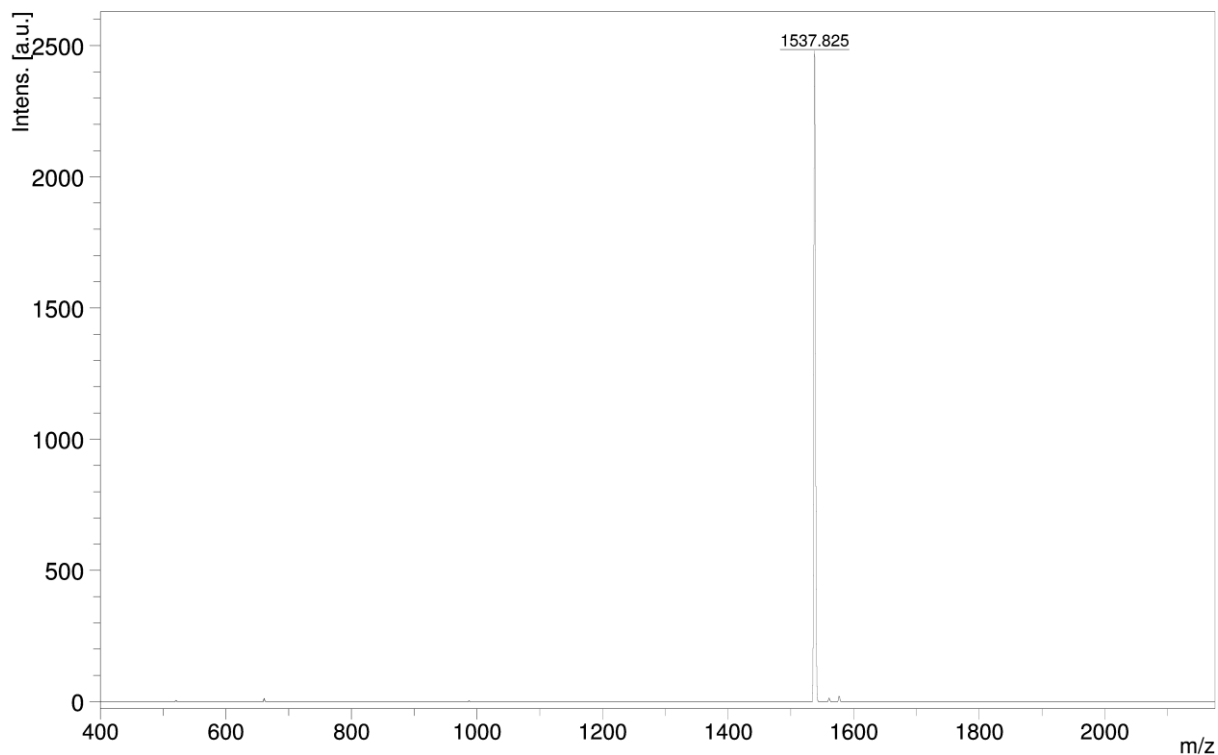


Calculated mass [M-H] of C₁₀₄H₁₆₁N₂₆O₃₆: 2350.16 g/mol

6.5.2 MALDI-TOF MS of the targeting peptides cmb and GE11



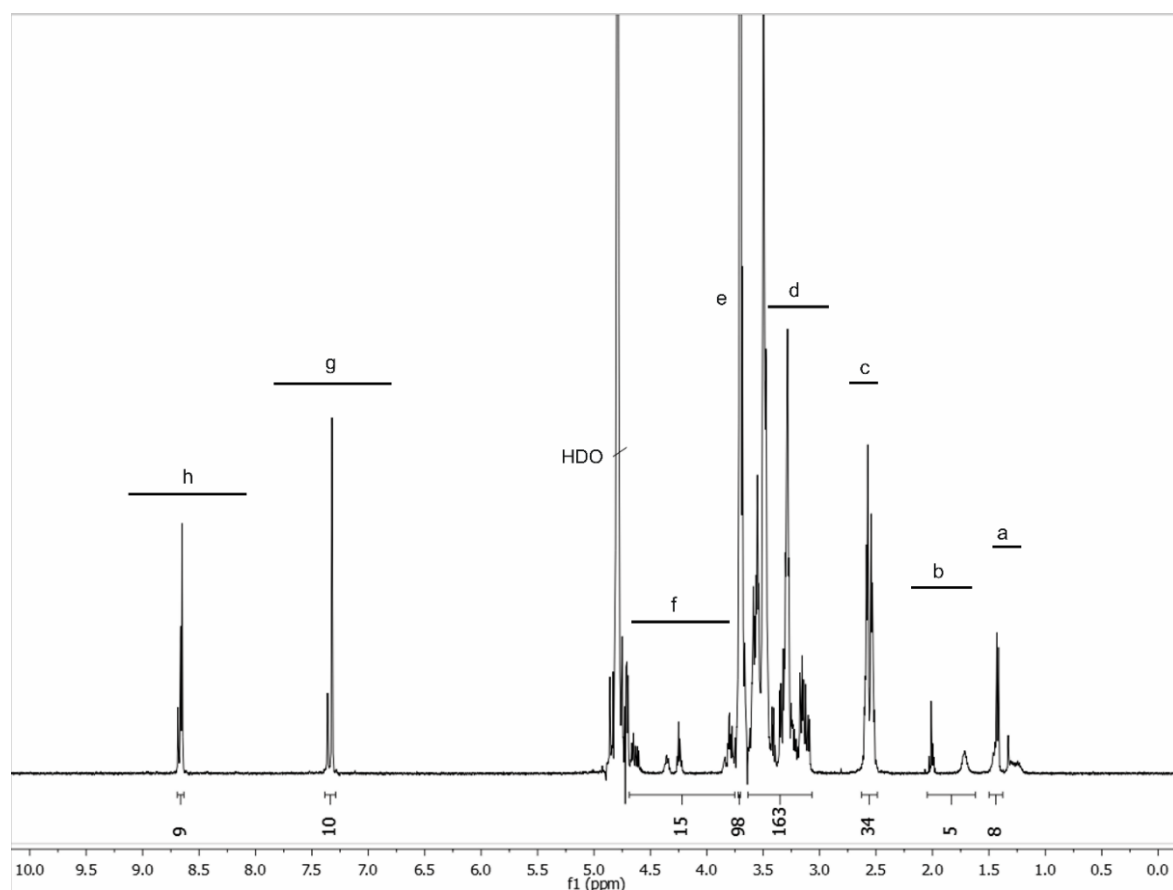
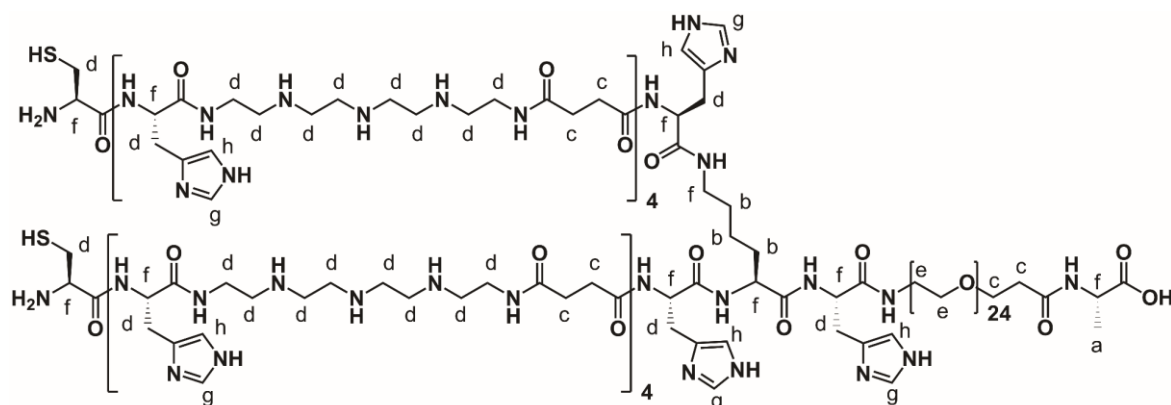
MALDI-MS of cmb peptide: Calculated mass [M+H] of $C_{70}H_{110}N_{28}O_{18}$: 1630.9 g/mol



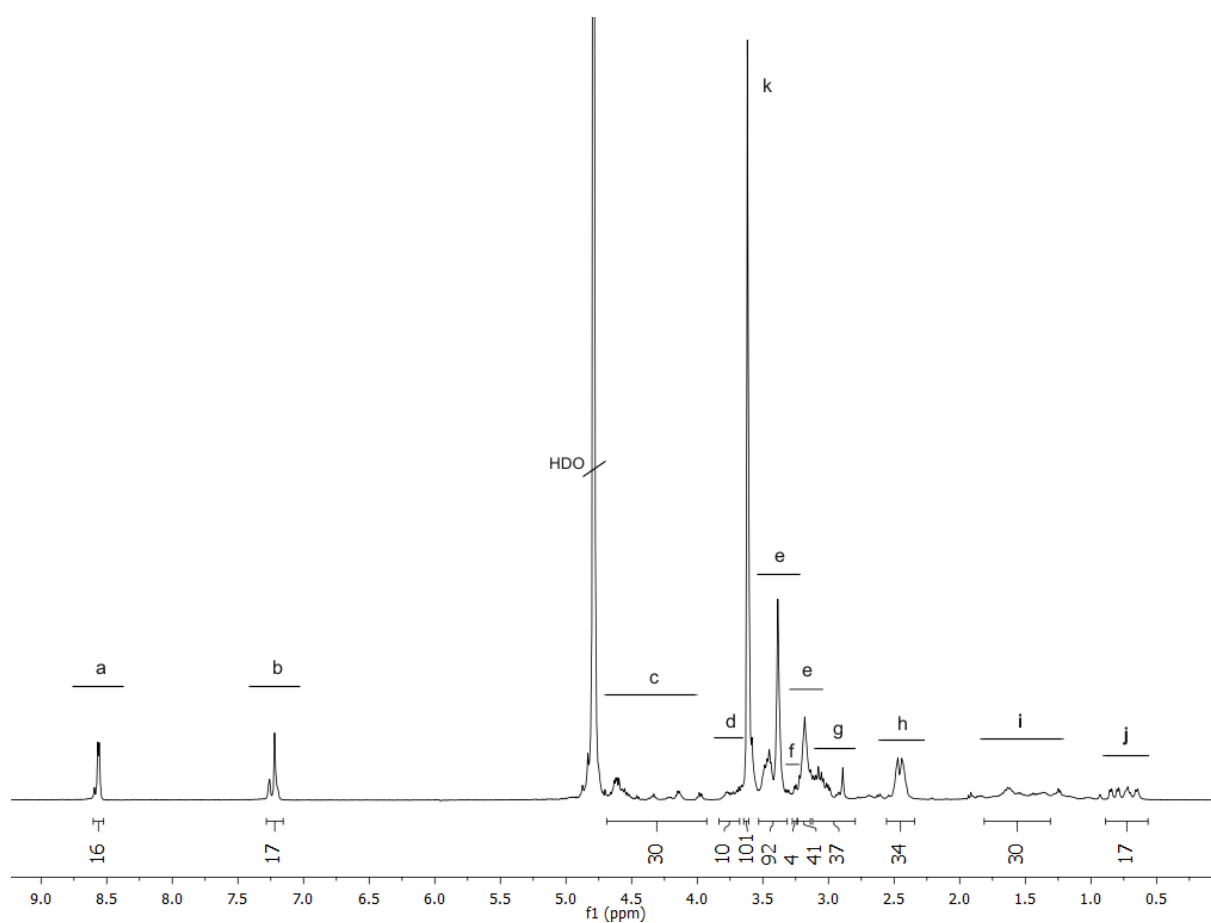
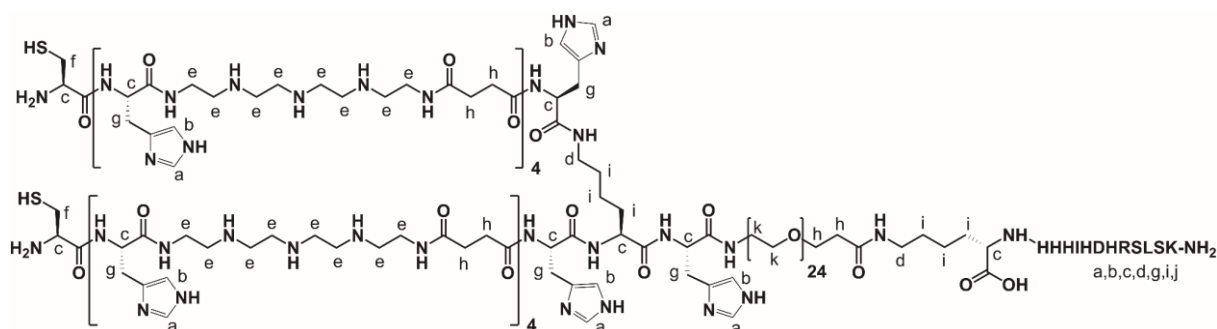
MALDI-MS of GE11 peptide: Calculated mass [M+H] of $C_{75}H_{97}N_{17}O_{19}$: 1541.7 g/mol

6.5.3 ^1H NMR spectra of oligomers

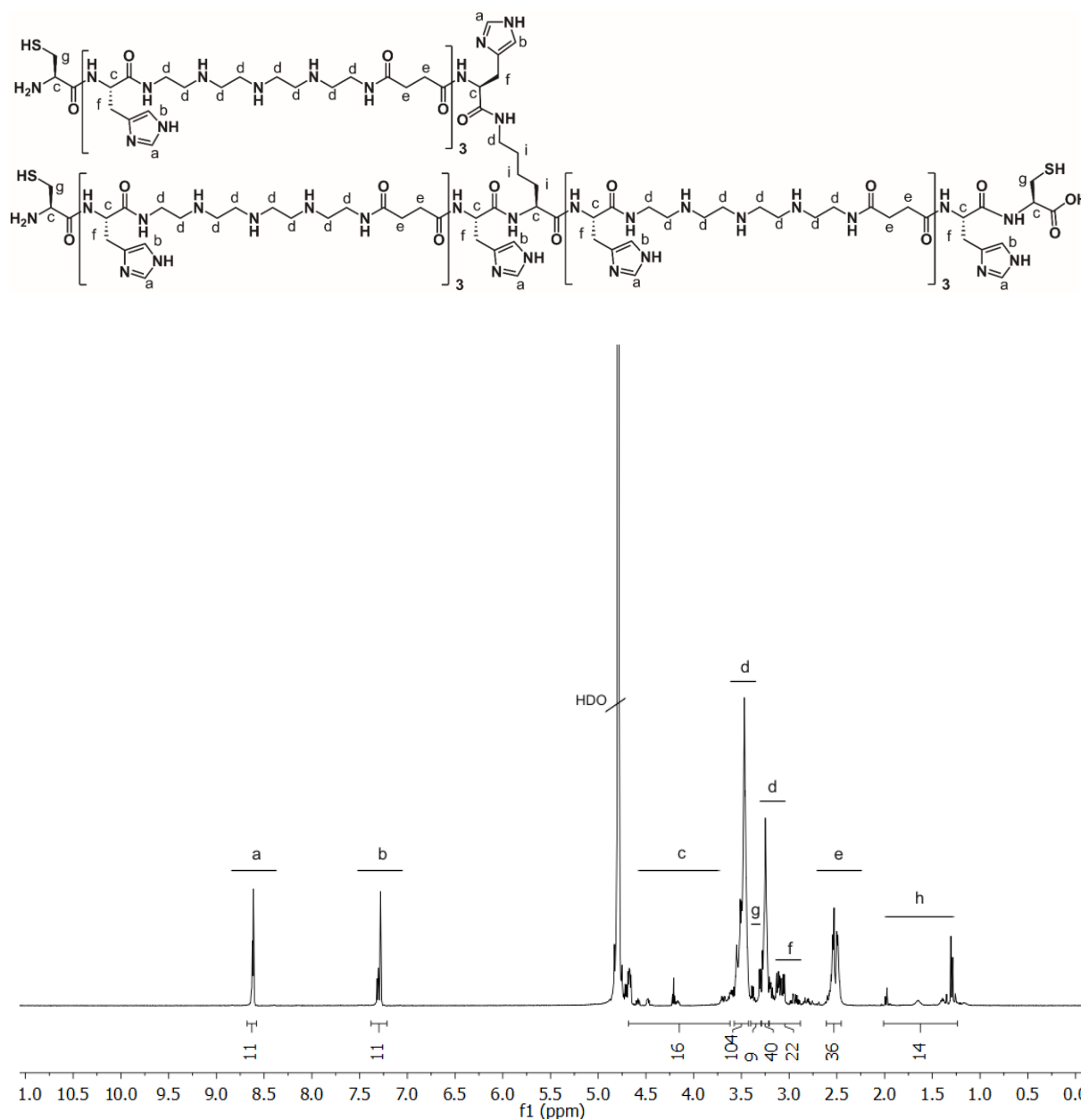
440: Sequence (N->C): $[\text{C}-(\text{H}-\text{Stp})_4-\text{H}]_{\alpha,\varepsilon}\text{-K-dPEG}_{24}\text{-A}$



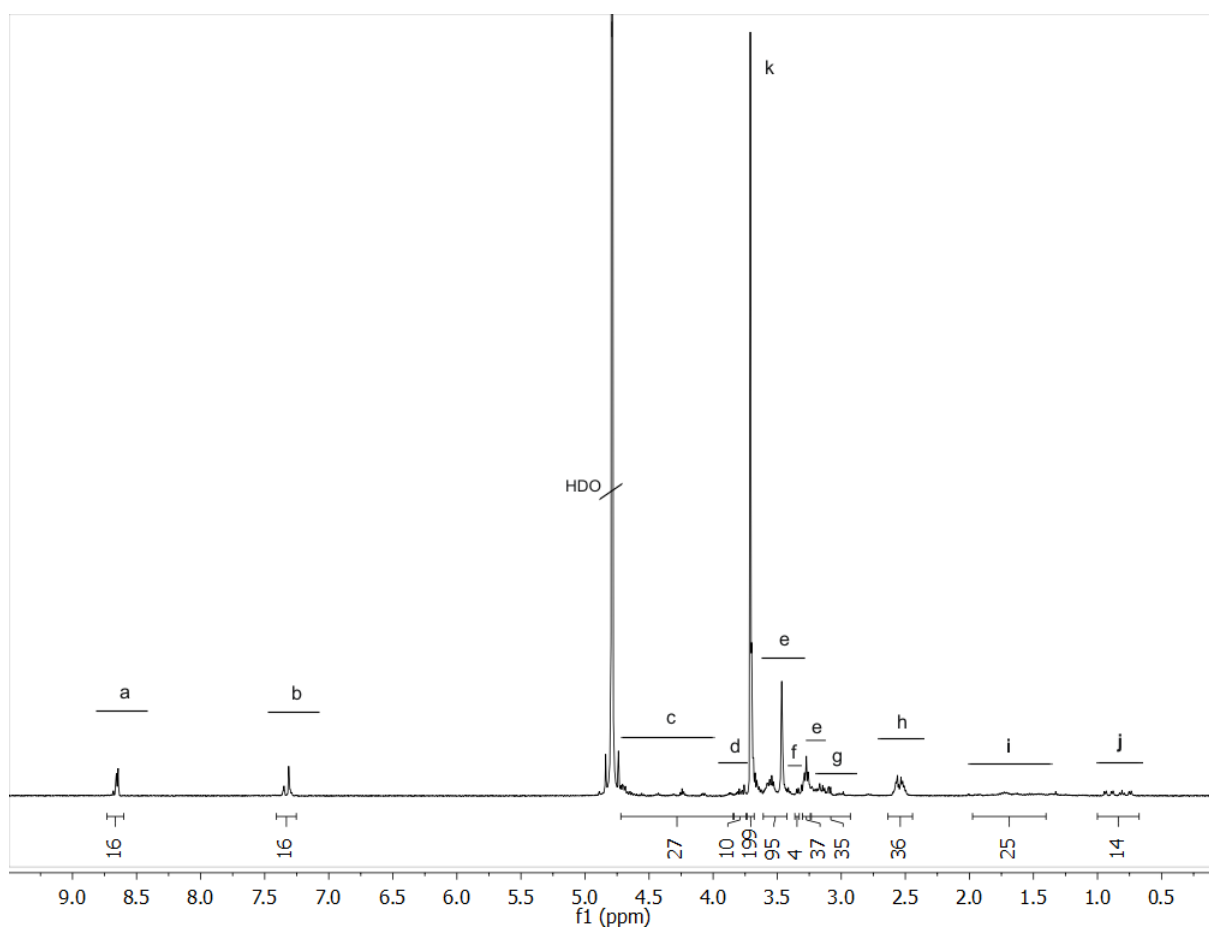
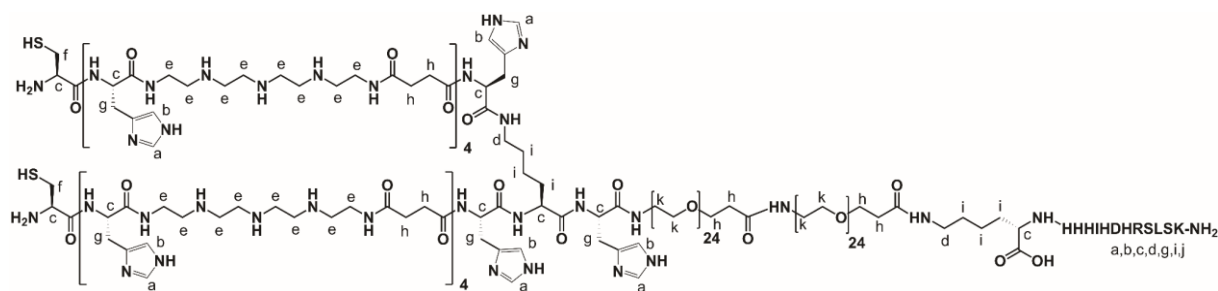
^1H NMR (500 MHz, Deuterium oxide) δ (ppm) = 1.3-1.45 (comp, 3H, βH alanine), 1.6-2.0 (comp, 6H, $\beta\gamma\delta\text{H}$ lysine), 2.4-2.6 (comp, 34 H, $-\text{CO}-\text{CH}_2-\text{CH}_2-\text{CO}-$ succinic acid - $\text{CO}-\text{CH}_2\text{-dPEG}_{24}$), 3.0 -3.65 (comp, 156 H, $-\text{CH}_2-$ tepa, εH lysine, βH cysteine, βH histidine), 3.70 (s, 98H, $-\text{CH}_2\text{-O-dPEG}_{24}$, $-\text{CH}_2\text{-N-dPEG}_{24}$), 3.75-4.75 (comp, 15 H, αH cysteine, lysine, histidine), 4.79 (s, HDO), 7.2-7.4 (m, 11 H, aromatic H histidine), 8.5-8.7 (m, 11 H, aromatic H histidine). comp indicates a group of overlaid protons.

442: Sequence (N->C): KSLSRHDHIIHHH -[(C-(H-Stp)₄-H)_{α,ε}K-H-dPEG₂₄]_ε-K


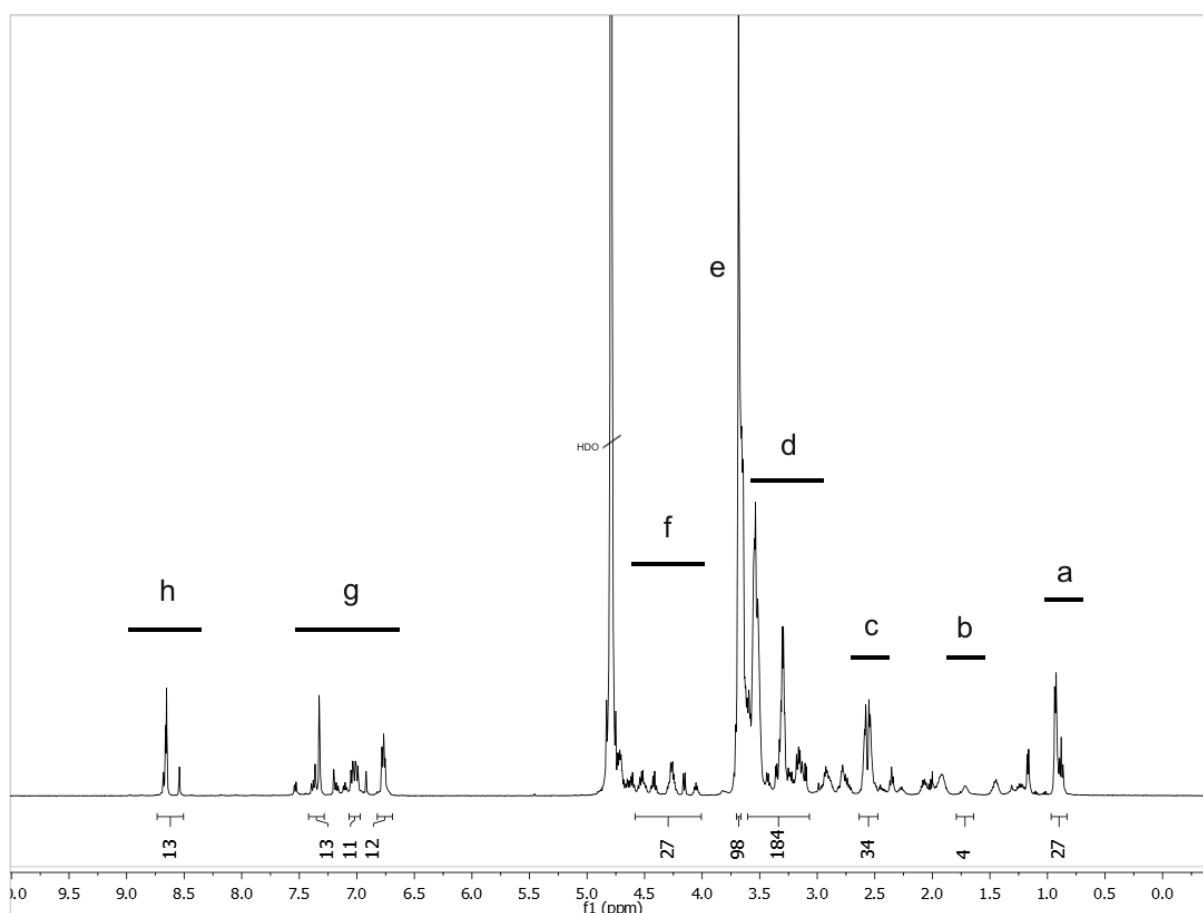
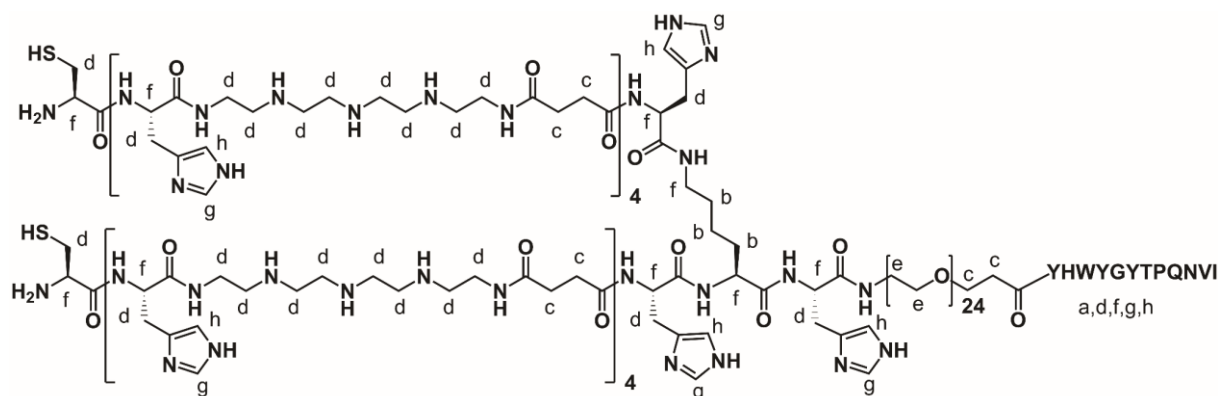
¹H NMR (500 MHz, Deuterium oxide) δ (ppm) = 0.7-0.95 (comp, 17H, βγδH leucine, βγδH isoleucine), 1.35-1.8 (comp, 24H, βγδH lysine, βγδH arginine), 2.3-2.7 (comp, 34 H, -CO-CH₂-CH₂-CO- succinic acid), 2.8 -3.15 (comp, 34 H, βH histidine, βH asparagine) 3.20-3.55 (comp, 132 H, -CH₂- tepa, βH cysteine), 3.6 (s, 98H, -CH₂-O-dPEG₂₄) 3.65-4.7 (comp, 37 H, αH amino acids, βH serine, εH lysine), 4.79 (s, HDO), 7.2-7.3 (m, 16 H, aromatic H histidine), 8.5-8.7 (m, 16 H, aromatic H histidine). comp indicates a group of overlaid protons.

689: Sequence (N->C): [C-(H-Stp)₃-H]_{α,ε}-K-H-(Stp-H)₃-C


¹H NMR (500 MHz, Deuterium oxide) δ (ppm) = 1.1-1.4 (comp, 6H, βγδH lysine), 2.3-2.7 (comp, 36 H, -CO-CH₂-CH₂-CO- succinic acid), 2.9-3.8 (comp, 176 H, -CH₂- tepe, βH cysteine, βH histidine, εH lysine), 4.1-4.7 (comp, 16 H, αH cysteine, lysine, histidine), 4.79 (s, HDO), 7.2-7.4 (m, 11 H, aromatic H histidine), 8.5-8.7 (m, 11 H, aromatic H histidine). comp indicates a group of overlaid protons.

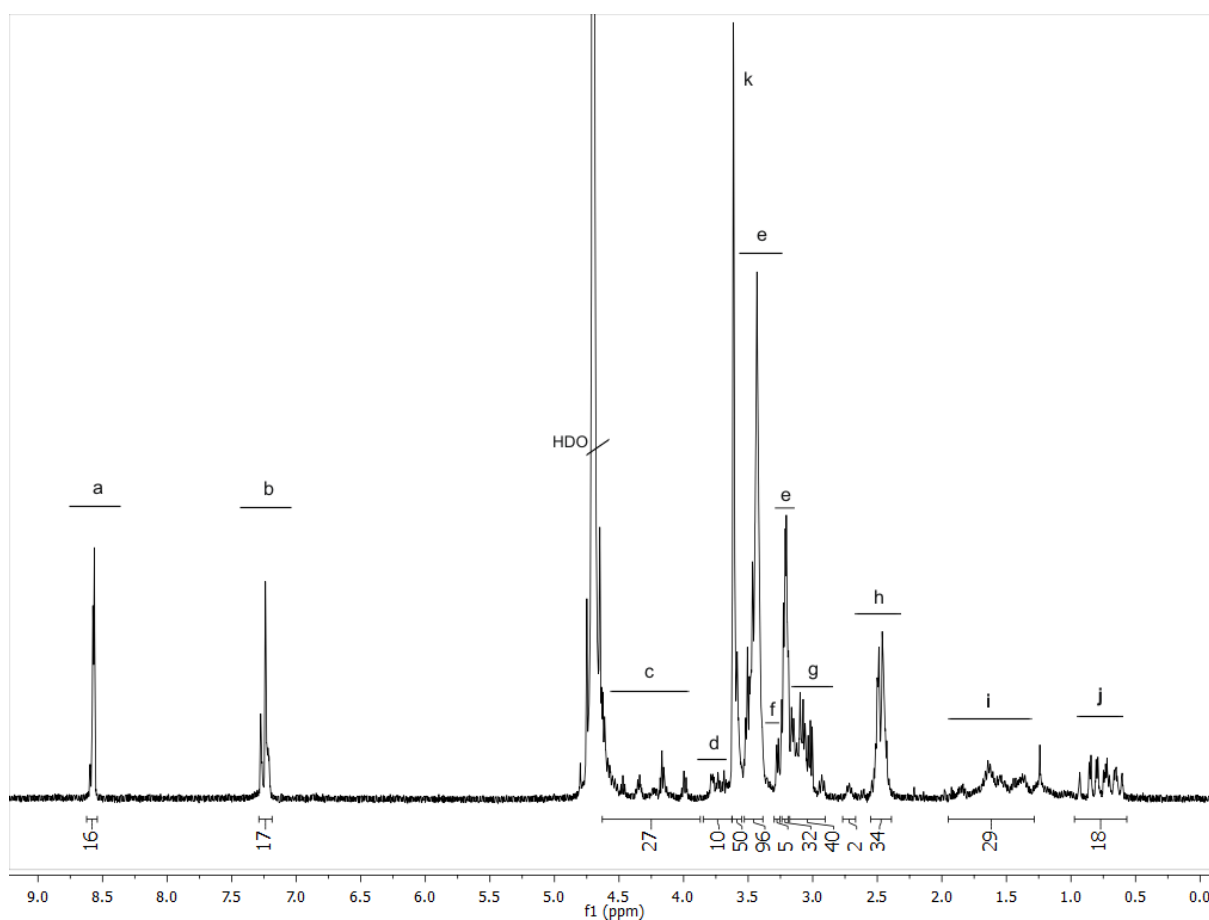
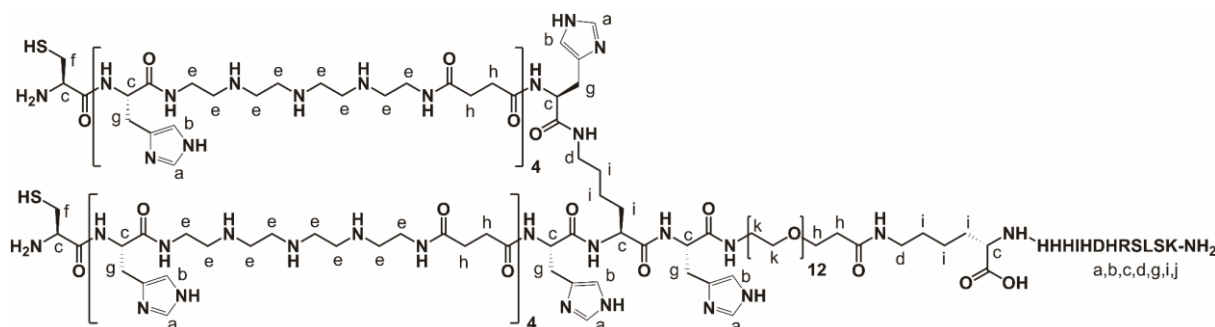
694: Sequence (N->C): KSLSRHDHIIHHH -[(C-(H-Stp)₄-H)_{α,ε}K-H-dPEG₂₄-dPEG₂₄]_ε-K

¹H NMR (500 MHz, Deuterium oxide) δ (ppm) = 0.7-0.95 (comp, 17H, βγδH leucine, βγδH isoleucine), 1.35-1.8 (comp, 24H, βγδH lysine, βγδH arginine), 2.3-2.7 (comp, 36 H, -CO-CH₂-CH₂-CO- succinic acid), 2.8 -3.15 (comp, 36H, βH histidine, βH asparagine) 3.20-3.55 (comp, 132H, -CH₂- tepe, βH cysteine), 3.7 (s, 196H, -CH₂-O-dPEG₂₄) 3.72-4.7 (comp, 37 H, αH amino acids, βH serine, εH lysine), 4.79 (s, HDO), 7.2-7.3 (m, 16 H, aromatic H histidine), 8.5-8.7 (m, 16H, aromatic H histidine). comp indicates a group of overlaid protons.

835: Sequence (N->C): [C-(H-Stp)₄-H]_{α,ε}-K-dPEG₂₄-YHWYGYTPQNVI

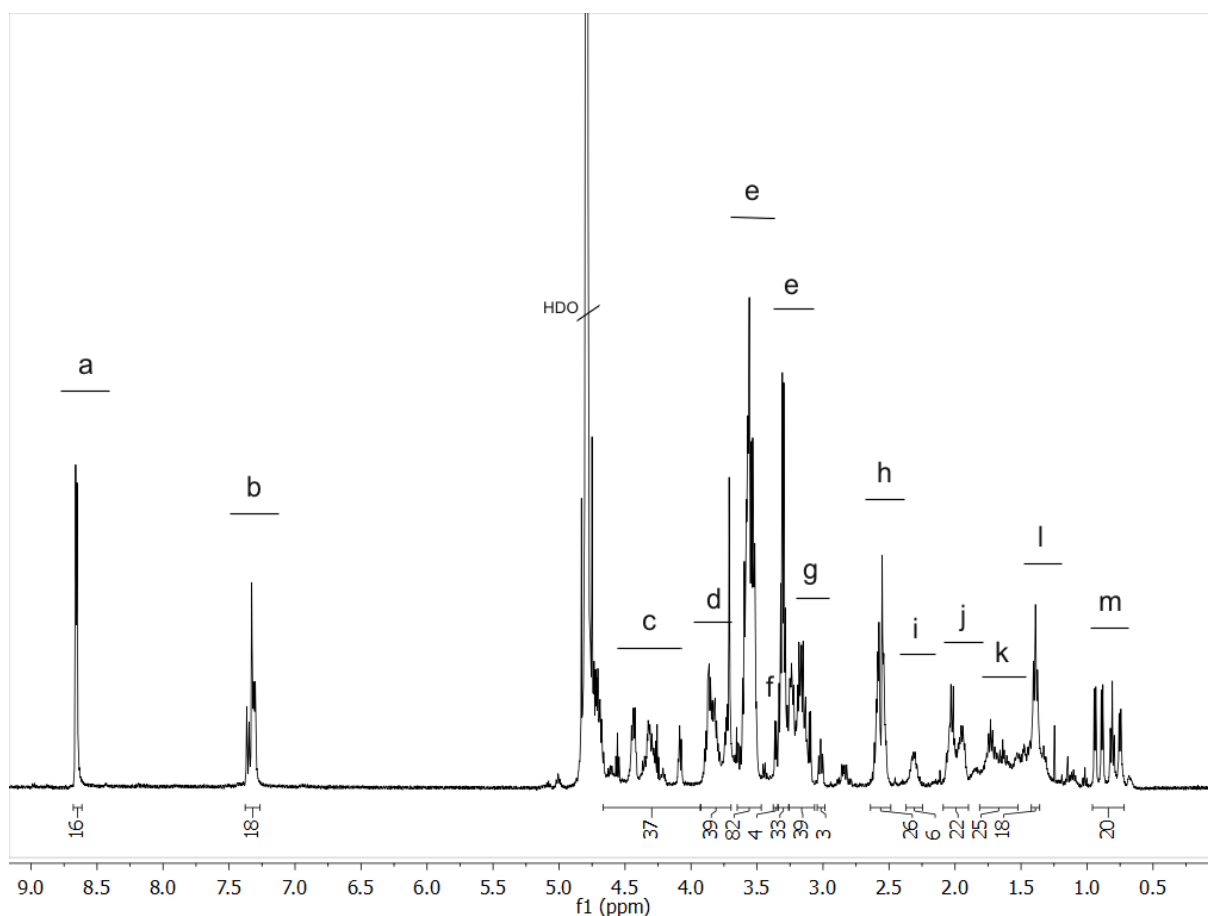
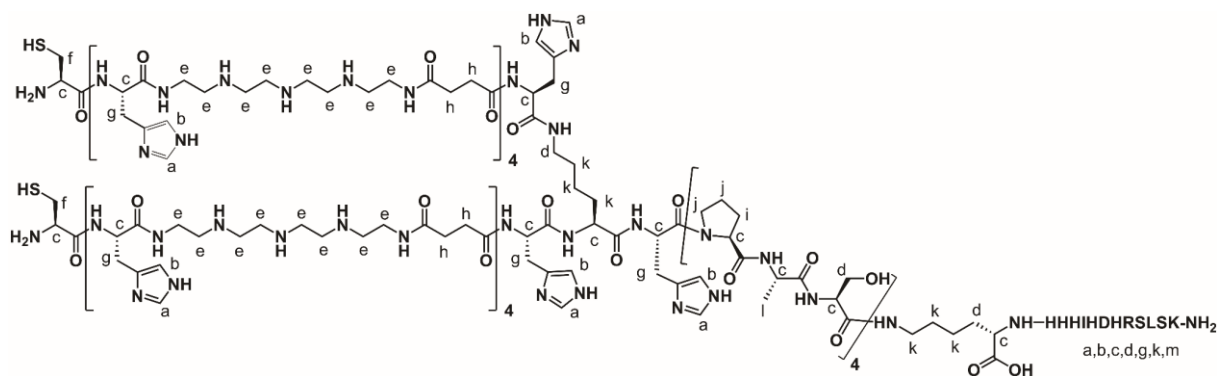
¹H NMR (500 MHz, Deuterium oxide) δ (ppm) = 0.75-1.0 (m, 19H, γH threonine β-CH₃ γδH isoleucine, β-CH₃ valine), 1.60-1.80 (m, 6H, βγδH lysine), 2.35-2.54 (m, 34 H, -CO-CH₂-CH₂-CO- succinic acid, -CO-CH₂- dPEG₂₄), 3.1-3.65 (m, 174 H, -CH₂-tepa, □H asparagine, βH cysteine, βH histidine, βH tryptophan, βH tyrosine, δH proline, βH asparagine, βH valine, εH lysine), 3.74-3.8 (m, 98 H, -CH₂-O- dPEG₂₄, -CH₂-N- dPEG₂₄), 4.1-4.65 (m, 26 H, αH amino acids), 4.75 (s, HDO), 6.7-7.42 (m, 29 H, aromatic ring H tyrosine, tryptophan, imidazole), 8.52-8.70 (m, 11 H, imidazole).

996: Sequence (N->C): KSLSRHDHIIHHH -[(C-(H-Stp)₄-H)_{α,ε}K-H-dPEG₁₂]_ε-K

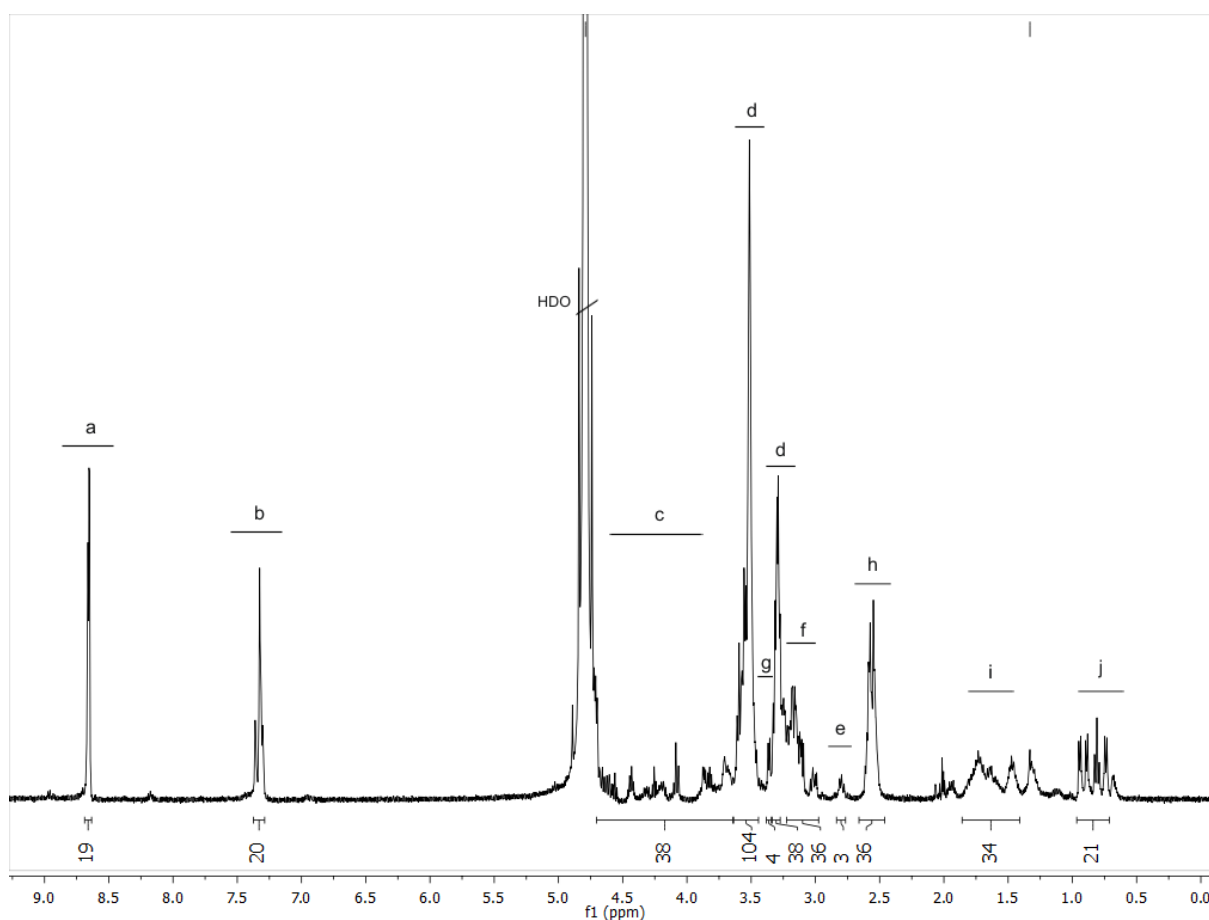
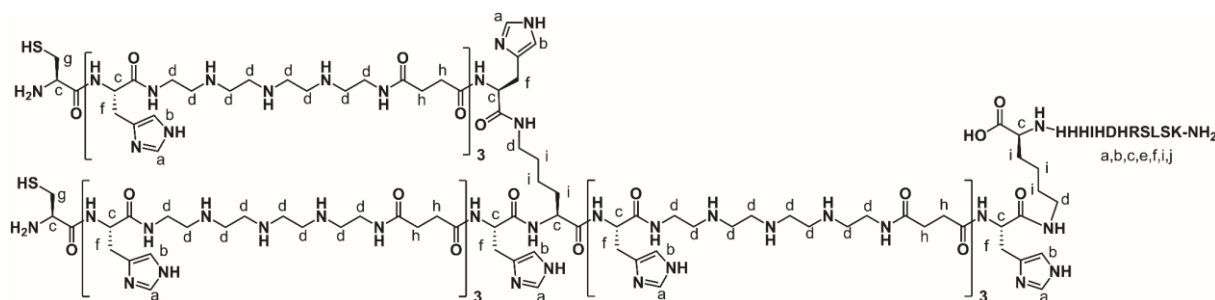


¹H NMR (500 MHz, Deuterium oxide) δ (ppm) = 0.7-0.95 (comp, 17H, βγδH leucine, βγδH isoleucine), 1.35-1.8 (comp, 24H, βγδH lysine, βγδH arginine), 2.3-2.7 (comp, 34 H, -CO-CH₂-CH₂-CO- succinic acid), 2.45-2.55 (t, 2 H, asparagine), 2.8 -3.15 (comp, 32 H, β histidine) 3.20-3.52 (comp, 132 H, -CH₂- tepe, βH cysteine), 3.6 (s, 50H, -CH₂-O-dPEG₁₂) 3.65-4.7 (comp, 37 H, αH amino acids, βH serine, εH lysine), 4.79 (s, HDO), 7.2-7.3 (m, 16 H, aromatic H histidine), 8.5-8.7 (m, 16 H, aromatic H histidine). comp indicates a group of overlaid protons.

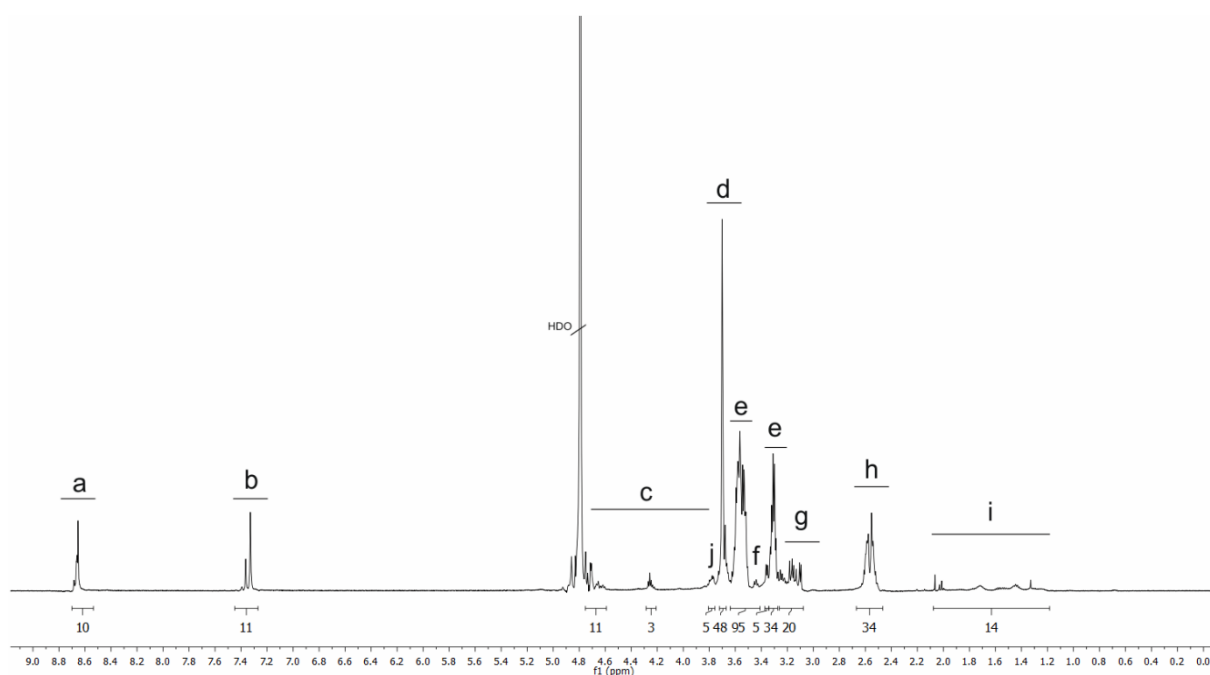
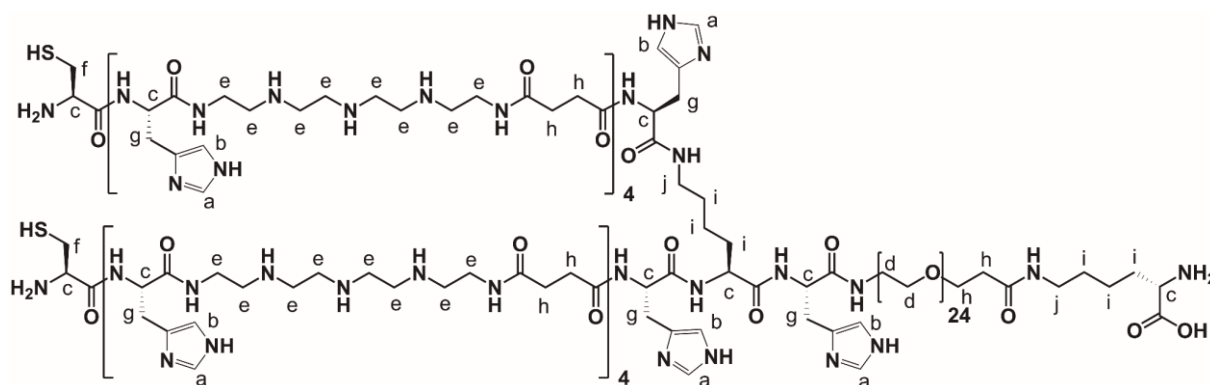
1000: Sequence (N->C): KLSLRHDHIIHHH-[(C-(H-Stp)₄-H)_{α,ε}K-H-(PAS)₄]_ε-K



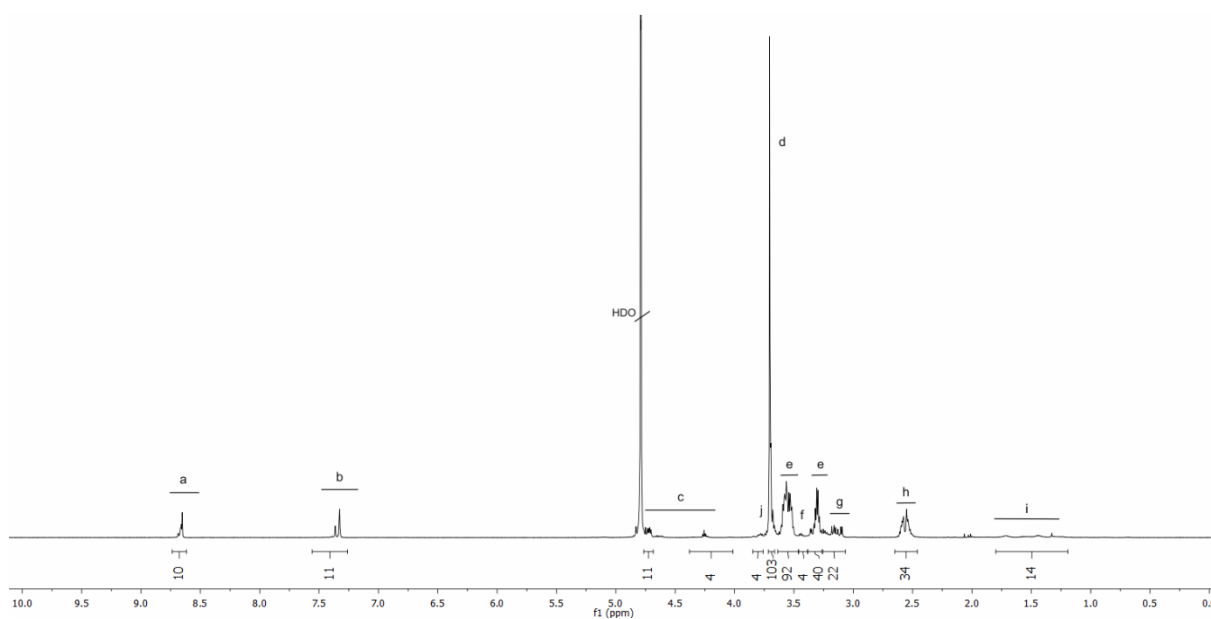
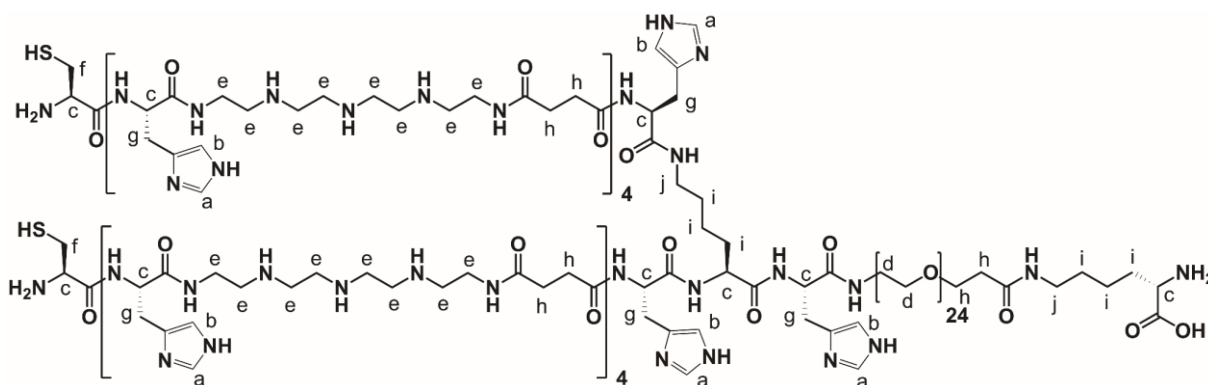
¹H NMR (500 MHz, Deuterium oxide) δ (ppm) = 0.7-0.95 (comp, 17H, βγδH leucine, βγδH isoleucine), 1.3-1.4 (td, 12H, -CH₃ H alanine), 1.5-1.9 (comp, 24H, βγδH lysine, βγδH arginine), 1.95-2.45 (comp, 24H, -CH₂ proline), 2.5-2.7 (comp, 36H, -CO-CH₂-CH₂-CO- succinic acid), 3.0 (t, 2 βH, asparagine), 3.15-3.3 (comp, 34H, βH histidine), 3.3-3.6 (comp, 132 H, -CH₂- tepla, βH cysteine), 3.75-4.7 (comp, 57H, βH serine, εH lysine, αH amino acids), 4.79 (s, HDO), 7.3-7.4 (m, 16 H, aromatic H histidine), 8.6-8.8 (m, 16 H, aromatic H histidine). comp indicates a group of overlaid protons.

1078: Sequence (N->C): KLSLRHDHIIHHH-[(C-(H-Stp)₃-H)_{α,ε}K-H-(Stp-H)₃]_ε-K

¹H NMR (500 MHz, Deuterium oxide) δ (ppm) = 0.7-0.95 (comp, 17H, βγδH leucine, βγδH isoleucine), 1.35-1.8 (comp, 24H, βγδH lysine, βγδH arginine), 2.3-2.7 (comp, 36 H, -CO-CH₂-CH₂-CO- succinic acid), 2.6-2.85 (t, 2 H, asparagine), 2.95 -3.2 (comp, 34 H, β histidine) 3.25-3.6 (comp, 150 H, -CH₂- tepe, βH cysteine), 3.65-4.7 (comp, 16 H, αH amino acids, βH serine, εH lysine), 4.79 (s, HDO), 7.2-7.4 (m, 17 H, aromatic H histidine), 8.5-8.7 (m, 17 H, aromatic H histidine). comp indicates a group of overlaid protons.

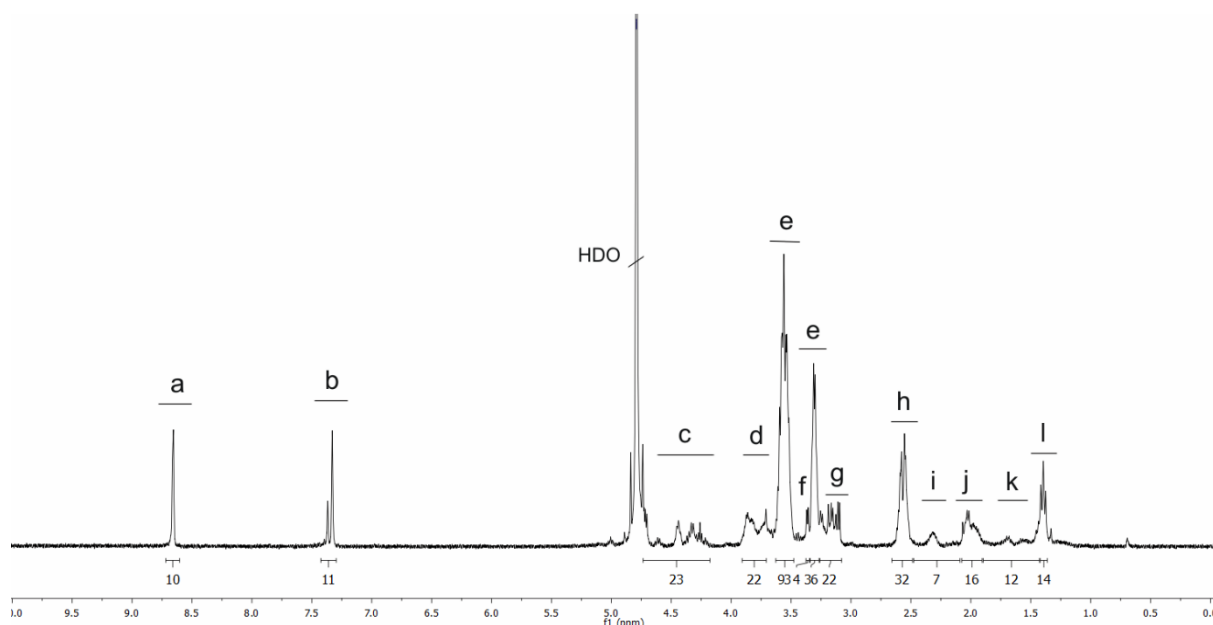
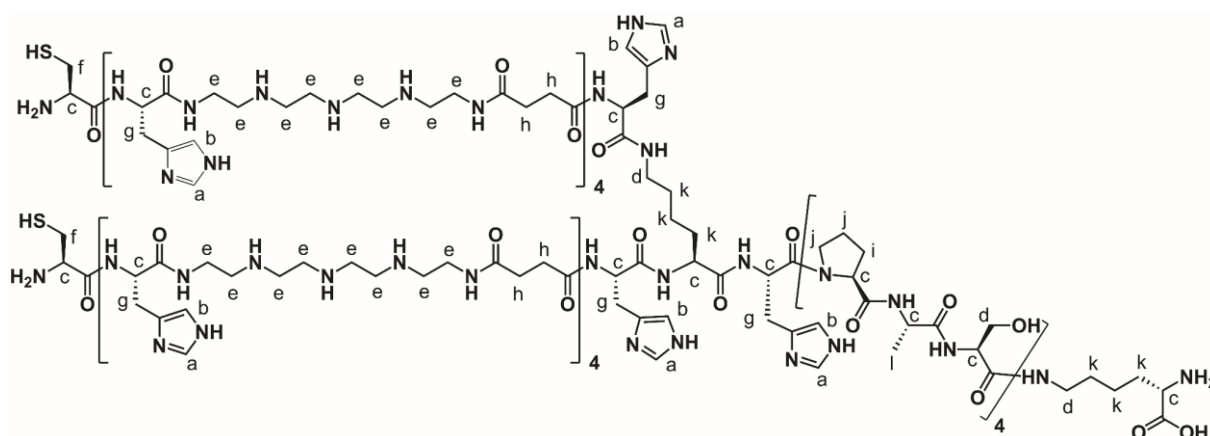
1088: Sequence (N->C): {[C-(H-Stp)₄-H]_{α,ε}-K-H-dPEG₁₂]_ε-K

¹H NMR (500 MHz, Deuterium oxide) δ (ppm) = 1.1-1.4 (comp, 12H, βγδH lysine), 2.3-2.7 (comp, 34 H, -CO-CH₂-CH₂-CO- succinic acid -CO-CH₂-dPEG₁₂), 2.9-3.65 (comp, 154 H, -CH₂- teпа, βH cysteine, βH histidine), 3.70 (s, 48H, -CH₂-O-dPEG₁₂, -CH₂-N-dPEG₁₂), 3.75-3.85 (m, 4H, εH lysine) 4.1-4.7 (comp, 15 H, αH cysteine, lysine, histidine), 4.79 (s, HDO), 7.2-7.4 (m, 11 H, aromatic H histidine), 8.5-8.7 (m, 11 H, aromatic H histidine). comp indicates a group of overlaid protons.

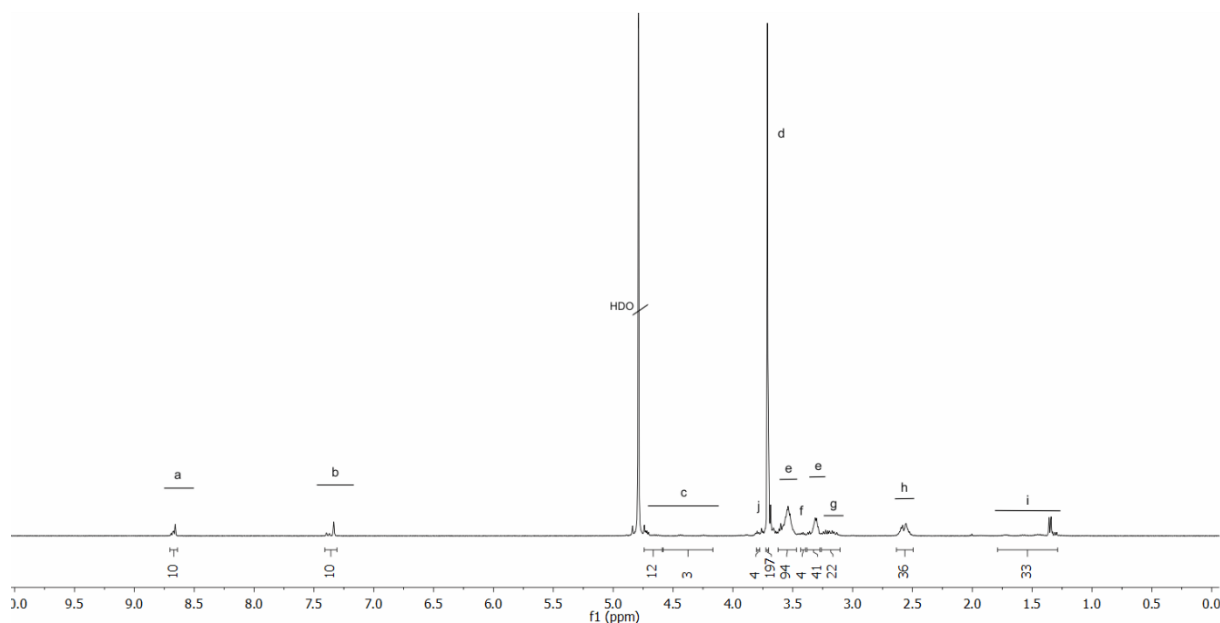
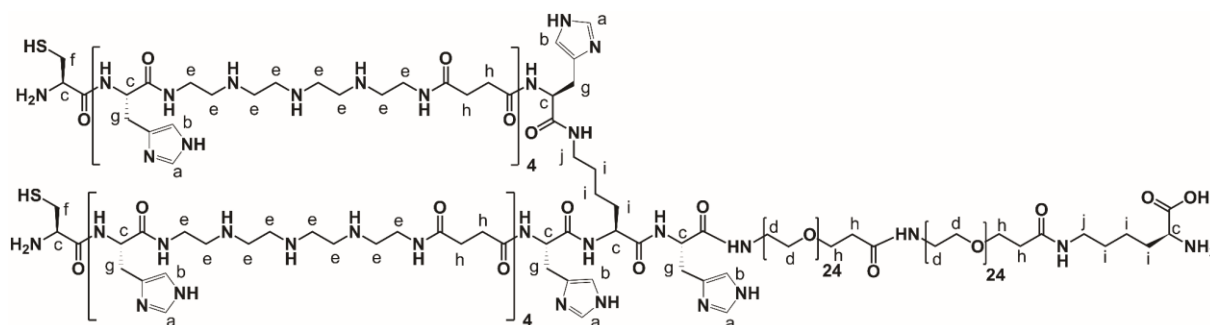
1091: Sequence (N->C): {[C-(H-Stp)₄-H]_{α,ε}-K-H-dPEG₂₄]_ε-K

¹H NMR (500 MHz, Deuterium oxide) δ (ppm) = 1.1-1.4 (comp, 12H, βγδH lysine), 2.3-2.7 (comp, 34 H, -CO-CH₂-CH₂-CO- succinic acid -CO-CH₂-dPEG₂₄), 2.9-3.65 (comp, 154 H, -CH₂- tepea, βH cysteine, βH histidine), 3.70 (s, 98H, -CH₂-O-dPEG₂₄, -CH₂-N-dPEG₂₄), 3.75-3.85 (m, 4H, εH lysine) 4.1-4.7 (comp, 15 H, αH cysteine, lysine, histidine), 4.79 (s, HDO), 7.2-7.4 (m, 11 H, aromatic H histidine), 8.5-8.7 (m, 11 H, aromatic H histidine). comp indicates a group of overlaid protons.

1094: Sequence (N->C): {[C-(H-Stp)₄-H]_{α,ε}-K-H-(PAS)₄]_ε-K



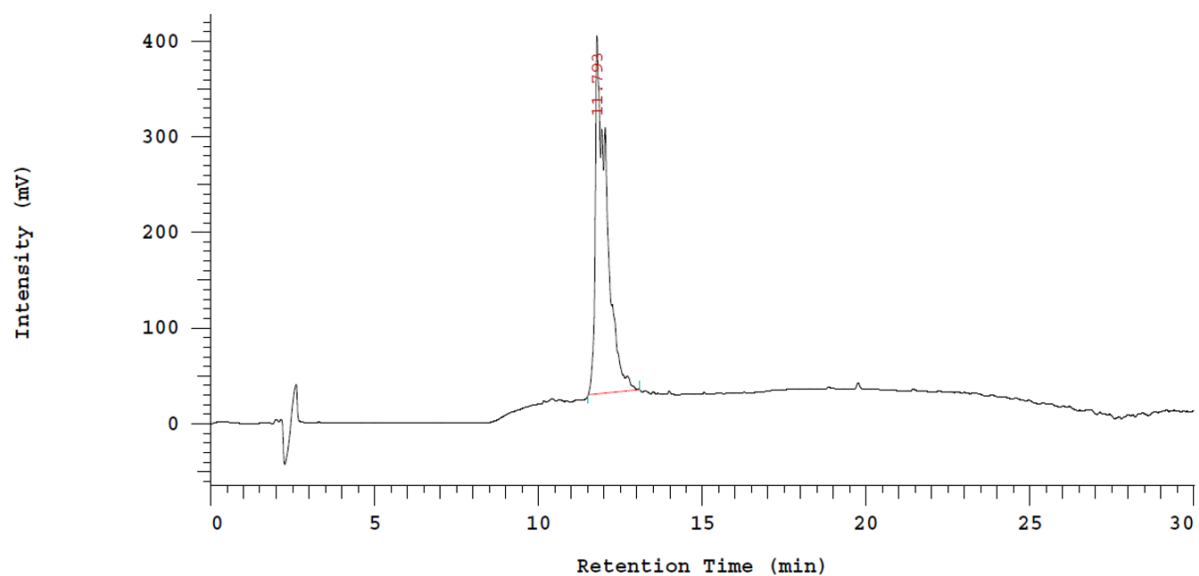
¹H NMR (500 MHz, Deuterium oxide) δ (ppm) = 1.3-1.4 (td, 12H, -CH₃ H alanine), 1.45-1.9 (comp, 12H βγδH lysine), 1.95-2.45 (comp, 24H, -CH₂ proline), 2.5-2.7 (comp, 32 H, -CO-CH₂-CH₂-CO- succinic acid), 3.1-3.65 (comp, 154 H, -CH₂- tepa, βH cysteine, βH histidine), 3.70-3.90 (m, 16H, αεH lysine, βH serine, αH cysteine) 4.1-4.7 (comp, 23 H, αH histidine, αH serine, αH proline, αH alanine), 4.79 (s, HDO), 7.2-7.4 (m, 11 H, aromatic H histidine), 8.5-8.7 (m, 11 H, aromatic H histidine). comp indicates a group of overlaid protons.

1120: Sequence (N->C): {[C-(H-Stp)₄-H]_{α,ε}-K-H-dPEG₂₄-dPEG₂₄]_ε-K


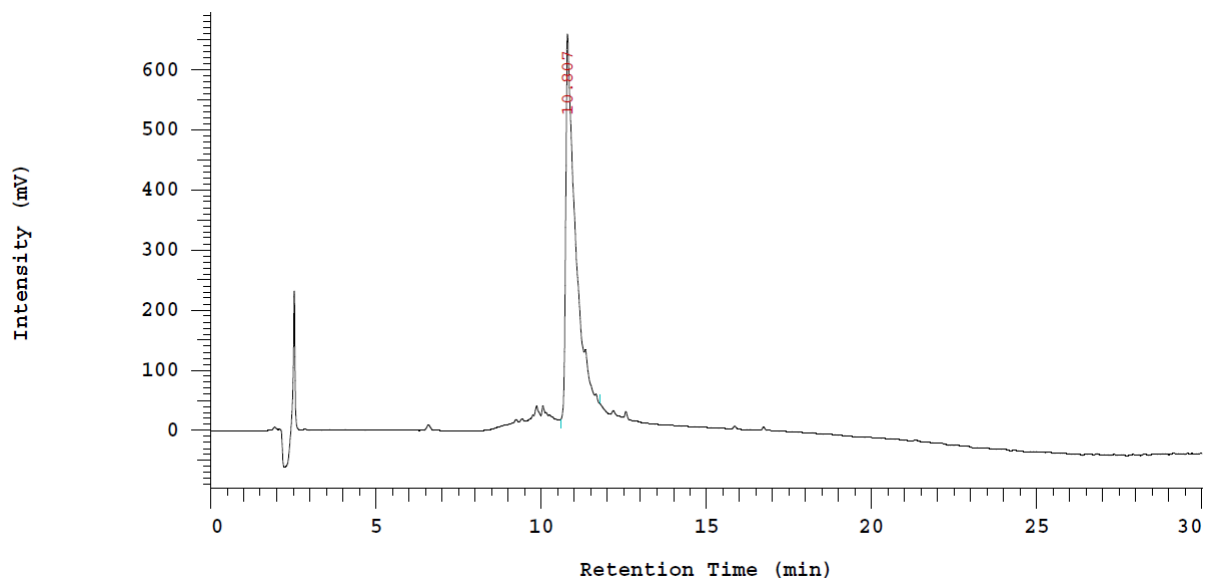
¹H NMR (500 MHz, Deuterium oxide) δ (ppm) = 1.1-1.4 (comp, 12H, βγδH lysine), 2.3-2.7 (comp, 34 H, -CO-CH₂-CH₂-CO- succinic acid -CO-CH₂-dPEG₂₄), 2.9-3.65 (comp, 154 H, -CH₂- tepe, βH cysteine, βH histidine), 3.70 (s, 196H, -CH₂-O-dPEG₂₄, -CH₂-N-dPEG₂₄), 3.75-3.85 (m, 4H, εH lysine) 4.1-4.7 (comp, 15 H, αH cysteine, lysine, histidine), 4.79 (s, HDO), 7.2-7.4 (m, 11 H, aromatic H histidine), 8.5-8.7 (m, 11 H, aromatic H histidine). comp indicates a group of overlaid protons.

6.5.4 RP-HPLC of oligomers

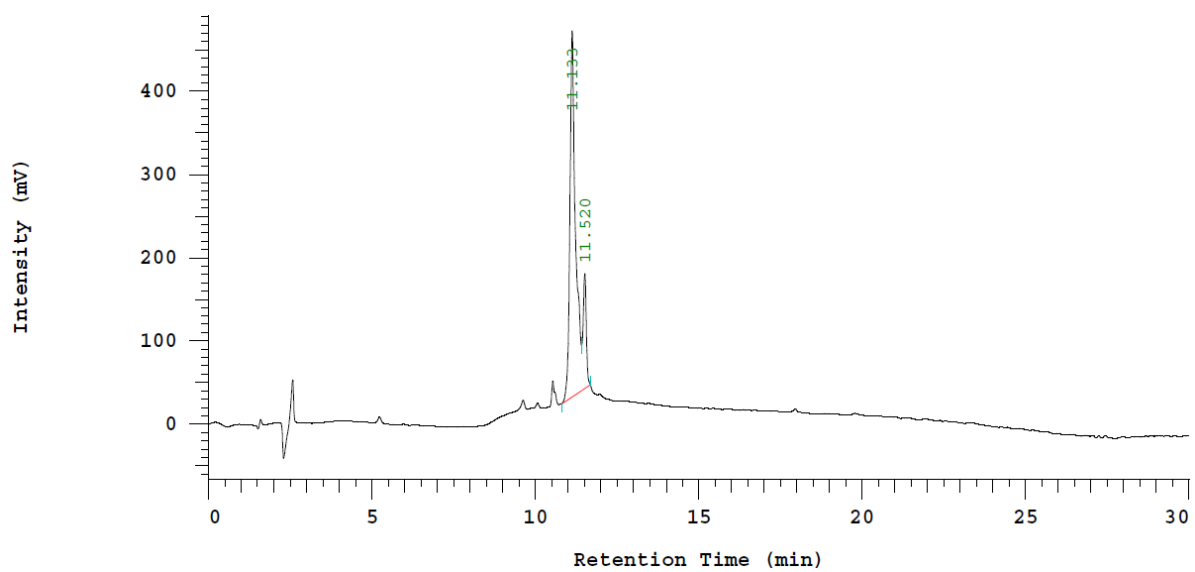
440:



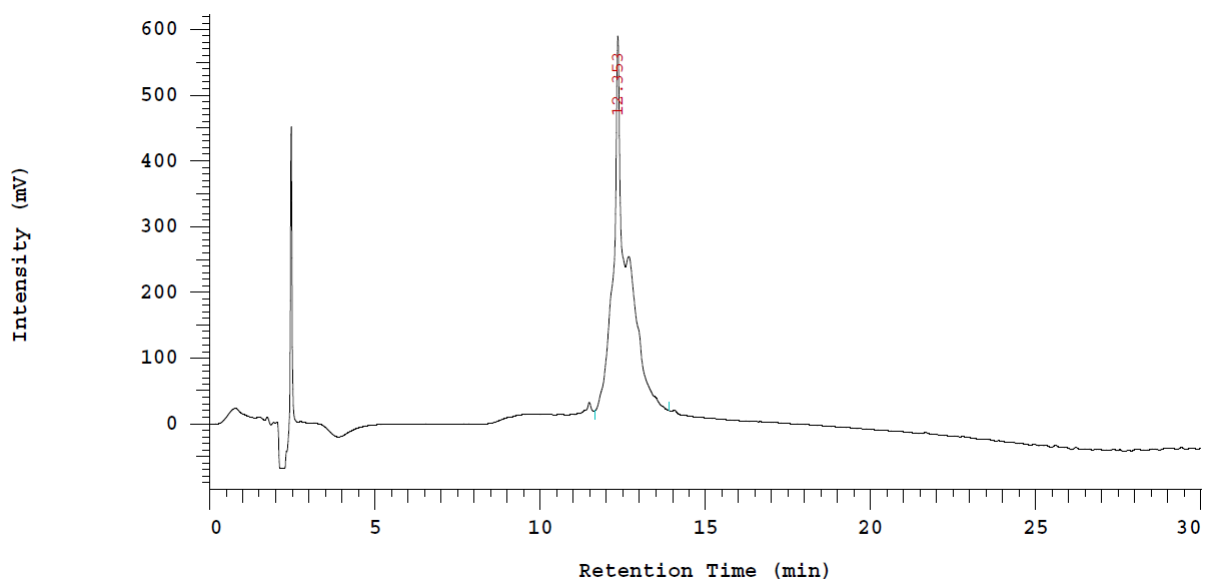
442:



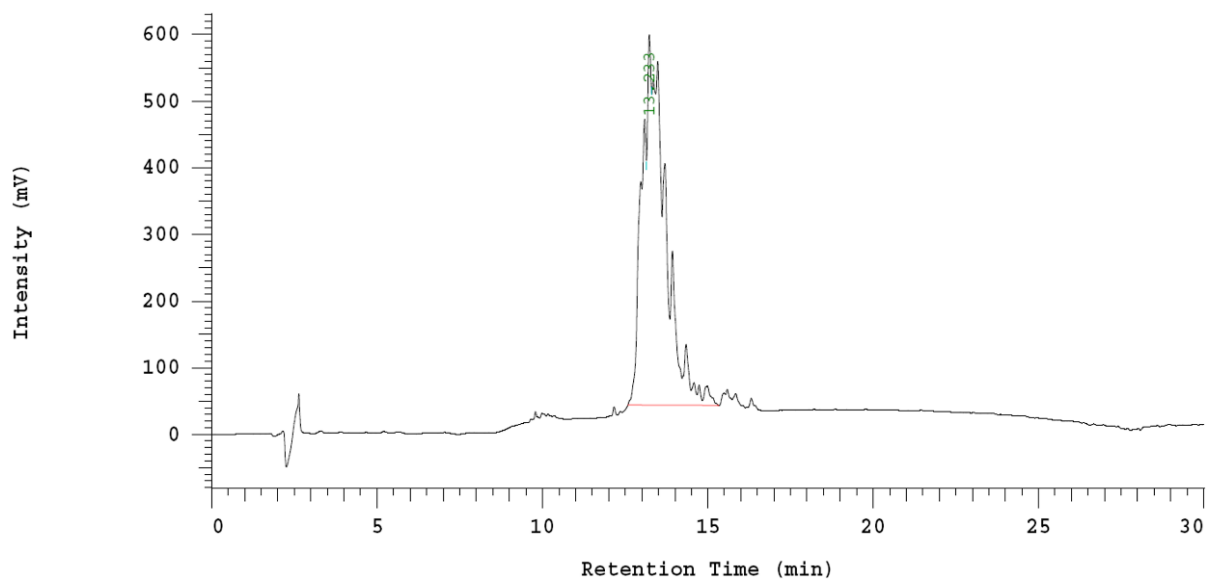
689:



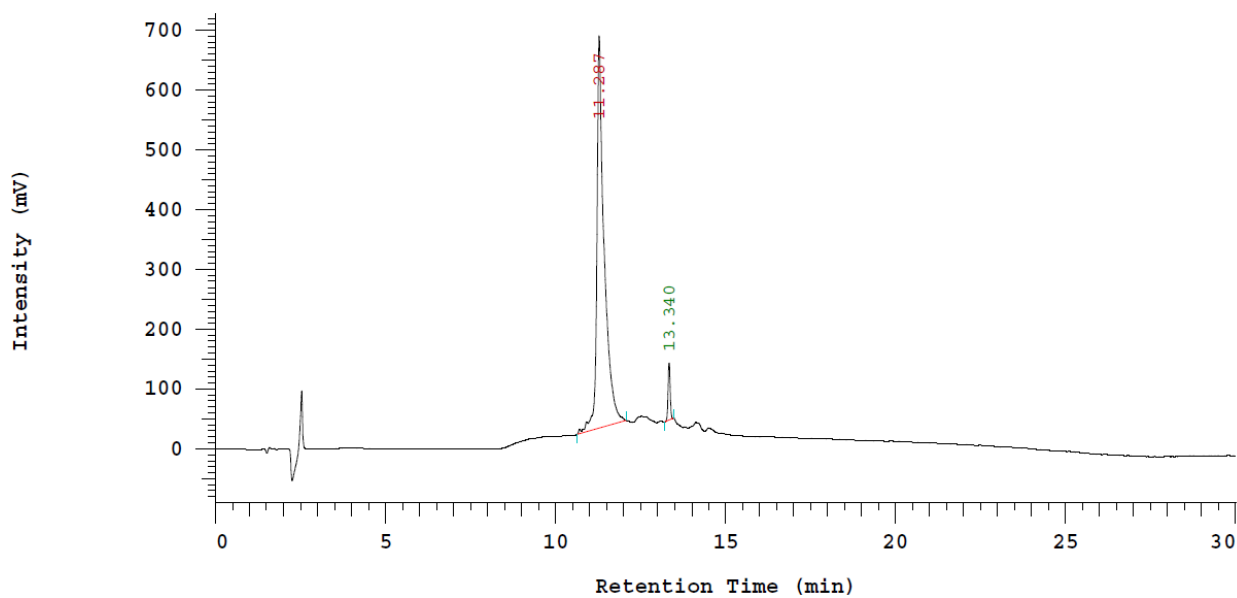
694:



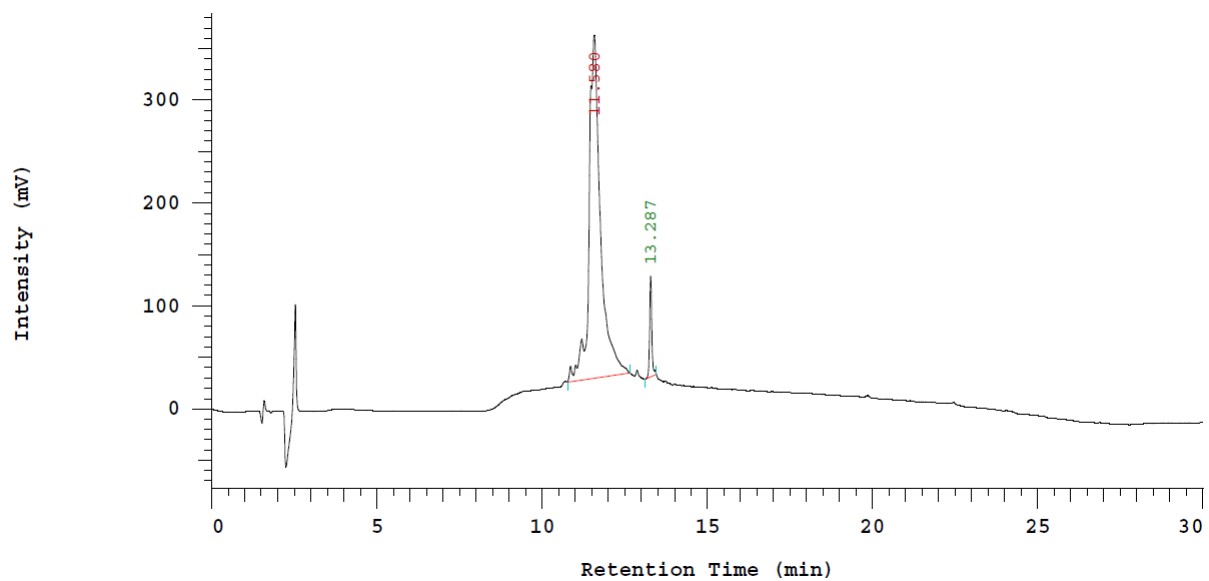
835:



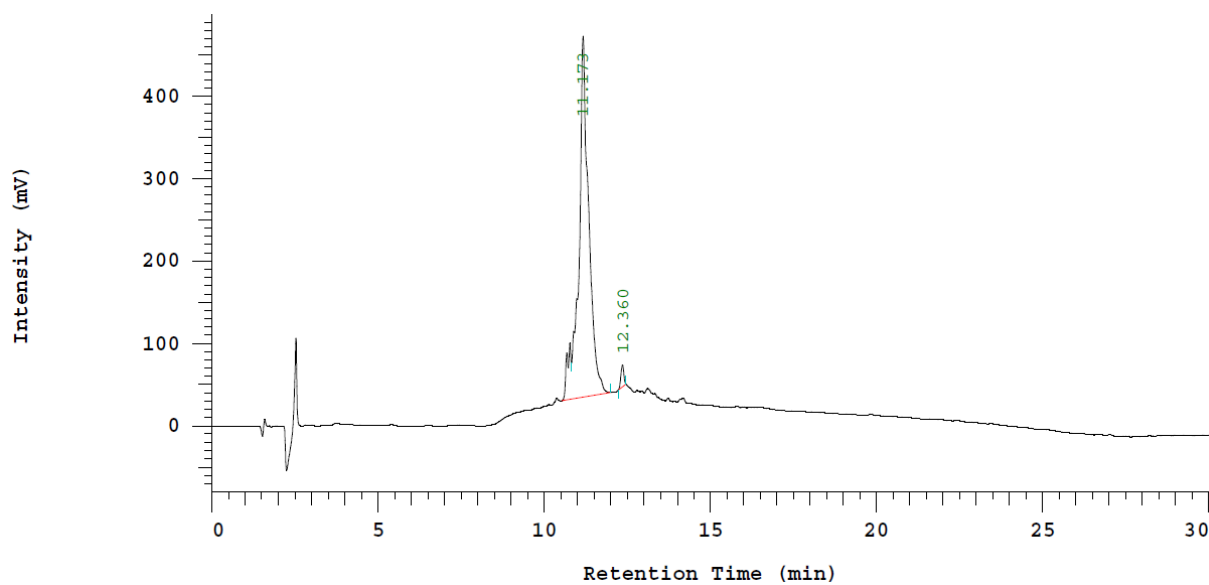
901:

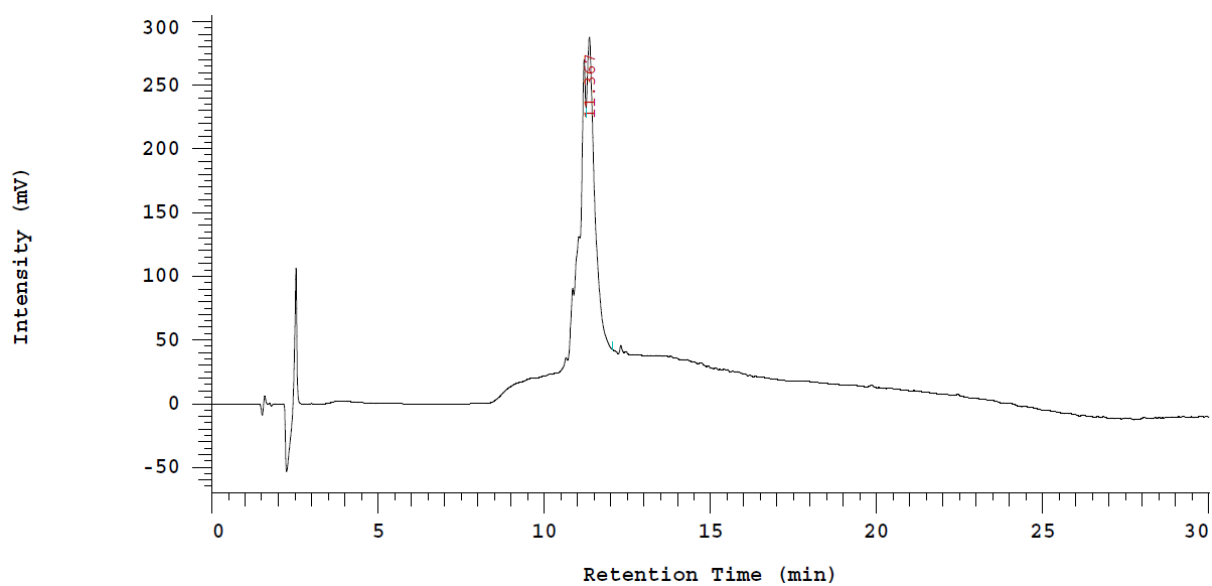
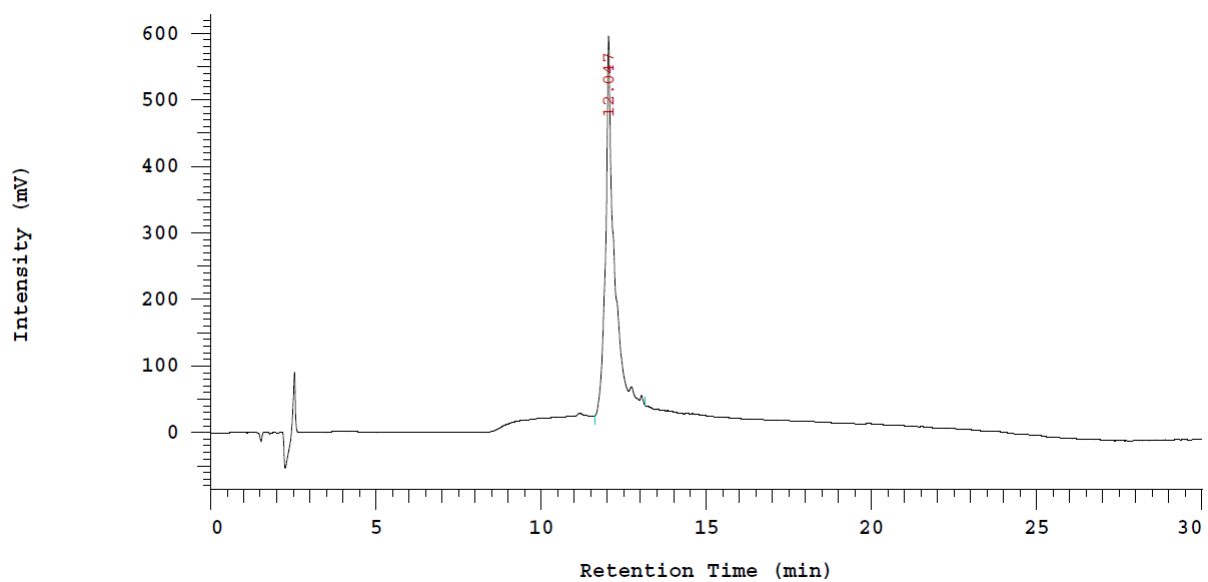


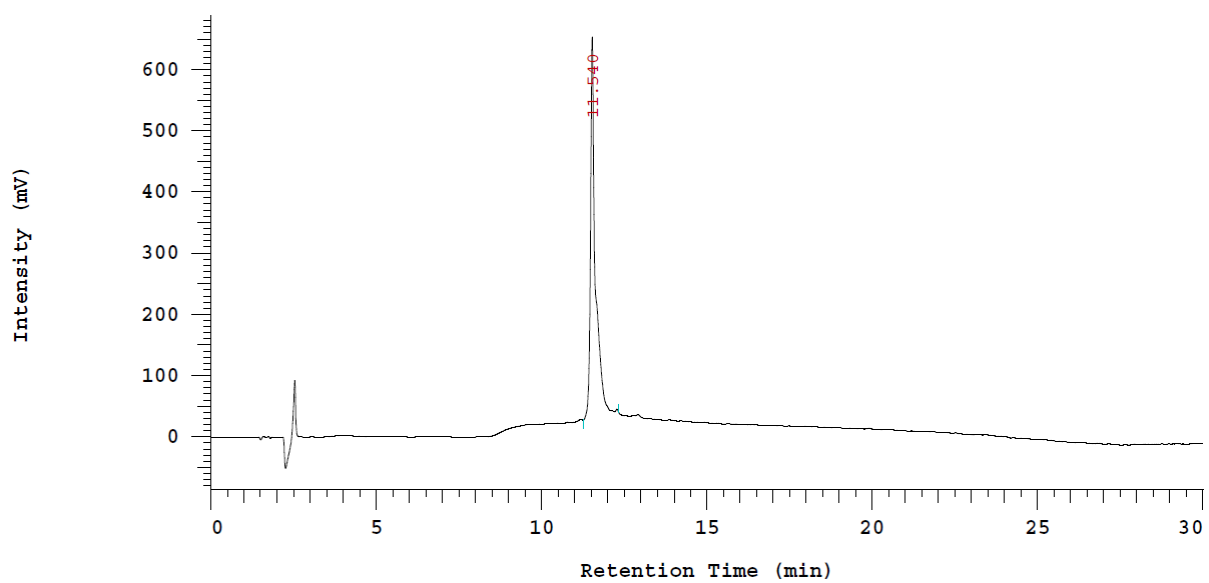
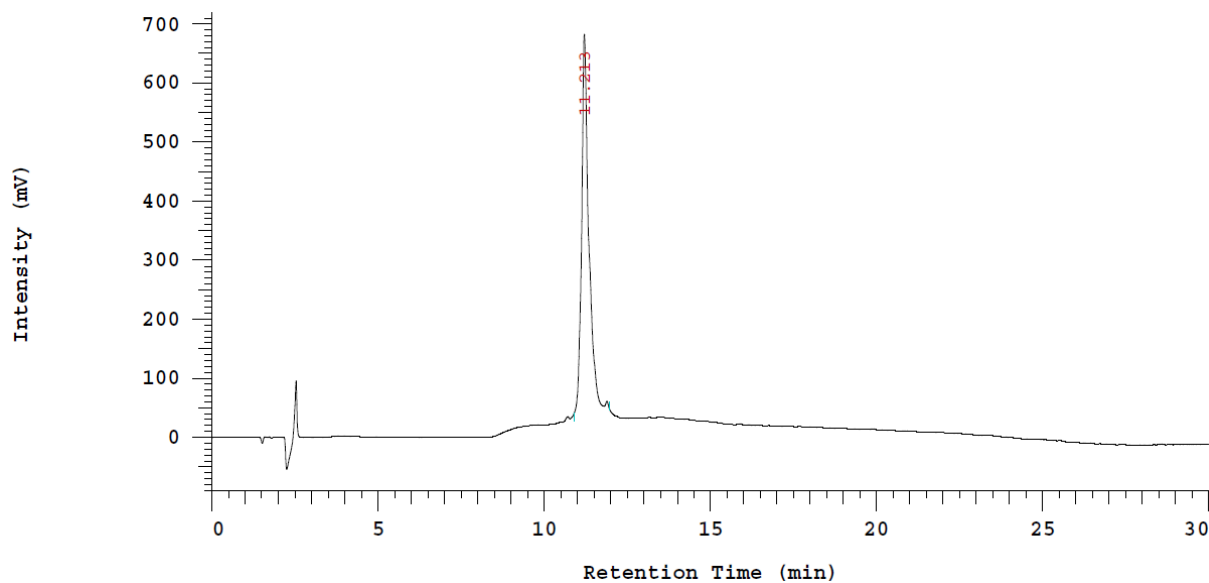
996:

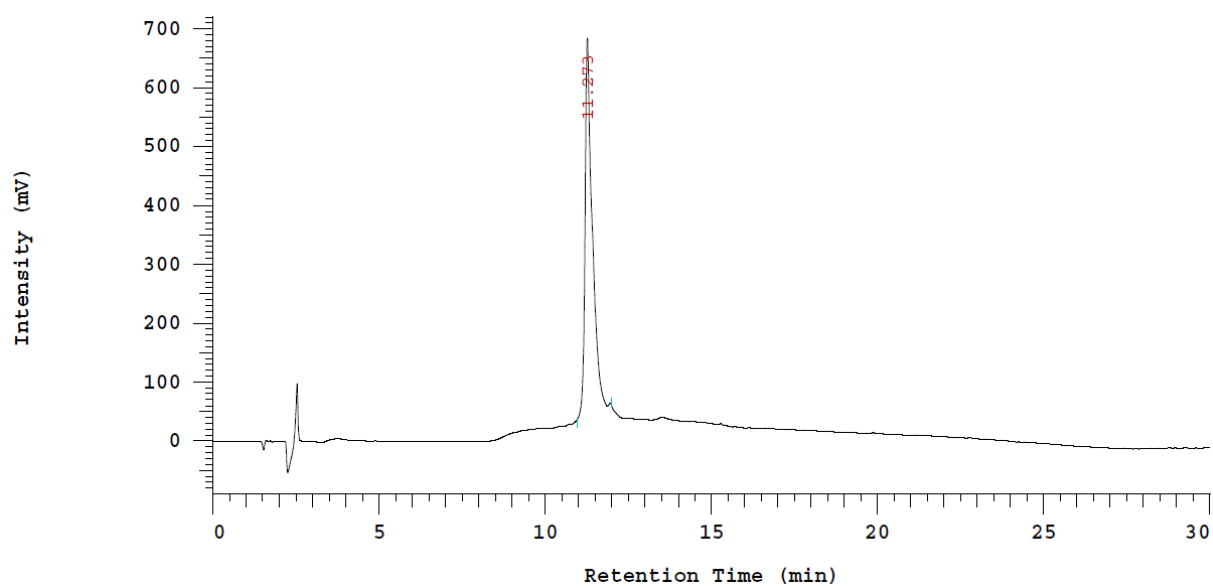
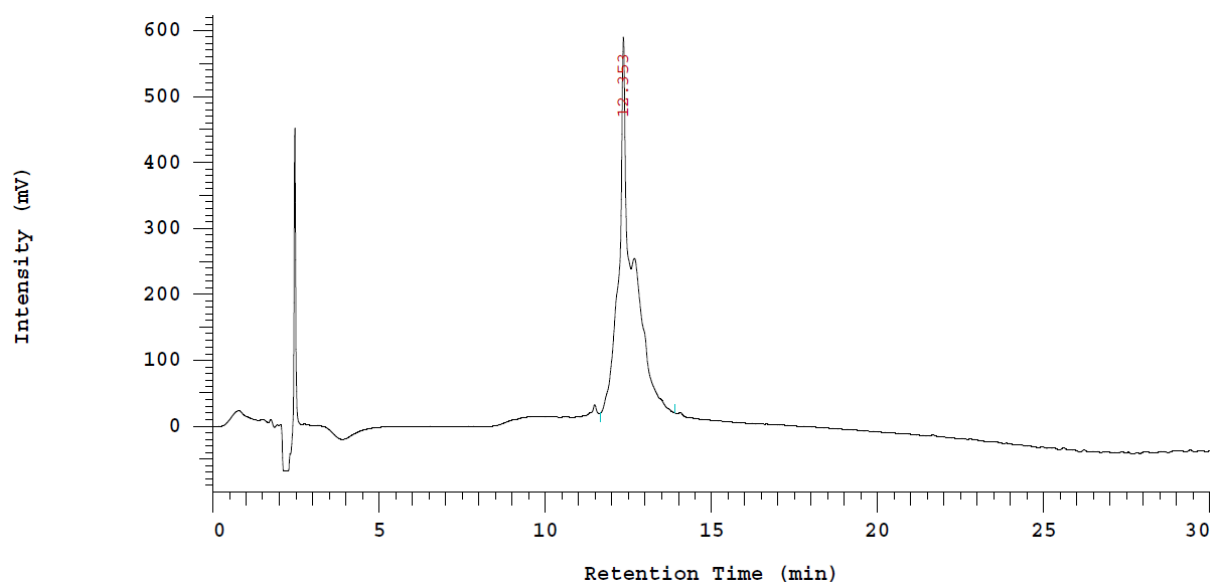


1000:



1078:**1088:**

1091:**1094:**

1097:**1120:**

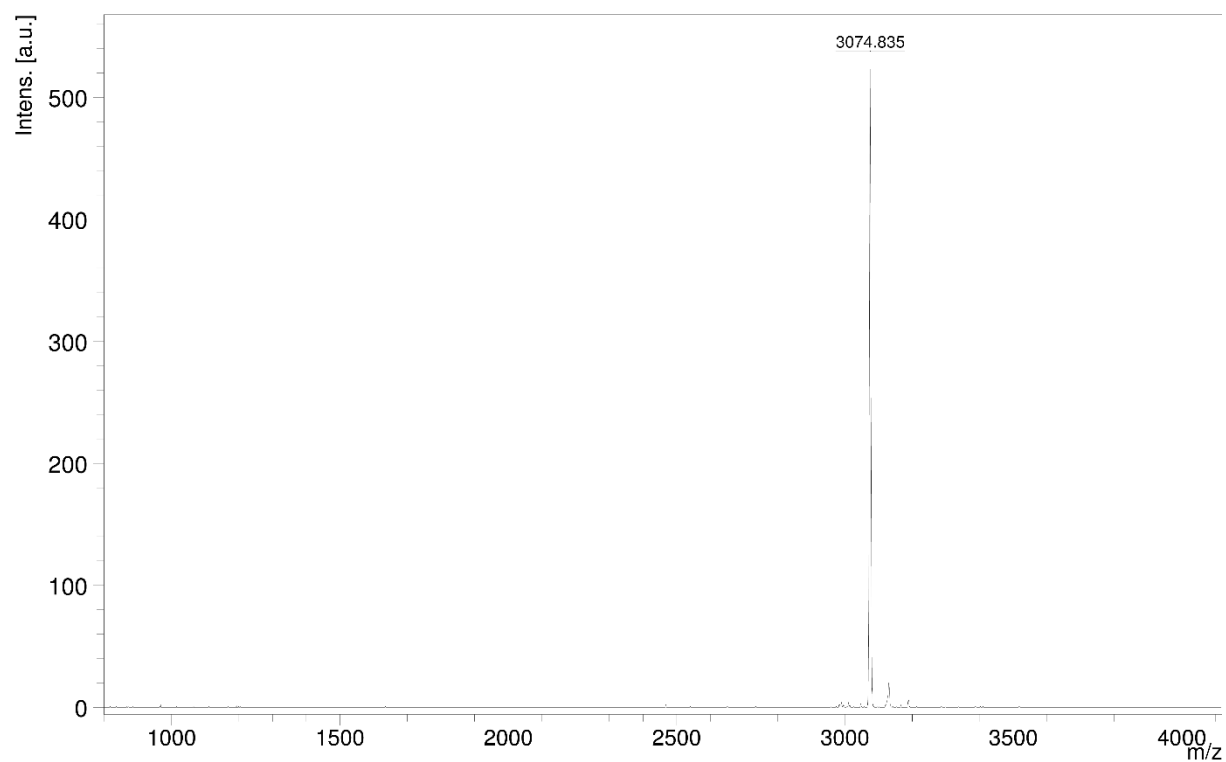
6.5.5 Mass spectra of oligomers

Table 23 Table summarizing mass data of oligomers. Mass data was recorded with a Bruker MALDI-TOF instrument

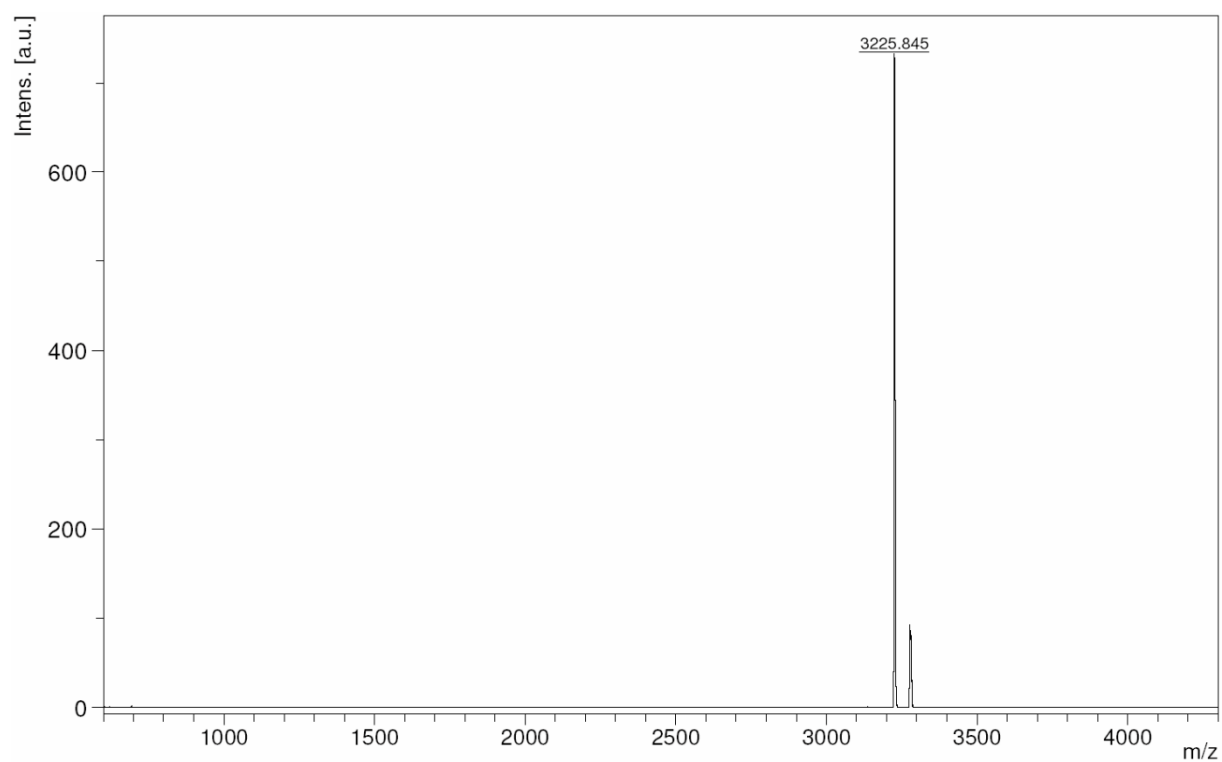
| Oligomer | Molecular formula | [M-H] ⁻ calc. | [M-H] ⁻ found |
|---|-------------------|--------------------------|--------------------------|
| 454 (Stp ₂ -Y ₃ -OleA) | | 3072.0 | 3074.8 |
| 1021 (Stp ₂ -Y ₃ -CholA) | | 3229.2 | 3225.9 |
| 1022 (Stp ₃ -Y ₃ -OleA) | | 3615.7 | 3615.8 |
| 1023 (Stp ₃ -Y ₃ -CholA) | | 3771.0 | 3769.2 |
| 1024 (Stp ₂ -H ₃ -Y ₃ -OleA) | | 3895.9 | 3893.7 |
| 1026 ((Stp-H) ₂ -H-Y ₃ -OleA) | | 3895.9 | 3893.1 |
| 1173 (Stp ₂ -Y ₆ -OleA) | | 4052.1 | 4047.9 |
| 1174 (Stp ₂ -Y ₆ -CholA) | | 4208.3 | 4205.9 |
| 1175 (Stp ₄ -Y ₃ -OleA) | | 4158.5 | 4154.5 |
| 1176 (Stp ₄ -Y ₃ -CholA) | | 4314.7 | 4312.4 |
| 1177 (Stp ₄ -Y ₆ -OleA) | | 5137.5 | 5133.2 |
| 1178 (Stp ₄ -Y ₆ -CholA) | | 5293.7 | 5286.2 |
| 1179 ((Stp-H) ₄ -H-Y ₃ -OleA) | | 5529.8 | 5525.9 |
| 1180 (Stp ₄ -H ₅ -Y ₃ -OleA) | | 5529.8 | 5522.7 |

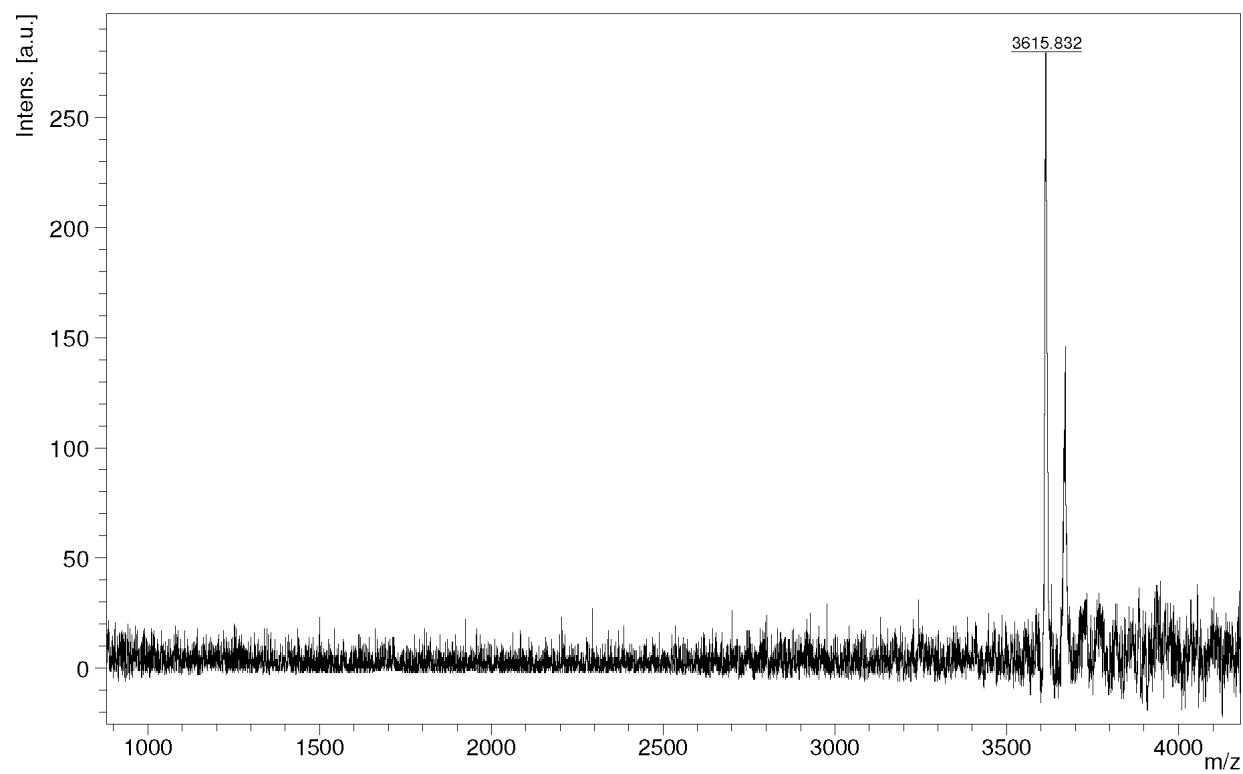
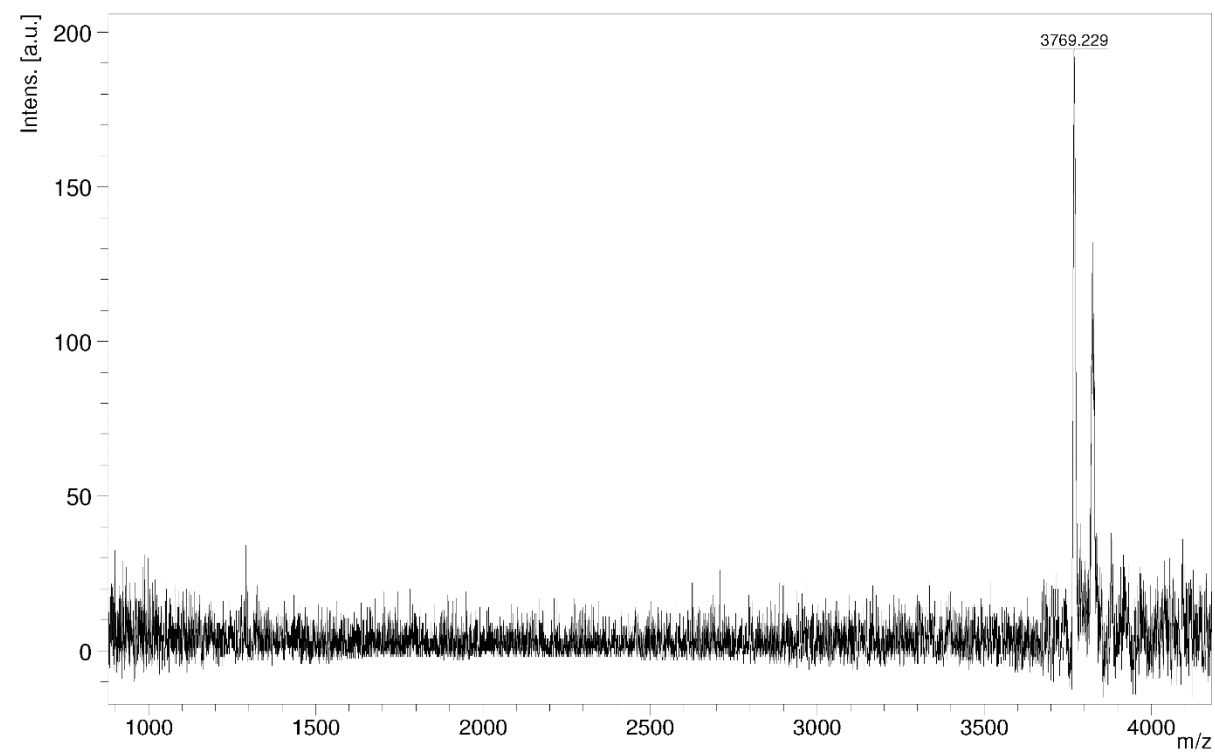
6.5.5.1 Full mass spectra of oligomers

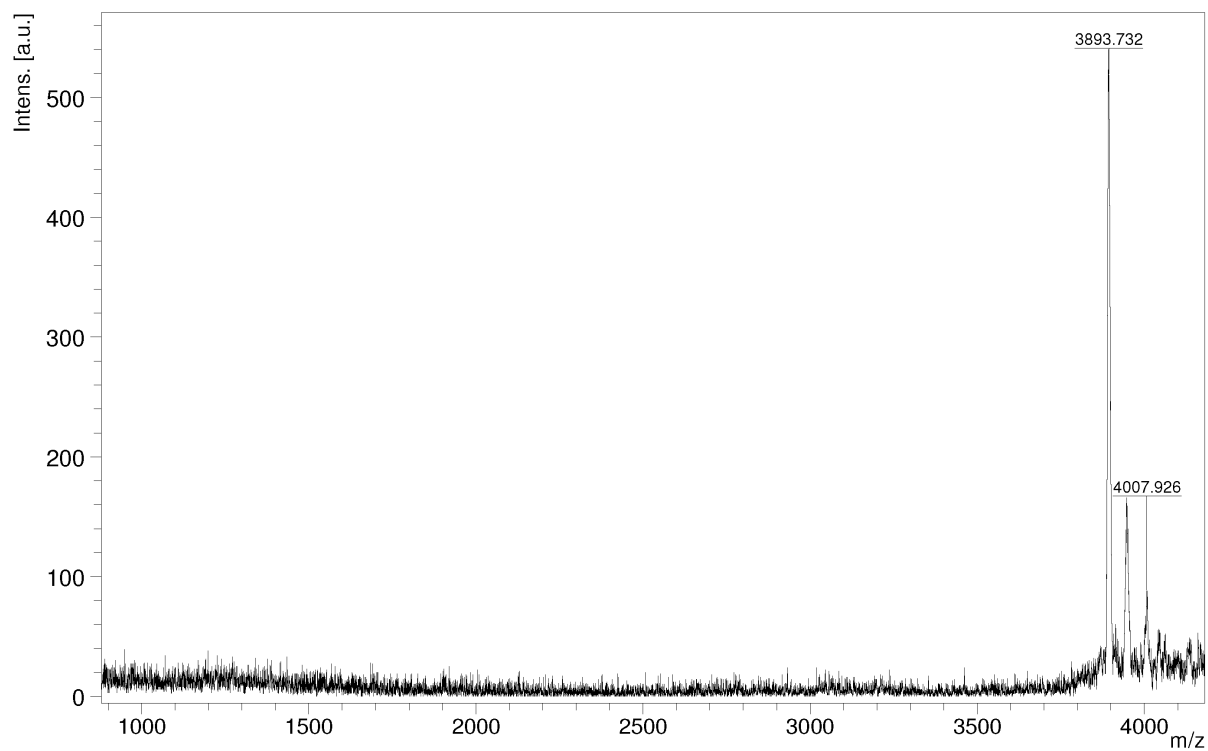
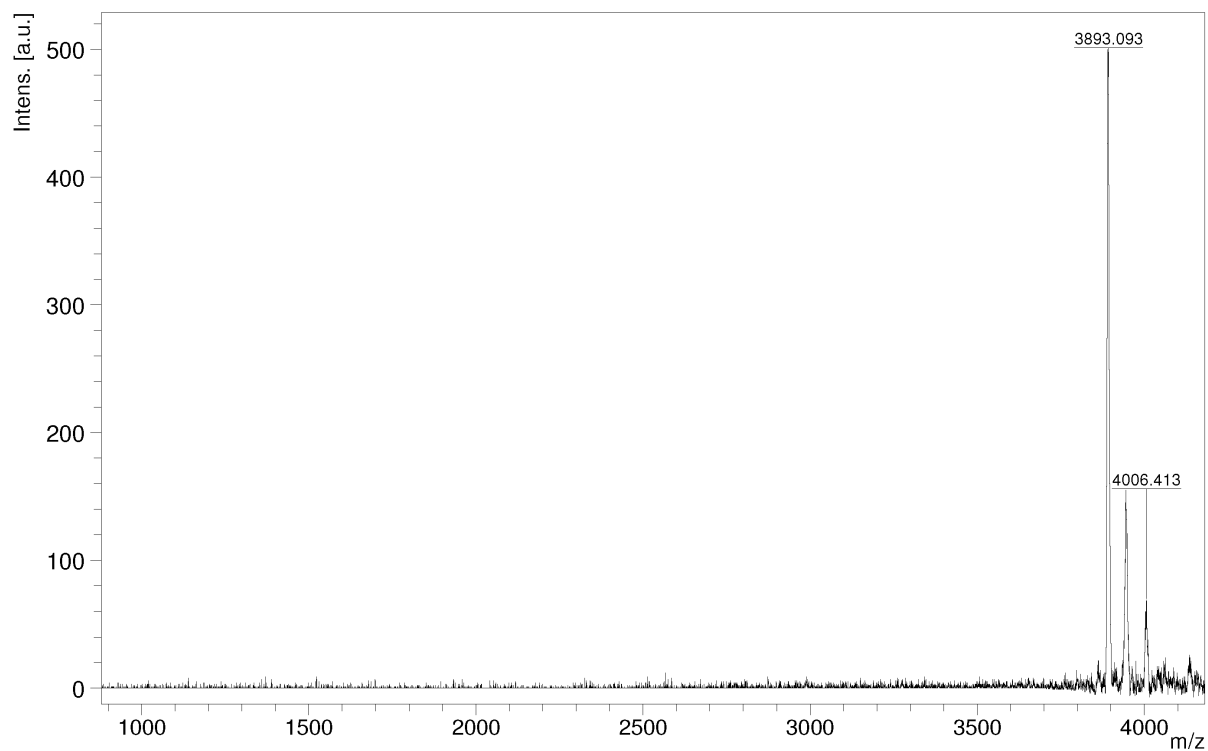
454:

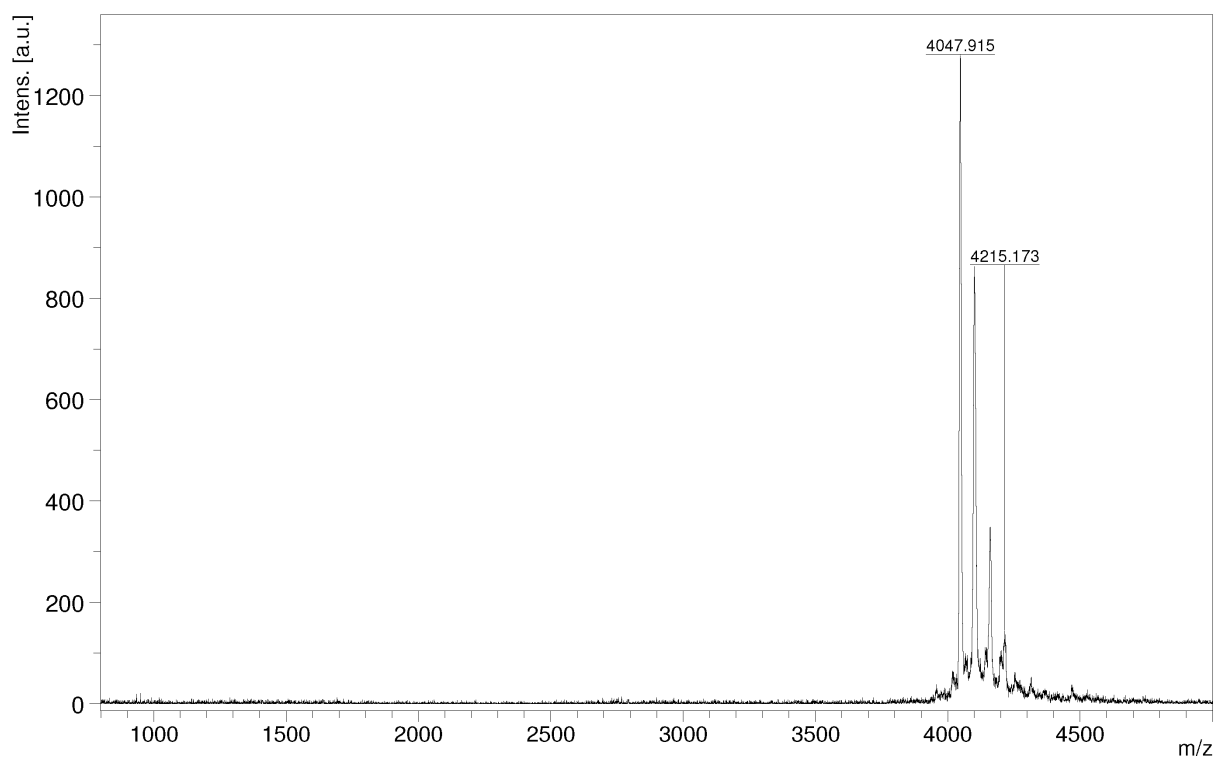
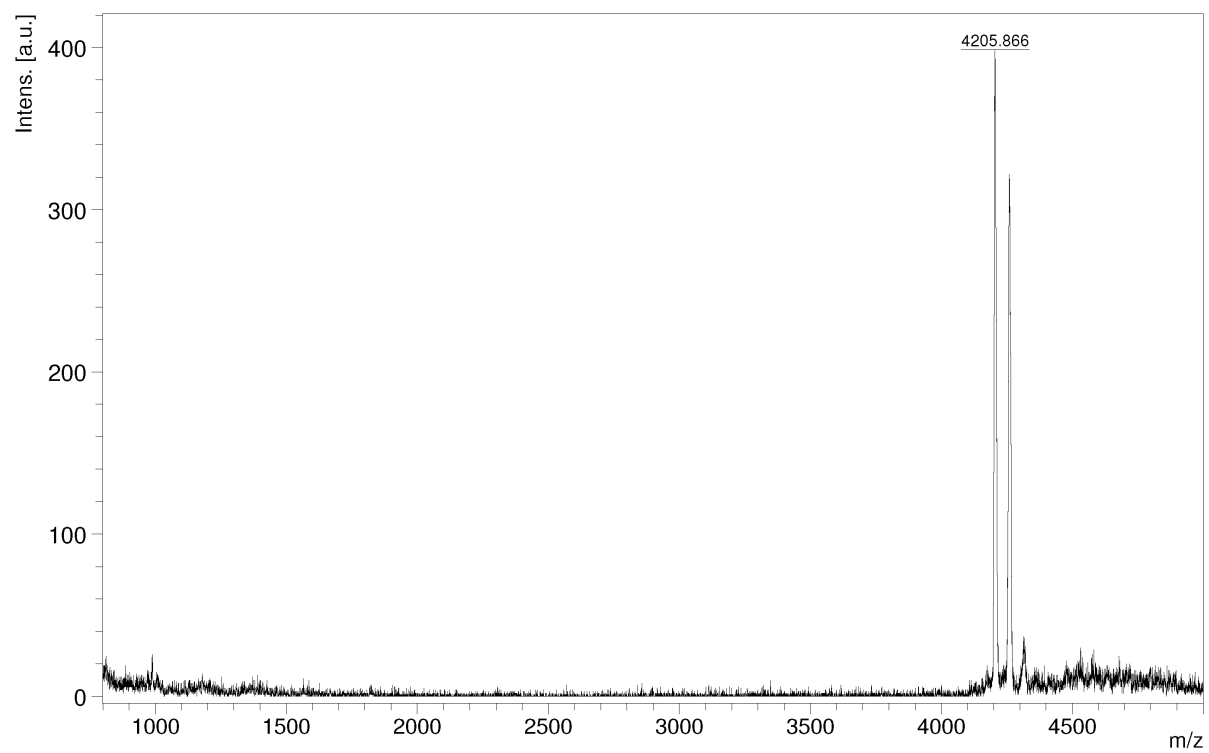


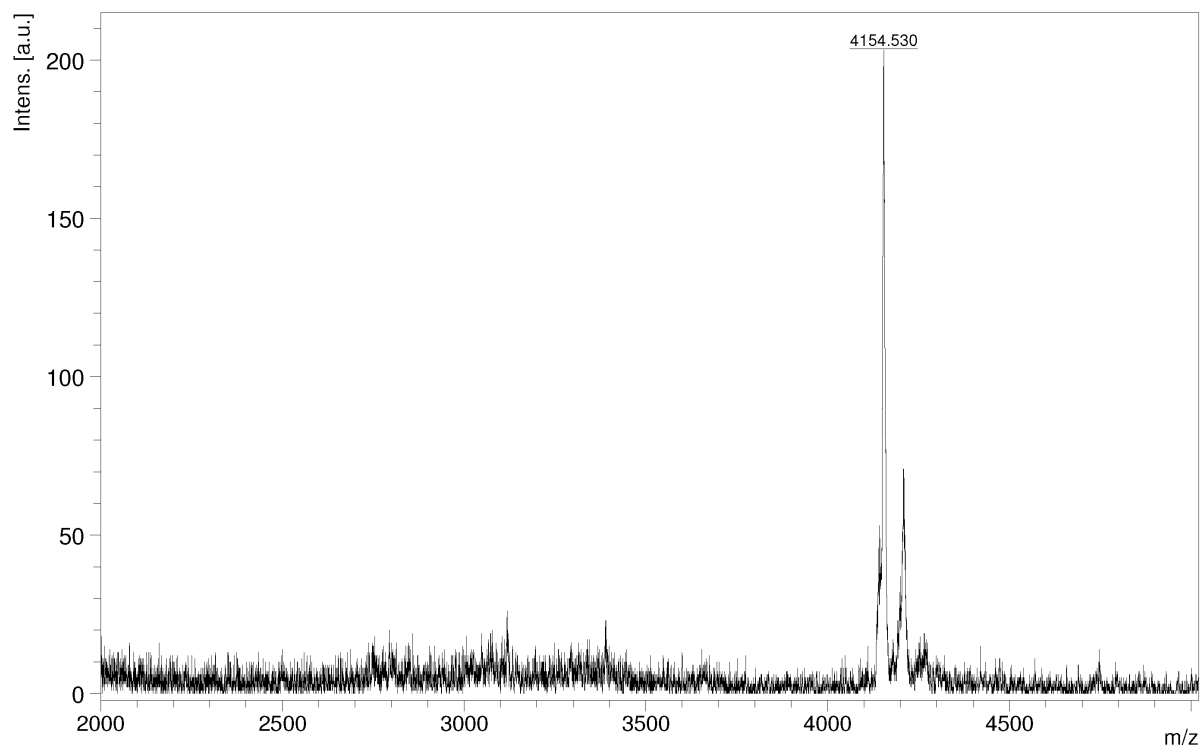
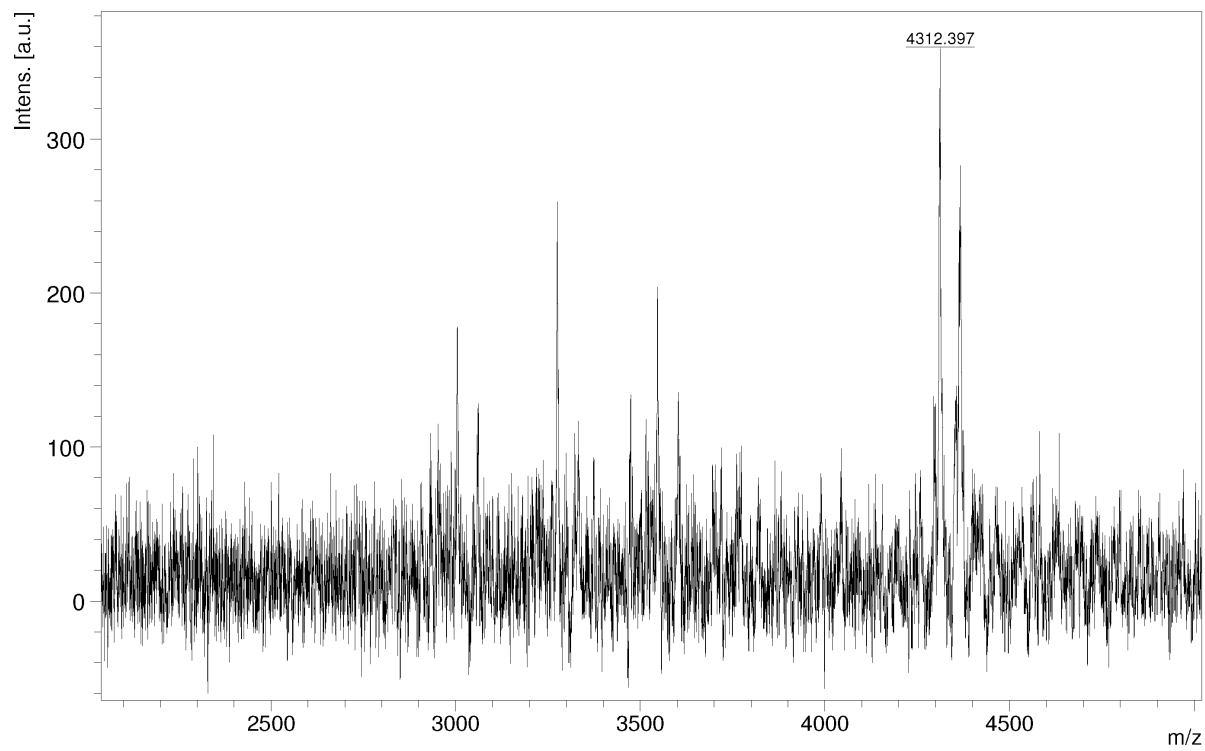
1021:

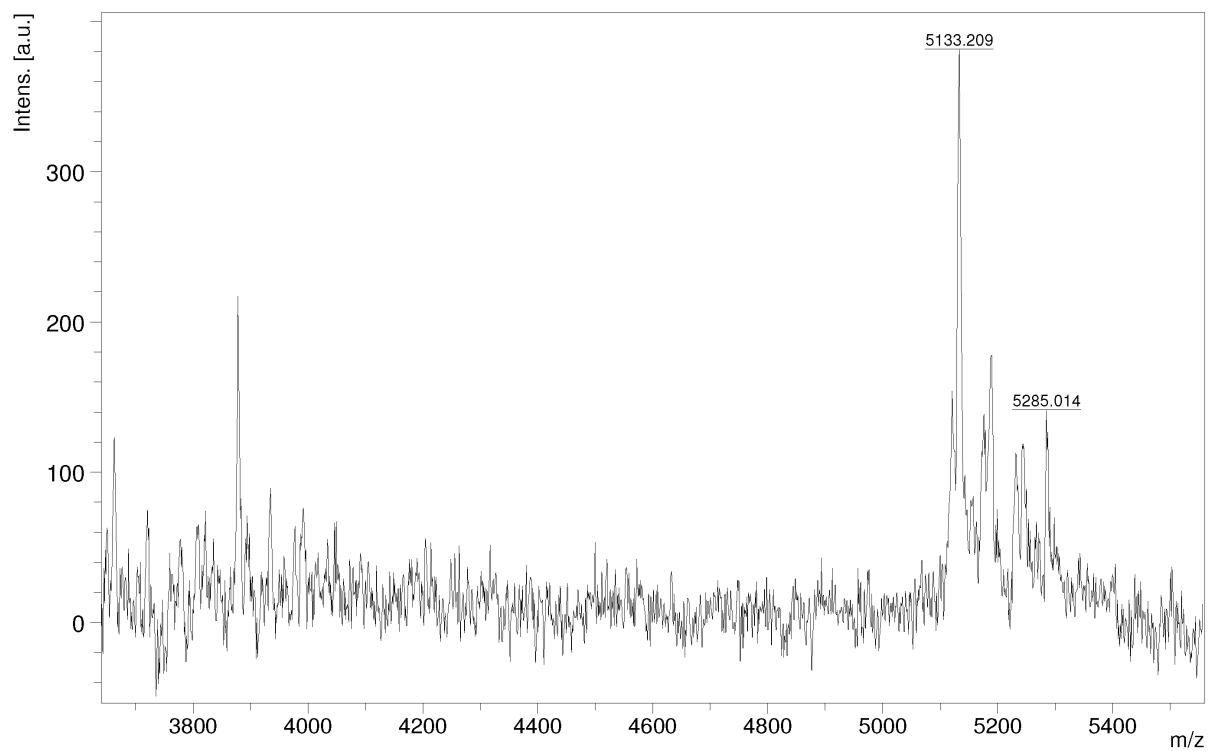
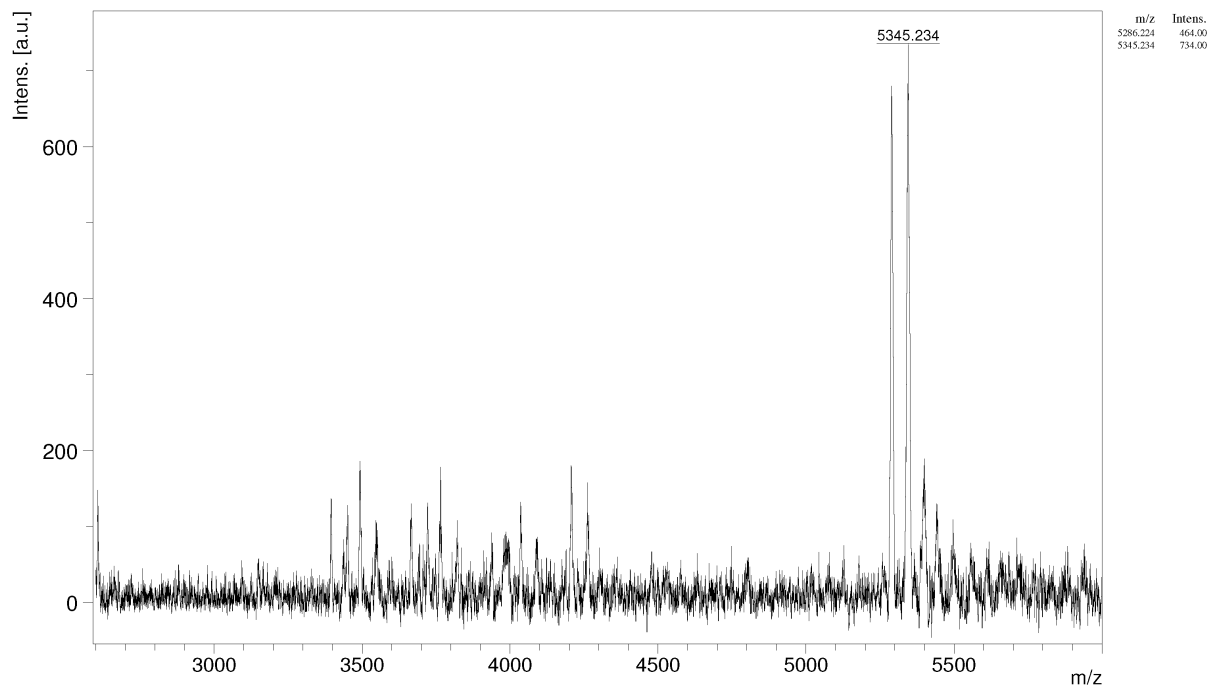


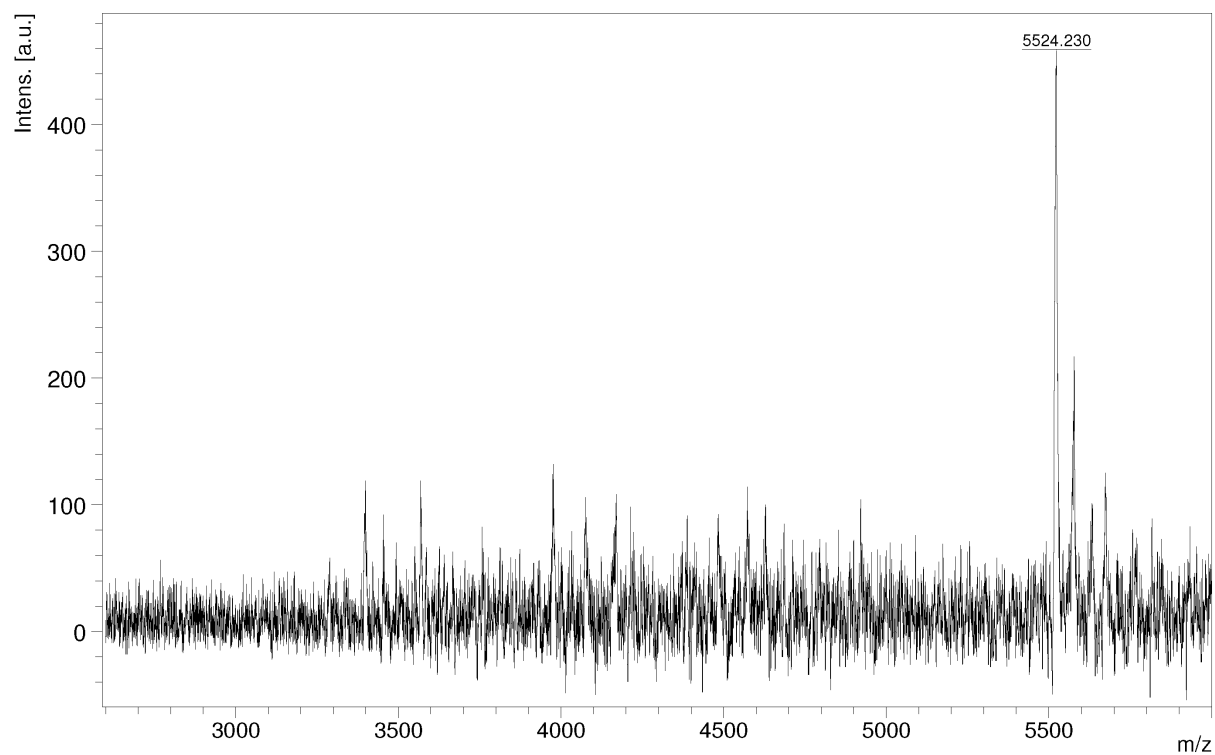
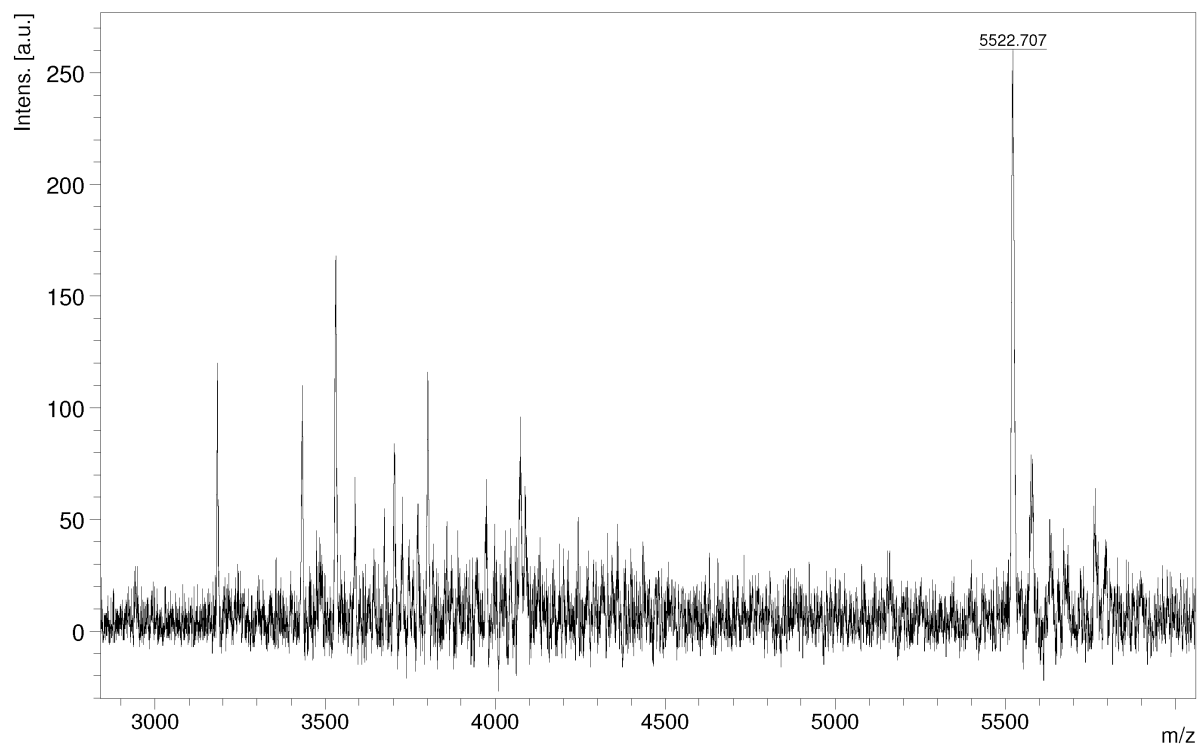
1022:**1023:**

1024:**1026:**

1173:**1174:**

1175:**1176:**

1177:**1178:**

1179:**1180:**

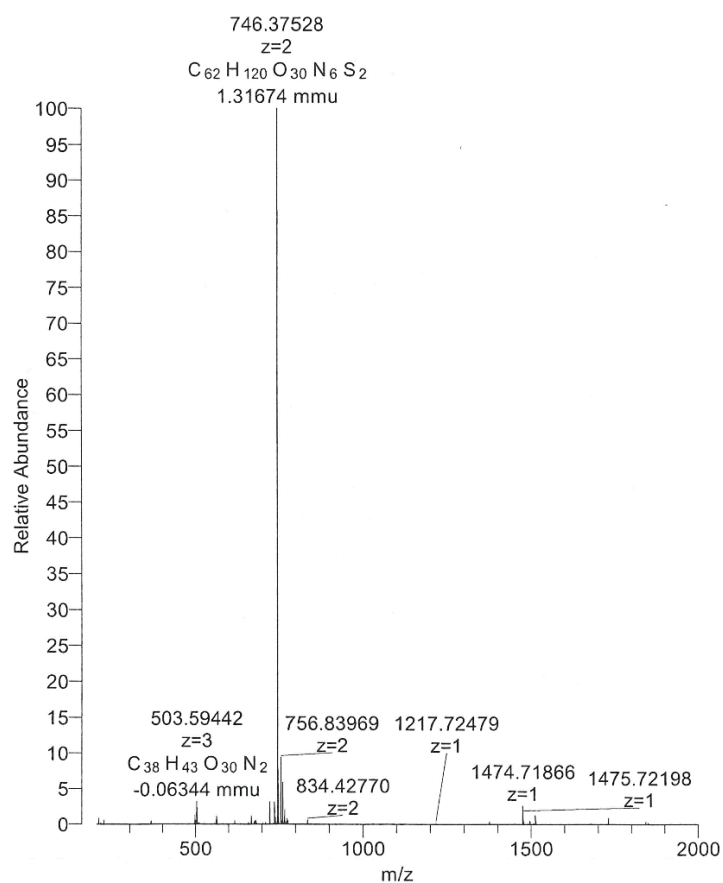
6.5.6 Mass spectra of shielding reagents

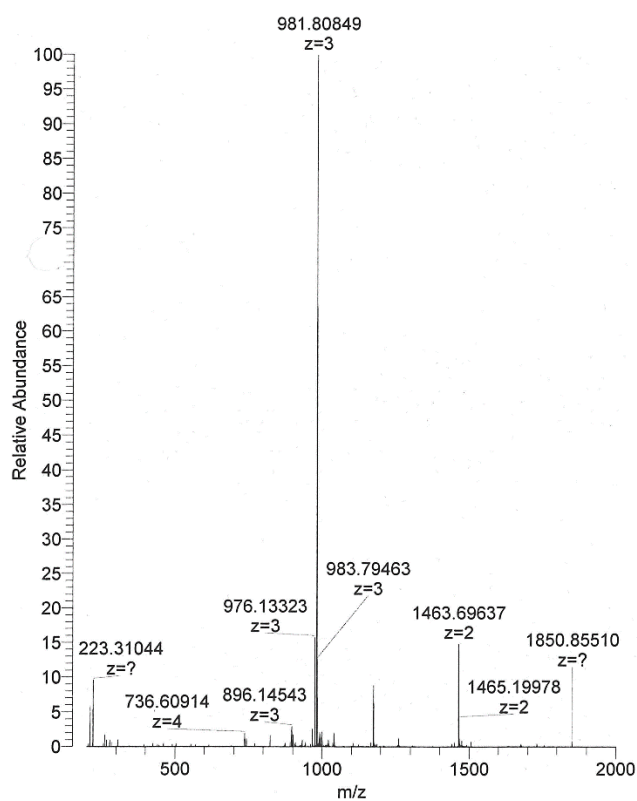
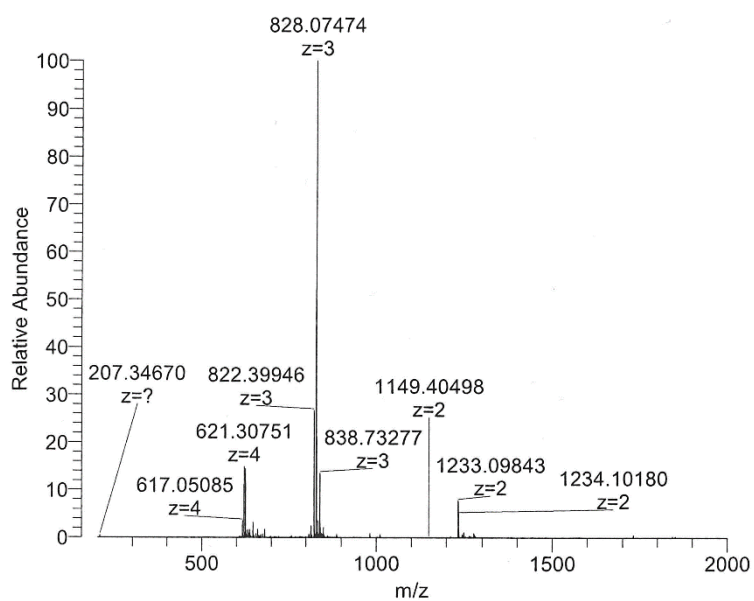
Table 24 Table summarizing mass data of shielding reagents. Mass data was recorded with a Thermoscientific LTQ FT Ultra Fourier transform ion cyclotron and an IonMax source.

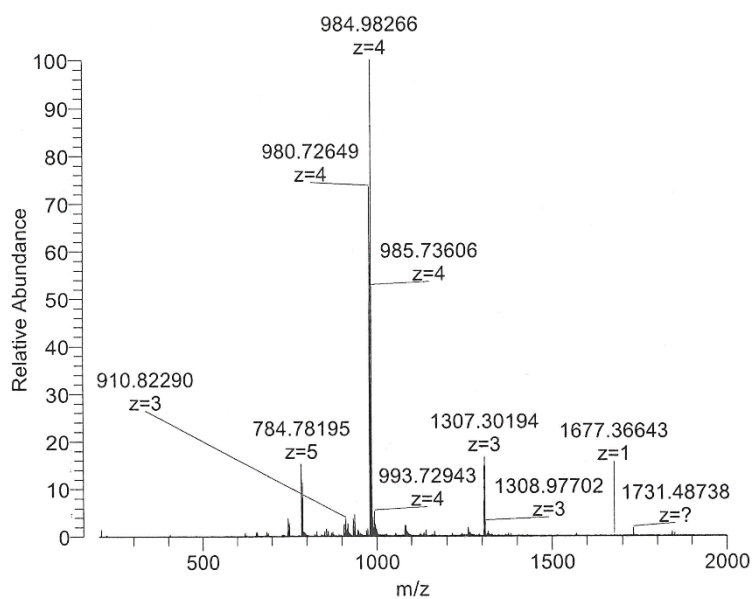
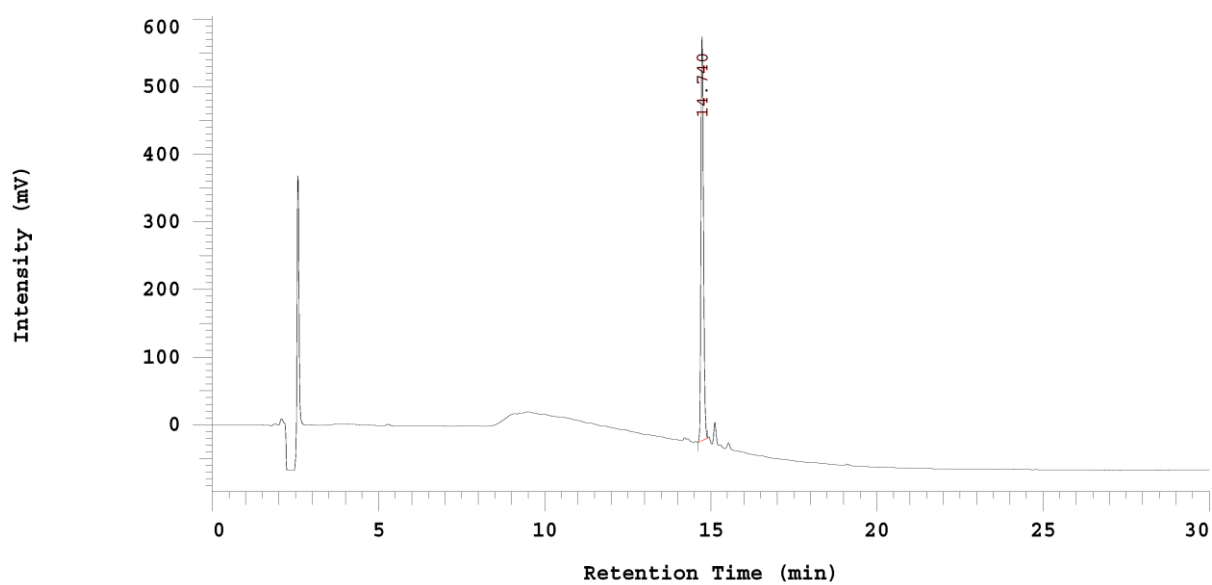
| Shielding agent | ID | Molecular formula | [M+X] ⁺ calc. | [M+X] ⁺ found |
|---|------|--|--------------------------|--------------------------|
| Cys(NPys)-PEG ₂₄ -Ala | 1059 | C ₆₂ H ₁₁₅ N ₅ O ₃₀ S ₂ | 1495.7 [Na] | 1492.8 [Na] |
| Cys(NPys)-PEG ₂₄ -GE11 | 999 | C ₁₃₄ H ₂₀₅ N ₂₁ O ₄₇ S ₂ | 2948.3 [Na] | 2945.4 [Na] |
| Cys(NPys) ₂ -PEG ₂₄ -Ala | 1060 | C ₁₀₄ H ₁₈₆ N ₁₄ O ₄₄ S ₄ | 2486.9 [Na] | 2484.3 [Na] |
| Cys(NPys) ₂ -PEG ₂₄ -GE11 | 1056 | C ₁₇₆ H ₂₇₆ N ₃₀ O ₆₁ S ₄ | 3938.5 [Na] | 3940.0 [Na] |

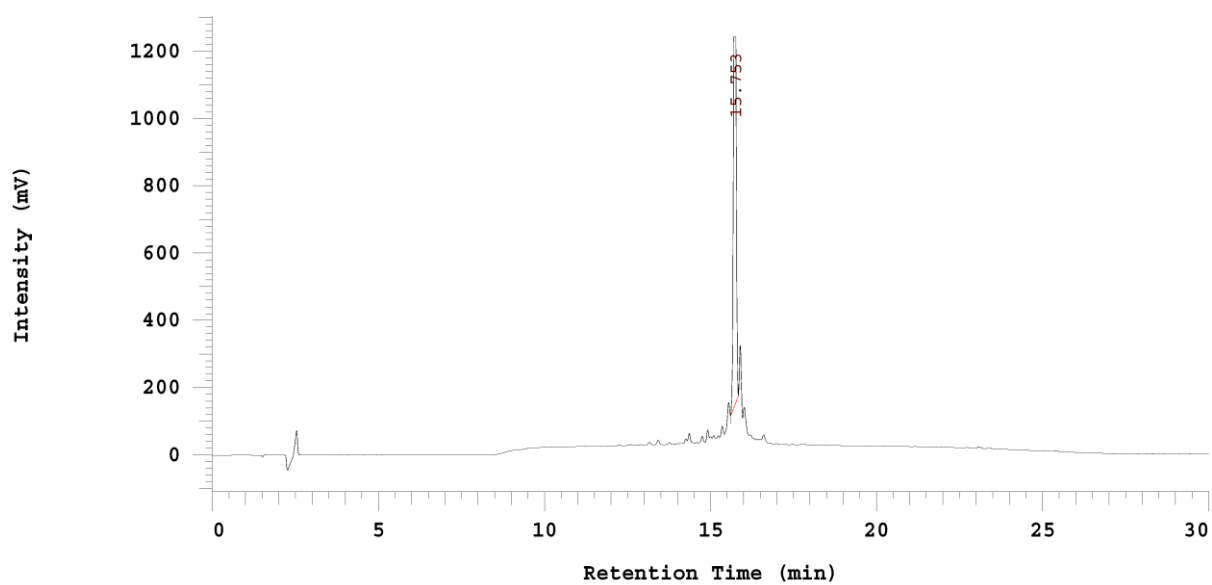
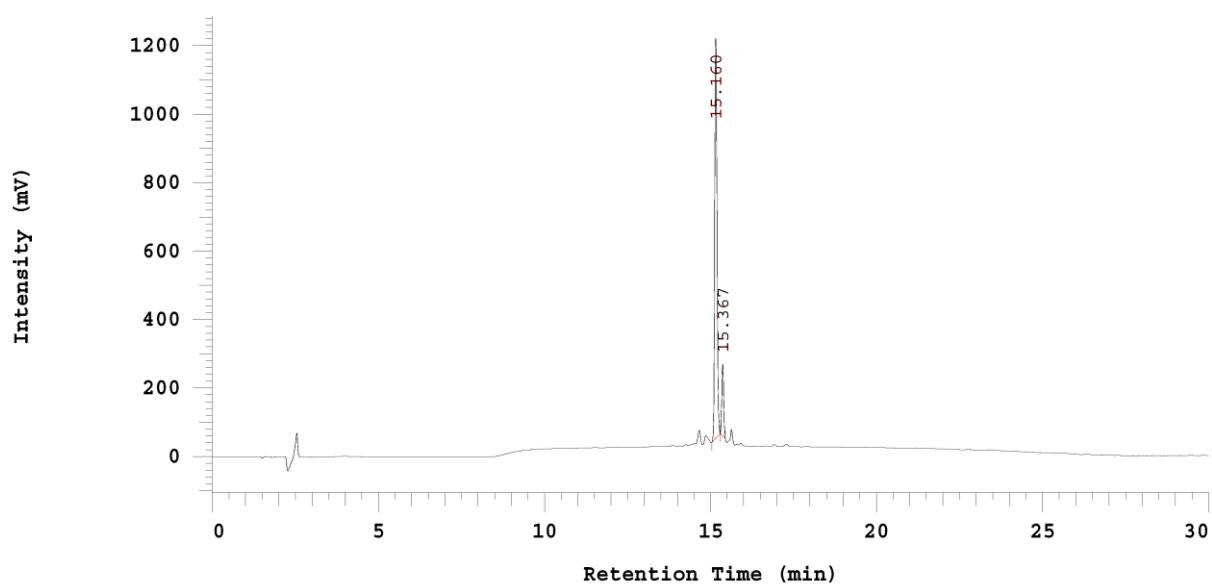
6.5.6.1 Full mass spectra of shielding reagents

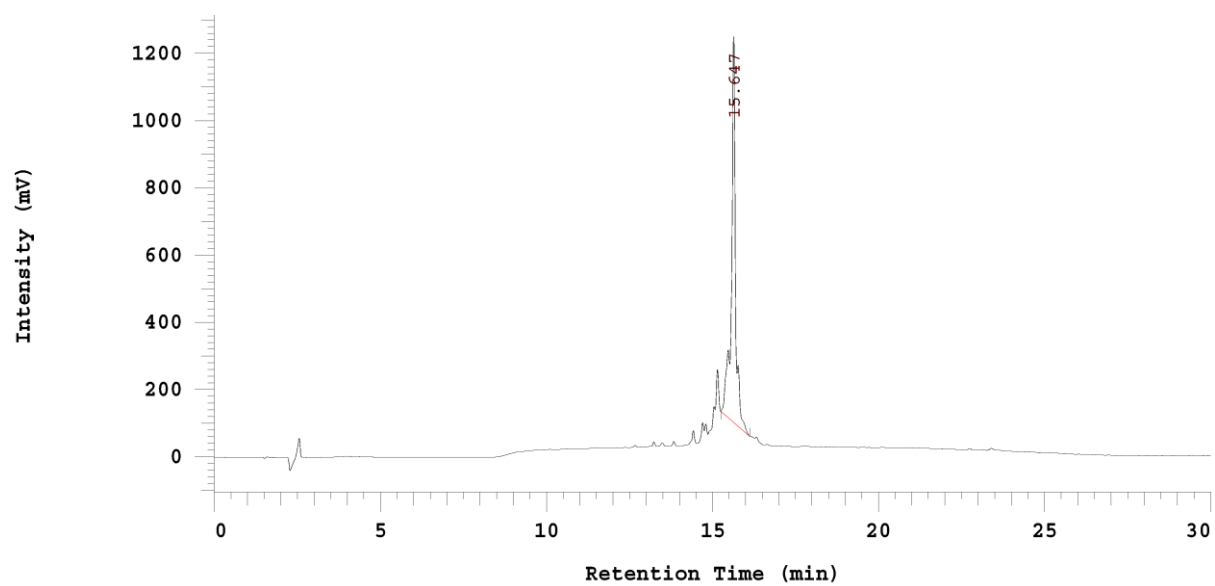
1059 (Cys(NPys)-PEG₂₄-Ala):



999 (Cys(NPys)- PEG₂₄-GE11):**1060 (Cys(NPys)₂-PEG₂₄-Ala):**

1056 (Cys(NPys)₂- PEG₂₄-GE11):**6.5.7 RP-HPLC of shielding reagents****1059 (Cys(NPys)-PEG₂₄-Ala):**

999 (Cys(NPys)- PEG₂₄-GE11):**1060 (Cys(NPys)₂-PEG₂₄-Ala):**

1056 (Cys(NPys)₂- PEG₂₄-GE11):

7 References

- [1] U. Lächelt, E. Wagner, Nucleic Acid Therapeutics Using Polyplexes: A Journey of 50 Years (and Beyond), *Chem. Rev.* 115(19) (2015) 11043-78.
- [2] S.R. Kumar, D.M. Markusic, M. Biswas, K.A. High, R.W. Herzog, Clinical development of gene therapy: results and lessons from recent successes, *Mol. Ther. Methods Clin. Dev.* 3 (2016) 16034.
- [3] J. Rosenecker, S. Huth, C. Rudolph, Gene therapy for cystic fibrosis lung disease: current status and future perspectives, *Curr. Opin. Mol. Ther.* 8(5) (2006) 439-45.
- [4] R.M. Blaese, K.W. Culver, A.D. Miller, C.S. Carter, T. Fleisher, M. Clerici, G. Shearer, L. Chang, Y. Chiang, P. Tolstoshev, J.J. Greenblatt, S.A. Rosenberg, H. Klein, M. Berger, C.A. Mullen, W.J. Ramsey, L. Muul, R.A. Morgan, W.F. Anderson, T lymphocyte-directed gene therapy for ADA- SCID: initial trial results after 4 years, *Science* 270(5235) (1995) 475-80.
- [5] D.W. Scott, J.N. Lozier, Gene therapy for haemophilia: prospects and challenges to prevent or reverse inhibitor formation, *Br. J. Haematol.* 156(3) (2012) 295-302.
- [6] P. Arumugam, P. Malik, Genetic therapy for beta-thalassemia: from the bench to the bedside, *Hematology Am. Soc. Hematol. Educ. Program* 2010 (2010) 445-50.
- [7] N. Cartier, S. Hacein-Bey-Abina, C.C. Bartholomae, G. Veres, M. Schmidt, I. Kutschera, M. Vidaud, U. Abel, L. Dal-Cortivo, L. Caccavelli, N. Mahlaoui, V. Kiermer, D. Mittelstaedt, C. Bellesme, N. Lahlou, F. Lefrere, S. Blanche, M. Audit, E. Payen, P. Leboulch, B. l'Homme, P. Bougneres, C. Von Kalle, A. Fischer, M. Cavazzana-Calvo, P. Aubourg, Hematopoietic stem cell gene therapy with a lentiviral vector in X-linked adrenoleukodystrophy, *Science* 326(5954) (2009) 818-23.
- [8] J.B. Rosenberg, S.M. Kaminsky, P. Aubourg, R.G. Crystal, D. Sondhi, Gene therapy for metachromatic leukodystrophy, *J. Neurosci. Res.* 94(11) (2016) 1169-79.
- [9] A.M. Maguire, F. Simonelli, E.A. Pierce, E.N. Pugh, Jr., F. Mingozzi, J. Bennicelli, S. Banfi, K.A. Marshall, F. Testa, E.M. Surace, S. Rossi, A. Lyubarsky, V.R. Arruda, B. Konkle, E. Stone, J. Sun, J. Jacobs, L. Dell'Osso, R. Hertle, J.X. Ma, T.M. Redmond, X. Zhu, B. Hauck, O. Zelenaia, K.S. Shindler, M.G. Maguire, J.F. Wright, N.J. Volpe, J.W. McDonnell, A. Auricchio, K.A. High, J. Bennett, Safety and efficacy of gene transfer for Leber's congenital amaurosis, *N. Engl. J. Med.* 358(21) (2008) 2240-8.
- [10] H. Ledford, Cell therapy fights leukaemia, *Nature* (2011).
- [11] P.A. LeWitt, A.R. Rezai, M.A. Leehey, S.G. Ojemann, A.W. Flaherty, E.N. Eskandar, S.K. Kostyk, K. Thomas, A. Sarkar, M.S. Siddiqui, S.B. Tatter, J.M. Schwalb, K.L. Poston, J.M. Henderson, R.M. Kurlan, I.H. Richard, L. Van Meter, C.V. Sapan, M.J. Doring, M.G. Kaplitt, A. Feigin, AAV2-GAD gene therapy for advanced Parkinson's disease: a double-blind, sham-surgery controlled, randomised trial, *Lancet Neurol.* 10(4) (2011) 309-19.
- [12] A. Aiuti, M.G. Roncarolo, L. Naldini, Gene therapy for ADA-SCID, the first marketing approval of an ex vivo gene therapy in Europe: paving the road for the next generation of advanced therapy medicinal products, *EMBO Mol. Med.* 9(6) (2017) 737-740.
- [13] A. Fire, S. Xu, M.K. Montgomery, S.A. Kostas, S.E. Driver, C.C. Mello, Potent and specific genetic interference by double-stranded RNA in *Caenorhabditis elegans*, *Nature* 391(6669) (1998) 806-11.
- [14] J.C. Burnett, J.J. Rossi, RNA-based therapeutics: current progress and future prospects, *Chem. Biol.* 19(1) (2012) 60-71.

- [15] M.D. Krebs, E. Alsborg, Localized, targeted, and sustained siRNA delivery, *Chemistry* 17(11) (2011) 3054-62.
- [16] M.A. Mintzer, E.E. Simanek, Nonviral vectors for gene delivery, *Chem. Rev.* 109(2) (2009) 259-302.
- [17] H. Herweijer, J.A. Wolff, Gene therapy progress and prospects: hydrodynamic gene delivery, *Gene Ther.* 14(2) (2007) 99-107.
- [18] D.L. Lewis, J.A. Wolff, Systemic siRNA delivery via hydrodynamic intravascular injection, *Adv. Drug Deliv. Rev.* 59(2-3) (2007) 115-23.
- [19] B. Martin, M. Sainlos, A. Aissaoui, N. Oudrhiri, M. Hauchecorne, J.P. Vigneron, J.M. Lehn, P. Lehn, The design of cationic lipids for gene delivery, *Curr. Pharm. Des.* 11(3) (2005) 375-94.
- [20] S. Chesnoy, L. Huang, Structure and function of lipid-DNA complexes for gene delivery, *Annu. Rev. Biophys. Biomol. Struct.* 29 (2000) 27-47.
- [21] A. Hirko, F. Tang, J.A. Hughes, Cationic lipid vectors for plasmid DNA delivery, *Curr. Med. Chem.* 10(14) (2003) 1185-93.
- [22] L. Dekie, V. Toncheva, P. Dubruel, E.H. Schacht, L. Barrett, L.W. Seymour, Poly-L-glutamic acid derivatives as vectors for gene therapy, *J. Control. Release* 65(1-2) (2000) 187-202.
- [23] G.Y. Wu, C.H. Wu, Receptor-mediated in vitro gene transformation by a soluble DNA carrier system, *J. Biol. Chem.* 262(10) (1987) 4429-32.
- [24] L. Gao, E. Wagner, M. Cotten, S. Agarwal, C. Harris, M. Romer, L. Miller, P.C. Hu, D. Curiel, Direct in vivo gene transfer to airway epithelium employing adenovirus-polylysine-DNA complexes, *Hum. Gene Ther.* 4(1) (1993) 17-24.
- [25] S. Schreiber, E. Kampgen, E. Wagner, D. Pirkhammer, J. Trcka, H. Korschan, A. Lindemann, R. Dorffner, H. Kittler, F. Kasteliz, Z. Kupcu, A. Sinski, K. Zatloukal, M. Buschle, W. Schmidt, M. Birnstiel, R.E. Kempe, T. Voigt, H.A. Weber, H. Pehamberger, R. Mertelsmann, E.B. Brocker, K. Wolff, G. Stingl, Immunotherapy of metastatic malignant melanoma by a vaccine consisting of autologous interleukin 2-transfected cancer cells: outcome of a phase I study, *Hum. Gene Ther.* 10(6) (1999) 983-93.
- [26] O. Boussif, F. Lezoualc'h, M.A. Zanta, M.D. Mergny, D. Scherman, B. Demeneix, J.P. Behr, A versatile vector for gene and oligonucleotide transfer into cells in culture and in vivo: polyethylenimine, *Proc. Natl. Acad. Sci. U.S.A.* 92(16) (1995) 7297-301.
- [27] K. Kunath, A. von Harpe, D. Fischer, H. Petersen, U. Bickel, K. Voigt, T. Kissel, Low-molecular-weight polyethylenimine as a non-viral vector for DNA delivery: comparison of physicochemical properties, transfection efficiency and in vivo distribution with high-molecular-weight polyethylenimine, *J. Control. Release* 89(1) (2003) 113-125.
- [28] A. von Harpe, H. Petersen, Y. Li, T. Kissel, Characterization of commercially available and synthesized polyethylenimines for gene delivery, *J. Control. Release* 69(2) (2000) 309-22.
- [29] M. Ogris, S. Brunner, S. Schuller, R. Kircheis, E. Wagner, PEGylated DNA/transferrin-PEI complexes: reduced interaction with blood components, extended circulation in blood and potential for systemic gene delivery, *Gene Ther.* 6(4) (1999) 595-605.
- [30] D. Goula, N. Becker, G.F. Lemkine, P. Normandie, J. Rodrigues, S. Mantero, G. Levi, B.A. Demeneix, Rapid crossing of the pulmonary endothelial barrier by polyethylenimine/DNA complexes 965, *Gene Ther.* 7(6) (2000) 499-504.
- [31] D. Goula, C. Benoist, S. Mantero, G. Merlo, G. Levi, B.A. Demeneix, Polyethylenimine-based intravenous delivery of transgenes to mouse lung, *Gene Ther.* 5(9) (1998) 1291-5.

- [32] J.M. Williford, M.M. Archang, I. Minn, Y. Ren, M. Wo, J. Vandermark, P.B. Fisher, M.G. Pomper, H.Q. Mao, Critical Length of PEG Grafts on IPEI/DNA Nanoparticles for Efficient in Vivo Delivery, *ACS Biomater. Sci. Eng.* 2(4) (2016) 567-578.
- [33] L. Wightman, R. Kircheis, V. Rossler, S. Carotta, R. Ruzicka, M. Kursa, E. Wagner, Different behavior of branched and linear polyethylenimine for gene delivery in vitro and in vivo, *J. Gene Med.* 3(4) (2001) 362-72.
- [34] D.A. Tomalia, H. Baker, J. Dewald, M. Hall, G. Kallos, S. Martin, J. Roeck, J. Ryder, P. Smith, Dendritic macromolecules: synthesis of starburst dendrimers, *Macromolecules* 19(9) (1986) 2466-2468.
- [35] G. Navarro, G. Maiwald, R. Haase, A.L. Rogach, E. Wagner, C.T. de Ilarduya, M. Ogris, Low generation PAMAM dendrimer and CpG free plasmids allow targeted and extended transgene expression in tumors after systemic delivery, *J. Control. Release* 146(1) (2010) 99-105.
- [36] R. Esfand, D.A. Tomalia, Poly(amidoamine) (PAMAM) dendrimers: from biomimicry to drug delivery and biomedical applications, *Drug Discov. Today* 6(8) (2001) 427-436.
- [37] P.L. Felgner, Y. Barenholz, J.P. Behr, S.H. Cheng, P. Cullis, L. Huang, J.A. Jessee, L. Seymour, F. Szoka, A.R. Thierry, E. Wagner, G. Wu, Nomenclature for synthetic gene delivery systems, *Hum. Gene Ther.* 8(5) (1997) 511-2.
- [38] V.A. Bloomfield, DNA condensation by multivalent cations, *Biopolymers* 44(3) (1997) 269-82.
- [39] H.S. Choi, W. Liu, F. Liu, K. Nasr, P. Misra, M.G. Bawendi, J.V. Frangioni, Design considerations for tumour-targeted nanoparticles, *Nat. Nanotechnol.* 5(1) (2010) 42-7.
- [40] F. Yuan, M. Dellian, D. Fukumura, M. Leunig, D.A. Berk, V.P. Torchilin, R.K. Jain, Vascular permeability in a human tumor xenograft: molecular size dependence and cutoff size, *Cancer Res.* 55(17) (1995) 3752-6.
- [41] H. Maeda, G.Y. Bharate, J. Daruwalla, Polymeric drugs for efficient tumor-targeted drug delivery based on EPR-effect, *Eur. J. Pharm. Biopharm.* 71(3) (2009) 409-19.
- [42] J. Wu, T. Akaike, K. Hayashida, T. Okamoto, A. Okuyama, H. Maeda, Enhanced vascular permeability in solid tumor involving peroxynitrite and matrix metalloproteinases, *J. Cancer Res.* 92(4) (2001) 439-51.
- [43] M.E. Davis, Z.G. Chen, D.M. Shin, Nanoparticle therapeutics: an emerging treatment modality for cancer, *Nat. Rev. Drug Discov.* 7(9) (2008) 771-82.
- [44] B. Smrekar, L. Wightman, M.F. Wolschek, C. Lichtenberger, R. Ruzicka, M. Ogris, W. Rödl, M. Kursa, E. Wagner, R. Kircheis, Tissue-dependent factors affect gene delivery to tumors in vivo, *Gene Ther.* 10(13) (2003) 1079-88.
- [45] H. Cabral, Y. Matsumoto, K. Mizuno, Q. Chen, M. Murakami, M. Kimura, Y. Terada, M.R. Kano, K. Miyazono, M. Uesaka, N. Nishiyama, K. Kataoka, Accumulation of sub-100 nm polymeric micelles in poorly permeable tumours depends on size, *Nat. Nanotechnol.* 6(12) (2011) 815-23.
- [46] P.M. Klein, E. Wagner, Bioreducible polycations as shuttles for therapeutic nucleic acid and protein transfection, *Antioxid. Redox Signal.* 21(5) (2014) 804-17.
- [47] M. Neu, O. Germershaus, S. Mao, K.H. Voigt, M. Behe, T. Kissel, Crosslinked nanocarriers based upon poly(ethylene imine) for systemic plasmid delivery: in vitro characterization and in vivo studies in mice, *J. Control Release* 118(3) (2007) 370-380.
- [48] V. Russ, T. Fröhlich, Y. Li, A. Halama, M. Ogris, E. Wagner, Improved in vivo gene transfer into tumor tissue by stabilization of pseudodendritic oligoethylenimine-based polyplexes, *J. Gene Med.* 12(2) (2010) 180-93.
- [49] D. Schaffert, C. Troiber, E.E. Salcher, T. Fröhlich, I. Martin, N. Badgujar, C. Dohmen, D. Edinger, R. Kläger, G. Maiwald, K. Farkasova, S. Seeber, K. Jahn-Hofmann, P. Hadwiger, E. Wagner, Solid-phase synthesis of sequence-defined T-, i-,

- and U-shape polymers for pDNA and siRNA delivery, *Angew. Chem. Int. Ed.* 50(38) (2011) 8986-9.
- [50] U. Lächelt, P. Kos, F.M. Mickler, A. Herrmann, E.E. Salcher, W. Rödl, N. Badgujar, C. Bräuchle, E. Wagner, Fine-tuning of proton sponges by precise diaminoethanes and histidines in pDNA polyplexes, *Nanomedicine* 10(1) (2014) 35-44.
- [51] T. Fröhlich, D. Edinger, R. Kläger, C. Troiber, E. Salcher, N. Badgujar, I. Martin, D. Schaffert, A. Cengizeroglu, P. Hadwiger, H.P. Vornlocher, E. Wagner, Structure-activity relationships of siRNA carriers based on sequence-defined oligo (ethane amino) amides, *J. Control. Release* 160(3) (2012) 532-41.
- [52] C. Troiber, D. Edinger, P. Kos, L. Schreiner, R. Kläger, A. Herrmann, E. Wagner, Stabilizing effect of tyrosine trimers on pDNA and siRNA polyplexes, *Biomaterials* 34(5) (2013) 1624-33.
- [53] A. Philipp, X. Zhao, P. Tarcha, E. Wagner, A. Zintchenko, Hydrophobically modified oligoethylenimines as highly efficient transfection agents for siRNA delivery, *Bioconjugate Chem.* 20(11) (2009) 2055-61.
- [54] M. Ogris, P. Steinlein, S. Carotta, S. Brunner, E. Wagner, DNA/polyethylenimine transfection particles: influence of ligands, polymer size, and PEGylation on internalization and gene expression, *AAPS PharmSci.* 3(3) (2001) E21.
- [55] K. de Bruin, N. Ruthardt, K. von Gersdorff, R. Bausinger, E. Wagner, M. Ogris, C. Bräuchle, Cellular dynamics of EGF receptor-targeted synthetic viruses, *Mol. Ther.* 15(7) (2007) 1297-305.
- [56] C. Munoz-Pinedo, N. El Mjiyad, J.E. Ricci, Cancer metabolism: current perspectives and future directions, *Cell Death Dis.* 3 (2012) e248.
- [57] E. Wagner, M. Zenke, M. Cotten, H. Beug, M.L. Birnstiel, Transferrin-polycation conjugates as carriers for DNA uptake into cells, *Proc. Natl. Acad. Sci. U.S.A.* 87(9) (1990) 3410-3414.
- [58] C.P. Leamon, P.S. Low, Folate-mediated targeting: from diagnostics to drug and gene delivery, *Drug Discov. Today* 6(1) (2001) 44-51.
- [59] M. Kurasa, G.F. Walker, V. Roessler, M. Ogris, W. Roedl, R. Kircheis, E. Wagner, Novel shielded transferrin-polyethylene glycol-polyethylenimine/DNA complexes for systemic tumor-targeted gene transfer, *Bioconjugate Chem.* 14(1) (2003) 222-31.
- [60] P.S. Low, W.A. Henne, D.D. Doorneweerd, Discovery and development of folic-acid-based receptor targeting for imaging and therapy of cancer and inflammatory diseases, *Acc. Chem. Res.* 41(1) (2008) 120-9.
- [61] G. Abourbeh, A. Shir, E. Mishani, M. Ogris, W. Rödl, E. Wagner, A. Levitzki, PolyIC GE11 polyplex inhibits EGFR-overexpressing tumors, *IUBMB Life* 64(4) (2012) 324-30.
- [62] A. Schäfer, A. Pahnke, D. Schaffert, W.M. van Weerden, C.M. de Ridder, W. Rödl, A. Vetter, C. Spitzweg, R. Kraaij, E. Wagner, M. Ogris, Disconnecting the yin and yang relation of epidermal growth factor receptor (EGFR)-mediated delivery: a fully synthetic, EGFR-targeted gene transfer system avoiding receptor activation, *Hum. Gene Ther.* 22(12) (2011) 1463-73.
- [63] K. Klutz, D. Schaffert, M.J. Willhauck, G.K. Grünwald, R. Haase, N. Wunderlich, C. Zach, F.J. Gildehaus, R. Senekowitsch-Schmidtke, B. Göke, E. Wagner, M. Ogris, C. Spitzweg, Epidermal Growth Factor Receptor-targeted ¹³¹I-therapy of Liver Cancer Following Systemic Delivery of the Sodium Iodide Symporter Gene, *Mol. Ther.* 19(4) (2011) 676-685.
- [64] P. Kos, U. Lächelt, A. Herrmann, F.M. Mickler, M. Döblinger, D. He, A. Krhac Levacic, S. Morys, C. Bräuchle, E. Wagner, Histidine-rich stabilized polyplexes for cMet-directed tumor-targeted gene transfer, *Nanoscale* 7(12) (2015) 5350-62.

- [65] S. Urnauer, S. Morys, A. Krhac Levacic, A.M. Müller, C. Schug, K.A. Schmohl, N. Schwenk, C. Zach, J. Carlsen, P. Bartenstein, E. Wagner, C. Spitzweg, Sequence-defined cMET/HGFR-targeted Polymers as Gene Delivery Vehicles for the Theranostic Sodium Iodide Symporter (NIS) Gene, *Mol. Ther.* 24(8) (2016) 1395-404.
- [66] K. Kunath, T. Merdan, O. Hegener, H. Haberlein, T. Kissel, Integrin targeting using RGD-PEI conjugates for in vitro gene transfer, *J. Gene Med.* 5(7) (2003) 588-599.
- [67] F.M. Mickler, Y. Vachutinsky, M. Oba, K. Miyata, N. Nishiyama, K. Kataoka, C. Bräuchle, N. Ruthardt, Effect of integrin targeting and PEG shielding on polyplex micelle internalization studied by live-cell imaging, *J. Control. Release* 156(3) (2011) 364-73.
- [68] F.M. Mickler, L. Möckl, N. Ruthardt, M. Ogris, E. Wagner, C. Bräuchle, Tuning nanoparticle uptake: live-cell imaging reveals two distinct endocytosis mechanisms mediated by natural and artificial EGFR targeting ligand, *Nano Lett.* 12(7) (2012) 3417-23.
- [69] F.R. Maxfield, T.E. McGraw, Endocytic recycling, *Nat. Rev. Mol. Cell Biol.* 5(2) (2004) 121-32.
- [70] I. Mellman, R. Fuchs, A. Helenius, Acidification of the endocytic and exocytic pathways, *Annu. Rev. Biochem.* 55 (1986) 663-700.
- [71] J.P. Behr, The proton sponge: A trick to enter cells the viruses did not exploit, *Chimia* 51(1-2) (1997) 34-36.
- [72] S.M. Moghimi, P. Symonds, J.C. Murray, A.C. Hunter, G. Debska, A. Szewczyk, A two-stage poly(ethylenimine)-mediated cytotoxicity: implications for gene transfer/therapy, *Mol. Ther.* 11(6) (2005) 990-5.
- [73] H. Uchida, K. Miyata, M. Oba, T. Ishii, T. Suma, K. Itaka, N. Nishiyama, K. Kataoka, Odd-even effect of repeating aminoethylene units in the side chain of N-substituted polyaspartamides on gene transfection profiles, *J. Am. Chem. Soc.* 133(39) (2011) 15524-32.
- [74] P. Midoux, M. Monsigny, Efficient gene transfer by histidylated polylysine/pDNA complexes, *Bioconjugate Chem.* 10(3) (1999) 406-11.
- [75] Q. Leng, P. Scaria, J. Zhu, N. Ambulos, P. Campbell, A.J. Mixson, Highly branched HK peptides are effective carriers of siRNA, *J. Gene Med.* 7(7) (2005) 977-86.
- [76] M. Zorko, U. Langel, Cell-penetrating peptides: mechanism and kinetics of cargo delivery, *Adv. Drug. Deliv. Rev.* 57(4) (2005) 529-45.
- [77] S. Fawell, J. Seery, Y. Daikh, C. Moore, L.L. Chen, B. Pepinsky, J. Barsoum, Tat-mediated delivery of heterologous proteins into cells, *Proc. Natl. Acad. Sci. U.S.A.* 91(2) (1994) 664-8.
- [78] T.B. Wyman, F. Nicol, O. Zelphati, P.V. Scaria, C. Plank, F.C. Szoka, Jr., Design, synthesis, and characterization of a cationic peptide that binds to nucleic acids and permeabilizes bilayers, *Biochemistry* 36(10) (1997) 3008-3017.
- [79] S.M. Shaheen, H. Akita, T. Nakamura, S. Takayama, S. Futaki, A. Yamashita, R. Katoono, N. Yui, H. Harashima, KALA-modified multi-layered nanoparticles as gene carriers for MHC class-I mediated antigen presentation for a DNA vaccine, *Biomaterials* 32(26) (2011) 6342-50.
- [80] W. Li, F. Nicol, F.C. Szoka, Jr., GALA: a designed synthetic pH-responsive amphipathic peptide with applications in drug and gene delivery, *Adv. Drug. Deliv. Rev.* 56(7) (2004) 967-85.
- [81] C. Plank, B. Oberhauser, K. Mechtler, C. Koch, E. Wagner, The influence of endosome-disruptive peptides on gene transfer using synthetic virus-like gene transfer systems, *J. Biol. Chem.* 269(17) (1994) 12918-12924.
- [82] E. Wagner, C. Plank, K. Zatloukal, M. Cotten, M.L. Birnstiel, Influenza virus hemagglutinin HA-2 N-terminal fusogenic peptides augment gene transfer by

- transferrin-polylysine-DNA complexes: toward a synthetic virus-like gene-transfer vehicle, *Proc. Natl. Acad. Sci. U.S.A.* 89(17) (1992) 7934-8.
- [83] S. Boeckle, J. Fahrmeir, W. Rödl, M. Ogris, E. Wagner, Melittin analogs with high lytic activity at endosomal pH enhance transfection with purified targeted PEI polyplexes, *J. Control. Release* 112(2) (2006) 240-248.
- [84] K. Ezzat, S.E. Andaloussi, E.M. Zaghoul, T. Lehto, S. Lindberg, P.M. Moreno, J.R. Viola, T. Magdy, R. Abdo, P. Guterstam, R. Sillard, S.M. Hammond, M.J. Wood, A.A. Arzumanov, M.J. Gait, C.I. Smith, M. Hallbrink, U. Langel, PepFect 14, a novel cell-penetrating peptide for oligonucleotide delivery in solution and as solid formulation, *Nucleic Acids Res.* 39(12) (2011) 5284-98.
- [85] S.E. Andaloussi, T. Lehto, I. Mager, K. Rosenthal-Aizman, Oprea, II, O.E. Simonson, H. Sork, K. Ezzat, D.M. Copolovici, K. Kurrikoff, J.R. Viola, E.M. Zaghoul, R. Sillard, H.J. Johansson, F. Said Hassane, P. Guterstam, J. Suhorutsenko, P.M. Moreno, N. Oskolkov, J. Halldin, U. Tedebark, A. Metspalu, B. Lebleu, J. Lehtio, C.I. Smith, U. Langel, Design of a peptide-based vector, PepFect6, for efficient delivery of siRNA in cell culture and systemically in vivo, *Nucleic Acids Res.* 39(9) (2011) 3972-87.
- [86] D.A. Dean, D.D. Strong, W.E. Zimmer, Nuclear entry of nonviral vectors, *Gene Ther.* 12(11) (2005) 881-90.
- [87] S. Brunner, T. Sauer, S. Carotta, M. Cotten, M. Saltik, E. Wagner, Cell cycle dependence of gene transfer by lipoplex, polyplex and recombinant adenovirus, *Gene Ther.* 7(5) (2000) 401-7.
- [88] H. Akita, D. Kurihara, M. Schmeer, M. Schleef, H. Harashima, Effect of the Compaction and the Size of DNA on the Nuclear Transfer Efficiency after Microinjection in Synchronized Cells, *Pharmaceutics* 7(2) (2015) 64-73.
- [89] J.-F. Lutz, Sequence-controlled polymerizations: the next Holy Grail in polymer science?, *Polym. Chem.* 1(1) (2010) 55-62.
- [90] J.F. Lutz, M. Ouchi, D.R. Liu, M. Sawamoto, Sequence-controlled polymers, *Science* 341(6146) (2013) 1238149.
- [91] M.H. Stenzel, RAFT polymerization: an avenue to functional polymeric micelles for drug delivery, *Chem. Commun.* (30) (2008) 3486-503.
- [92] V. Vazquez-Dorbatt, J. Lee, E.W. Lin, H.D. Maynard, Synthesis of glycopolymers by controlled radical polymerization techniques and their applications, *ChemBioChem* 13(17) (2012) 2478-87.
- [93] H. Mori, T. Endo, Amino-acid-based block copolymers by RAFT polymerization, *Macromol. Rapid Commun.* 33(13) (2012) 1090-107.
- [94] C. Boyer, V. Bulmus, T.P. Davis, V. Ladmiral, J. Liu, S. Perrier, Bioapplications of RAFT polymerization, *Chem. Rev.* 109(11) (2009) 5402-36.
- [95] M.S. Wadhwa, W.T. Collard, R.C. Adami, D.L. McKenzie, K.G. Rice, Peptide-mediated gene delivery: influence of peptide structure on gene expression, *Bioconjugate Chem.* 8(1) (1997) 81-8.
- [96] R.C. Adami, W.T. Collard, S.A. Gupta, K.Y. Kwok, J. Bonadio, K.G. Rice, Stability of peptide-condensed plasmid DNA formulations, *J. Pharm. Sci.* 87(6) (1998) 678-83.
- [97] S.M. van Rossenberg, A.C. van Keulen, J.W. Drijfhout, S. Vasto, H.K. Koerten, F. Spies, J.M. van 't Noordende, T.J. van Berkel, E.A. Biessen, Stable polyplexes based on arginine-containing oligopeptides for in vivo gene delivery, *Gene Ther.* 11(5) (2004) 457-64.
- [98] D.L. McKenzie, E. Smiley, K.Y. Kwok, K.G. Rice, Low molecular weight disulfide cross-linking peptides as nonviral gene delivery carriers, *Bioconjugate Chem.* 11(6) (2000) 901-909.

- [99] A.L. Parker, K.D. Fisher, D. Oupicky, M.L. Read, S.A. Nicklin, A.H. Baker, L.W. Seymour, Enhanced gene transfer activity of peptide-targeted gene-delivery vectors, *J. Drug Target.* 13(1) (2005) 39-51.
- [100] M.L. Read, K.H. Bremner, D. Oupicky, N.K. Green, P.F. Searle, L.W. Seymour, Vectors based on reducible polycations facilitate intracellular release of nucleic acids, *J. Gene Med.* 5(3) (2003) 232-45.
- [101] M.L. Read, S. Singh, Z. Ahmed, M. Stevenson, S.S. Briggs, D. Oupicky, L.B. Barrett, R. Spice, M. Kendall, M. Berry, J.A. Preece, A. Logan, L.W. Seymour, A versatile reducible polycation-based system for efficient delivery of a broad range of nucleic acids, *Nucleic Acids Res.* 33(9) (2005) e86.
- [102] T. Lehto, R. Abes, N. Oskolkov, J. Suhorutsenko, D.M. Copolovici, I. Mager, J.R. Viola, O.E. Simonson, K. Ezzat, P. Guterstam, E. Eriste, C.I. Smith, B. Lebleu, A. Samir El, U. Langel, Delivery of nucleic acids with a stearylated (RxR)₄ peptide using a non-covalent co-incubation strategy, *J. Control. Release* 141(1) (2010) 42-51.
- [103] A. Kwok, D. McCarthy, S.L. Hart, A.D. Tagalakis, Systematic Comparisons of Formulations of Linear Oligolysine Peptides with siRNA and Plasmid DNA, *Chem. Biol. Drug Des.* 87(5) (2016) 747-63.
- [104] C. Plank, M.X. Tang, A.R. Wolfe, F.C. Szoka, Jr., Branched cationic peptides for gene delivery: role of type and number of cationic residues in formation and in vitro activity of DNA polyplexes, *Hum. Gene Ther.* 10(2) (1999) 319-32.
- [105] Q.R. Chen, L. Zhang, S.A. Stass, A.J. Mixson, Branched co-polymers of histidine and lysine are efficient carriers of plasmids, *Nucleic Acids Res.* 29(6) (2001) 1334-40.
- [106] Q. Leng, A.J. Mixson, Small interfering RNA targeting Raf-1 inhibits tumor growth in vitro and in vivo, *Cancer Gene Ther.* 12(8) (2005) 682-90.
- [107] Q. Leng, A.J. Mixson, Modified branched peptides with a histidine-rich tail enhance in vitro gene transfection, *Nucleic Acids Res.* 33(4) (2005) e40.
- [108] S.T. Chou, K. Hom, D. Zhang, Q. Leng, L.J. Tricoli, J.M. Hustedt, A. Lee, M.J. Shapiro, J. Seog, J.D. Kahn, A.J. Mixson, Enhanced silencing and stabilization of siRNA polyplexes by histidine-mediated hydrogen bonds, *Biomaterials* 35(2) (2014) 846-55.
- [109] Q. Leng, A.J. Mixson, The neuropilin-1 receptor mediates enhanced tumor delivery of H2K polyplexes, *J. Gene Med.* 18(7) (2016) 134-44.
- [110] E. Dauty, J.-S. Remy, T. Blessing, J.-P. Behr, Dimerizable Cationic Detergents with a Low cmc Condense Plasmid DNA into Nanometric Particles and Transfect Cells in Culture, *J. Am. Chem. Soc.* 123(38) (2001) 9227-9234.
- [111] P.M. Klein, S. Reinhard, D.J. Lee, K. Müller, D. Ponader, L. Hartmann, E. Wagner, Precise redox-sensitive cleavage sites for improved bioactivity of siRNA lipopolyplexes, *Nanoscale* 8(42) (2016) 18098-18104.
- [112] X.L. Wang, R. Xu, Z.R. Lu, A peptide-targeted delivery system with pH-sensitive amphiphilic cell membrane disruption for efficient receptor-mediated siRNA delivery, *J. Control. Release* 134(3) (2009) 207-13.
- [113] X.L. Wang, S. Ramusovic, T. Nguyen, Z.R. Lu, Novel polymerizable surfactants with pH-sensitive amphiphilicity and cell membrane disruption for efficient siRNA delivery, *Bioconjugate Chem.* 18(6) (2007) 2169-77.
- [114] X.L. Wang, R. Jensen, Z.R. Lu, A novel environment-sensitive biodegradable polydisulfide with protonatable pendants for nucleic acid delivery, *J. Control. Release* 120(3) (2007) 250-8.
- [115] L. Hartmann, E. Krause, M. Antonietti, H.G. Börner, Solid-phase supported polymer synthesis of sequence-defined, multifunctional poly(amidoamines), *Biomacromolecules* 7(4) (2006) 1239-44.

- [116] L. Hartmann, S. Häfele, R. Peschka-Süss, M. Antonietti, H.G. Börner, Sequence Positioning of Disulfide Linkages to Program the Degradation of Monodisperse Poly(amidoamines), *Macromolecules* 40(22) (2007) 7771-7776.
- [117] L. Hartmann, S. Häfele, R. Peschka-Süss, M. Antonietti, H.G. Börner, Tailor-made poly(amidoamine)s for controlled complexation and condensation of DNA, *Chemistry* 14(7) (2008) 2025-33.
- [118] L. Hartmann, H.G. Börner, Precision polymers: monodisperse, monomer-sequence-defined segments to target future demands of polymers in medicine, *Adv. Mater.* 21(32-33) (2009) 3425-31.
- [119] S. Mosca, F. Wojcik, L. Hartmann, Precise positioning of chiral building blocks in monodisperse, sequence-defined polyamides, *Macromol. Rapid Commun.* 32(2) (2011) 197-202.
- [120] F. Wojcik, S. Mosca, L. Hartmann, Solid-phase synthesis of asymmetrically branched sequence-defined poly/oligo(amidoamines), *J. Org. Chem.* 77(9) (2012) 4226-34.
- [121] D. Ponader, F. Wojcik, F. Beceren-Braun, J. Dervede, L. Hartmann, Sequence-defined glycopolymer segments presenting mannose: synthesis and lectin binding affinity, *Biomacromolecules* 13(6) (2012) 1845-52.
- [122] D.J. Lee, E. Kessel, D. Edinger, D. He, P.M. Klein, L. Voith von Voithenberg, D.C. Lamb, U. Lächelt, T. Lehto, E. Wagner, Dual antitumoral potency of EG5 siRNA nanoplexes armed with cytotoxic bifunctional glutamyl-methotrexate targeting ligand, *Biomaterials* 77 (2016) 98-110.
- [123] R.B. Merrifield, Solid Phase Peptide Synthesis. I. The Synthesis of a Tetrapeptide, *J. Am. Chem. Soc.* 85(14) (1963) 2149-2154.
- [124] L.A. Carpino, G.Y. Han, 9-Fluorenylmethoxycarbonyl function, a new base-sensitive amino-protecting group, *J. Am. Chem. Soc.* 92(19) (1970) 5748-5749.
- [125] E. Atherton, H. Fox, D. Harkiss, C.J. Logan, R.C. Sheppard, B.J. Williams, A mild procedure for solid phase peptide synthesis: use of fluorenylmethoxycarbonylaminoacids, *Chem. Commun.* (13) (1978) 537.
- [126] C.D. Chang, J. Meienhofer, Solid-phase peptide synthesis using mild base cleavage of N alpha-fluorenylmethoxycarbonylamino acids, exemplified by a synthesis of dihydrosomatostatin, *Int. J. Pept. Protein Res.* 11(3) (1978) 246-9.
- [127] W.C. Chan, P.D. White, *Fmoc solid phase peptide synthesis : a practical approach*, Oxford University Press, New York, 2000.
- [128] D. Orain, J. Ellard, M. Bradley, Protecting groups in solid-phase organic synthesis, *J. Comb. Chem.* 4(1) (2002) 1-16.
- [129] I.A. Nash, B.W. Bycroft, W.C. Chan, Dde — A selective primary amine protecting group: A facile solid phase synthetic approach to polyamine conjugates, *Tetrahedron Letters* 37(15) (1996) 2625-2628.
- [130] E. Kaiser, R.L. Colescott, C.D. Bossinger, P.I. Cook, Color test for detection of free terminal amino groups in the solid-phase synthesis of peptides, *Anal. Biochem.* 34(2) (1970) 595-8.
- [131] D. Schaffert, N. Badgujar, E. Wagner, Novel Fmoc-polyamino acids for solid-phase synthesis of defined polyamidoamines, *Org. Lett.* 13(7) (2011) 1586-9.
- [132] E.E. Salcher, P. Kos, T. Fröhlich, N. Badgujar, M. Scheible, E. Wagner, Sequence-defined four-arm oligo(ethanamino)amides for pDNA and siRNA delivery: Impact of building blocks on efficacy, *J. Control. Release* 164(3) (2012) 380-6.
- [133] S. Morys, A. Krhac Levacic, S. Urnauer, S. Kempter, S. Kern, J.O. Rädler, C. Spitzweg, U. Lächelt, E. Wagner, Influence of Defined Hydrophilic Blocks within Oligoaminoamide Copolymers: Compaction versus Shielding of pDNA Nanoparticles, *Polymers* 9(4) (2017).

- [134] D. Schaffert, C. Troiber, E. Wagner, New sequence-defined polyaminoamides with tailored endosomolytic properties for plasmid DNA delivery, *Bioconjugate Chem.* 23(6) (2012) 1157-65.
- [135] C. Dohmen, D. Edinger, T. Fröhlich, L. Schreiner, U. Lächelt, C. Troiber, J. Rädler, P. Hadwiger, H.P. Vornlocher, E. Wagner, Nanosized multifunctional polyplexes for receptor-mediated siRNA delivery, *ACS Nano* 6(6) (2012) 5198-208.
- [136] P.M. Klein, K. Müller, C. Gutmann, P. Kos, A. Krhac Levacic, D. Edinger, M. Höhn, J.C. Leroux, M.A. Gauthier, E. Wagner, Twin disulfides as opportunity for improving stability and transfection efficiency of oligoaminoethane polyplexes, *J. Control. Release* 205 (2015) 109-19.
- [137] D. He, K. Müller, A. Krhac Levacic, P. Kos, U. Lächelt, E. Wagner, Combinatorial Optimization of Sequence-Defined Oligo(ethan amino)amides for Folate Receptor-Targeted pDNA and siRNA Delivery, *Bioconjugate Chem.* 27(3) (2016) 647-59.
- [138] P. Kos, U. Lächelt, D. He, Y. Nie, Z. Gu, E. Wagner, Dual-targeted polyplexes based on sequence-defined peptide-PEG-oligoamino amides, *Journal of pharmaceutical sciences* 104(2) (2015) 464-75.
- [139] I. Martin, C. Dohmen, C. Mas-Moruno, C. Troiber, P. Kos, D. Schaffert, U. Lächelt, M. Teixido, M. Günther, H. Kessler, E. Giralt, E. Wagner, Solid-phase-assisted synthesis of targeting peptide-PEG-oligo(ethane amino)amides for receptor-mediated gene delivery, *Org. Biomol. Chem.* 10(16) (2012) 3258-68.
- [140] S. Wang, S. Reinhard, C. Li, M. Qian, H. Jiang, Y. Du, U. Lächelt, W. Lu, E. Wagner, R. Huang, Antitumoral Cascade-Targeting Ligand for IL-6 Receptor-Mediated Gene Delivery to Glioma, *Mol. Ther.* 25(7) (2017) 1556-1566.
- [141] A. Krhac Levacic, S. Morys, S. Kempfer, U. Lächelt, E. Wagner, Minicircle versus plasmid DNA delivery by receptor-targeted polyplexes, *Hum. Gene Ther.* 28(10) (2017) 862-874.
- [142] L. Beckert, L. Kostka, E. Kessel, A. Krhac Levacic, H. Kostkova, T. Etrych, U. Lächelt, E. Wagner, Acid-labile pHPMA modification of four-arm oligoaminoamide pDNA polyplexes balances shielding and gene transfer activity in vitro and in vivo, *Eur. J. Pharm. Biopharm.* 105 (2016) 85-96.
- [143] A. Hall, U. Lächelt, J. Bartek, E. Wagner, S.M. Moghimi, Polyplex Evolution: Understanding Biology, Optimizing Performance, *Mol. Ther.* 25(7) (2017) 1476-1490.
- [144] C. Scholz, P. Kos, E. Wagner, Comb-like oligoaminoethane carriers: change in topology improves pDNA delivery, *Bioconjugate Chem.* 25(2) (2014) 251-61.
- [145] K.A. Mislick, J.D. Baldeschwieler, Evidence for the role of proteoglycans in cation-mediated gene transfer, *Proc. Natl. Acad. Sci. U.S.A.* 93(22) (1996) 12349-54.
- [146] I. Kopatz, J.S. Remy, J.P. Behr, A model for non-viral gene delivery: through syndecan adhesion molecules and powered by actin, *J. Gene Med.* 6(7) (2004) 769-776.
- [147] E. Wagner, Polymers for siRNA delivery: inspired by viruses to be targeted, dynamic, and precise, *Acc. Chem. Res.* 45(7) (2012) 1005-13.
- [148] A. Yousefi, G. Storm, R. Schiffelers, E. Mastrobattista, Trends in polymeric delivery of nucleic acids to tumors, *J. Control. Release* 170(2) (2013) 209-18.
- [149] C. Plank, K. Mechtler, F.C. Szoka, Jr., E. Wagner, Activation of the complement system by synthetic DNA complexes: a potential barrier for intravenous gene delivery, *Hum. Gene Ther.* 7(12) (1996) 1437-46.
- [150] O.M. Merkel, R. Urbanics, P. Bedocs, Z. Rozsnyay, L. Rosivall, M. Toth, T. Kissel, J. Szebeni, In vitro and in vivo complement activation and related anaphylactic effects associated with polyethylenimine and polyethylenimine-graft-poly(ethylene glycol) block copolymers, *Biomaterials* 32(21) (2011) 4936-42.

- [151] R.S. Burke, S.H. Pun, Extracellular barriers to in Vivo PEI and PEGylated PEI polyplex-mediated gene delivery to the liver, *Bioconjugate Chem.* 19(3) (2008) 693-704.
- [152] J.M. Rabanel, P. Hildgen, X. Banquy, Assessment of PEG on polymeric particles surface, a key step in drug carrier translation, *J. Control. Release* 185 (2014) 71-87.
- [153] K. Knop, R. Hoogenboom, D. Fischer, U.S. Schubert, Poly(ethylene glycol) in drug delivery: pros and cons as well as potential alternatives, *Angew. Chem. Int. Ed.* 49(36) (2010) 6288-308.
- [154] D.W. Pack, A.S. Hoffman, S. Pun, P.S. Stayton, Design and development of polymers for gene delivery, *Nat. Rev. Drug Discovery* 4(7) (2005) 581-93.
- [155] J. DeRouchey, G.F. Walker, E. Wagner, J.O. Rädler, Decorated rods: a "bottom-up" self-assembly of monomolecular DNA complexes, *J. Phys. Chem. B.* 110(10) (2006) 4548-54.
- [156] C. Fella, G.F. Walker, M. Ogris, E. Wagner, Amine-reactive pyridylhydrazone-based PEG reagents for pH-reversible PEI polyplex shielding, *Eur. J. Pharm. Sci.* 34(4-5) (2008) 309-20.
- [157] O.M. Merkel, D. Librizzi, A. Pfestroff, T. Schurrat, K. Buyens, N.N. Sanders, S.C. De Smedt, M. Behe, T. Kissel, Stability of siRNA polyplexes from poly(ethylenimine) and poly(ethylenimine)-g-poly(ethylene glycol) under in vivo conditions: effects on pharmacokinetics and biodistribution measured by Fluorescence Fluctuation Spectroscopy and Single Photon Emission Computed Tomography (SPECT) imaging, *J. Control. Release* 138(2) (2009) 148-59.
- [158] S. Khargharia, K. Kizzire, M.D. Ericson, N.J. Baumhover, K.G. Rice, PEG length and chemical linkage controls polyacridine peptide DNA polyplex pharmacokinetics, biodistribution, metabolic stability and in vivo gene expression, *J. Control. Release* 170(3) (2013) 325-33.
- [159] R.S. Burke, S.H. Pun, Synthesis and characterization of biodegradable HPMA-oligolysine copolymers for improved gene delivery, *Bioconjugate Chem.* 21(1) (2010) 140-50.
- [160] D. Oupicky, M. Ogris, K.A. Howard, P.R. Dash, K. Ulbrich, L.W. Seymour, Importance of lateral and steric stabilization of polyelectrolyte gene delivery vectors for extended systemic circulation, *Mol. Ther.* 5(4) (2002) 463-72.
- [161] M. Noga, D. Edinger, R. Kläger, S.V. Wegner, J.P. Spatz, E. Wagner, G. Winter, A. Besheer, The effect of molar mass and degree of hydroxyethylation on the controlled shielding and deshielding of hydroxyethyl starch-coated polyplexes, *Biomaterials* 34(10) (2013) 2530-8.
- [162] P. Heller, A. Birke, D. Huesmann, B. Weber, K. Fischer, A. Reske-Kunz, M. Bros, M. Barz, Introducing PeptoPlexes: polylysine-block-polysarcosine based polyplexes for transfection of HEK 293T cells, *Macromol. Biosci.* 14(10) (2014) 1380-95.
- [163] H. Hatakeyama, H. Akita, H. Harashima, A multifunctional envelope type nano device (MEND) for gene delivery to tumours based on the EPR effect: a strategy for overcoming the PEG dilemma, *Adv. Drug Deliv. Rev.* 63(3) (2011) 152-60.
- [164] S. Mishra, P. Webster, M.E. Davis, PEGylation significantly affects cellular uptake and intracellular trafficking of non-viral gene delivery particles, *Eur. J. Cell Biol.* 83(3) (2004) 97-111.
- [165] G.F. Walker, C. Fella, J. Pelisek, J. Fahrmeir, S. Boeckle, M. Ogris, E. Wagner, Toward synthetic viruses: endosomal pH-triggered deshielding of targeted polyplexes greatly enhances gene transfer in vitro and in vivo, *Mol. Ther.* 11(3) (2005) 418-25.
- [166] K. Miyata, N. Nishiyama, K. Kataoka, Rational design of smart supramolecular assemblies for gene delivery: chemical challenges in the creation of artificial viruses, *Chem. Soc. Rev.* 41(7) (2012) 2562-74.

- [167] H. Hatakeyama, H. Akita, H. Harashima, The polyethyleneglycol dilemma: advantage and disadvantage of PEGylation of liposomes for systemic genes and nucleic acids delivery to tumors, *Biol. Pharm. Bull.* 36(6) (2013) 892-9.
- [168] T. Blessing, M. Kursa, R. Holzhauser, R. Kircheis, E. Wagner, Different strategies for formation of pegylated EGF-conjugated PEI/DNA complexes for targeted gene delivery, *Bioconjugate Chem.* 12(4) (2001) 529-37.
- [169] K. Müller, E. Kessel, P.M. Klein, M. Höhn, E. Wagner, Post-PEGylation of siRNA Lipo-oligoamino Amide Polyplexes Using Tetra-glutamylated Folic Acid as Ligand for Receptor-Targeted Delivery, *Mol. Pharm.* 13(7) (2016) 2332-45.
- [170] W. Zhang, K. Müller, E. Kessel, S. Reinhard, D. He, P.M. Klein, M. Höhn, W. Rödl, S. Kemper, E. Wagner, Targeted siRNA Delivery Using a Lipo-Oligoaminoamide Nanocore with an Influenza Peptide and Transferrin Shell, *Adv. Healthcare Mater.* 5(12) (2016) 1493-504.
- [171] K. Müller, P.M. Klein, P. Heissig, A. Roidl, E. Wagner, EGF receptor targeted lipo-oligocation polyplexes for antitumoral siRNA and miRNA delivery, *Nanotechnology* 27(46) (2016) 464001.
- [172] V. Knorr, L. Allmendinger, G.F. Walker, F.F. Paintner, E. Wagner, An acetal-based PEGylation reagent for pH-sensitive shielding of DNA polyplexes, *Bioconjugate Chem.* 18(4) (2007) 1218-25.
- [173] V. Knorr, M. Ogris, E. Wagner, An acid sensitive ketal-based polyethylene glycol-oligoethylenimine copolymer mediates improved transfection efficiency at reduced toxicity, *Pharm. Res.* 25(12) (2008) 2937-2945.
- [174] V. Knorr, V. Russ, L. Allmendinger, M. Ogris, E. Wagner, Acetal linked oligoethylenimines for use as pH-sensitive gene carriers, *Bioconjugate Chem.* 19(8) (2008) 1625-1634.
- [175] J. Rejman, V. Oberle, I.S. Zuhorn, D. Hoekstra, Size-dependent internalization of particles via the pathways of clathrin- and caveolae-mediated endocytosis, *Biochem. J.* 377(Pt 1) (2004) 159-69.
- [176] J. Rejman, A. Bragonzi, M. Conese, Role of clathrin- and caveolae-mediated endocytosis in gene transfer mediated by lipo- and polyplexes, *Mol. Ther.* 12(3) (2005) 468-74.
- [177] J. Fang, H. Nakamura, H. Maeda, The EPR effect: Unique features of tumor blood vessels for drug delivery, factors involved, and limitations and augmentation of the effect, *Adv. Drug Delivery Rev.* 63(3) (2011) 136-51.
- [178] E. Wagner, M. Cotten, R. Foisner, M.L. Birnstiel, Transferrin-polycation-DNA complexes: the effect of polycations on the structure of the complex and DNA delivery to cells, *Proc. Natl. Acad. Sci. U.S.A.* 88(10) (1991) 4255-9.
- [179] D. Hanahan, R.A. Weinberg, The hallmarks of cancer, *Cell* 100(1) (2000) 57-70.
- [180] N.E. Hynes, H.A. Lane, ERBB receptors and cancer: the complexity of targeted inhibitors, *Nat. Rev. Cancer* 5(5) (2005) 341-54.
- [181] E.M. Kim, E.H. Park, S.J. Cheong, C.M. Lee, D.W. Kim, H.J. Jeong, S.T. Lim, M.H. Sohn, K. Kim, J. Chung, Characterization, biodistribution and small-animal SPECT of I-125-labeled c-Met binding peptide in mice bearing c-Met receptor tyrosine kinase-positive tumor xenografts, *Nucl. Med. Biol.* 36(4) (2009) 371-8.
- [182] M.E. Davis, The first targeted delivery of siRNA in humans via a self-assembling, cyclodextrin polymer-based nanoparticle: from concept to clinic, *Mol. Pharm.* 6(3) (2009) 659-68.
- [183] R. Hennig, K. Pollinger, A. Vesper, M. Breunig, A. Goepferich, Nanoparticle multivalency counterbalances the ligand affinity loss upon PEGylation, *J. Control. Release* 194 (2014) 20-7.

- [184] J.E. Silpe, M. Sumit, T.P. Thomas, B. Huang, A. Kotlyar, M.A. van Dongen, M.M. Banaszak Holl, B.G. Orr, S.K. Choi, Avidity modulation of folate-targeted multivalent dendrimers for evaluating biophysical models of cancer targeting nanoparticles, *ACS Chem. Biol.* 8(9) (2013) 2063-71.
- [185] T.A. Martin, W.G. Jiang, Hepatocyte growth factor and its receptor signalling complex as targets in cancer therapy, *Anti-Cancer Agents Med. Chem.* 10(1) (2010) 2-6.
- [186] B. Peruzzi, D.P. Bottaro, Targeting the c-Met signaling pathway in cancer, *C Clin. Cancer Res.* 12(12) (2006) 3657-60.
- [187] X. Chen, G. Ding, Q. Gao, J. Sun, Q. Zhang, L. Du, Z. Qiu, C. Wang, F. Zheng, B. Sun, J. Ni, Z. Feng, J. Zhu, A human anti-c-Met Fab fragment conjugated with doxorubicin as targeted chemotherapy for hepatocellular carcinoma, *PloS one* 8(5) (2013) e63093.
- [188] R.M. Lu, Y.L. Chang, M.S. Chen, H.C. Wu, Single chain anti-c-Met antibody conjugated nanoparticles for in vivo tumor-targeted imaging and drug delivery, *Biomaterials* 32(12) (2011) 3265-74.
- [189] M.J. Vosjan, J. Vercammen, J.A. Kolkman, M. Stigter-van Walsum, H. Revets, G.A. van Dongen, Nanobodies targeting the hepatocyte growth factor: potential new drugs for molecular cancer therapy, *Mol. Cancer Ther.* 11(4) (2012) 1017-25.
- [190] E.S. Mittra, H. Fan-Minogue, F.I. Lin, J. Karamchandani, V. Sriram, M. Han, S.S. Gambhir, Preclinical efficacy of the anti-hepatocyte growth factor antibody ficlatuzumab in a mouse brain orthotopic glioma model evaluated by bioluminescence, PET, and MRI, *Clin. Cancer Res.* 19(20) (2013) 5711-21.
- [191] E.M. Kim, E.H. Park, S.J. Cheong, C.M. Lee, H.J. Jeong, D.W. Kim, S.T. Lim, M.H. Sohn, In vivo imaging of mesenchymal-epithelial transition factor (c-Met) expression using an optical imaging system, *Bioconjugate Chem.* 20(7) (2009) 1299-306.
- [192] K.A. Schmohl, A. Gupta, G.K. Grünwald, M. Trajkovic-Arsic, K. Klutz, R. Braren, M. Schwaiger, P.J. Nelson, M. Ogris, E. Wagner, J.T. Siveke, C. Spitzweg, Imaging and targeted therapy of pancreatic ductal adenocarcinoma using the theranostic sodium iodide symporter (NIS) gene, *Oncotarget* 8(20) (2017) 33393-33404.
- [193] Y. Yarden, The EGFR family and its ligands in human cancer. signalling mechanisms and therapeutic opportunities, *Eur. J. Cancer* 37 Suppl 4 (2001) S3-8.
- [194] R.I. Nicholson, J.M. Gee, M.E. Harper, EGFR and cancer prognosis, *Eur. J. Cancer* 37 Suppl 4 (2001) 9-15.
- [195] F. Ciardiello, G. Tortora, EGFR antagonists in cancer treatment, *N. Engl. J. Med.* 358(11) (2008) 1160-74.
- [196] A. Shir, M. Ogris, E. Wagner, A. Levitzki, EGF receptor-targeted synthetic double-stranded RNA eliminates glioblastoma, breast cancer, and adenocarcinoma tumors in mice, *PLoS Med.* 3(1) (2006) e6.
- [197] D. Schaffert, M. Kiss, W. Rödl, A. Shir, A. Levitzki, M. Ogris, E. Wagner, Poly(I:C)-mediated tumor growth suppression in EGF-receptor overexpressing tumors using EGF-polyethylene glycol-linear polyethylenimine as carrier, *Pharm. Res.* 28(4) (2011) 731-41.
- [198] Z. Li, R. Zhao, X. Wu, Y. Sun, M. Yao, J. Li, Y. Xu, J. Gu, Identification and characterization of a novel peptide ligand of epidermal growth factor receptor for targeted delivery of therapeutics, *FASEB J.* 19(14) (2005) 1978-85.
- [199] S. Morys, E. Wagner, U. Lächelt, From Artificial Amino Acids to Sequence-Defined Targeted Oligoaminoamides, *Methods Mol. Biol.* 1445 (2016) 235-58.
- [200] S. Reinhard, W. Zhang, E. Wagner, Optimized solid-phase assisted synthesis of oleic acid-containing siRNA nanocarriers, *ChemMedChem* 12(17) (2017) 1464-1470.

- [201] E. Broda, F.M. Mickler, U. Lächelt, S. Morys, E. Wagner, C. Bräuchle, Assessing potential peptide targeting ligands by quantification of cellular adhesion of model nanoparticles under flow conditions, *J. Control. Release* 213 (2015) 79-85.
- [202] M. Ogris, P. Steinlein, M. Kursa, K. Mechtler, R. Kircheis, E. Wagner, The size of DNA/transferrin-PEI complexes is an important factor for gene expression in cultured cells, *Gene Ther.* 5(10) (1998) 1425-1433.
- [203] Q. Leng, L. Goldgeier, J. Zhu, P. Cambell, N. Ambulos, A.J. Mixson, Histidine-lysine peptides as carriers of nucleic acids, *Drug News Perspect.* 20(2) (2007) 77-86.
- [204] R.J. Smith, R.W. Beck, L.E. Prevette, Impact of molecular weight and degree of conjugation on the thermodynamics of DNA complexation and stability of polyethylenimine-graft-poly(ethylene glycol) copolymers, *Biophys. Chem.* 203-204 (2015) 12-21.
- [205] T.A. Tockary, K. Osada, Y. Motoda, S. Hiki, Q. Chen, K.M. Takeda, A. Dirisala, S. Osawa, K. Kataoka, Rod-to-Globule Transition of pDNA/PEG-Poly(L-Lysine) Polyplex Micelles Induced by a Collapsed Balance Between DNA Rigidity and PEG Crowdedness, *Small* 12(9) (2016) 1193-200.
- [206] S. Schottler, G. Becker, S. Winzen, T. Steinbach, K. Mohr, K. Landfester, V. Mailander, F.R. Wurm, Protein adsorption is required for stealth effect of poly(ethylene glycol)- and poly(phosphoester)-coated nanocarriers, *Nat. Nanotechnol.* 11(4) (2016) 372-7.
- [207] N.P. Truong, J.F. Quinn, M.R. Whittaker, T.P. Davis, Polymeric filomicelles and nanoworms: two decades of synthesis and application, *Polym. Chem.* 7(26) (2016) 4295-4312.
- [208] C.A. Hunter, J.K.M. Sanders, The nature of π - π interactions, *J. Am. Chem. Soc.* 112(14) (1990) 5525-5534.
- [209] A.L. Fink, Protein aggregation: folding aggregates, inclusion bodies and amyloid, *Fold Des.* 3(1) (1998) R9-23.
- [210] F.M. Veronese, A. Mero, F. Caboi, M. Sergi, C. Marongiu, G. Pasut, Site-specific pegylation of G-CSF by reversible denaturation, *Bioconjugate Chem.* 18(6) (2007) 1824-30.
- [211] I. Truebenbach, J. Gorges, J. Kuhn, S. Kern, E. Baratti, U. Kazmaier, E. Wagner, U. Lächelt, Sequence-Defined Oligoamide Drug Conjugates of Pretubulysin and Methotrexate for Folate Receptor Targeted Cancer Therapy, *Macromol. Biosci.* 17(10) (2017).
- [212] G. Saito, J.A. Swanson, K.D. Lee, Drug delivery strategy utilizing conjugation via reversible disulfide linkages: role and site of cellular reducing activities, *Adv. Drug Deliv. Rev.* 55(2) (2003) 199-215.
- [213] P.A. Smanik, Q. Liu, T.L. Furminger, K. Ryu, S. Xing, E.L. Mazzaferri, S.M. Jhiang, Cloning of the Human Sodium Iodide Symporter, *Biochem. Biophys. Res. Commun.* 226(2) (1996) 339-345.
- [214] S. Ravera, A. Reyna-Neyra, G. Ferrandino, L.M. Amzel, N. Carrasco, The Sodium/Iodide Symporter (NIS): Molecular Physiology and Preclinical and Clinical Applications, *Annu. Rev. Physiol.* 79 (2017) 261-289.
- [215] A.M. Müller, K.A. Schmohl, K. Knoop, C. Schug, S. Urnauer, A. Hagenhoff, D.A. Clevert, M. Ingrisch, H. Niess, J. Carlsen, C. Zach, E. Wagner, P. Bartenstein, P.J. Nelson, C. Spitzweg, Hypoxia-targeted ¹³¹I therapy of hepatocellular cancer after systemic mesenchymal stem cell-mediated sodium iodide symporter gene delivery, *Oncotarget* 7(34) (2016) 54795-54810.
- [216] K. Klutz, V. Russ, M.J. Willhauck, N. Wunderlich, C. Zach, F.J. Gildehaus, B. Göke, E. Wagner, M. Ogris, C. Spitzweg, Targeted radioiodine therapy of

- neuroblastoma tumors following systemic nonviral delivery of the sodium iodide symporter gene, *Clin. Cancer Res.* 15(19) (2009) 6079-86.
- [217] K. Klutz, M.J. Willhauck, C. Dohmen, N. Wunderlich, K. Knoop, C. Zach, R. Senekowitsch-Schmidtke, F.J. Gildehaus, S. Ziegler, S. Fürst, B. Göke, E. Wagner, M. Ogris, C. Spitzweg, Image-guided tumor-selective radioiodine therapy of liver cancer after systemic nonviral delivery of the sodium iodide symporter gene, *Hum. Gene Ther.* 22(12) (2011) 1563-74.
- [218] K. Klutz, M.J. Willhauck, N. Wunderlich, C. Zach, M. Anton, R. Senekowitsch-Schmidtke, B. Göke, C. Spitzweg, Sodium iodide symporter (NIS)-mediated radionuclide (^{131}I , ^{188}Re) therapy of liver cancer after transcriptionally targeted intratumoral in vivo NIS gene delivery, *Hum. Gene Ther.* 22(11) (2011) 1403-12.
- [219] G.K. Grünwald, K. Klutz, M.J. Willhauck, N. Schwenk, R. Senekowitsch-Schmidtke, M. Schwaiger, C. Zach, B. Göke, P.S. Holm, C. Spitzweg, Sodium iodide symporter (NIS)-mediated radiovirotherapy of hepatocellular cancer using a conditionally replicating adenovirus, *Gene Ther.* 20(6) (2013) 625-33.
- [220] G.K. Grünwald, A. Vetter, K. Klutz, M.J. Willhauck, N. Schwenk, R. Senekowitsch-Schmidtke, M. Schwaiger, C. Zach, E. Wagner, B. Göke, P.S. Holm, M. Ogris, C. Spitzweg, EGFR-Targeted Adenovirus Dendrimer Coating for Improved Systemic Delivery of the Theranostic NIS Gene, *Mol. Ther. Nucleic Acids* 2 (2013) e131.
- [221] G.K. Grünwald, A. Vetter, K. Klutz, M.J. Willhauck, N. Schwenk, R. Senekowitsch-Schmidtke, M. Schwaiger, C. Zach, E. Wagner, B. Göke, P.S. Holm, M. Ogris, C. Spitzweg, Systemic image-guided liver cancer radiovirotherapy using dendrimer-coated adenovirus encoding the sodium iodide symporter as theranostic gene, *J. Nucl. Med.* 54(8) (2013) 1450-7.
- [222] C. Spitzweg, S. Zhang, E.R. Bergert, M.R. Castro, B. McIver, A.E. Heufelder, D.J. Tindall, C.Y. Young, J.C. Morris, Prostate-specific antigen (PSA) promoter-driven androgen-inducible expression of sodium iodide symporter in prostate cancer cell lines, *Cancer Res.* 59(9) (1999) 2136-41.
- [223] S. Urnauer, K. Klutz, G.K. Grünwald, S. Morys, N. Schwenk, C. Zach, F.J. Gildehaus, W. Rödl, M. Ogris, E. Wagner, C. Spitzweg, Systemic tumor-targeted sodium iodide symporter (NIS) gene therapy of hepatocellular carcinoma mediated by B6 peptide polyplexes, *J. Gene Med.* 19(5) (2017).
- [224] C. Scholz, P. Kos, L. Leclercq, X. Jin, H. Cottet, E. Wagner, Correlation of length of linear oligo(ethan amino) amides with gene transfer and cytotoxicity, *ChemMedChem* 9(9) (2014) 2104-10.
- [225] C.D. Churchill, S.D. Wetmore, Noncovalent interactions involving histidine: the effect of charge on pi-pi stacking and T-shaped interactions with the DNA nucleobases, *J. Phys. Chem. B* 113(49) (2009) 16046-58.
- [226] S. Morys, S. Urnauer, C. Spitzweg, E. Wagner, EGFR Targeting and Shielding of pDNA Lipopolyplexes via Bivalent Attachment of a Sequence-Defined PEG Agent, *Macromol. Biosci.* (2017).
- [227] K. Itaka, A. Harada, Y. Yamasaki, K. Nakamura, H. Kawaguchi, K. Kataoka, In situ single cell observation by fluorescence resonance energy transfer reveals fast intra-cytoplasmic delivery and easy release of plasmid DNA complexed with linear polyethylenimine, *J. Gene Med.* 6(1) (2004) 76-84.
- [228] P. Midoux, C. Mendes, A. Legrand, J. Raimond, R. Mayer, M. Monsigny, A.C. Roche, Specific gene transfer mediated by lactosylated poly-L-lysine into hepatoma cells, *Nucleic Acids Res.* 21(4) (1993) 871-8.

- [229] S. Boeckle, K. von Gersdorff, S. van der Piepen, C. Culmsee, E. Wagner, M. Ogris, Purification of polyethylenimine polyplexes highlights the role of free polycations in gene transfer, *J. Gene Med.* 6(10) (2004) 1102-11.
- [230] Y. Yue, F. Jin, R. Deng, J. Cai, Y. Chen, M.C. Lin, H.F. Kung, C. Wu, Revisit complexation between DNA and polyethylenimine - Effect of uncomplexed chains free in the solution mixture on gene transfection, *J. Control. Release* 155(1) (2011) 67-76.
- [231] J.F. Stefanick, J.D. Ashley, T. Kiziltepe, B. Bilgicer, A systematic analysis of peptide linker length and liposomal polyethylene glycol coating on cellular uptake of peptide-targeted liposomes, *ACS Nano* 7(4) (2013) 2935-47.
- [232] K.D. Fisher, K. Ulbrich, V. Subr, C.M. Ward, V. Mautner, D. Blakey, L.W. Seymour, A versatile system for receptor-mediated gene delivery permits increased entry of DNA into target cells, enhanced delivery to the nucleus and elevated rates of transgene expression, *Gene Ther.* 7(15) (2000) 1337-1343.
- [233] D. Oupicky, K.A. Howard, C. Konak, P.R. Dash, K. Ulbrich, L.W. Seymour, Steric stabilization of poly-L-Lysine/DNA complexes by the covalent attachment of semitelechelic poly[N-(2-hydroxypropyl)methacrylamide], *Bioconjugate Chem.* 11(4) (2000) 492-501.
- [234] L. Peeters, N.N. Sanders, A. Jones, J. Demeester, S.C. De Smedt, Post-pegylated lipoplexes are promising vehicles for gene delivery in RPE cells, *J. Control. Release* 121(3) (2007) 208-17.
- [235] S.M. Liao, Q.S. Du, J.Z. Meng, Z.W. Pang, R.B. Huang, The multiple roles of histidine in protein interactions, *Chem. Cent. J.* 7(1) (2013) 44.
- [236] H. Maeda, The enhanced permeability and retention (EPR) effect in tumor vasculature: the key role of tumor-selective macromolecular drug targeting, *Adv. Enzyme Regul.* 41 (2001) 189-207.
- [237] S. Urnauer, A.M. Müller, C. Schug, K.A. Schmohl, M. Tutter, N. Schwenk, W. Rödl, S. Morys, M. Ingrisich, J. Bertram, P. Bartenstein, D.-A. Clevert, E. Wagner, C. Spitzweg, EGFR-targeted nonviral NIS gene transfer for bioimaging and therapy of disseminated colon cancer metastases, *Oncotarget* (2017).
- [238] P. Erbacher, A.C. Roche, M. Monsigny, P. Midoux, Putative role of chloroquine in gene transfer into a human hepatoma cell line by DNA/lactosylated polylysine complexes, *Exp. Cell Res.* 225(1) (1996) 186-94.
- [239] J. Cheng, R. Zeidan, S. Mishra, A. Liu, S.H. Pun, R.P. Kulkarni, G.S. Jensen, N.C. Bellocq, M.E. Davis, Structure-function correlation of chloroquine and analogues as transgene expression enhancers in nonviral gene delivery, *J. Med. Chem.* 49(22) (2006) 6522-31.
- [240] S.M. Moghimi, Mechanisms regulating body distribution of nanospheres conditioned with pluronic and tetronic block co-polymers, *Adv. Drug Deliv. Rev.* 16(2-3) (1995) 183-193.
- [241] C. Monfardini, F.M. Veronese, Stabilization of substances in circulation, *Bioconjugate Chem.* 9(4) (1998) 418-50.
- [242] V. Subr, C. Konak, R. Laga, K. Ulbrich, Coating of DNA/poly(L-lysine) complexes by covalent attachment of poly[N-(2-hydroxypropyl)methacrylamide], *Biomacromolecules* 7(1) (2006) 122-30.
- [243] P.R. Dash, M.L. Read, K.D. Fisher, K.A. Howard, M. Wolfert, D. Oupicky, V. Subr, J. Strohalm, K. Ulbrich, L.W. Seymour, Decreased binding to proteins and cells of polymeric gene delivery vectors surface modified with a multivalent hydrophilic polymer and retargeting through attachment of transferrin, *J. Biol. Chem.* 275(6) (2000) 3793-802.

8 Publications

Original articles (*indicates equal contributions)

Urnauer S., Schmohl K.A., Tutter M., Schug C., Schwenk N., **Morys S.**, Ziegler S., Bartenstein P., Clevert D.A., Wagner E., Spitzweg C. *Dual-targeting strategy for improved nonviral gene transfer of the theranostic sodium iodide symporter*, **2017**, submitted.

Krhac Levacic A., **Morys S.**, Kempter S., Lächelt U., Wagner E. Minicircle versus plasmid DNA delivery by receptor-targeted polyplexes, *Hum Gene Ther.*, **2017**, 28 (10),862-74.

Urnauer S., Müller A. M., Schug C., Schmohl K. M., Tutter M., Schwenk N., Rödl W., **Morys S.**, Ingrisich M., Bertram J., Bartenstein P., Clevert A., Wagner E., Spitzweg C. *EGFR-targeted nonviral NIS gene transfer for bioimaging and therapy of disseminated colon cancer metastases*. *Oncotarget*, **2017**, doi: 10.18632/oncotarget.21028

Morys S.*, Urnauer S.*, Spitzweg C., Wagner E. *EGFR targeting and shielding of pDNA lipopolyplexes via bivalent attachment of a sequence-defined PEG agent*. *Macromol. Biosci.*, **2017**, doi: 10.1002/mabi.201700203

Urnauer S., Klutz K., Grünwald G. K., **Morys S.**, Schwenk N., Zach C., Gildehaus F. J., Rödl W., Ogris M., Wagner E., Spitzweg C. *Systemic tumor-targeted sodium iodide symporter (NIS) gene therapy of hepatocellular carcinoma mediated by B6 peptide polyplexes*. *J. Gene Med.* **2017**, 19 (5).

Morys S., Krhac Levacic A.; Urnauer S., Kempter S., Kern S., Rädler J.O., Spitzweg C., Lächelt U., Wagner E. *Influence of Defined Hydrophilic Blocks within Oligoaminoamide Copolymers: Compaction versus Shielding of pDNA Nanoparticles*. *Polymers* **2017**, 9, 142.

Urnauer S., **Morys S.**, Krhac Levacic A., Müller A. M., Schug C., Schmohl K. A., Schwenk N., Zach C., Carlsen J., Bartenstein P., Wagner E., Spitzweg C. *Sequence-defined cMET/HGFR-targeted Polymers as Gene Delivery Vehicles for the Theranostic Sodium Iodide Symporter (NIS) Gene*. *Mol. Ther.* **2016**, 24 (8), 1395-404.

Broda E., Mickler F. M., Lächelt U., **Morys S.**, Wagner E., Bräuchle C. *Assessing potential peptide targeting ligands by quantification of cellular adhesion of model nanoparticles under flow conditions. J. Control. Release* **2015**, 213, 79-85.

Kos, P.*, Lächelt U.*, Herrmann A., Mickler F. M., Döblinger M., He D., Krhac Levacic A., **Morys S.**, Bräuchle C., Wagner E. *Histidine-rich stabilized polyplexes for cMet-directed tumor-targeted gene transfer. Nanoscale* **2015**, 7 (12), 5350-62.

Bookchapter

Morys S.; Wagner, E.; Lächelt, U., *From Artificial Amino Acids to Sequence-Defined Targeted Oligoaminoamides. Methods Mol. Biol.* **2016**, 1445, 235-58.

Review

Krhac Levacic A., **Morys S.**, Wagner E. *Solid-phase Supported Design of Carriers for Therapeutic Nucleic Acid Delivery. Bioscience Reports* **2017**, 37 (5).

Meeting abstracts and poster presentations

Urnauer S., Schmohl K. A., **Morys S.**, Tutter M., Schwenk N., Schug C., Oos R., Bartenstein P., Clevert D. A., Wagner E., Spitzweg C. *Dual receptor targeting for improved systemic tumor-specific delivery of the sodium iodide symporter (NIS) gene. 87th Annual Meeting of the American Thyroid Association, Victoria, Canada, October 2017.*

Urnauer S., Müller A. M., Schug C., Schmohl K. A., Tutter M., Schwenk N., Rödl W., **Morys S.**, Ingrisich M., Bertram J., Bartenstein P., Clevert D. A., Wagner E., Spitzweg C. *EGFR-targeted polyplex-mediated NIS gene therapy of metastatic colorectal cancer. 60th Annual Meeting of the German Society of Endocrinology, Würzburg, Germany, April 2017.*

Urnauer S., Müller A. M., Schug C., Schmohl K. A., Tutter M., Schwenk N., Rödl W., **Morys S.**, Ingrisich M., Bertram J., Bartenstein P., Clevert D. A., Wagner E., Spitzweg C. *EGFR-targeted nonviral NIS gene transfer for bioimaging and therapy of*

disseminated colon cancer metastases. 40th Annual Meeting of the European Thyroid Association, Belgrade, Serbia, September 2017.

Urnauer S., Müller A.M., **Morys S.**, Oos R., Bartenstein P., Clevert D. A., Wagner E., Spitzweg C. *Systemic epidermal growth factor receptor-targeted sodium iodide symporter (NIS) gene therapy in an advanced tumor model of hepatic colon cancer metastasis*. 86th Annual Meeting of the American Thyroid Association, Denver, USA, October 2016.

Urnauer S., **Morys S.**, Müller A. M., Oos R., Carlsen J., Bartenstein P., Wagner E., Spitzweg C. *Systemic epidermal growth factor receptor-targeted gene delivery using the theranostic sodium iodide symporter (NIS) gene in an advanced orthotopic tumor model*. 59th Annual Meeting of the German Society of Endocrinology, Munich, Germany, May 2016.

Urnauer S., **Morys S.**, Krhac Levacic A., Müller A. M., Schug C., Schmohl K. A., Schwenk N., Zach C., Carlsen J., Bartenstein P., Wagner E., Spitzweg C. *Sequence defined cMET/HGFR-targeted polymers as gene delivery vehicles for the theranostic sodium iodide symporter (NIS) gene*. 59th Annual Meeting of the German Society of Endocrinology, Munich, Germany, May 2016.

Urnauer S., **Morys S.**, Krhac Levacic A., Müller A. M., Schug C., Schmohl K. A., Schwenk N., Zach C., Carlsen J., Bartenstein P., Wagner E., Spitzweg C. *Sequence defined cMET/HGFR-targeted polymers as gene delivery vehicles for the theranostic sodium iodide symporter (NIS) gene*. 18th Congress of European Endocrinology, Munich, Germany, May 2016.

Urnauer S., **Morys S.**, Müller A. M., Oos R., Carlsen J., Bartenstein P., Wagner E., Spitzweg C. *Systemic epidermal growth factor receptor-targeted gene delivery using the theranostic sodium iodide symporter (NIS) gene in an advanced orthotopic tumor model*. 18th Congress of European Endocrinology, Munich, Germany, May 2016.

Urnauer S., **Morys S.**, Krhac Levacic A., Schug C., Schwenk C., Carlsen J., Zach C., Wagner E., Spitzweg C. *Systemic non-viral cMET/HGFR-targeted gene delivery using the theranostic function of the sodium iodide symporter (NIS)*. 15th International Thyroid Congress, Orlando, Florida, USA, October 2015.

9 Acknowledgements

After an intensive period of almost four years, my PhD study comes to an end. It has been a period of intense learning for me, not only in the scientific area, but also on a personal level. Writing this dissertation has had a big impact on me. I would like to reflect on the people who have supported and helped me so much throughout the years.

First of all, I thank my supervisor Professor Dr. Ernst Wagner for giving me the opportunity to work on my dissertation within his research group. I am very grateful for his wise supervision and personal as well as scientific support during the whole time. Also, I want to thank for his encouragement to develop own projects and experiments.

I want to thank Professor Dr. Christine Spitzweg for providing funding of my PhD work and offering help whenever needed! I also specially want to thank her PhD student Sarah Urnauer for a very close and fruitful collaboration in several projects over the years. Not only did she essentially contribute to our joint project of post-modification of lipopolyplexes, but also provided innumerable transfections of my generated compounds. Thank you so much for this!

I also specially want to thank Ana for spending so much time on cell culture work to test my synthesized oligomers. All synthetic work would be irrelevant without your contribution! It was great teamwork that added up perfectly within different projects.

Many thanks to Sarah and Jasmin for carrying out *in vivo* animal experiments, and Markus for taking care of the animals.

I thank Philipp and Uli for teaching me solid phase synthesis during my very first weeks in the lab and scientific advice, whenever needed.

Many thanks to Wolfgang for the support with our technical equipment, for repairing almost any broken instrument or computer and for ensuring the technical maintenance, as well as the good atmosphere within room D3.002. Also, I want to thank the remaining team of technicians: Anna, Ursula, Miriam and Melinda for keeping the everyday life in the lab running. I'm also grateful for Olga's support, when ever needed, with her organizational skills. Also, I want to thank Ursula for all the delicious cakes she baked.

I greatly appreciate the efforts of Dr. Martina Ruffer for the organization of hiking events, the Christmas party (including “Wichteln”) and the traditional Weißwurst Frühstück. Lately, these traditions have been luckily preserved and continued by Dr. Ulrich Lächelt, many thanks!

My thanks also go out to Dr. Martina Ruffer and Dr. Andreas Roidl for organizing practical courses for the students and correcting the student’s exams, thereby leaving us time to do research.

I want to thank Ruth, Katharina, Philipp H., and Bojan for a quick familiarization into the group on a personal as well as scientific level.

I want to thank all (current) members of the Wagner research group for the great atmosphere during my time in the AK. We were not only able to support each other by deliberating over our problems and findings, but also happily by talking about things other than just our papers. Here I specially want to thank Sören, Philipp, Ines, Dominik and Jasmin for good (scientific) discussions during working times or coffee breaks. Within the years, the whole lab had a lot of great events and we spent time together not only as colleagues but also as friends on ski trips to Kühtai, several BBQs, lab dinners, PhD celebrations, Fasching and Christmas parties, soccer and basketball games, Oktoberfest, celebrations for new publications and many more occasions. Special thanks also go out to Ines for proofreading my thesis for spelling and punctuation mistakes.

I would like to thank the Rolling Stones for providing with “You can’t always get what you want” a hymn that helped me through all the failings within PhD life and everyone in room D3.002 for standing my taste of music or enriching it.

Finally, I would also like to thank my parents and my brother Christoph for my carefree childhood and for supporting me all my life, as well as Brigitte for always having an “open ear” and her kindness.